

Attention Microfiche User,

The original document from which this microfiche was made was found to contain some imperfection or imperfections that reduce full comprehension of some of the text despite the good technical quality of the microfiche itself. The imperfections may be:

- missing or illegible pages/figures
- wrong pagination
- poor overall printing quality, etc.

We normally refuse to microfiche such a document and request a replacement document (or pages) from the National INIS Centre concerned. However, our experience shows that many months pass before such documents are replaced. Sometimes the Centre is not able to supply a better copy or, in some cases, the pages that were supposed to be missing correspond to a wrong pagination only. We feel that it is better to proceed with distributing the microfiche made of these documents than to withhold them till the imperfections are removed. If the removals are subsequently made then replacement microfiche can be issued. In line with this approach then, our specific practice for microfiching documents with imperfections is as follows:

1. A microfiche of an imperfect document will be marked with a special symbol (black circle) on the left of the title. This symbol will appear on all masters and copies of the document (1st fiche and trailer fiches) even if the imperfection is on one fiche of the report only.
2. If imperfection is not too general the reason will be specified on a sheet such as this, in the space below.
3. The microfiche will be considered as temporary, but sold at the normal price. Replacements, if they can be issued, will be available for purchase at the regular price.
4. A new document will be requested from the supplying Centre.
5. If the Centre can supply the necessary pages/document a new master fiche will be made to permit production of any replacement microfiche that may be requested.

The original document from which this microfiche has been prepared has these imperfections:

- missing pages/figures numbered: _____
- wrong pagination
- poor overall printing quality
- combinations of the above
- other ; Page 92. Fig 2 not printed ^{few lines of text under} INIS Clearinghouse
IAEA

P. O. Box 100
A-1400, Vienna, Austria

FR 8002140

FR NG - CONF - 201



a
2212

International Conference on
**NUCLEAR BEHAVIOUR AT
HIGH ANGULAR MOMENTUM**

Contributions

Shasburg - April 22-24, 1980



INTERNATIONAL CONFERENCE
ON
NUCLEAR BEHAVIOUR AT HIGH ANGULAR MOMENTUM

CONTRIBUTIONS

STRASBOURG , APRIL 22-24, 1980

INTERNATIONAL CONFERENCE

ON

NUCLEAR BEHAVIOUR AT HIGH ANGULAR MOMENTUM

HELD IN STRASBOURG FROM APRIL 22-24, 1980

ORGANIZED BY THE CENTRE DE RECHERCHES NUCLÉAIRES DE STRASBOURG

INTERNATIONAL ADVISORY COMMITTEE

R. BOCK
R.M. DIAMOND
V. GILLET
A. GIZON
B. HERSKIND
M. LEFORT
J.O. NEWTON

G.C. MORRISON
R.A. RICCI
J.P. SCHIFFER
A.W. SUNYAR
Z. SZYMANSKI
J. VERVIER
D. WARD

ORGANIZING COMMITTEE

F.A. BECK
T. BYRSKI
J.P. COFFIN
G. COSTA
D. DISDIER
R.M. FREEMAN

B. HAAS
F. HAAS
J.C. MERDINGER
Y. SCHUTZ
J.P. VIVIEN

The Proceedings of the International Conference on Nuclear Behaviour at High Angular Momentum, held in Strasbourg, April 22-24, 1980, are published in two volumes.

The present volume contains the contributions to the Conference. All papers have been reproduced by direct photoreproduction.

The invited talks and the contributions presented during the Conference will be published in a special issue of the JOURNAL DE PHYSIQUE.

March 31, 1980

C O N T E N T S

	page
THE SPIN POLARIZATION OF ROTATING NUCLEAR MATTER S.Frauenthorf, K.Neergård	FR8002141 1
A SEMI-CLASSICAL MODEL FOR HEAVY ION POTENTIALS AT HIGH SPIN B.Grammaticos, T.Sami	— 2142 3
g-FACTOR OF THE FIRST EXCITED 4^+ STATE IN BACKBENDING ^{20}Ne K.H.Speidel, G.J.Kumbartzki, W.Knauer, V.Mertens, P.N.Tandon, N.Ayres de Campos, J.Gerber, M.B.Goldberg	— 2143 5
HIGH SPIN STATES OF ^{34}Cl C.J.van der Poel	— 2144 7
DECAY MODES OF HIGH SPIN STATES IN LIGHT NUCLEI P.A.Butler, R.Daniel, A.D.Irving, P.J.Nolan, J.F.Sharpey- Schafer	— 2145 9
HIGH SPIN STATES IN ^{40}K , ^{42}Ca , ^{55}Fe and ^{56}Fe P.Kofahl, H.Fromm, H.V.Klapdor, T.Oda	— 2146 11
STRUCTURE ABOVE AND FEEDING OF THE YRAST LINE IN ^{48}Ti F.Glatz, P.Betz, J.Siefert and H.Röpke	— 2147 13
MEASUREMENT OF GROUND-STATE SIDE FEEDING BY MEANS OF IN-BEAM AND RADIOACTIVITY γ -RAY SPECTROMETRY F.Terrasi, M.G.Saint-Laurent, A.D'Onofrio, H.Dumont and J.Delaunay	— 2148 15

HIGH SPIN STATES FOR ^{55}Fe VIA HEAVY ION INDUCED FUSION EVAPORATION REACTIONS FR 8002149

M.G. Saint-Laurent, H.Dumont, B.Delaunay and J.Delaunay	17
A MICROSCOPIC CLASSIFICATION OF HIGH-SPIN STATES IN ^{56}Fe	2150
P.W.M.Glaudemans	19
TWO-NUCLEON HIGH-SPIN STATES IN ODD-ODD COPPER : THE ^{66}Cu CASE	
Tsan Ung Chan, J.F.Bruandet, B.Chambon, A.Dauchy, D.Drain, A.Giorni, F.Glasser and C.Morand ISN 80-04	21
GAMMA-SPECTROSCOPIC INVESTIGATIONS ON ^{67}Ge	2151
V.Zobel, L.Cleemann, J.Eberth, T.Heck and W.Neumann	23
A NEUTRON MULTIPLICITY TECHNIQUE FOR STUDYING WEAK REACTION CHANNELS IN IN-BEAM γ -RAY SPECTROSCOPY AND ITS APPLICATION TO ^{74}Kr	2152
J.Roth, L.Cleemann, J.Eberth, W.Neumann, R.B.Piercey, A.V.Ramaya, J.H.Hamilton	25
CALCULATION OF CONTINUUM FEEDING TIMES IN HEAVY ION FUSION REACTIONS	2153
F.P.Hellmeister and K.P.Lieb	27
DECOUPLED $g_{3/2}$ PROTON BAND IN ^{79}Rb	2154
J.Panqueva, H.P.Hellmeister, F.J.Bergmeister and K.P.Lieb	29
LIFETIME MEASUREMENTS FOR HIGH-SPIN STATES IN $^{83,85}\text{Sr}$	2155
D.Bucurescu, G.Constantinescu, M.Ivascu, N.V.Zamfir and M.Avrigeanu	31
IN BEAM GAMMA-RAY SPECTROSCOPY OF ^{84}Sr	2156
A.Dewald, W.Gast, A.Gelberg, H.-W.Schuh, K.O.Zell, P.von Brentano	33
THREE-QUASIPARTICLE STATES OF THE NUCLEI ^{85}Y AND ^{87}Y	2157
S.E.Arnell, A.Nilsson, O.Skeppstedt, E.Wallander	35

FR 800 2158

EVIDENCE OF A BAND STRUCTURE IN ODD-ODD ^{104}Ag	
R.Béraud, A.Charvet, R.Duffait, M.Meyer, J.Genevey, J.Tréherne, F.Beck, T.Byrski	37
HIGH SPIN STATES OF THE ODD-ODD ^{110}In NUCLEUS	— 2159
R.Béraud, A.Charvet, R.Duffait, M.Meyer, J.Genevey, J.Tréherne, F.Beck, T.Byrski	39
GAMMA-GAMMA CORRELATIONS FOLLOWING COMPOUND NUCLEUS REACTIONS WITH 118 MeV ^{12}C -IONS	— 2160
C.J.Herrlander, L.Hildingsson, A.Johnson, A.Kerek, W.Klamra, A.Källberg, Th.Lindblad, C.G.Lindén, J.Starker, K.Wikström, J.Bialowski, J.Kownacki, B.Fant, T.Lönnroth	41
MULTIPLICITY OF THE STATISTICAL γ -RAYS FOLLOWING (HI,xn) REACTIONS	— 2161
S.H.Sie, R.M.Diamond, J.O.Newton, J.R.Leigh	43
BAND CROSSING IN THE INTERACTING BOSON MODEL	— 2162
A.Gelberg, A.Zemel	45
GAMMA TRANSITION-ENERGY CORRELATIONS IN BARIUM NUCLEI	— 2163
M.A.Deleplanque, O.Andersen, J.D.Garrett, B.Herskind, F.S.Stephens, C.G.Lindén, S.A.Hjorth, A.Johnson and Th.Lindblad	47
MAGNETIC MOMENTS OF ^{134}Ce LEVELS AT BACKBENDING	— 2164
M.B.Goldberg, C.Broude, A.Zemel, J.Gerber, G.J.Kumbartzki, K.H.Speidel	49
THE g-FACTOR OF THE $I^\pi = 10^+$ ISOMERS IN ^{138}Ce AND ^{140}Nd	— 2165
J.C.Merdinger, F.A.Beck, T.Byrski, C.Gehring, Y.Schutz, J.P.Vivien, E.Božek	51
HIGH SPIN LEVEL STRUCTURE OF ^{147}Sm	— 2166
M.Piiparinen, Y.Nagai, J.Styczen, P.Kleinheinz	53

DEFORMATION OF A HIGH-SPIN YRAST ISOMER IN ^{147}Gd	FR8002167	
H.-E.Mahnke, O.Häusser, T.K.Alexander, H.R.Andrews, J.F.Sharpey-Schafer, M.Swanson, P.Taras, D.Ward		55
ON THE STRUCTURE OF THE HIGH SPIN ISOMERS IN ^{147}Gd	—	2168
T.Dössing, K.Neergård, H.Sagawa		57
IDENTIFICATION OF HIGH SPIN ISOMERS NEAR $N = 82$		
S.André, J.Genevey, A.Gizon, J.Gizon, J.Jastrzebski, J.Łukasiak, M.Moszyński, Z.Preibisz	15150007	59
HOW PARTICLE-OCTUPOLE EXCHANGE COUPLING AFFECTS THE YRAST LINES OF DYSPROSIUM NUCLEI	—	2169
P.J.Daly, P.Kleinheinz, R.Broda, S.Lunardi, H.Backe, J.Blomqvist		61
HIGH SPIN SHELL MODEL EXCITATIONS IN ^{149}Gd		
M.Piiparinen, R.Pengo, Y.Nagai, P.Kleinheinz, N.Roy, L.Carlen, H.Ryde, Th.Lindblad, A.Johnson, S.A.Hjorth, E.Hammarén	—	2170
		63
A STUDY OF THE γ -RAY CONTINUUM FEEDING HIGH SPIN STATES IN $^{151,152}\text{Dy}$	—	2171
J.F.Sharpey-Schafer, A.J.Ferguson, H.R.Andrews, O.Häusser, H.-E.Mahnke, D.Ward		65
HIGH SPIN YRAST STATES IN ^{151}Ho		
J.Gizon, A.Gizon, S.André, J.Genevey, J.Jastrzebski, J.Łukasiak, M.Moszyński, Z.Preibisz	—	2172
		67
ROTATION-ALIGNED BAND IN THE ODD-ODD ^{152}Eu NUCLEUS	—	2173
J.A.Pinston, R.Bengtsson, D.Barneoud, A.Monnand, F.Schussler		69
THE X-(OR Δ) TRANSITION IN ^{152}Dy	—	2174
Y.Nagai, J.Styczen, M.Piiparinen, P.Kleinheinz		71

CONTINUUM γ -RAY SPECTRA AND EXCITATION FUNCTIONS OF YRAST STATES IN ^{152}Dy

FR8002175

I.Ahmad, J.Borggreen, P.Chowdhury, T.L.Khoo, R.K.Smither,
S.R.Faber, C.L.Dors, J.Wilson, P.J.Daly 73

K-SHELL IONIZATION YIELDS FOR ($^{40}\text{Ar}, 4n$) REACTIONS LEADING TO THE NUCLEI ^{152}Dy AND ^{162}Yb — 2175

K.Cornelis, R.Holzmann, M.Huyse, R.Janssens, G.Lhersonneau,
J.Lukasiak, C.Michel, Z.Sujkowski, M.A.Van Hove, J.Verplancke,
J.Vervier 75

PATHS OF γ -DECAYS FROM HIGHLY EXCITED STATES AND THE EFFECT OF THE K-QUANTUM NUMBER — 2177

M.Wakai, M.Sano, A.Faessler 77

HIGH SPIN ISOMERIC STATES IN THE $N = 84$ NUCLEUS ^{152}Er — 2178

R.Holzmann, Y.El Masri, C.Michel, M.A.Van Hove and
J.Vervier 79

HIGH SPIN ISOMERS IN ^{153}Er — 2179

D.Horn, G.R.Young, C.J.Lister, C.Baktash 81

NATURE OF HIGH SPIN STATES IN NEUTRON DEFICIENT ERBIUM ISOTOPES — 2180

P.Aguer, G.Bastin, A.Péghaire, J.P.Thibaud, N.Perrin,
H.Sergolle, Ph.Hubert 83

CALCULATIONS OF THE CONTINUUM γ -RAY SPECTRA IN (HI, xn) REACTIONS

Ph.Hubert, F.Leccia, R.Liotta, P.Mennrath, M.M.Villard 85
29786-8015

IRREGULARITIES IN THE YRAST LINE OF ^{156}Er

T.Byrski, F.A.Beck, C.Gehringer, J.C.Merdinger, Y.Schutz
and J.P.Vivien — 2181
87

GAMMA-RAY TRANSITION ENERGY CORRELATIONS IN ^{156}Er AND ^{160}Yb

J.P.Vivien, Y.Schutz, F.A.Beck, T.Byrski, C.Gehringer
and J.C.Merdinger — 2182
89

B(E2) - VALUES OF HIGH SPIN STATES IN Dy-ISOTOPES	FR 800 2183
H.Emling, P.Fuchs, E.Grosse, R.Kulesa, D.Schwalm, R.S.Simon and H.J.Wollersheim	91
DISCRETE γ -RAYS ABOVE 1-MeV IN Er NUCLEI	— 2184
H.Yamada, D.C.Hensley, A.V.Ramayya, C.F.Maguire, J.H.Hamilton, and A.Ahmed	93
ALIGNMENT OF PARTICLE ANGULAR MOMENTUM IN DEFORMED NUCLEI	— 2185
L.K.Peker, J.H.Hamilton, J.O.Rasmussen	95
YRST SPECTRUM AND g-FACTOR FOR ^{158}Dy	— 2186
M.Diebel, A.N.Mantri and U.Mosel	97
HIGH SPIN STATES IN NEUTRON RICH DEFORMED NUCLEI	— 2187
H.Bohn, T.Faestermann, F.v.Feilitzsch, P.Kienle, H.Emling, P.Fuchs, E.Grosse, D.Schwalm and H.J.Wollersheim	99
HIGH FREQUENCY BAND CROSSING IN ^{161}Yb	— 2188
J.J.Gaardhøje, O.Andersen, J.D.Garrett, G.B.Hagemann, B.Herskind, L.L.Riedinger, P.O.Tjøm	101
THE MICROSCOPIC STRUCTURE OF THE VIBRATIONAL LEVELS IN ^{164}Er AT LARGE ANGULAR MOMENTA	— 2189
J.L.Egido, H.J.Mang, P.Ring	103
ANALYSIS OF ANGULAR DISTRIBUTIONS IN (PARTICLE,XN) REACTIONS	— 2190
V.A.Ionescu, J.Kern, Cl.Nordmann, S.Olbrich	105
γ_{21} PAIRING AND THE PARTICLE-ROTOR DESCRIPTION OF ^{167}Er	— 2191
J.Almberger, I.Hamamoto and G.Leander	107
ON THE YRST-YRARE INTERACTION IN THE CRANKED HFB MODEL	— 2192
H.-B.Håkansson	109

STUDY OF BAND CROSSINGS IN ^{182}Os

FR 800 2193

R.M.Lieder, G.Sletten, O.Bakander, S.Bjørnholm, J.Borggreen,
J.Pedersen 111

ALIGNED QUASIPARTICLES IN EVEN $^{190-198}\text{Hg}$ ISOTOPES

M.Guttormsen and H.Hübel 113

HIGH SPIN STATES AND E2 TRANSITION STRENGTHS IN $^{194,196}\text{Pt}$,

J.Idzko, K.Stelzer, Th.W.Elze, H.Ower, H.J.Wollersheim,
H.Emling, P.Fuchs, E.Grosse, R.Piercey, D.Schwalm 115

MULTI-STEP SHELL MODEL METHOD

C.Pomar and R.Liotta 117

HIGH SPIN STATES IN ^{232}Th , ^{234}U and ^{236}U

H.Ower, Th.W.Elze, J.Idzko, K.Stelzer, H.Emling, P.Fuchs,
E.Grosse, D.Schwalm, H.J.Wollersheim, N.Kaffrell, N.Trautmann 119

A COMPTON SUPPRESSION SPECTROMETER FOR COINCIDENCE MEASUREMENTS ; LARGE SOLID ANGLE AND GOOD SUPPRESSION

H.J.M.Aarts 121

SPIN POLARIZATION OF LIGHT FRAGMENTS FROM $^{16}\text{O} + ^{58}\text{Ni}$ REACTIONS

W.Trautmann, W.Dahme, W.Dünneberger, W.Hering, C.Lauterbach,
H.Puchta, W.Kühn, J.P.Wurm 123

ALPHA EMISSION WITH 10 MeV/A ^{14}N PROJECTILES

R.K.Bhowmik, E.C.Pollacco, J.B.A.England, N.E.Sanderson
and G.C.Morrison 125

HOW FAST α PARTICLES ARE EMITTED IN "MASSIVE TRANSFER" REACTIONS ?

C.Gerschel, N.Perrin, L.Valentin, H.Tricoire, B.Ader,
D.Paya 127

EMITTED PARTICLES AND GAMMA DEEXCITATION IN THE REACTION

$^{12}\text{C} + ^{55}\text{Mn}$ AT $E(^{12}\text{C}) = 55$ MeV

F.Azgui, J.F.Bruandet, F.Glasser, B.Chambon, A.Dauchy,
D.Drain, A.Giorni, J.P.Longequeue, C.Morand, C.Pastor,
Tsan Ung Chan, J.C.Wells, H.Dumont

129

MEASUREMENT OF CHARGED PARTICLE MULTIPLICITIES BY PARTICLE- γ COINCIDENCES : THEIR POSSIBLE ROLE FOR SPECTROSCOPY AND MECHANISM STUDIES

FR 800 2202

M.G.Saint-Laurent, H.Dumont, H.Yoshikawa and J.Delaunay

131

THE $^{18}\text{O} + ^{12}\text{C}$ FUSION-EVAPORATION REACTION

2203

B.Heusch, C.Beck, J.P.Coffin, R.M.Freeman, A.Gallmann,
F.Haas, F.Rami, P.Wagner and D.E.Alburger

133

STUDY OF THE DOMINANT CHANNELS IN THE REACTIONS INDUCED BY LIGHT-HEAVY IONS ON MEDIUM-MASS ($A \sim 50$) TARGETS

2204

A.D'Onofrio, H.Dumont, M.G.Saint-Laurent, F.Terrasi,
B.Delaunay, J.Delaunay and D.Rizzo

135

EVAPORATION RESIDUE AND FISSION CROSS-SECTIONS FOR THE SYSTEM

2205

$^{40}\text{Ar} + ^{110}\text{Pd}$

C.Cabot, H.Gauvin, Y.Le Beyec, H.Delagrance, J.P.Dufour,
A.Fleury, Y.Llabador, J.M.Alexander

137

CROSS SECTION DISTRIBUTION IN NUCLEAR REACTIONS INDUCED BY ^{12}C ,

^{14}N AND ^{16}O IONS ON TARGETS NEAR $N = 82$

J.Jastrzebski, R.Kossakowski, J.Łukasiak, M.Moszyński,
Z.Preibisz, P.Rymuza, S.André, J.Genevey, A.Gizon, J.Gizon

139

NEW RESULTS ON ANGULAR MOMENTUM TRANSFER FROM SEQUENTIAL FISSION IN $^{255}\text{MeV Ar} + \text{Bi}$ AND $^{435}\text{MeV Ni} + \text{Pb}$ DEEP INELASTIC COLLISIONS

2206

C.Le Brun, J.F.Lecolley, F.Lefèbvres, M.L'Haridon,
J.P.Patry, J.C.Steckmeyer, R.Chechik

141

FR 800 2193

STUDY OF BAND CROSSINGS IN ^{182}Os	
R.M.Lieder, G.Sletten, O.Bakander, S.Bjørnholm, J.Borggreen, J.Pedersen	111
ALIGNED QUASIPARTICLES IN EVEN $^{190-198}\text{Hg}$ ISOTOPES	— 2194
M.Guttormsen and H.Hübel	113
HIGH SPIN STATES AND E2 TRANSITION STRENGTHS IN $^{194,196}\text{Pt}$,	— 2195
J.Idzko, K.Stelzer, Th.W.Elze, H.Ower, H.J.Wollersheim, H.Emling, P.Fuchs, E.Grosse, R.Piercey, D.Schwalm	115
MULTI-STEP SHELL MODEL METHOD	— 2196
C.Pomar and R.Liotta	117
HIGH SPIN STATES IN ^{232}Th , ^{234}U and ^{236}U	— 2197
H.Ower, Th.W.Elze, J.Idzko, K.Stelzer, H.Emling, P.Fuchs, E.Grosse, D.Schwalm, H.J.Wollersheim, N.Kaffrell, N.Trautmann	119
A COMPTON SUPPRESSION SPECTROMETER FOR COINCIDENCE MEASUREMENTS ; LARGE SOLID ANGLE AND GOOD SUPPRESSION	— 2198
H.J.M.Aarts	121
SPIN POLARIZATION OF LIGHT FRAGMENTS FROM $^{16}\text{O} + ^{58}\text{Ni}$ REACTIONS	— 2199
W.Trautmann, W.Dahme, W.Dünnweber, W.Hering, C.Lauterbach, H.Puchta, W.Kühn, J.P.Wurm	123
ALPHA EMISSION WITH 10 MeV/A ^{14}N PROJECTILES	— 2200
R.K.Bhowmik, E.C.Pollacco, J.B.A.England, N.E.Sanderson and G.C.Morrison	125
HOW FAST α PARTICLES ARE EMITTED IN "MASSIVE TRANSFER" REACTIONS ?	— 2201
C.Gerschel, N.Perrin, L.Valentin, H.Tricoire, B.Ader, D.Paya	127

COMPETITION BETWEEN FISSION AND NEUTRON EMISSION OF ^{210}Po AT HIGH SPINS AND EXCITATION ENERGIES

M.Ploszajczak, M.Faber

FR 800 2207
143

FAST FISSION PHENOMENA IN HEAVY ION REACTIONS,

C.Grégoire, R.Lucas, C.Ngô, H.Ngô and B.Schlürmann

CEA CONF-5214

145

PRE-EQUILIBRIUM EMISSION IN PROTON-INDUCED REACTIONS ON COBALT AND NICKEL IN THE ENERGY RANGE 18-84 MeV

S.J.Mills and F.J.Haasbroek

2208
147

FORMATION AND DEEXCITATION OF THE ^{79}Rb COMPOUND NUCLEUS

J.Barreto, M.Langevin and C.Détraz

2209
149

POST DEAD-LINE CONTRIBUTED PAPERS

p. 153

FR 800 2210

(F. Grümmer)

p. 155

2211

(Khadkikar)

AUTHOR INDEX

p. 157

2212

(Radford)

CONTRIBUTIONS

THE SPIN POLARIZATION OF ROTATING NUCLEAR MATTER[†]

S. Frauendorf

Zentralinstitut für Kernforschung Rossendorf, Dresden, DDR

K. Neergård

Justus-Liebig-Universität Giessen, Giessen, BRD

Rotating nuclear matter can be defined in analogy with the ordinary nuclear matter as a system of infinitely many nucleons where the forces that would destabilize states with a finite, homogeneous density are switched off. In a rotating frame of reference, these forces are (i) the Coulomb interaction, and (ii) the centrifugal force. We have studied the structure of rotating nuclear matter in an effective Hartree-Fock model, using for the density dependent two-nucleon interaction Sprung's and Banerjee's local approximation^{1,2} to a Brueckner reaction matrix calculated from the Reid soft core potential. The shortest range part of the Sprung-Banerjee force was adjusted, in accordance with the authors' suggestion, so that the model gives the empirical values for the binding and symmetry energies and saturation density of nuclear matter.

It is assumed that the reaction matrix, and therefore the effective interaction, is unaffected by a local spin polarization. This assumption is supported by a consideration of the relative weights of s- and d-waves in the intermediate steps of the virtual scattering of two nucleons starting in the ³S channel. The transition to an intermediate d-state shifts the direction of the total intrinsic spin. Taking into account the quantal fluctuations, and using the values for the respective defect integrals given by Siemens³, one finds that the average effect of the spin polarization felt by the two interacting nucleons is practically zero. Under the assumption that the effective interaction is independent of the local spin polarization, we get the results for the isoscalar and isovector spin symmetry energies shown in the table. For comparison are shown also the corresponding numbers derived from the phenomenological spin-spin force of Bauer *et al.*⁴

Spin symmetry energy (MeV)
isoscalar isovector

	isoscalar	isovector
Present work	24.4	35.1
Bauer <i>et al.</i>	31.4	36.2

For a given type of particles, the spin density in rotating nuclear matter is roughly proportional to the Fermi momentum. Due to the non-central spin-orbit and tensor forces, the spin polarization is anisotropically distributed on the Fermi sphere. The figure shows the distribution calculated in the case of normal density and equal numbers of neutrons and protons.

The spin polarization is induced by the spin part of the Coriolis field, $-\omega \cdot s$, and the spin-orbit interaction between the single particle spin and the local curl of the momentum density. The last-named contribution is roughly proportional to the density. The restoring force is composed of the usual Fermi gas term modified by the factor M/M^* , which equals 0.7^{-1} for our effective

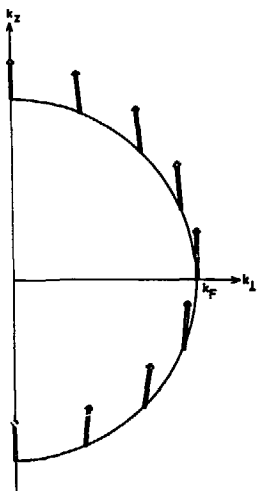


Figure. The arrows indicate the relative magnitude and direction of the spin polarization for different directions of the Fermi momentum. The z-axis is parallel to the axis of rotation.

interaction, and a term arising from the spin-spin forces. At normal density, the enhancements of both the driving and the restoring force amount to about a factor 2 with the net result that the spin density is given very closely by the Fermi gas estimate. This corresponds to a spin ("Pauli") contribution to the moment of inertia of finite nuclei equal to $3A/8\epsilon_F$, or $0.8A^{-2/3}$ times the rigid sphere value.

The "Landau" contribution⁵, which for the non-interacting nucleonic gas equals $-A/2\epsilon_F$, is modified by the factor $M^*/M = 0.7$. Thus, due to the interactions, we get a practically exact cancellation between the "Pauli" and the "Landau" term. This entails that, apart of shell effects, the nuclear moment of inertia is given, with a very high accuracy, as that of a rigid body with the same distribution of masses.

⁺Work partly supported by the BMFT and GSI Darmstadt

1. D.W.L.Sprung and P.K.Banerjee, Nucl. Phys. A168, 273 (1971)
2. D.W.L.Sprung, Nucl. Phys. A182, 97 (1972)
3. P.J.Siemens, Nucl. Phys. A141, 225 (1970)
4. R.Bauer et al. Nucl. Phys. A209, 535 (1973)
5. J.Dabrowski, Phys. Lett. 59B, 132 (1975)

A SEMI-CLASSICAL MODEL FOR HEAVY ION POTENTIALS AT HIGH SPIN

B. Grammaticos, T. Sami

Laboratoire de Physique Théorique, C.R.N. Strasbourg, France

In a recent work ¹ we have presented an application of the Thomas-Fermi approximation to rotating nuclei. It was actually shown that under the effect of the rotation the Fermi sea preserves its sphericity although its center is shifted by a quantity proportional to the rotational frequency. In a subsequent work ² we have developed systematic quantal corrections for the lowest order Thomas-Fermi. However these smooth quantal corrections, surface peaked,

do not contribute appreciably to the moment of inertia of the nucleus.

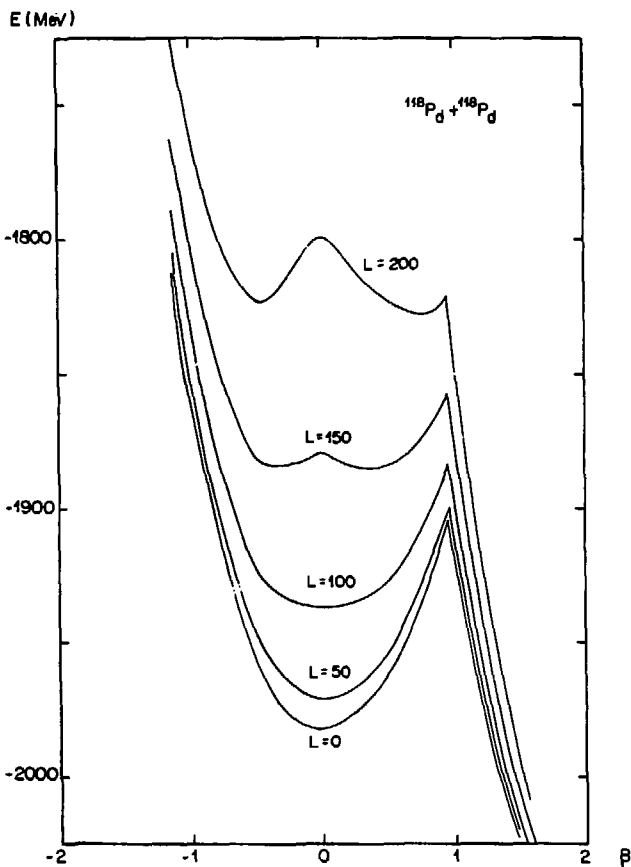
Once the calculation of the kinetic energy is performed the potential energy is obtained by means of a simple functional depending only on the density ρ of the nucleus and its derivatives. We have thus :

$$E = \int d^3r \left(\frac{\hbar^2}{2m} \tau + a\rho^2 + b\rho^{7/3} + c \frac{(\nabla\rho)^2}{\rho} \right) + E_{\text{coul}} \quad (1)$$

where

$$\tau = \frac{3}{5} \left(\frac{3\pi^2}{2} \right)^{2/3} \rho^{5/3} + \frac{m^2}{\hbar^2} (\vec{\omega} \times \vec{r})^2 \rho \quad (2)$$

as given by the Thomas-Fermi approximation and where $\frac{m^2}{\hbar^2} (\vec{\omega} \times \vec{r})^2 \rho$ is the rotational energy. The analogy with the liquid droplet ³ approach can be explicitated once one performs the leptodermous expansion ⁴ in(1). In ref. (1) this model has been used for the investigation of shape transition of nuclei at high spins. In this contribution we wish to report a recent application of the model to the computation of heavy-ion potentials. This is done in the framework of the two-sphere model ^{5,6}. In the figure such a potential is shown for the system of ¹¹⁸Pd + ¹¹⁸Pd (which leads to ²³⁶U for a compound system). The calculation of heavy-ion potentials for asymmetric systems is equally feasible.



Collective potential $E(\beta)$ for $^{118}\text{Pd} - ^{118}\text{Pd}$ for various values of angular momentum L .

References.

1. B. Grammaticos, Phys. Rev. C17 (1978) 1244.
2. B. Grammaticos, A. Voros, Ann. of Phys. 123 (1979) 359.
3. S. Cohen, F. Plasil and W.J. Swiatecki, Ann. of Phys. 82 (1974) 557.
4. W.D. Myers, Nucl. Phys. A204 (1973) 465.
5. M. Gaudin, Journ. de Phys. 35 (1979) 885.
6. B. Grammaticos, Phys. Lett. 44B (1973) 343.

g-FACTOR OF THE FIRST EXCITED 4^+ STATE IN BACKBENDING ^{20}Ne

K.H. Speidel, G.J. Kumbartzki, W. Knauer, V. Mertens, P.N. Tandon⁺,
 N. Ayres de Campos⁺⁺
 Institut für Strahlen- und Kernphysik, Uni. Bonn, W. Germany.
 J. Gerber
 Centre de Recherches Nucléaires, Strasbourg, France
 M.B. Goldberg
 Weizmann Institute of Science, Rehovot, Israel.

The backbending behaviour is not unique to heavy nuclei. Indeed $^{20,22}\text{Ne}$ not only exhibit a clear rotational band structure but also show strong backbending at relatively low angular momentum ¹. In many cases measurement of magnetic moments of states in the backbending region can distinguish between the roles of neutrons and protons in this process. We report here the measurement of the g-factor of the first excited 4^+ state in ^{20}Ne which is two units of angular momentum lower than the backbending state. The large transient magnetic field experienced by Ne nuclei recoiling at 0.057c through polarized iron has been utilized². The field was calibrated with the known g-factor of the 2^+ state.

The 2^+ ($\tau = 1.05$ ps) and the 4^+ ($\tau = 93$ fs) states in ^{20}Ne were populated in the reaction $^{12}\text{C}(^{12}\text{C}, \alpha)^{20}\text{Ne}$. Targets consisted of 200 $\mu\text{g}/\text{cm}^2$ thick layers of carbon deposited on discharge cleaned 2 μm thick iron foils which were magnetized in an external magnetic field of 0.015 T. The perturbed angular correlation technique was used to measure the spin precession ². In view of the large difference in the lifetime of the 2^+ and the 4^+ states, and hence the uncertainties involved in the velocity dependence of the transient field, the precession of the 2^+ state was restricted to 150 fs which was provided by populating this state directly and also by observing it via the 4^+ state. The precessions, corrected for decay and feeding, are summarized in the table below. With the known value of $g(2^+) = + 0.54$ (4)³,

we obtain : $g(4^+) = - 0.10$ (19).

TABLE

STATE	Φ mrad
Direct 2^+	$3.70 \pm 1.29^+$
2^+ via 4^+	$4.95 \pm 1.54^{+,++}$
4^+	-0.55 ± 1.04

} 4.22 ± 0.98

+ corresponding to the transit time of 150 fs

++ corrected for the 4^+ precession.

In the shell model basis, Arima et al ⁴ have explained most of the properties of the ground state band in ^{20}Ne . However, their prediction for the 4^+ state $g(4^+) = + 0.5$ is in contradiction to the present result. The fact that the g-factor of the 4^+ state is very much reduced compared to the 2^+ state is surprising for a $T = 0$ state in a self conjugate nucleus. This strong reduction however, can be understood if rotationally aligned $d_{5/2}$ neutrons contribute to the g-factor.

1. E.M. Szanto, A. Szanto de Toledo, H.V. Klapdor, M. Diebel, J. Fleckner and U. Mosel, Phys. Rev. Lett. 42, 622 (1979).

2. G.J. Kumbartzki, K. Hagemeyer, W. Knauer, G. Krösing, R. Kuhnen, V. Mertens, K.H. Speidel, J. Gerber and W. Nagel, *Hyp. Int.* 7, 253 (1979).
3. R.E. Horstman, J.L. Eberhard, H.A. Doubt, C.M.E. Otten and G. Van Middelkoop, *Nucl. Phys.* A248, 291 (1975).
4. A. Arima, M. Sakakura and T. Sebe, *Nucl. Phys.* A170, 273 (1971).
5. A. Bohr, B.R. Mottelson, *Nuclear Structure*, Vol. II (W.A. Benjamin, 1975).

+ On leave from Tata Institute, Bombay, India.

++ On leave from Coimbra University, Portugal.

HIGH SPIN STATES OF ^{34}Cl

C.J. van der Poel

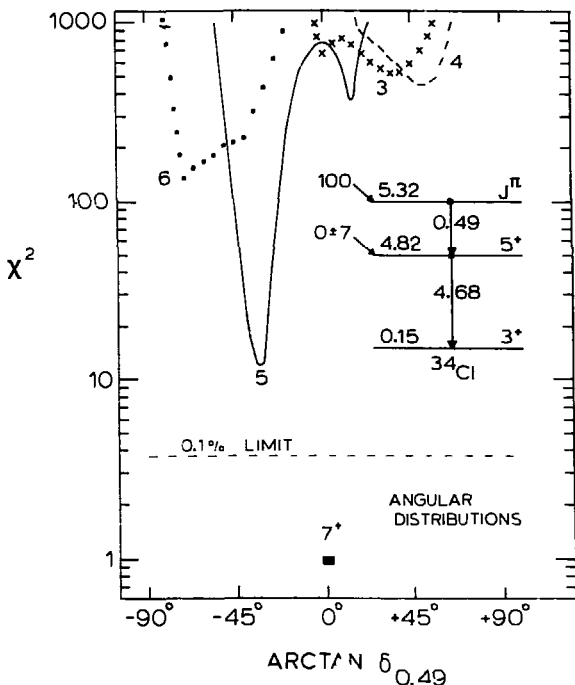
Fysisch Laboratorium, Rijksuniversiteit, Utrecht, The Netherlands

High-spin states of ^{34}Cl have been studied with the $^{24}\text{Mg}(^{12}\text{C},\text{pn}\gamma)^{34}\text{Cl}$ reaction at $E(^{12}\text{C}) = 35$ MeV and with the $^{31}\text{P}(\alpha,\text{n}\gamma)^{34}\text{Cl}$ reaction at α -energies between 11.7 and 16.3 MeV. Gamma-gamma coincidences and γ -ray angular distributions are measured in the $^{24}\text{Mg} + ^{12}\text{C}$ reaction with a Compton suppression spectrometer.

Generally, a γ - γ coincidence measurement is not sufficient to give the relative order of the γ -rays in the decay scheme. Therefore, the $^{31}\text{P}(\alpha,\text{n}\gamma)^{34}\text{Cl}$ reaction ($Q = -5.65$ MeV) was used at various α -energies to obtain approximate excitation energies of the levels of interest from threshold measurements. In combination with accurate E_γ -values, these measurements result in a firmly established level scheme and accurate excitation energies. Results obtained involve levels at excitation energies of $E_x = 4743.2 \pm 0.2$, 4824.2 ± 0.3 , 5315.0 ± 0.3 , 7250.1 ± 0.6 and 7802.4 ± 1.0 keV. The latter two (not observed previously) exclusively decay to the $J^\pi = 7^+$ level at 5.32 MeV.

The (α, n) reaction is also used to eliminate unwanted γ -ray feeding in the lifetime measurements. Lifetimes are obtained of 450 ± 200 , 200 ± 70 and 100 ± 70 fs for the levels at $E_x = 4.82$, 7.25 and 7.80 MeV, respectively.

The absence of side feeding to the 4.82 MeV level in the $^{24}\text{Mg} + ^{12}\text{C}$ reaction at $E(^{12}\text{C}) =$



35 MeV makes it possible to obtain the J^π values of the lowest three states listed above from angular distributions alone. With the alignment parameters as free parameters a χ^2 -search results in unambiguous J^π assignments of 6^- , 5^+ and 7^+ for the levels at 4.74, 4.82 and 5.32 MeV, respectively (see figure for the 5.32 MeV level). These assignments agree with the work of ref.¹. Angular correlations will be measured to obtain information on the J values of the new levels at $E_x = 7.25$ and $E_x = 7.80$ MeV which are speculated to have $J^\pi = 9^+$.

DECAY MODES OF HIGH SPIN STATES IN LIGHT NUCLEI

P.A. Butler, R. Daniel, A.D. Irving, P.J. Nolan, J.F. Sharpey-Schafer
University of Liverpool, Liverpool L69 3BX, United Kingdom

In this experiment the decay properties of high spin states in nuclei near $A = 40$, populated by the reaction $^{28}\text{Si} + ^{16}\text{O}$, were studied using a Si ΔE -E telescope to detect charged particles emitted in the reaction. The emitted particles passed through a thin (250 μm) ΔE detector, positioned at 0° to the beam direction, and were then stopped in a thicker (5 mm) detector placed ~ 1 cm behind the ΔE counter. The angle subtended by the telescope at the target was $\sim 25^\circ$. The high geometry of this system ensured that the probability of detecting two charged particles simultaneously in the forward direction was $\sim 10\%$ of the detection probability for one of the particles. Analysis of the energy deposited in each detector enabled the $2p$ channel in this reaction, leading to ^{42}Ca , to be clearly distinguished from the αp channel, leading to ^{39}K . In both cases the total kinetic energy removed by the evaporated particles could be measured.

By demanding coincidences between the particle telescope and a Ge(Li) detector, also placed at 0° , the Doppler broadening of the γ -ray line shapes in the Ge(Li) spectrum was reduced because of the restriction of the range of linear momentum of the residual nuclei. In this way, it was possible to observe fast ($\tau < 1$ ps) γ -ray transitions from high spin states in these nuclei not previously observed in heavy-ion reactions.

At the same time the variation of angular momentum left in the nucleus by particle emission with the total energy removed by the particles was studied. Preliminary measurements for ^{42}Ca indicate that the γ -ray de-excitation pattern via the yrast states observed in this nucleus¹ does not change with total two proton energy. This behaviour is consistent with the constancy observed for the γ -ray multiplicity as a function of $2p$ energy, which was measured at the same time using a 3" x 3" NaI detector. The data suggests that for states of high angular momentum ($J > 10$) α -particle emission is the dominant mode of decay.

1. Eggenhuisen et al Nucl.Phys. A305, 245-261 (1978).

HIGH SPIN STATES IN ^{40}K , ^{42}Ca , ^{55}Fe AND ^{56}Fe

P. Kofahl, H. Fromm, H.V. Klapdor, T. Oda
 Max-Planck-Institut für Kernphysik, Heidelberg, W. Germany

In extension of our recent work on high spin states in $^{34,37}\text{Cl}$ ¹⁾ we have investigated high spin states in ^{40}K , ^{42}Ca , ^{55}Fe , ^{56}Fe by the reactions $^{27}\text{Al}(^{19}\text{F}, \text{xyzy})$ and $^{46}\text{Ti}/^{13}\text{C}(\text{xyzy})$ at the Heidelberg MP-Tandem. Using an Anticompton spectrometer device ²⁾ $\gamma\gamma$ -coincidences and angular distributions have been measured at $E_{\text{lab}} = 72$ MeV and 49-55 MeV, respectively. An excitation function has been measured for the reaction $^{27}\text{Al}(^{19}\text{F}, \text{xyzy})$ between $E_{\text{lab}}=50$ and 110 MeV. The bombarding energies, at which the coincidence measurements have been performed, were expected, on the basis of CASCADE calculations, to give the highest selectivity for the excitation of high spin states (see, e.g. ref. 3).

For the level scheme of ^{40}K a new state (in addition to the work of ref. 4) has been found at $E^* = 7.48$ MeV ($J=9$) (fig. 1). Spin $J=8$ has been assigned to the $E^* = 6.23$ MeV state. In ^{42}Ca up to the $J=9^-$ state at $E^* = 6.55$ MeV the results of recent investigations ^{5,6)} have been confirmed. New states have been found at $E^* = 8.52$ MeV ($J=10$) and 8.68 MeV ($J=10$) (fig. 3). To the states at $E^* = 7.37$ and 7.75 MeV we assign $J^\pi=10^-$ and 11^- , respectively. The coincidence spectra show that the $E_\gamma = 929$ keV transition has to be placed upon the 11^- state. In $^{55,56}\text{Fe}$ up to now two new states at $E^* = 7.60$ MeV (decaying to the 6.52 MeV ($J=21/2$) state) and $E^* = 7.08$ MeV (decaying to the 6.11 MeV state), respectively, have been identified.

The restriction of the possible spin values according to the ΔJ determined from the angular distributions was possible on the basis of the excitation function measurements like shown in fig. 2. With increasing bombarding energy the feeding of the states "inside" of the yrast line decreases when the primary population in the E^*-J plane shifts to much higher spins while at the same time the γ -flux through the yrast states increases relative to low-lying yrast transitions. This occurs in our case of ^{42}Ca , ^{40}K at bombarding energies $E_{\text{lab}} \geq 80$ MeV. The angular distributions give $\Delta J=1$ for all observed transitions above $E^* = 6.55$ MeV in ^{42}Ca and $E^* = 4.88$ MeV in ^{40}K . The above argument about the excitation func-

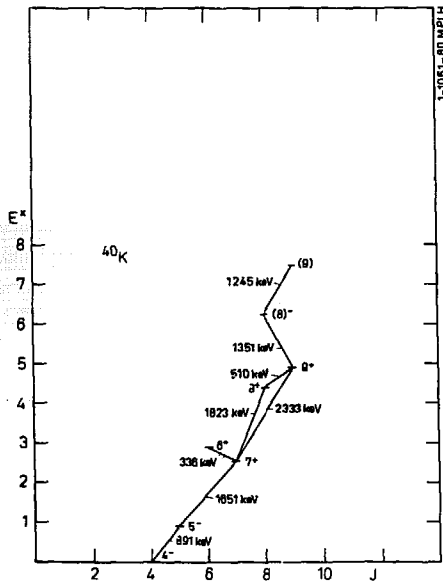
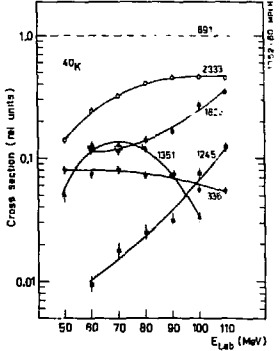


Fig. 1: Level scheme of ^{40}K .

Fig. 2: Excitation functions of ^{40}K normalized to the $E_\gamma=891$ keV transition.



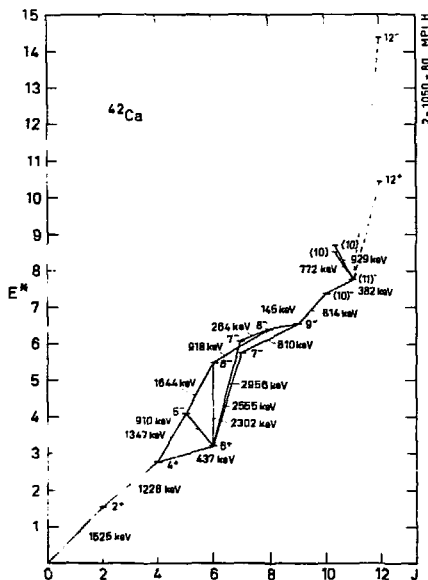


Fig. 3: Level scheme of ^{42}Ca . The dashed lines show predictions of weak-coupling calculations.

from Sherr et al. ⁷⁾ Multiplets from one nucleon excitation generating spins less than 9 are dropped. The lowest $J^\pi=12^-$ state in this configuration is expected at $E^* \approx 14.4$ MeV. Three nucleon excitations are lying about 3 MeV higher than the corresponding one nucleon excitations. The lowest-lying $J^\pi=12^+$ state which is produced by the $(\pi d_{3/2}^{-2})0^+ \otimes {}^4\text{Ti}(12^+)$ configuration is expected at $E^* \approx 10.4$ MeV. However, the matrix element for an E1 transition to the 11^- state vanishes. Fig. 2 shows that the $J^\pi=9^+$ yrast state in ^{40}K at $E_{\text{lab}} = 100$ MeV is fed by more than 90% from unobserved high spin states.

1. P. Baumann, A.M. Berdolt, G. Bergdolt, A. Huck, G. Klotz, G. Walter, H.V. Klapdor, H. Fromm and H. Wilmes, PR C18, 247 and 2110 (1978).
2. P. Kofahl, H.V. Klapdor, Annual Report MPI Heidelberg, p. 24 (1978).
3. H.V. Klapdor, Lecture Notes in Physics 92 125 (1979).
4. H.H. Eggenhuisen, L.P. Ekström, G.A.P. Engelbertink, H.J.M. Aarts and J.A.J. Hermans, Nucl.Phys. A285 167 (1977).
5. H.H. Eggenhuisen, L.P. Ekström, G.A.P. Engelbertink and H.J.M. Aarts, Nucl. Phys. A305 245 (1978).
6. E.K. Warburton, J.J. Kolata and J.W. Olneso, Phys.Rev. C11 700 (1975).
7. R. Sherr, R. Konzes and R. del Vecchio, Phys.Lett. 52B 401 (1974).

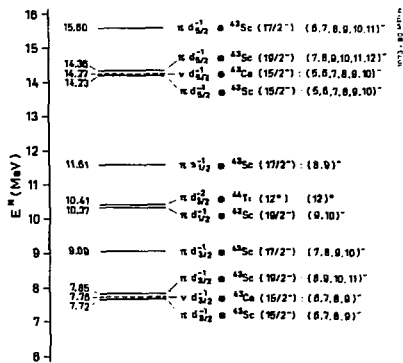


Fig. 4: Level scheme of ^{42}Ca expected from weak-coupling calculations.

tions leads to the spin values given in figs. 1,3.

STRUCTURE ABOVE AND FEEDING OF THE YRAST LINE IN ^{48}Ti *

F. Glatz, P. Betz, J. Siefert and H. Röpke
Fakultät für Physik der Universität Freiburg, Freiburg/Brsg., West-Germany

The yrast states of ^{48}Ti arise, up to $I^\pi = 12^+$, from the $(f_{7/2})^8$ configuration. The complete level scheme from this configuration has been calculated in ref. 1. We have recently observed and investigated² the majority of the predicted levels by p- γ coincidence measurements in the $^{45}\text{Sc}(\alpha, p\gamma)$ reaction. It became evident that in addition to the $(f_{7/2})^8$ configuration the $(f_{7/2})^7 p_{3/2}$ configuration is playing a role in the structure of high-spin states. Two levels at 7427 and 8323 keV were interpreted as the lowest $I^\pi = 9^+$ and 10^+ levels, respectively, of this configuration.

In the present work a search for further $(f_{7/2})^7 p_{3/2}$ levels was performed with the $^{45}\text{Sc}(\alpha, p\gamma)$ reaction at $E_\alpha = 14$ MeV. Good resolution in the proton and γ -ray spectra allowed the identification of high-spin ($I \geq 7$) states on the basis of their γ -decay modes up to $E_\gamma = 11$ MeV. A sample of 36 such levels was observed while the $(f_{7/2})^8$ configuration provides only 19. Thus the presence of the $(f_{7/2})^7 p_{3/2}$ configuration is definitely established without the need for rigorous spin-assignments. The experiment yielded in addition unambiguous candidates for the lowest $I^\pi = 11^+$, 12^+ and 13^+ levels of the configuration. These levels, which are displayed in fig. 1, are connected with the 7427 keV and 8323 keV levels by a cascade of low energy γ -ray transitions which is the basis of their identification. A weak coupling calculation which equalizes the positions of the theoretical and experimental 9^+ states, reproduces (fig. 1) the observed sequence of levels very well.

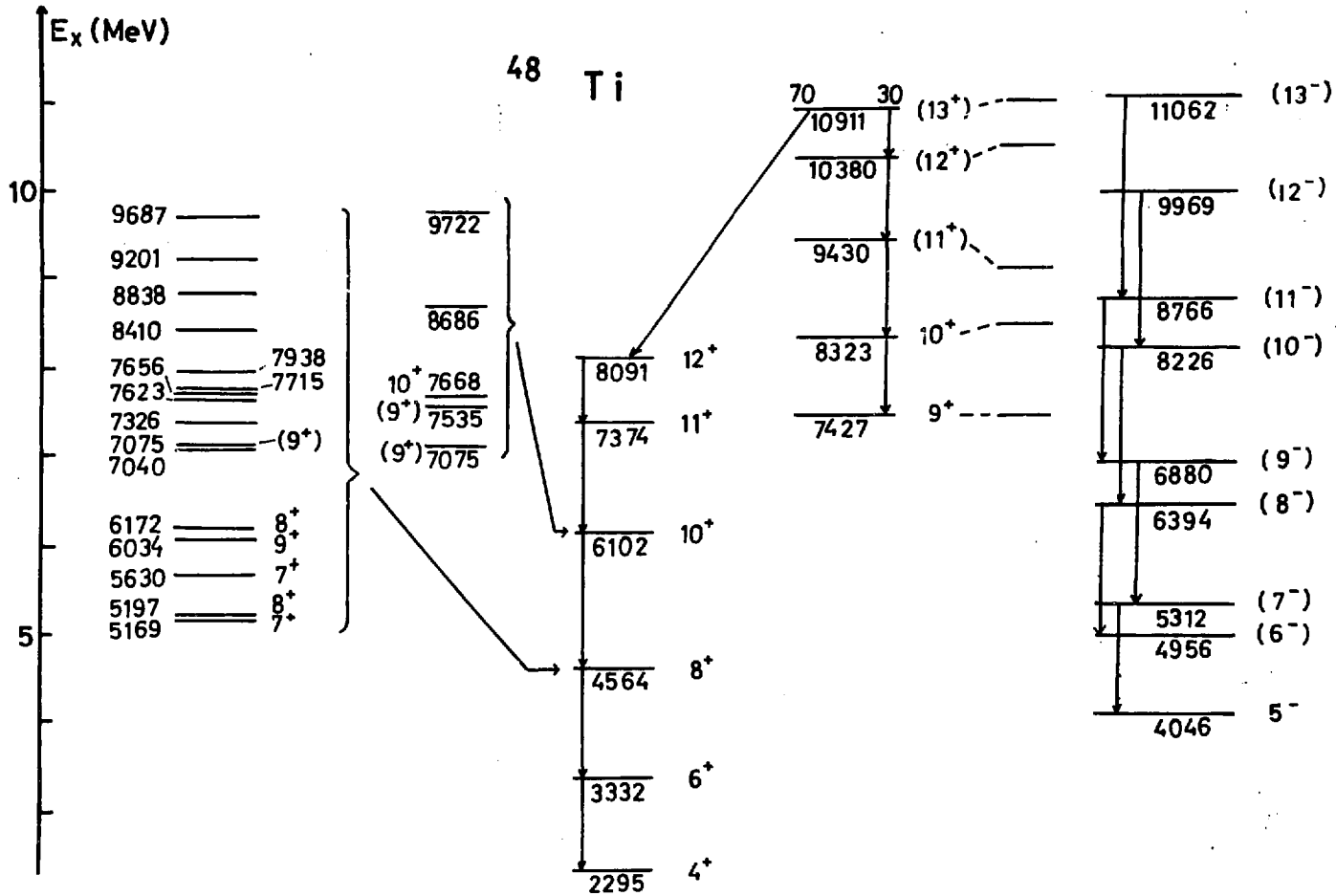
The present work gives insight into the feeding mechanism of yrast states from higher excited states. While the $I^\pi = 8^+$ and 10^+ levels are fed quite frequently, the $I^\pi = 11^+$ and 12^+ levels are fed only once via the 10911 keV level. This explains the failure to observe these levels³ in the $^{44}\text{Ca}(^7\text{Li}, p2n)$ and $^{27}\text{Al}(^{24}\text{Mg}, 3p)$ reactions with γ - γ coincidence techniques.

The present work also yielded new levels which, from their γ -decay, are suspect to have negative parity. It appears that the proposed² $K^\pi = 5^-$ band can be extended (fig. 1) from $I^\pi = 9^-$ towards $I^\pi = 13^-$.

* Work supported by Deutsche Forschungsgemeinschaft

1. W. Kutschera, B.A. Brown, K. Ogawa; Rivista Nuov. Cim. 1 no. 12,1 (1978)
2. F. Glatz et al., Z. Physik A 293, 57 (1978)
3. G. Fortuna et al., Nuovo Cim. 34 A, 321 (1976)

Fig. 1. From left to right: Feeding of the 8^+ yrast state, feeding of the 10^+ yrast state, the $(f_{7/2})^8$ yrast states (0^+ and 2^+ omitted), the lowest $(f_{7/2})^7 p_{3/2}$ states, their predicted energies from weak coupling, the proposed $k^- = 5^-$ band.



MEASUREMENT OF GROUND-STATE SIDE FEEDING BY MEANS OF IN-BEAM
AND RADIOACTIVITY γ -RAY SPECTROMETRY

F. Terrasi*, M.G. Saint-Laurent, A. D'Onofrio*, H. Dumont and J. Delaunay
DPh-N/BE, CEN Saclay, BP 2, 91190 Gif-sur-Yvette, France

In the last few years in-beam γ -ray spectrometry following fusion-evaporation reactions induced by "light-heavy" ions on medium and heavy mass nuclei has been extensively utilized in order to study the spectroscopy of high-spin states.

More recently, it has become evident that the possibility of both atomic and mass number identification of residual nuclei yields a powerful tool for detailed absolute reaction cross section measurements as an aid in the reaction mechanism understanding¹. For this reason an extensive program of absolute residual nuclei cross section measurements in the f-p shell region has been undertaken at the Van de Graaff tandem accelerator in Saclay². By comparing several independent normalization methods, a precision of a few percent has been obtained, at least in the most favourable cases³. It has been realized that the major limitation in this kind of measurements arises from the so-called ground state side feeding (GSSF), i.e. the statistical γ -ray or particle feeding of residual ground states.

An attempt to evaluate the importance of such contribution is currently underway at Saclay : residual cross sections are measured by in-beam detection at 55° of discrete γ -ray transitions feeding ground states. Spectrum accumulation is then switched by the beam stopper insertion to another detector in close geometry and radioactivity measured. Beam intensity instabilities are corrected by numerical integration. The comparison of the two measurements yields directly the GSSF.

Preliminary results concerning ^{62}Zn and ^{63}Zn residual nuclei produced both in $^{52}\text{Cr} + ^{13}\text{C}$ and $^{49}\text{Ti} + ^{16}\text{O}$ reactions and ^{53}Fe produced in $^{28}\text{Si} + ^{28}\text{Si}$ reaction show that extrapolation procedures usually employed to evaluate GSSF in heavier mass investigations may conduct to misleading results in our mass region.

Even if a systematic study is not possible in this region, due to the relatively small percentage of suitable radioactive residual nuclei, we intend to continue this kind of investigation in order to check possible regular behaviours of GSSF versus entrance channel and incident energy for given residual and compound nuclei.

REFERENCE

1. J. Delaunay et al., XVIII Int. Conf. Winter Meeting on Nuclear Physics in Bormio (January 1980).
2. A. D'Onofrio, Thesis, Orsay 1979 and A. D'Onofrio et al., to be published.
3. F. Terrasi et al., to be published.

* On leave of absence from Istituto di Fisica Sperimentale dell'Università,
Via. A. Tari 3, Napoli. Italy.

HIGH SPIN STATES FOR ^{55}Fe VIA HEAVY ION INDUCED FUSION EVAPORATION REACTIONS

M.G. Saint-Laurent, H. Dumont, B. Delaunay and J. Delaunay
 DPh-N/BE, CEN Saclay, BP 2, 91190 Gif-sur-Yvette, France

Nuclei near closed shells can give valuable information on the interaction matrix elements of the residual forces and are sensitive to the configurations involved in the nuclear structure. ^{55}Fe , near the double closed shell nucleus ^{56}Ni , is very interesting from this point of view ; extensive shell model calculations have been performed recently¹ for this nucleus. The authors demonstrated that the shell model is able to reproduce correctly many properties of this nucleus but more information is required - in particular high spin states - to test their predictions.

^{55}Fe has been investigated at the Saclay tandem Van de Graaff by γ spectroscopic methods with an intrinsic Ge detector (for the singles), with an efficiency of $\sim 15\%$ and a one-line resolution ≤ 2 keV at 1.33 MeV. Information on ^{55}Fe were gathered through the different studies :

$^{30}\text{Si}(^{28}\text{Si},2\text{pn})^{55}\text{Fe}$: an excitation function was performed from 67.5 MeV to 82.5 MeV by 2.5 MeV step ;

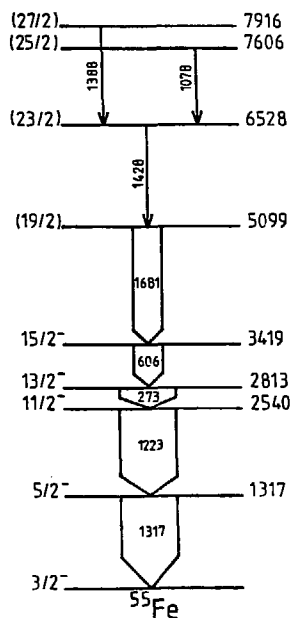
$^{46}\text{Ti}(^{13}\text{C},2\text{p}2\text{n})^{55}\text{Fe}$: at 36, 46, 56 MeV where this channel is dominant in the reaction ;

$^{48}\text{Ti}(^{13}\text{C},\alpha 2\text{n})^{55}\text{Fe}$: a) an excitation function from 25 MeV to 60 MeV by 2.5 MeV step ; b) at 46 MeV γ angular distribution ; c) at the same energy $\gamma\gamma$ coincidences both prompt and delayed were performed with two Ge(Li), 15% efficiency, and ≈ 2 keV resolution at 1.33 MeV ; d) at 46 MeV also, particles- γ coincidences³.

An extensive study of this reaction at this energy² shows that the $\alpha 2\text{n}$ channel represents a large cross section of the order of 250 mb.

From all these data, not yet fully reduced, it is nevertheless possible to build the level scheme shown in Fig. 1 ; we have a good agreement with the level scheme obtained previously by Poletti et al.⁴ with the $^{51}\text{V}(^7\text{Li},3\text{n})^{55}\text{Fe}$ reaction. In addition we obtained two new transitions above the 6.258 MeV level. The preliminary results of the excitation function for the reaction $^{30}\text{Si}(^{28}\text{Si},2\text{pn})^{55}\text{Fe}$ and the γ angular distribution with the reaction $^{48}\text{Ti}(^{13}\text{C},\alpha 2\text{n})^{55}\text{Fe}$ show that the spins of these two new states are rather high. At present, these spin determinations are only tentative ; analysis is in progress to ascertain these spin assignments.

Figure 1 - Partial level scheme of ^{55}Fe . The intensity of the observed γ rays was determined from the $^{28}\text{Si}(^{30}\text{Si},2\text{pn})^{55}\text{Fe}$ reaction at 77.5 MeV ; for the transitions 1428 keV, 1078 keV and 1388 keV, the Doppler effect does not permit to extract their intensity. Notice the important side feeding for the 2.813 MeV level.



REFERENCES

1. R. Vennink and P.W.M. Glaudemans, preprint, to be published.
2. A. D'Onofrio, Thesis Orsay 1979, et al., to be published.
3. H. Dumont et al., Winter meeting Bormio, Italy, January 1980.
4. A.R. Poletti, B.A. Brown, D.B. Fossan, E.K. Warburton, Phys. Rev. C10, 2312 (1974).

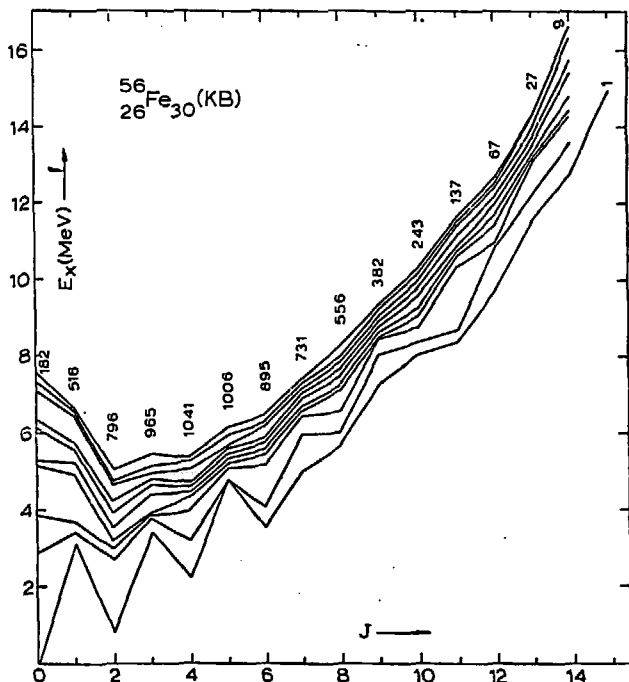
A MICROSCOPIC CLASSIFICATION OF HIGH-SPIN STATES IN ^{56}Fe

P.W.M. Glaudemans

Fysisch Laboratorium, Rijksuniversiteit, Utrecht, The Netherlands

Recent large-scale shell-model calculations on nuclei in the middle of the fp-shell indicate that a microscopic description works very well for most properties of low-lying states. Presently I would like to discuss some remarkable properties of positive-parity high-spin states ($J = 8-15$) in ^{56}Fe which have been obtained with the same interactions (KB and SDI) and model space as used in the reference.

The calculated excitation energies obtained with KB for the ten lowest eigenstates of each J are presented in the figure. The excitation energies obtained with the very different SDI matrix elements show a nearly identical behaviour. It is seen that the yrast and yrast-plus-one states for $J \leq 6$ follow a collective pattern, with the typical oscillatory behaviour. For $J > 6$ the excitation energies increase almost linearly with J . Moving away from the yrast line one finds a smooth behaviour of the excitation energies as a function of J with a



Excitation energies of the lowest ten states with positive parity of each J obtained with the KB interaction for ^{56}Fe . The vertically placed numbers represent the total number of states for each J in the present model space.

dip at about $J=3$ (see figure). The level density as a function of J turns out to be largely independent of the dimensions of the matrices which are also shown in the figure. One should note also that the yrast and yrast-plus-one states are sometimes barely depressed with respect to the other states.

A detailed investigation of the electromagnetic properties of the lowest four states of each J reveals that the states can be divided into two groups (i) those connected by rather large $M1$ and/or $E2$ transition strengths and (ii) states not fed or deexcited by strong transitions. The first group contains nearly all yrast states and many yrast-plus-one states. These states are also interesting since they are described by typical wave functions, which distinguish them clearly from all other states. Although the number of components for each wave function is rather large (in general several hundreds; see figure) the main intensity, i.e. more than 50%, is concentrated in at most ten components. Moreover states in one group all have the same structure.

Except for the $J = 0, 2, 4$ and 6 states of the ground-state band the holes are always coupled to maximum spin J_{hole} which is constant within each group. The particles are coupled to J_{particle} which increases with J . Where possible one has $J = J_{\text{hole}} + J_{\text{particle}}$ in a stretched coupling scheme.

Experimental investigations on ^{56}Fe as a test of the present predictions would be most interesting for a better understanding of the relation between microscopic and collective-type properties.

I would like to thank drs. F. van Hees, B.C. Metsch, R. Vennink and D. Zwarts for their assistance with the calculations.

Reference: R. Vennink and P.W.M. Glaudemans, Z. Physik, to be published.

TWO-NUCLEON HIGH-SPIN STATES IN ODD-ODD COPPER : THE ^{66}Cu CASE

Tsan Ung Chan, J.F. Bruandet, B. Chambon⁺, A. Dauchy, D. Drain⁺, A. Giorni, F. Glasser and C. Morand

Institut des Sciences Nucléaires, 53 Avenue des Martyrs, 38026 - Grenoble Cedex

⁺Institut de Physique Nucléaire, 43 Boulevard du 11 novembre, 69621 Villeurbanne

From the high selectivity of the (α, d) reaction, C.C. Lu et al¹⁾ have located $(\pi g_{9/2} \nu g_{9/2})_{9+}$ state in several isotopes of Cu and Ga. In fact, the $(\pi g_{9/2} \nu g_{9/2})_{9+}$ states are not the only states strongly excited by the (α, d) reaction. Particularly, the $(\pi p_{3/2} \nu g_{9/2})_{6-}$ states are also strongly excited. These high-spin states which correspond to a maximum coupling of two nucleons, are often yrast states so they are sometimes also excited in fusion-evaporation reaction and it is possible to observe their γ decay.

We have proposed²⁾ a very simple calculation (based on the crudest shell model picture) of the excitation energies of two nucleon high-spin states, the two nucleons being coupled to their maximum spin value : the energy of such a two-nucleon state is simply equal to the sum of the two individual single particle energies plus a pairing energy when the two nucleons are identical. Such a simple shell-model description has been satisfactorily applied to many two-nucleon high-spin states in various nuclei. In ^{66}Cu , this model predicts the $(\pi p_{3/2} \nu g_{9/2})_{6-}$ at 1.013 MeV and the $(\pi g_{9/2} \nu g_{9/2})_{9+}$ at 3.544 MeV.

We have performed the $^{64}\text{Ni}(\alpha, d)^{66}\text{Cu}$ reaction at $E_{\alpha} = 50$ MeV. Two peaks are strongly excited ; one is the $(\pi p_{3/2} \nu g_{9/2})_{6-}$ state at 1.154 MeV, known from previous work by (d, p) reaction³⁾ (as expected it is selectively excited), the other one located at 3.7 MeV is probably the $(\pi g_{9/2} \nu g_{9/2})_{9+}$ state (see Fig. 1). Fig. 2 shows the striking correlation between the excitation energies of the 6^{-} and 9^{+} states and the $g_{9/2}$ single particle energies in odd-odd copper.

The $^{64}\text{Ni}(\alpha, d\gamma)$, $^{64}\text{Ni}(\alpha, p\gamma)$ and $^{64}\text{Ni}({}^7\text{Li}, \alpha\gamma)$ reactions have also been performed. The low cross-section of the 9^{+} state prevents us to determine directly the γ decay of the 9^{+} state from $d-\gamma$ coincidences. Delayed $\gamma\gamma$ coincidences show that the following γ lines feed the isomeric 6^{-} state ($\tau = 860$ ns) 1597, 1098, 972, 1377, 584 keV, these γ -rays are also seen in particle - γ coincidence in the $^{64}\text{Ni} + \alpha$ reaction at $E_{\alpha} = 50$ MeV.

1. C.C. Lu et al, Phys. Rev. 186 (1969) 1086.
2. Tsan Ung Chan et al, Phys. Rev. C 19 (1979) 244.
3. W.W. Dachnick et al, Phys. Rev 180 (1969) 1062.

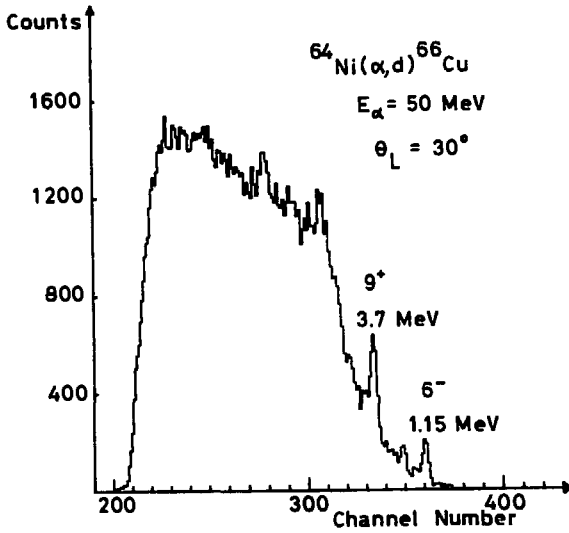


Fig. 1 : Deuteron energy spectrum from the reaction $^{64}\text{Ni}(\alpha, d)$.

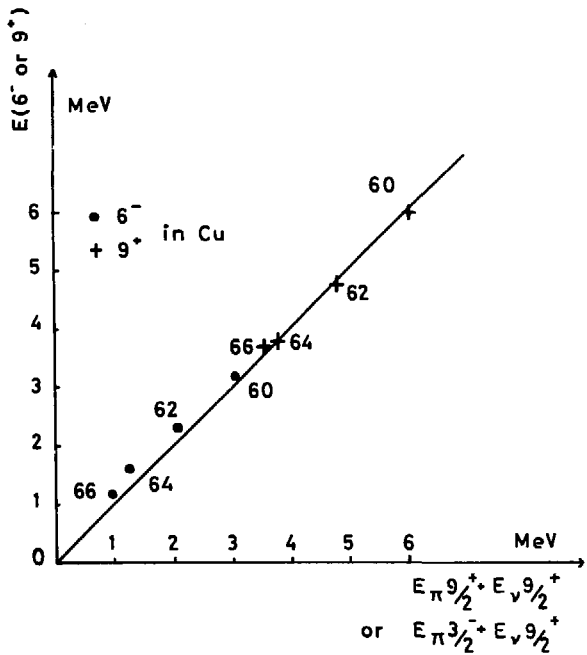


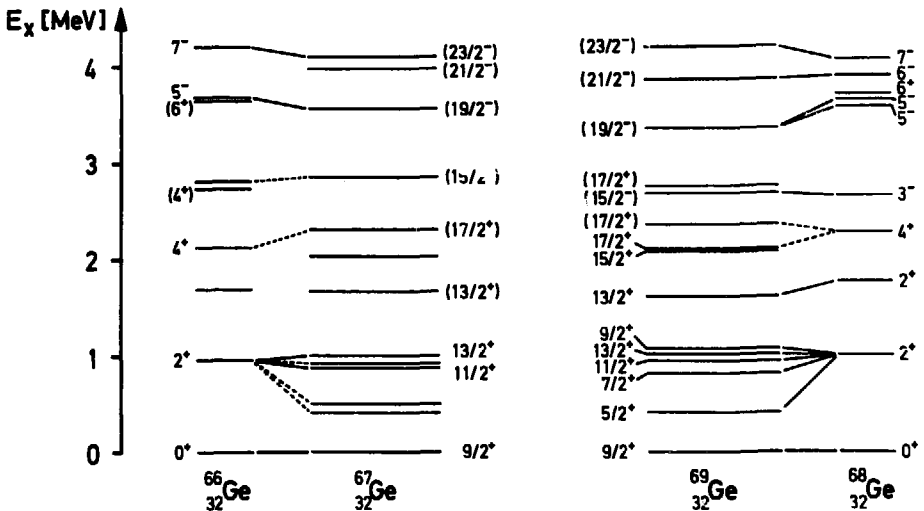
Fig. 2 : Experimental energy of the $J^\pi = 6^-$ and 9^+ states in odd-odd Cu isotopes as a function of the sum of two single particle energies.

γ-RAY SPECTROSCOPIC INVESTIGATIONS ON ^{67}Ge

V. Zobel, L. Cleemann, J. Eberth, T. Heck and W. Neumann
 Institut für Kernphysik, Köln, Germany

By γ -coincidence measurements following the $^{57}\text{Fe} + ^{12}\text{C}$ reaction at $E_{12} = 42$ MeV several new states above 1.5 MeV excitation energy in ^{67}Ge could be established. Spin and parity assignments on the basis of angular distribution, linear polarization and γ -ray yield function indicate very similar structures of $^{67,69}\text{Ge}$.

The significant role of the $1g_{9/2}$ orbital among the degrees of freedom of high spin states in the mass region around $A=70$ as found in all neighbouring nuclei is apparent also in the level scheme of ^{67}Ge . Based on the $9/2^+$ -single particle state at 751.7 keV, a similar structure as in ^{69}Ge is observed as seen in the figure. Recent results of Al-Naser et al.¹⁾ on low energy excitations up to $E_x = 2.8$ MeV carry on the correspondence between both odd Ge-isotopes if the five levels around 1.5 MeV excitation energy were identified with the one phonon multiplet. Our spin and parity assignments to the levels at 1642 and 2421 keV of $11/2^+$ and $13/2^+$, respectively, support this assumption as well as the fact that the other three levels with expected spins of $9/2^+$, $7/2^+$ $5/2^+$ have not been excited in our heavy-ion induced reaction.



Although the energy levels obviously correspond in $^{66,67}\text{Ge}$ and $^{68,69}\text{Ge}$ (see the figure), a simple description in terms of the weak coupling picture is too restrictive when data on transition probabilities are considered²⁾. Recent CVM (Cluster-Vibration-Model) calculations³⁾ for $^{66,70}\text{Ge}$ where a two-proton-cluster was coupled to quadrupole vibrations of the respective even Zn-cores provided good overall agreement in the energy spectra as well as in transition probabilities. Consequently, mixed two-proton-one-neutron cluster in the $2p1f_{5/2}1g_{9/2}$ -orbitals should be used for describing the odd Ge isotopes in this model. The assumption of mixed configurations seems to be necessary since at least the $23/2^-$ state cannot be built of a three particle excitation of identical type because of the Pauli exclusion principle while the strongly retarded $23/2^- \rightarrow 19/2^-$ transition in ^{69}Ge with a transition probability of $B(E2)=0.3$ W.u.²⁾ indicates strong particle admixtures to the configuration of the initial state.

1. A.M. Al-Naser, A.H.Behbehani, P.A.Butler, L.L.Green, A.N. James, C.J.Lister, P.J.Nolan, N.R.F.Rammo, J.F.Sharpey-Schafer, H.M.Sheppard, L.H.Zybert and R.Zybart, J.Phys. G5, 423 (1979)
2. V.Zobel, L.Cleemann, J.Eberth, W.Neumann and N.Wiehl, Phys. Rev. C19, 811 (1979)
3. L.Cleemann, J.Eberth, W.Neumann, N.Wiehl and V.Zobel, Nucl. Phys., in print

A NEUTRON MULTIPLICITY TECHNIQUE FOR STUDYING WEAK REACTION CHANNELS IN IN-BEAM γ -RAY SPECTROSCOPY AND ITS APPLICATION TO ^{74}Kr .

J.Roth, L.Cleemann, J.Eberth, W.Neumann,
University of Köln, Germany[†]

R.B.Piercey, A.V.Ramayya, J.H.Hamilton,
Vanderbilt University, Nashville, USA.

A neutron deficient compound nucleus produced in a heavy ion induced reaction mainly will evaporate charged particles which leads to residual nuclei near the line of stability. Consequently, in the reaction ^{19}F on ^{58}Ni the major cross-section is for the evaporation of three protons (^{74}Se), while the 2pn channel to ^{74}Br and $\text{p}2\text{n}$ to ^{74}Kr are rather weak. At the 9 MV FN Tandem in Köln we studied these weak reaction channels by detecting the γ -rays in coincidence with the evaporated neutrons. The detector was a large liquid scintillator (35 cm diameter, 10 cm thick) divided into 4 independently working segments. The experimental setup is shown in fig. 1. The measurement of 1 to 4 fold n coincidences by a multiplicity logic leads to a good identification of the residual nuclei.

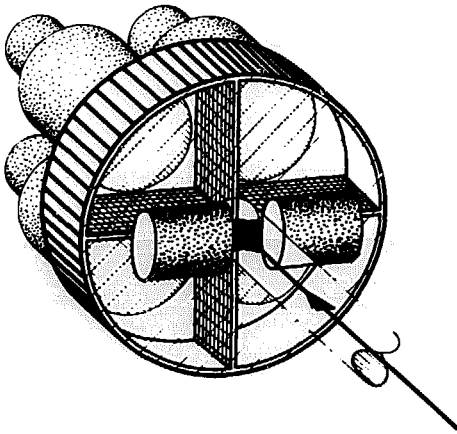


Fig. 1: Experimental setup.

fig. 3. So far, 10 new levels in ^{74}Kr could be identified. The experimental results are in excellent agreement with the predictions

Fig. 2 shows a comparison of γ -singles, $\text{n-}\gamma$ - and $\text{n-n-}\gamma$ -coincidences of the reaction ^{19}F on ^{58}Ni . The ratio of ^{74}Kr to ^{74}Se was enhanced by a factor of >200 in the $\text{n-n-}\gamma$ -coincidence compared to the singles. A previously unassigned γ -ray group is now unambiguously placed in $^{74}\text{Br}^1$ and many unknown transitions in ^{74}Kr could be identified. From $\text{n-}\gamma$ and $\text{n-n-}\gamma$ yield function measured from $E(^{19}\text{F}) = 58$ MeV to 68 MeV and $\text{n-}\gamma$ - γ -coincidences a preliminary level scheme of ^{74}Kr was constructed which is shown in

[†]Supported in part by the German BMFT.

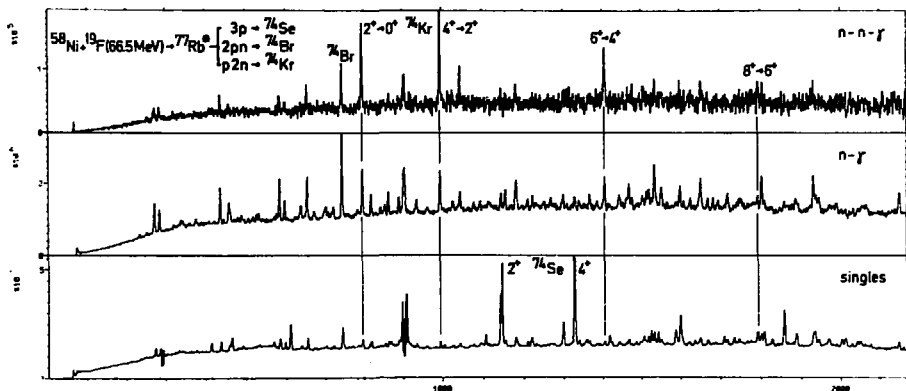


Fig. 2: Comparison of γ -singles, n- γ - and n-n- γ -coincidences of the reaction ^{19}F on ^{58}Ni .

of the Interacting Boson Model (IBM) calculated by Kaup and Gelberg² which supports the interpretation that the lighter Kr-isotopes change their character from an axial symmetric rotator in ^{74}Kr to a triaxial or γ -instable structure in ^{82}Kr .

The first application of the system to ^{74}Kr has shown that the neutron multiplicity technique is an excellent tool to study very neutron deficient nuclei produced by heavy ion induced fusion-evaporation reactions and can complement the β decay investigations with on line separators.

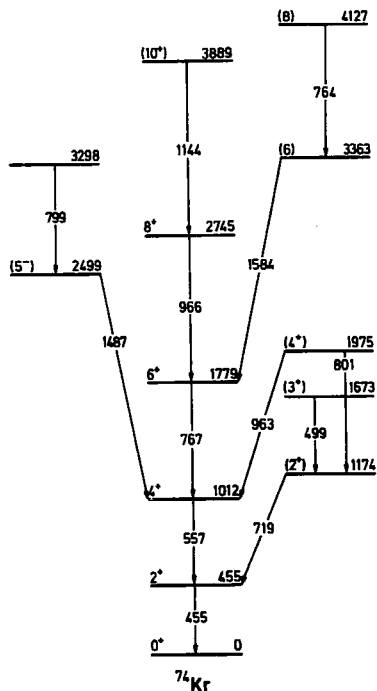


Fig.3: Level scheme of ^{74}Kr .

1. R.B.Piercey et al., Bull. Am. Phys. Soc. 22, 488 (1977)
2. U. Kaup, A.Gelberg, Z. Physik A 293, 311 (1979)

CALCULATION OF CONTINUUM FEEDING TIMES IN HEAVY ION FUSION REACTIONS

H. P. Hellmeister and K. P. Lieb,
II. Physikalisches Institut der Universität Göttingen, 3400 Göttingen, FRG
and Institut für Kernphysik der Universität zu Köln, 5000 Köln 41, FRG

In recent years, a detailed investigation of the "continuum" γ -radiation in heavy ion fusion reactions preceding the population of discrete yrast states has been undertaken. In many cases, the spectral shapes, multipolarities and multiplicity distributions of the continuum γ -rays have been measured, as well as angular and energy correlations. All these available data were found in remarkably good agreement with the assumed statistical nature of the deexcitation process, as has been shown by several authors ¹⁻³.

A further essential parameter of the continuum radiation is the feeding time τ_F , defined as the average delay time between the compound nucleus formation and the population of the discrete state in consideration. In the present work we used a Hauser-Feshbach code to compute the population of the entry states, and a newly developed Monte Carlo program (SPHINX) to calculate the flux and time development of the subsequent γ -deexcitation. Obviously, the feeding time depends mostly on

- (a) the level density (ρ), calculated with the back-shifted Fermi gas formula and a variable moment of inertia:

$$\theta(E) = \theta_0 (1 + a_0 \exp(-bE))$$

- (b) the γ -ray transition strengths in the continuum:

$$\Gamma_{\gamma}(i \rightarrow f) = C_{EL} (E_i - E_f)^{2L+1} \rho_f / \rho_i.$$

Only E1 and E2 transitions have been considered in the calculation. As in ref. 2, "statistical" E2-transitions feeding the yrast region, and "collective" E2-transitions along or parallel to the yrast line have been incorporated.

Fig. 1 shows as an example the calculated distribution of feeding times for some members of the ground state band in ⁷⁸Kr populated in the reaction ⁶⁸Zn(¹²C,2n) at 36 MeV bombarding energy. The parameters $a_0 = 0.716$, $b = 0.168 \text{ MeV}^{-1}$ and $\theta_0 = \theta_{\text{rigid}}$ were fixed as to reproduce the energies of the gsb. The strengths of the continuum E1 transitions (0.5 mWu) and collective E2 transitions (20 Wu) were taken from the compilation of Endt ⁶, whereas the statistical E2 transitions were assumed to proceed with single particle strength. The arrows in Fig. 1 indicate the centers of gravity, i.e. the average feeding times, which as function of the spin are illustrated in Fig. 2. It is noteworthy that these values of $\langle \tau_F \rangle$ are in all cases considerably lower than the measured lifetimes ⁵. The area under each distribution in Fig. 1 is proportional to the side feeding intensity, whereas the dashed line indicates the experimental limit of the feeding time of the highest observable states of the gsb ^{3,5} (feeding time: $\tau_F \leq 0.1 \text{ ps}$).

Further calculations for heavier systems are in progress.

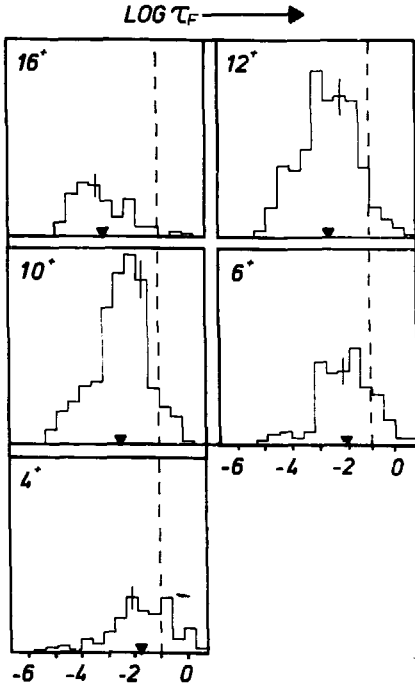


Fig. 1:
Calculated distribution of feeding times for the 4^+ , 6^+ , 10^+ , 12^+ and 16^+ states of the gsb in ^{78}Kr .

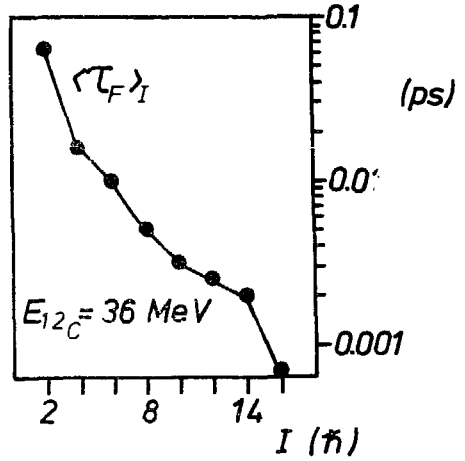


Fig. 2:
Spin dependence of the average feeding time of the reaction $^{68}\text{Zn}(^{12}\text{C},2n)^{78}\text{Kr}$ at 36 MeV beam energy.

1. R. J. Liotta and R. A. Sorensen, Nucl. Phys. A297, 196 (1978)
2. M. Wakai and A. Faessler, Nucl. Phys. A307, 279 (1978)
3. H. P. Hellmeister et al., Nucl. Phys. A307, 519 (1978);
K. P. Lieb, J. J. Kolata, Phys. Rev. D11, 1177 (1975)
4. M. Uhl, Acta Phys. Austr. 31, 245 (1978)
5. H. P. Hellmeister et al., Nucl. Phys. A312, 141 (1979)
6. P. M. Endt, submitted to Atomic and Nuclear Data Tables (1979)

supported by BMFT

DECOUPLED $g_{9/2}$ PROTON BAND IN ^{79}Rb

J. Panqueva, H. P. Hellmeister, F. J. Bergmeister, and K. P. Lieb
 Institut für Kernphysik der Universität zu Köln, 5000 Köln 41, FRG and
 II. Physikalisches Institut der Universität Göttingen, 3400 Göttingen, FRG

Ekström et al.¹ and Liptak and Kristiak² recently assigned $I^\pi = 5/2^+$ to the ground state of ^{79}Rb . Clements et al.³ proposed a decoupled $g_{9/2}$ band extending up to $21/2^+$. By using the Köln FN tandem accelerator, we studied high spin states in ^{79}Rb via the reactions $^{63}\text{Cu}(^{19}\text{F}, p2n)$, $^{65}\text{Cu}(^{16}\text{O}, 2n)$ and $^{66}\text{Zn}(^{16}\text{O}, p2n)$ at 40-58 MeV beam energy. On the basis of $\gamma\gamma$ -coincidences, angular distributions and excitation functions we were able to extend the level sequence up to the probable $29/2^+$ state (Fig. 1). However, no conclusive evidence for the presumed 97 keV $9/2^+ \rightarrow 5/2^+$ transition has been obtained, neither in the singles, $\gamma\gamma$ -coincidence nor a pulsed beam experiment. Recoil distance and DSA measurements gave the following lifetimes:

$$\begin{aligned} \tau(13/2^+) &= 12.2(7) \text{ ps} \\ \tau(17/2^+) &= 1.2(2) \text{ ps} \\ \tau(21/2^+) &= 0.5(1) \text{ ps} \quad \text{and} \\ \tau(25/2^+) &= 0.4(2) \text{ ps}. \end{aligned}$$

In Table 1, the transition energies and B(E2) values in ^{79}Rb are compared with the corresponding core transitions in ^{78}Kr ⁴. The experimental ratios

$$R_1 = \frac{B(E2, 13/2 \rightarrow 9/2)}{B(E2, 2 \rightarrow 0)} = 1.62(14); \quad R_2 = \frac{B(E2, 17/2 + 13/2)}{B(E2, 13/2 \rightarrow 9/2)} = 1.30(23)$$

agree well with the predictions $R_1 = 1.5$, $R_2 = 1.23$ of the Coriolis coupling model⁵ with a triaxial core ($\gamma = 25^\circ$). The B(E2) values of the high transitions, however, tend to be lower than predicted by this model. The Interacting Boson Model⁶, on the other hand, relates such lowering of the transition strengths to the cut-off in boson number. Preliminary IBA-1 calculations in the SU(3) and O(6) limits with $N = 8$ are in agreement with the data, as shown in Fig. 2.

Table 1:

Transition energies and B(E2) values in ^{79}Rb and ^{78}Kr .

Transition	^{78}Kr		Transition	^{79}Rb	
	E_γ (keV)	B(E2) ($e^2\text{fm}^4$)		E_γ (keV)	B(E2) ($e^2\text{fm}^4$)
$2^+ \rightarrow 0^+$	455	1309(82)	$13/2^+ \rightarrow 9/2^+$	501	2120(120)
$4^+ \rightarrow 2^+$	665	1760(160)	$17/2^+ \rightarrow 13/2^+$	756	2760(460)
$6^+ \rightarrow 4^+$	859	1950^{+390}_{-280}	$21/2^+ \rightarrow 17/2^+$	962	1970^{+490}_{-330}
$8^+ \rightarrow 6^+$	1016	1690^{+250}_{-200}	$25/2^+ \rightarrow 21/2^+$	1142	1042^{+1040}_{-350}
$10^+ \rightarrow 8^+$	1112	>960	$29/2^+ \rightarrow 25/2^+$	1316	---

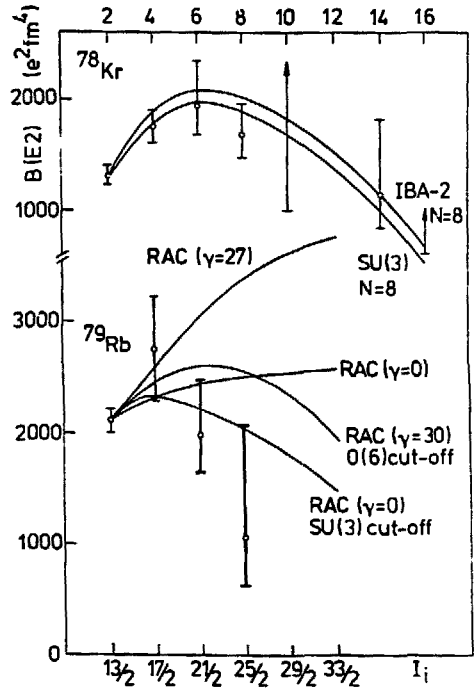
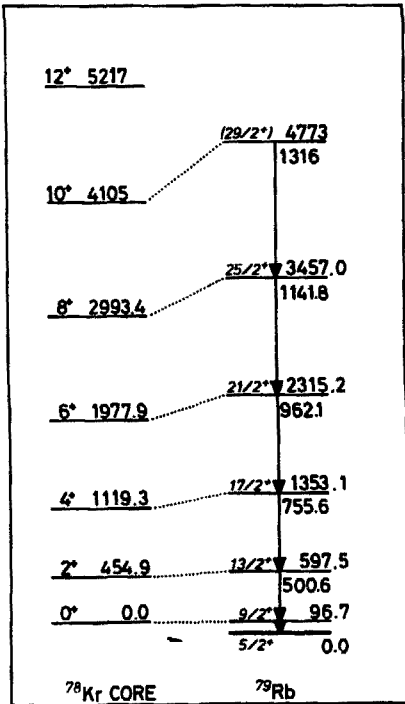


Fig. 1:
Level sequence of the $g_{9/2}$ decoupled band in ^{79}Rb

Fig. 2:
Experimental $B(E2)$ values and model predictions (see text)

1. C. Ekström et al., Nucl. Phys. A 311, 269 (1978)
2. J. Liptak and J. Kristiak, Nucl. Phys. A 311, 421 (1978)
3. J. S. Clements et al., Phys. Rev. C20, 164 (1979)
4. H. P. Hellmeister et al., Nucl. Phys. A332, 241 (1979)
5. H. Toki and A. Faessler, Phys. Lett. 63B, 121 (1976)
6. A. Arima and F. Iachello, Ann. of Phys. 111, 201 (1978)

supported by BMFT

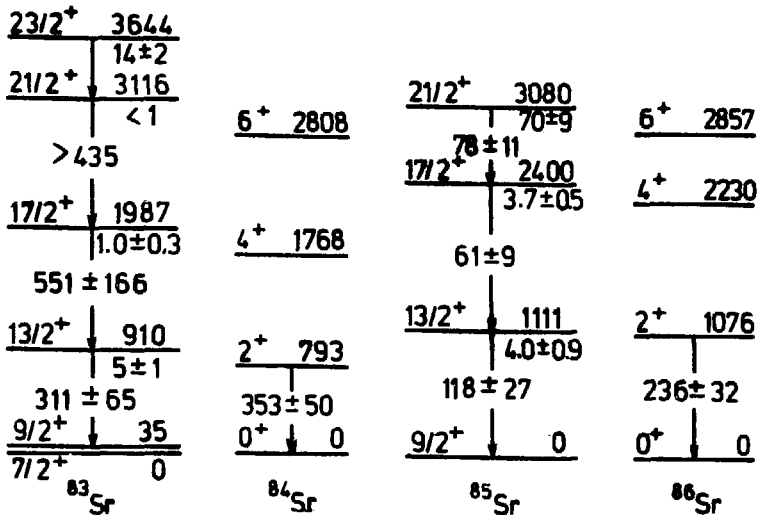
LIFETIME MEASUREMENTS FOR HIGH-SPIN STATES IN $^{63,85}\text{Sr}$

D.Bucurescu, G.Constantinescu, M.Ivaşcu, N.V.Zamfir
and M.Avrigeanu

Central Institute of Physics, P.O.Box MG-6, Bucharest
Romania

The neutron deficient Sr isotopes studied so far are transitional nuclei, their collectivity increasing with decreasing N^1 . Very little is known about how this evolution towards stable (?) deformation manifests itself in the structure of the odd isotopes, e.g., in the interplay between the single particle and the collective aspects. Electromagnetic transition probabilities would bring valuable information in this respect.

We report here lifetime measurements for several positive parity high-spin yrast states in ^{83}Sr and ^{85}Sr , with the recoil-distance method. The reactions used were $^{74,76}\text{Ge} (^{12}\text{C}, 3n\gamma)$ at 43 and 40 MeV, respectively, performed at the Bucharest FN tandem accelerator. Results for the lifetimes of the states forming the main gamma ray cascades populated in the two nuclei are shown in the figure.



The partial decay schemes and the spin-parity values are from refs.²⁻⁴. The measured lifetimes are given (in ps) under each level, and the E2 transitions are labelled with their B values (in $e^2\text{fm}^4$). The first yrast levels and the $B(E2, 2^+ \rightarrow 0^+)$ values (from N.D.S.) in $^{84,86}\text{Sr}$ are also shown for comparison. The values (not shown) for the $23/2^+ \rightarrow 21/2^+$ transition in ^{83}Sr are $B(M1) = 0.027(4)$ n.m.² and $B(E2) = 27(16) e^2\text{fm}^4$.

The $B(E2)$ values in ^{85}Sr are rather little enhanced (3 to 5 W.u), indicating a reduced contribution of collective degrees of freedom. The $13/2^+ \rightarrow 9/2^+$ transition is slower than the $2^+ \rightarrow 0^+$ transition in ^{86}Sr . It is also a factor of 7 slower than the prediction of three-hole cluster-vibration coupling model calculations⁵.

The $B(E2)$ values in ^{83}Sr are more enhanced and suggest that the band $21/2^+ - 17/2^+ - 13/2^+$ results from the coupling of the $g_{9/2}$ neutron hole to the almost collective 6^+ , 4^+ and 2^+ states of the ^{34}Sr core. Preliminary results of calculations based on coupling a $g_{9/2}$ orbital to an asymmetric rotor with VMI (the model of ref. 6) account reasonably well for the positive parity high spin levels in ^{83}Sr observed so far³, as well as for the $B(E2)$ values given in the above figure.

References

1. E.Kolte et al., Z.Physik 268, 267 (1974)
2. E.Arnell et al., Nucl.Phys. A280, 72 (1977)
3. E.Arnell, private communication
4. M.Ivaşcu et al., Rev.Roum.Physique, 23, 162 (1978)
5. S.K.Bassu, A.P.Patro, V.Paar, J.Phys. G5, 585 (1979)
6. H.Toki, A.Faessler, Nucl.Phys. A253, 231 (1975)

IN BEAM GAMMA-RAY SPECTROSCOPY OF $^{84}\text{Sr}^+$

A. Dewald, W. Gast, A. Gelberg, H.-W. Schuh, K. O. Zell, P. von Brentano, Institut für Kernphysik der Universität zu Köln, D-5000 Köln, W-Germany

Excited levels in ^{84}Sr were populated in the reaction $^{76}\text{Ge}(^{12}\text{C},4n)$ and $^{81}\text{Br}(^6\text{Li},3n)$. The particle energies were 35-60 MeV for the ^{12}C -beam and 19-32 MeV for the ^6Li -beam, respectively. Singles and coincidence gamma spectra as well as angular distributions were measured. Lifetime measurements by the recoil distance method were carried out using the $^{76}\text{Ge}(^{12}\text{C},4n)^{84}\text{Sr}$ reaction. Lifetimes and $B(E2)$'s are given in Tab. 1.

The level scheme already known ^{1,2,3} was completed by adding 22 new levels and is shown in Fig. 1. The yrast cascade goes along the ground state band (gsb) up to 6^+ . The strong backbending points out to a band crossing. We assume that the isomeric level 8^+ is a quasiparticle $(g_9/2)^{-2}$ state; the low value of $B(E2, 8^+ \rightarrow 6^+)$ of only a few WU favours this assumption. Similar states are known in $^{86,88}\text{Zr}$, ^{86}Sr , ^{84}Kr . The 10^+ state should also belong to the two-quasiparticle band although it is probably strongly mixed. The yrast band undergoes a new crossing and goes along a third positive parity band down to an 8^+ state. If we assume that the band continues over 6^+ and 4^+ down to the already known 2^+ γ -band, we could identify the $2^+ - 14^+$ cascade with the γ -band. We also identified the odd-spin members of the γ -band up to 9^+ .

The negative parity band was extended up to an 11^- state. We also populated in the $^{81}\text{Br}(^6\text{Li},3n)^{84}\text{Sr}$ reaction a 6^- and 8^- state as well as a second 5^- and 7^- state. In order to describe this structure we have to assume the existence of two negative parity bands, possibly one with $K^\pi = 0^-$ and the other with $K^\pi = 1^-$.

The large $B(E2)$ values point out the collective nature of most levels. In order to understand the appearance of a rather large number of positive parity states we have to use a more sophisticated classification than that provided by the β - γ -band scheme.

The structure observed is very similar to that predicted by the Interacting Boson Model ^{4,5}, as a matter of fact it is intermediate between the $O(6)$ and the $SU(5)$ limits of the model.

Table 1:

E (keV)	I_i	I_f	τ (psec)	$B(E2)$ ($e^2\text{fm}^4$)	$B(E2)$ WU
524.0	8^+	6^+	226.0 ± 7.0	92 ± 3	4.2 ± 0.14
718.8	7^-	5^-	6.3 ± 0.7	678 ± 75	31.0 ± 3.4
793.2	2^+	0^+	4.6 ± 0.5	568 ± 62	26.0 ± 2.8
808.3	11^-	9^-	10.8 ± 1.4	220 ± 29	10.1 ± 1.3
854.1	10^+	8^+	2.4 ± 0.2	751 ± 63	34.4 ± 2.9
872.0	8^+	6^+	4.8 ± 0.2	339 ± 14	15.5 ± 0.6
974.5	4^+	2^+	2.5 ± 0.3	373 ± 45	17.1 ± 2.1
1040.1	6^+	4^+	1.5 ± 0.3	449 ± 90	20.5 ± 4.2
1115.7	10^+	8^+	3.2 ± 0.5	148 ± 23	6.8 ± 1.1
1119.0	12^+	10^+	1.2 ± 0.4	389 ± 130	17.8 ± 6.0
1148.1	9^-	7^-	3.6 ± 0.6	114 ± 19	5.2 ± 0.8
1001.3	5^-	4^+	13.7 ± 0.8	-	-

The presence of the isomeric 8^+ state as well as the irregularities of some energy intervals and branching ratios indicate a perturbation of the collective structure, possibly through mixing with two-quasiparticle states.

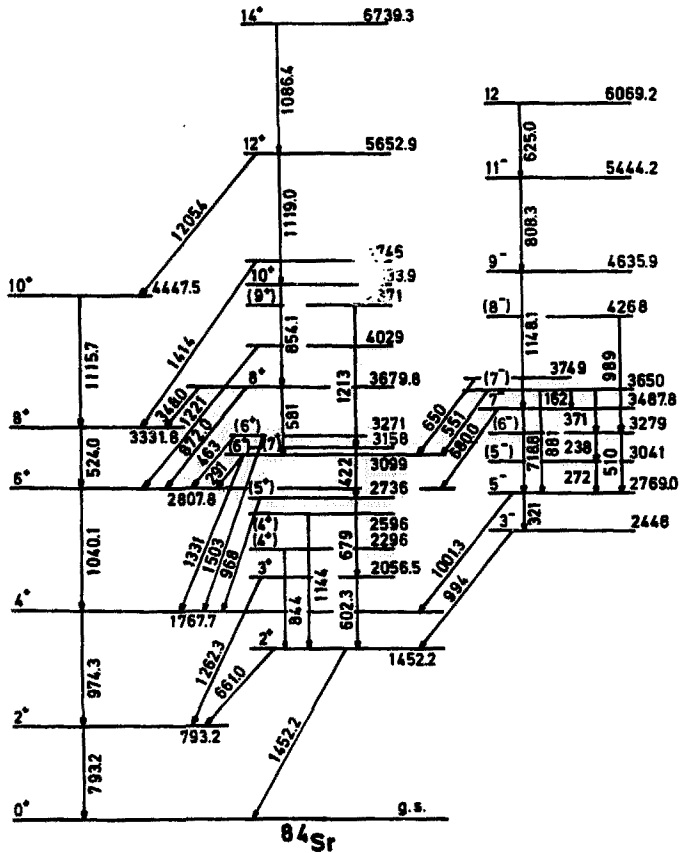


Fig. 1:
Level scheme of ^{84}Sr

1. R. L. Auble, Nucl. Data Sheets B5, 109 (1971)
2. J. B. Ball, J. J. Ponajian, J. S. Larsen, and A. C. Rester, Phys. Rev. C8, 1438 (1973)
3. N. Yoshikawa, Y. Shida, O. Hashimoto, and M. Sakai, Nucl. Phys. A327, 477 (1979)
4. A. Arima, F. Iachello, Annals of Physics, Vol. 99, No. 2, 253 (1976)
5. A. Arima, F. Iachello, Phys. Rev. Lett. Vol. 35, No. 16, 1069 (1975)

+ supported by BMFT

THREE-QUASIPARTICLE STATES OF THE NUCLEI ^{85}Y AND ^{87}Y .

S.E. Arnell⁺, A. Nilsson⁺⁺, Ö Skeppstedt⁺, E. Wallander⁺

⁺ Chalmers University of Technology, Gothenburg, Sweden

⁺⁺ Research Institute of Physics, Stockholm, Sweden

In our current program for investigating neutron-deficient odd nuclei in the $80 < A < 90$ region we have obtained information on ^{85}Y and ^{87}Y . In the spin region ($11/2 \leq J \leq 25/2$) the structure of these nuclei is dominated by the generalized seniority-three states of the configuration $\pi g_{9/2} \nu g_{9/2}^{-4}$ and $\pi g_{9/2} \nu g_{9/2}^{-2}$, respectively, which makes it amenable to relatively simple shell-model calculations.

The two yttrium nucleides were produced by the $^{84,86}\text{Sr}(\alpha, p2n)^{85,87}\text{Y}$ reactions at $E_{\alpha} = 51$ MeV. Identification of the yttrium γ -rays was performed by studying coincidences between the Ge(Li) detector and an annular detector that recorded outgoing charged particles. Almost half of the total reaction yield from the ^{86}Sr target went into the $(\alpha, p2n)$ channel, whereas for the ^{84}Sr target the corresponding figure was above 80 %.

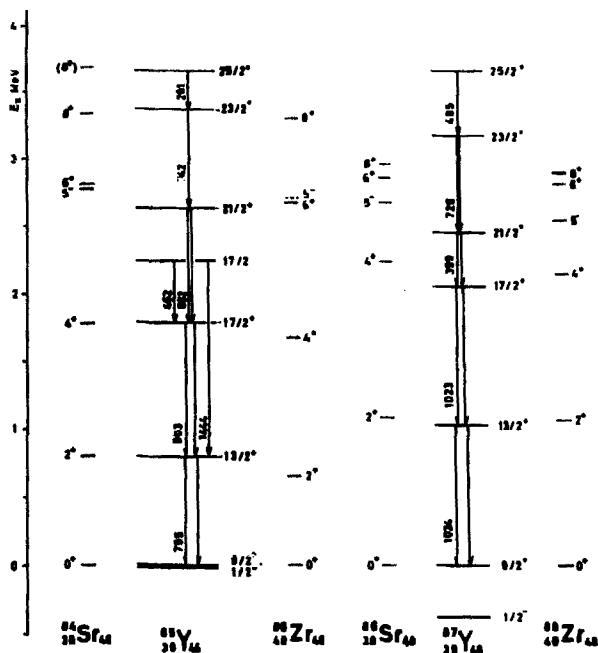


Fig. 1. Yrast cascades of ^{85}Y and ^{87}Y . The two lowest levels of these nuclei are taken from refs. 4 and 5. Pertinent levels of neighbouring even nuclei are also shown.

Standard in-beam γ -ray spectroscopy was used to obtain the two level schemes shown in Fig. 1. It is seen that the $13/2^+$ and $17/2^+$ levels lie close to the 2^+ and 4^+ levels of the neighbouring even-even nuclei. The $21/2^+$ levels (which are probably mostly $\pi g_{9/2} (u g_{9/2}^{-2})_8^+$, in analogy with the structure of the corresponding level of ^{91}Mo as derived from g-factor measurements ^{1/}) follow the pronounced rising of the 8^+ level that occurs when passing from $N = 48$ to $N = 46$. The $25/2^+$ levels - which represent maximal alignment of the three $g_{9/2}$ orbitals - on the other hand fall at about the same excitation energy. The $23/2^+$ and $25/2^+$ levels are both very short-lived ($T_{1/2} < 1$ ps), in analogy with what is found experimentally ^{1/} and theoretically ^{2/} for the corresponding generalized-seniority-three levels of ^{91}Mo .

REFERENCES

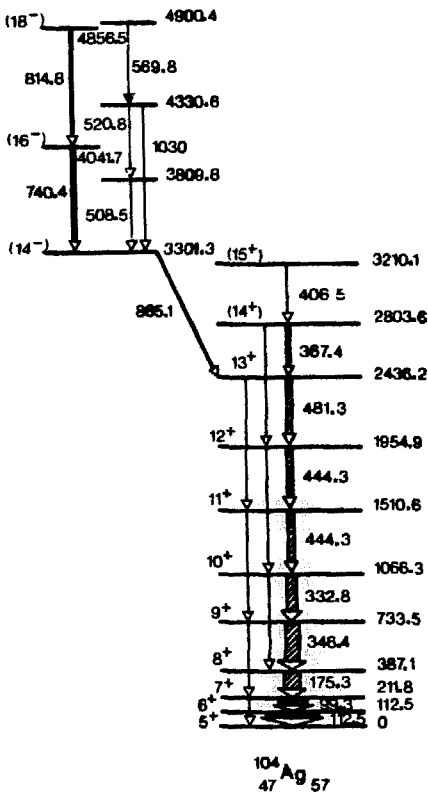
1. O. Häusser, T. Faestermann, I.S. Towner, T.K. Alexander, H.R. Andrews, J.R. Beene, D. Horn and D. Ward, *Hyperfine Int.* 4, 196 (1978).
2. A. Nilsson and M. Grecescu, *Nucl. Phys.* A212, 448 (1973).
3. F.J.D. Serduke, R.D. Lawson and D.H. Gloeckner, *Nucl. Phys.* A256, 45 (1976).
4. R. Iafigliola, H. Huang, J.K.P. Lee and T.Y. Li, *J. Inorg. Nucl. Chem.* 39, 7 (1977).
5. C.M. Lederer and V.S. Shirley, *Table of Isotopes*, Wiley, New York 1978.

EVIDENCE OF A BAND STRUCTURE IN ODD-ODD ^{104}Ag

R. Béraud, A. Charvet, R. Duffait, M. Meyer,
 Institut de Physique Nucléaire (and IN2P3), Université Claude-Bernard
 Lyon-I, 43, Bd du 11 Novembre 1918, 69622 Villeurbanne Cedex (France)

J. Genevey, J. Tréherne,
 Institut des Sciences Nucléaires de Grenoble, 53, Avenue des Martyrs,
 38026 Grenoble Cedex (France)

F. Beck, T. Byrski,
 Centre de Recherches Nucléaires de Strasbourg, 23, rue du Loess,
 Cronenbourg, 67037 Strasbourg Cedex (France)



In the framework of our systematic study of neutron-deficient nuclei of the In-Cd-Ag region, we have reinvestigated at the CEV of the Grenoble Institute the odd-odd ^{104}Ag , already studied by J. Ludziejewski ¹ et al. via $^{103}\text{Rh}(\alpha, 3n)$ reaction by means of the heavy-ion $^{94}\text{Mo}(^{12}\text{C}, pn)$ ^{104}Ag reaction. A level scheme has been established up to 5 MeV excitation energy from excitation functions and γ - γ coincidence results. Spins and parities have been assigned with the help of angular distributions $\gamma(\theta)$, electron conversion (with the Orange spectrometer of Grenoble-ISN) and linear polarization measurements (by means of the 5- intrinsic Ge detectors Compton polarimeter ² of the CRN Strasbourg).

A strongly populated cascade of $\Delta I = 1$ transitions based on the ground state 5^+ is observed up to 15^+ state at 3210.1 keV. The E1 nature of the 865.1 keV transition allows to identify unambiguously a sequence of negative parity states from the 3301.3 keV state. Fig. 1 shows a partial level scheme of ^{104}Ag involving the strongest transitions observed in this reaction.

The existence of a strong positive parity cascade in ^{104}Ag in contrast of a negative one in ^{106}Ag ³ could be explained by the different neutron configurations involved.: if the proton configuration is clear

($\Omega = 7/2, 9/2$ of g $9/2$), the neutron one gives rise to a strong negative decoupled band $\Delta I = 2$, based on a $11/2^-$ state, in ^{107}Cd ($\Omega = 1/2, 3/2$ of h $11/2$), while the dominant cascade in ^{103}Cd is a positive one, based on the $7/2^+$ state and interpreted as a ($\Omega = 1/2, 3/2$ of g $7/2$ and d $5/2$) decoupled band ⁴. So in the slightly deformed rotor plus particle model including coriolis interaction, it is possible to interpret the structure of ^{104}Ag : the preliminary results of the calculation indicates that the band built in fact on the 6^+ state is mainly composed of $K = 6$ bands ($\Omega_v = 3/2$ d $5/2$ \boxtimes $\Omega_\pi = 9/2$ g $9/2$), ($\Omega_v = 3/2$ g $7/2$ \boxtimes $\Omega_\pi = 9/2$ g $9/2$) and $K = 5$ band ($\Omega_v = 1/2$ g $7/2$ \boxtimes $\Omega_\pi = 9/2$ g $9/2$). The presence of $\Delta I = 2$ transitions suggests a collective nature for the excited levels observed here and supports our interpretation in terms of bands. More complete results will be soon published.

1. J. Ludziejewski, J. Bron, W.H.A. Hesselink, A.W.B. Kalshoven, L.K. Peker, A. van Poelgeest, H. Verheul and M.J.A de Voigt, in Proceedings of the Int. Conf. on Nuclear Physics, Tokyo, Japan, 1977.
2. F.A. Beck and R. Henck, Rapport Annuel CRN Strasbourg, 1979.
3. L.E. Samuelson, R.A. Emigh, D.E. Prull, R.E. Anderson, J.J. Kraushaar, R.A. Ristinen and B.M. Kluger-Bell, Rapport NPL-845 Nov 1, 1979, University of Colorado, Boulder Col 80309.
4. M. Meyer, J. Danière, J. Letessier and P. Quentin, Nucl. Phys. A 316 (1979) 93.

HIGH SPIN STATES OF THE ODD-ODD ^{110}In NUCLEUS

R. Béraud, A. Charvet, R. Duffait, M. Meyer
Institut de Physique Nucléaire (and IN2P3), Univ. Cl. Bernard Lyon-1,
43, Bd du 11 Novembre 1918, 69622 Villeurbanne Cedex (France)

J. Genevey, J. Tréherne,
Institut des Sciences Nucléaires de Grenoble,
53, Avenue des Martyrs, 38026 Grenoble Cedex (France)

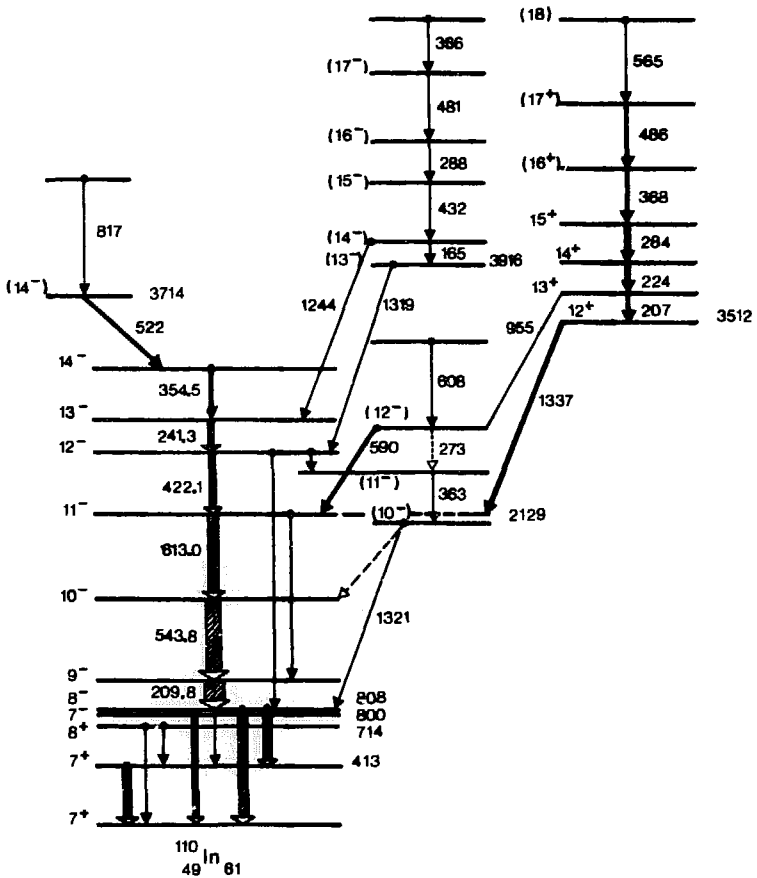
F. Beck, T. Byrski,
Centre de Recherches Nucléaires de Strasbourg,
23, rue du Loess, Cronembourg, 67037 Strasbourg Cedex (France)

This investigation is the continuation of a previous study ¹ of high spin states in ^{108}In . In odd -A nuclei of 48 Cd and 49 In adjacent to odd-odd indium, two different bands built on high j orbitals are excited : one perturbed on $\pi g 9/2$ ($\Omega = 9/2, 7/2$) and the other decoupled ($\Delta I = 2$) based on $\nu h 11/2$ ($\Omega = 1/2, 3/2$). The aim of the high-spin study of odd-odd indium is to investigate the resulting structure of such a conflicting case.

The level scheme of ^{110}In has been established from γ -ray spectroscopy and γ - γ coincidence experiments using the $^{100}\text{Mo} (^{14}\text{N}, 4n)^{110}\text{In}$ reaction at 65 MeV and all carried out at the Grenoble Cyclotron. Spin and parities have been assigned from excitation functions, γ - angular distributions, conversion electron (with the Grenoble Orange Spectrometer) and γ -ray linear polarization (with the five detectors Compton polarimeter ² of the CRN Strasbourg) measurements.

A partial level scheme of ^{110}In is presented in fig. 1 where different level sequences are displayed. Above the ground state and the first positive parity states (involving the $\pi g 9/2$ and $\nu g 7/2, \nu d 5/2$ orbitals) an intense cascade is observed from 7^- to 14^- . This sequence has been previously reported only up to 10^- and interpreted in the frame of quadrupole neutron-proton interaction as $\pi g 9/2 \otimes \nu h 11/2$ multiplet states ³. From the 11^- state, these states cannot be interpreted with this configuration. In the present work, negative parity levels have been compared to the results of a slightly deformed rotor + two quasi-particle calculation using H. F. self consistent wave functions. Preliminary results of this calculation show that the experimental sequence is well reproduced, especially the nearness of the 7^- and 8^- states. Moreover, the coexistence of E2 and M1 transitions supports this sequence looks like a rotational band based on the 8^- level composed of K = 6, 7, 8 band-mixing arising from $\nu h 11/2$ ($\Omega_n = 3/2, 5/2, 7/2$) \otimes $\pi g 9/2$ ($\Omega_p = 9/2$) states. Other sequences located much higher in the scheme cannot be easily interpreted with a two quasi-particle description.

1. R. Duffait, R. Béraud, A. Charvet, N. Elias, S. André, J. Genevey, S. Tedesco, J. Tréherne, F. Beck and T. Byrski, Comm. Rhodes, 1979, to be published.
2. F.A. Beck and R. Henck, Rapport Annuel 1979, CRN Strasbourg.
3. M. Eibert, A.K. Gaigalas and N.I. Greenberg, J. Phys. G 2 L 203 (1976).



GAMMA-GAMMA CORRELATIONS FOLLOWING
COMPOUND NUCLEUS REACTIONS WITH 118 MeV ^{12}C -IONS

C.J. Herrlander, L. Hildingsson, A. Johnson, A. Kerek, W. Klamra,
A. Källberg, Th. Lindblad, C.G. Lindén, J. Starker and K. Wikström
Research Institute of Physics, S-104 05 Stockholm, Sweden

J. Bialkowski and J. Kownacki
Swierk, Warsaw, Poland

B. Fant
University of Helsinki, Finland

T. Lönnroth
University of Jyväskylä, Finland

ABSTRACT. Investigations of correlations between γ -ray transitions following ^{12}C induced reactions on $^{116,118,120,122}\text{Sn}$, ^{124}Te , ^{161}Dy , ^{176}Yb and ^{197}Au have been performed using 118 MeV ^{12}C -ions from the Stockholm cyclotron. From these data the collective moments of inertia are deduced in spin regions above what is known from conventional γ -ray spectroscopy. Band-crossing structures are evidenced in the correlation spectra.

EXPERIMENTAL PROCEDURE AND RESULTS. The $\gamma\gamma$ -correlation technique¹ allows studies of rotational properties of nuclei to very high values of spin. In these measurements, individual bands are not isolated but the technique reveals general properties of "yrast-like" cascades in unresolved "E2-bumps", familiar from multiplicity and multipolarity measurements. In a previous experiment², a target of ^{124}Sn was bombarded with 118 MeV ^{12}C -ions to produce mainly $^{128-130}\text{Ba}$ and ^{126}Xe . There, a rotational-like structure was observed up to transition energies of about 1300 keV, corresponding to a collective spin of about 32 \hbar , whereas the information on discrete lines stops around 900 keV. A "bridge" in the correlation spectrum at about 1120 keV indicates a so far unknown band-crossing.

In the present experiments a systematic study of Ba- and Xe-isotopes, populated in (^{12}C , xn) and (^{12}C , axn) reactions on Sn-isotopes, is performed. No direct separation of final channels is performed in these experiments but the systematic study from the chain of stable Sn-isotopes and the fragmentation of angular momentum, will partly allow us to ascribe certain structures to definite final nuclei. The additional targets were tested mainly to find out if the resolution of the NaI-detectors is sufficient to resolve the structures in heavier nuclei where the larger moments of inertia cause compressed rotational spectra.

The experimental setup consisted of six 7,5 x 7,5 cm NaI(Tl)-detectors and one Ge(Li)-detector. The two and higher fold NaI-coincidence events, including the times relative to the beam bursts of the cyclotron, were stored on magnetic tape. The Ge(Li)-events were recorded whenever in coincidence with two or more NaI(Tl)-detectors in order to identify the final products and to get the multiplicities. For each target 80 - 250 million events were recorded.

The analysis of the data, which mainly consists of separating the correlated photopeak-photopeak events from all other possible events, is still in progress. Some preliminary results, concerning energy correlations are already available. As an example the results from about half of the data from 118 MeV

^{12}C on ^{116}Sn can be mentioned. The main channels here lead to $^{118,120,122}\text{Xe}$ and ^{122}Ba . The h_{5^0} valley in the correlation spectrum is here observed up to about 1100 keV and several pronounced bridges across the valley are observed giving indications on band-crossing structures.

1. O. Andersen, J.D. Garrett, G.B. Hagemann, B. Herskind, D.L. Hillis, L.L. Riedinger, Phys.Rev.Lett. 43, 687 (1979).
2. O. Andersen, M.A. Deleplanque, J.D. Garrett, B. Herskind, F.S. Stephens, S.A. Hjorth, A. Johnson and Th. Lindblad, to be published.

MULTIPLICITY OF THE STATISTICAL γ -RAYS FOLLOWING (HI,xn) REACTIONS

S.H. Sie, R.M. Diamond*, J.O. Newton, J.R. Leigh
 Department of Nuclear Physics, Australian National University, Canberra,
 Australia

We have studied the quasi-continuum γ -rays following the reactions $^{122}\text{Sn}(^{16}\text{O},4n)^{134}\text{Ce}$, $^{110}\text{Pd}(^{16}\text{O},4n)^{122}\text{Xe}$ at 65 and 83 MeV and the reactions $^{149}\text{Sm}(^{16}\text{O},3n)^{162}\text{Yb}$, $^{150}\text{Sm}(^{16}\text{O},4n)^{162}\text{Yb}$ and $^{154}\text{Sm}(^{16}\text{O},4n)^{166}\text{Yb}$ at 73 and 85 MeV bombarding energies. The continuum gamma rays were detected in a 7.6×7.6 cm NaI detector in coincidence with the discrete lines from the residual nuclei, detected in a Ge(Li) detector. Contributions to the spectra due to neutrons in the NaI were removed utilizing time of flight effects. Analysis of the data is similar to and described in more detail in ref.1.

A systematic variation of the number of γ -rays above 2 MeV, well beyond the range of the yrast cascade and discrete lines, was observed. Assuming that the statistical spectra follow the distribution $N(E_\gamma) = E_\gamma^3 e^{-E_\gamma/T}$, the total number of the statistical γ -rays M_S can be derived. This, shown plotted in fig. 1 against the total multiplicity M_T , clearly increases with increasing M_T . If the remaining continuum gamma rays and the discrete lines are stretched E2 and the statistical gamma rays carry no angular momentum, the quantity $\bar{L}_\gamma = 2(M_T - M_S)$ should be the average input angular momentum \bar{L} . In Table 1 \bar{L}_γ is compared with \bar{L} , calculated with the IWB Bass model², and the method of partitioning into various xn channels due to Sikkeland³. It can be seen that the usual fixed value of 4 for M_S^4 would give poorer agreement, again suggesting that M_S varies with M_T . This effect may be related to an increase (decrease) in the average excitation energy above the yrast line with increasing (decreasing) bombarding energy relative to the optimum bombarding energy for the particular reaction.

TABLE 1				
	E_{lab} (MeV)	\bar{L}	\bar{L}_γ	M_S
$^{122}\text{Sn}(^{16}\text{O},4n)^{134}\text{Ce}$	65	10.6	12	2.7
	83	24.3	23	6.2
$^{110}\text{Pd}(^{16}\text{O},4n)^{122}\text{Xe}$	65	12.6	16	2.4
	83	25.2	27	6.8
$^{149}\text{Sm}(^{16}\text{O},3n)^{162}\text{Yb}$	73	10.7	16	4.9
	85	23.8	26	7.2
$^{150}\text{Sm}(^{16}\text{O},4n)^{162}\text{Yb}$	73	9.1	11	2.7
	85	19.3	20	4.5
$^{154}\text{Sm}(^{16}\text{O},4n)^{166}\text{Yb}$	73	11.0	14	4.1
	85	22.6	21	5.6

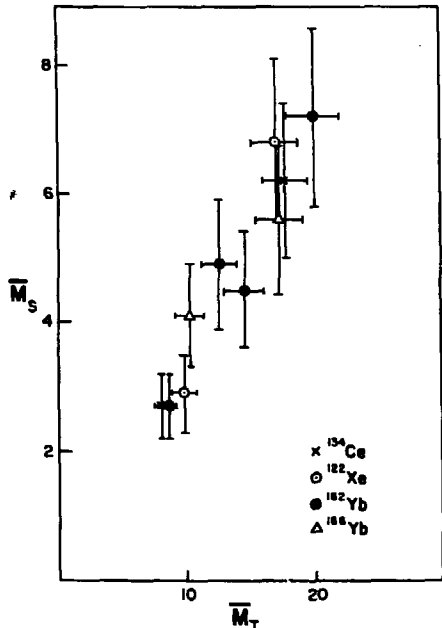


Fig. 1. \longrightarrow

Refs.

1. J.O. Newton, S.H. Sie and G.D. Dracoulis, Phys.Rev.Lett. 40, 625 (1978);
J.O. Newton, S.H. Sie, Nuclear Physics in press.
 2. R. Bass, Nucl.Phys. A231, 45 (1974); R. Broda et al. Nucl.Phys. A248,
356 (1975).
 3. T. Sikkeland, Arkiv.Fys. 36, 539 (1966).
 4. R.S. Simon et al., Nucl.Phys. A313, 909 (1979).
- * Nuclear Science Division, Lawrence Berkeley Laboratory, University of California, Berkeley, USA.

BAND CROSSING IN THE INTERACTING BOSON MODEL

A. Gelberg, Institut für Kernphysik, Universität zu Köln, Köln, W-Germany
 A. Zemel, Physics Department, Weizmann Institute, Rehovot, Israel

In the Interacting Boson Model (IBM)¹ the total number of s- and d-bosons with angular momentum 0 and 2 respectively is a finite number $N = n_s + n_d$; it is roughly equal to half the number of nucleons outside closed shells.

The main aim of this investigation was to study the way in which this boson cutoff manifests itself in the case of band crossing, as well as to extend IBM energy calculations to the backbending region. Energies, $B(E2)$'s and g-factors were calculated in the SU(3) limit of IBM¹.

A two-particle state is described by the boson-like operator

$$b_{\ell m}^+ = \sum_{m_1 m_2} \langle j m_1 j m_2 | j m \rangle a_{j m_1}^+ a_{j m_2}^+ \quad (1)$$

where $a_{j m}^+$ is the creation operator for a particle in the state (j, m) .

The core plus two particle hamiltonian is:

$$H = \alpha L(L+1) + \epsilon_{\ell} + \gamma \left[(b_{\ell}^+ b_{\ell})^{(1)} (d^+ d)^{(1)} \right]^{(0)} \quad (2)$$

$$+ Z \left\{ (b_{\ell}^+ b_{\ell})^{(2)} \left[(d^+ s + s^+ d)^{(2)} - (\sqrt{7})/2 (d^+ d)^{(2)} \right] \right\} + H_{\text{mix}}$$

where L is the core angular momentum, $d^+(d)$ and $s^+(s)$ are the creation (annihilation) operators of the d- and s-boson respectively, and ϵ_{ℓ} is the energy of the two-particle state. H_{mix} , which mixes different two-particle states, has been approximated by the constant $\beta\alpha$. We consider only two two-particle states with $\ell = 0$ ($\epsilon_0 = 0$) and $\ell = J$.

Energies and $B(E2)$'s were calculated for several transition nuclei which display backbending. The results for ^{126}Ba are shown as an example in figs. 1 and 2. We assumed $J = 10$, corresponding to a $(h_{11/2})^2$ configuration. This assignment is supported by the existence of decoupled bands based on $11/2^-$ states in adjacent odd-even nuclei.

Although the SU(3) limit is very simple, since it considers a constant inertial parameter, and the Hamiltonian (2) can mix only core states belonging to the ground state band¹, the main trends of the excitation energies are correctly reproduced. In particular, the energy intervals in the two-particle band are larger than the corresponding ones in the ground state band, e.g. $E(12^+) - E(10^+) = 3.1 E(2^+)$. This is due to the mixing of the core states by the quadrupole operator present in (2).

As can be seen in fig. 2, the drop in $B(E2)$, compared to the rotational value, starts already at low spins, contrary to the predictions based on the Nilsson model³. A similar trend can be observed in $^{130,132,134}\text{Ce}$ ⁴.

The overall agreement with our calculations allows us to ascribe this behaviour to the boson cutoff effect predicted by IBM. The extension of our calculations to the O(6) limit of IBM is under way.

1. A. Arima and F. Iachello, *Annals of Phys. (NY)* 99, 253 (1976) and 111, 201 (1978)
2. G. Seiler-Clark, D. Husar, R. Novotny, H. Graf, and D. Pelte, *Phys. Lett.* 80B, 345 (1979)
3. M. Reinecke and H. Ruder, *Z. Phys.* A282, 353 (1977)
4. D. Husar, S. J. Mills, H. Gräf, U. Neumann, D. Pelte, and G. Seiler-Clark, *Nucl. Phys.* A292, 267 (1977)

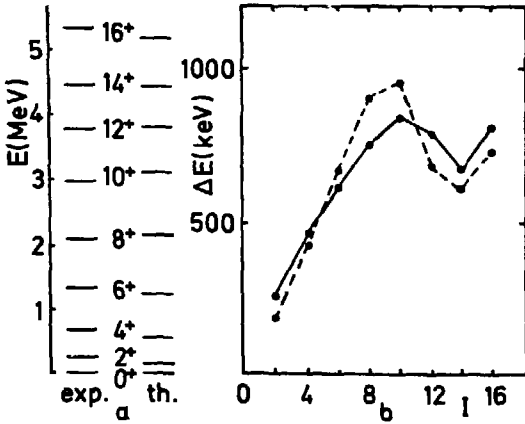


Fig. 1:
 a) Energies² and
 b) Energy intervals.
 Solid curve, experiment;
 dashed line, theory.

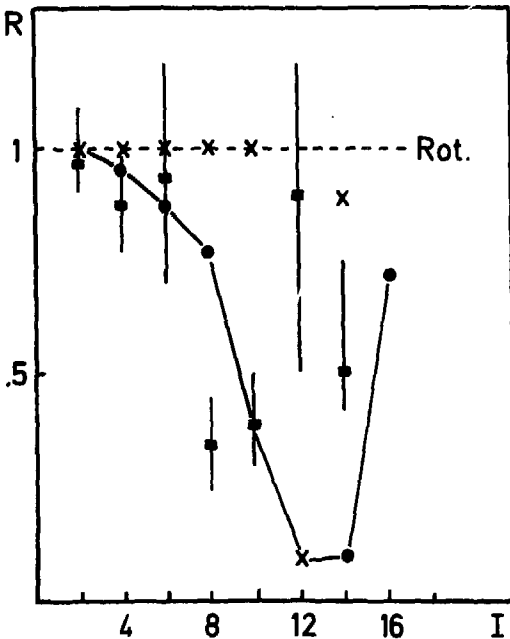


Fig. 2:
 Normalized $B(E2)$'s for ^{126}Ba

$$B = \frac{B(E2; I+2 \rightarrow I) / B(E2; 2 \rightarrow 0)}{[B(E2; I+2 \rightarrow I) / B(E2; 2 \rightarrow 0)]_{\text{rot}}}$$

 closed squares, experiment²;
 solid curve, IBM calculations;
 crosses, calculation Ref. 3.

GAMMA TRANSITION-ENERGY CORRELATIONS IN BARIUM NUCLEI

M.A.Deleplanque, O.Andersen, J.D.Garrett, B.Herskind and F.S.Stephens
The Niels Bohr Institute, University of Copenhagen, Copenhagen, Denmark

C.G.Lindén, S.A.Hjorth, A.Johnson and Th.Lindblad
The Research Institute of Physics, Stockholm, Sweden

The two-dimensional "correlated"¹ spectrum (fig.1) obtained (with NaI detectors) after subtraction of an uncorrelated background from an E_{γ} - E_{γ} coincidence matrix, has been studied for the reaction $^{12}\text{C}+^{124}\text{Sn}$ at 118 MeV performed at the Stockholm cyclotron. The maximum angular momentum I_{\max} at the top of the γ -cascade is estimated² to be $\approx 40 \hbar$. Four residual nuclei are produced: $^{128,129,130}\text{Ba}$ and ^{126}Xe . Projections of the channels along the valley (open circles) and along the ridge (closed squares), shown in fig.2, indicate that these features are statistically significant.

A valley is clearly observed from about 500 keV up to the top of the yrast bump (≈ 1300 keV), reflecting the rotational (or quasirotational) properties of these nuclei. The width of the valley decreases up to a transition-energy of 800 keV, corresponding to an increasing moment of inertia in the known ground band of these nuclei. These moments of inertia (I/ω , where ω is the frequency) can be fitted by the Harris formula $I/\omega = \mathcal{J}_0 + \omega^2 \mathcal{J}_1$ (fig.3). The width of the valley, directly related to $d\omega/dI$ agrees with the calculated values, although the nucleus probably decays through many different paths in that frequency region.

Both in the 800-1050 keV and in the 1200-1300 keV regions the half-width of the valley, W , (defined as half the energy separating the first ridge on either side of the valley) remains nearly constant and corresponds to collective moments of inertia³, $2\mathcal{J}_{\text{coll}}/\hbar^2 = 80$ and 95 MeV^{-1} , respectively. The $\mathcal{J}_{\text{coll}}$ obtained from W (i.e. the consecutive intraband transitions) corresponds to the moment of inertia of the core. In contrast, an effective moment of inertia, $2\mathcal{J}_{\text{eff}}/\hbar^2 \approx 115 \text{ MeV}^{-1}$ is indicated by the maximum energy of the correlated pattern seen on fig.1, $E_{\gamma}=1400$, and the estimated I_{\max} . If j_a is the "aligned angular momentum", $\mathcal{J}_{\text{coll}} = \mathcal{J}_{\text{eff}}(I-j_a)/I$. Therefore, at the maximum angular momentum $j_a \approx 7 \hbar$ units. One decay path then is visualized as a succession of several bands with different values of j_a and $\mathcal{J}_{\text{coll}}$. The crossings of a large number of these bands at a specific $\hbar\omega = 1/2 E_{\gamma}$ appear as bridges (see figs.1 and 2). Of particular interest in the present case is the bridge at around 1120 keV which collects a large intensity, suggesting that many band crossings occur at $\hbar\omega = 560$ keV.

Such crossings, which probably correspond to a specific alignment along the rotational axis⁴, are consistent with the observed difference between \mathcal{J}_{eff} and $\mathcal{J}_{\text{coll}}$. Cranking model calculations indicate that the aligned angular momentum near I_{\max} may be the result of the occupation of $h/2$ or $i_{13/2}$ neutron orbitals.

1. O.Andersen et al., Phys.Rev.Lett. 43, 687 (1979).
2. K.Siwiek-Wilczyńska et al., Phys.Rev.Lett. 42, 1599 (1979).
3. M.A.Deleplanque et al., submitted to Phys.Rev.Lett.
4. L.L.Riedinger et al., Phys.Rev.Lett. (in press).

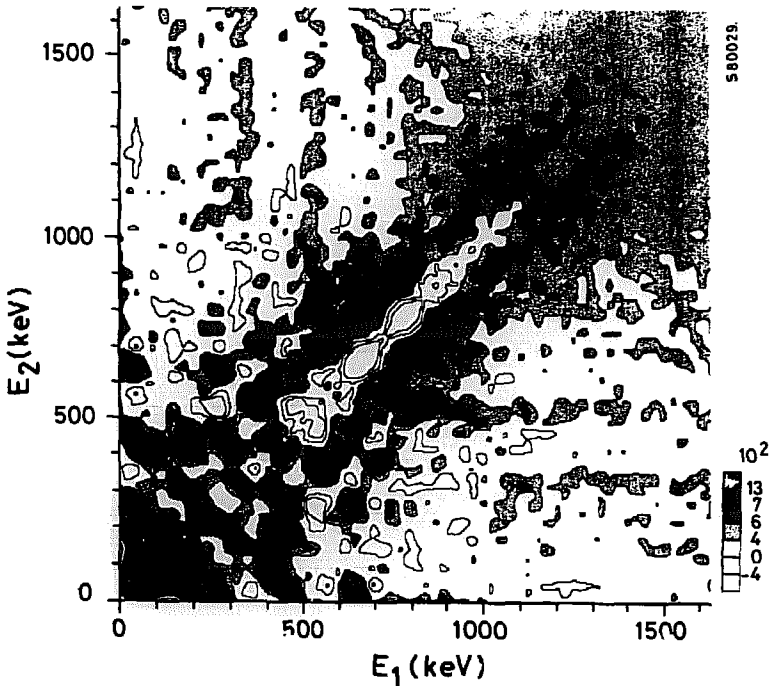


Fig.1. Contour plot of the correlated spectrum.

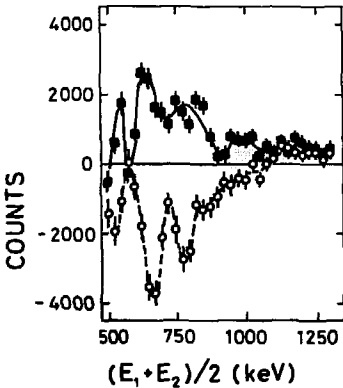


Fig.2. Projections of the channels along the valley (open circles) and along the first ridge (closed squares).

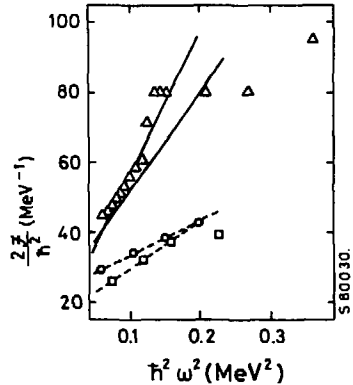


Fig.3. Moment of inertia (I/w) for the ground band of ^{128}Ba (circles) and ^{130}Ba (squares) and their fit by $I/w = I_0 + w^2 I_1$ (dashed lines). dI/dw (full lines) compared to 8:W (triangles).

MAGNETIC MOMENTS OF ^{134}Ce LEVELS AT BACKBENDING

M.B. Goldberg, C. Broude, A. Zemel
Weizmann Institute, Rehovot, Israel

J. Gerber
Centre de Recherches Nucléaires, Strasbourg, France

G.J. Kumbartzki, K.H. Speidel
Institut für Strahlen-und Kernphysik, Bonn, Germany.

^{134}Ce is in the middle of the $h_{11/2}$ neutron shell and exhibits strong backbending above the 8^+ state ¹⁾ the backbending mechanism is sensitively probed by magnetic moment measurements, since negative values unambiguously imply decoupled neutron pairs in $j=1+1/2$ orbits. It is also of interest to relate the structure at backbending to that of the isomeric 10^+ state at comparable excitation, since the corresponding isomers in $^{136,138}\text{Ce}$ have been assigned to the same neutron configuration ^{2,3)}. The spin-parity of the ^{134}Ce isomer was tentative prior to the present work.

We report here on internal (external) field gamma-ray PAC measurements on ^{134}Ce levels on recoil in magnetized Fe, Gd (Pb) backings respectively. Ground-state-band members up to 16^+ were populated via $^{122}\text{Sn}(^{160,4n})$ with 62-80 MeV beams from the Strasbourg MP tandem and Rehovot Pelletron accelerators.

For a better understanding of the ^{134}Ce yrast line feeding pattern, the precession data were supplemented by precision gamma angular distributions, recoil-distance time spectra and gamma-gamma coincidence runs. These confirmed most previous spectroscopic assignments ^{1,2,4)}, an exception being the 397.5 keV transition, which is contaminated by an adjacent line with strong negative anisotropy, probably from ^{133}Ce . We obtain $A_2(397.5) = + 0.20(4)$, substantiating the 10^+ assignment to the isomeric 3209 keV level.

We find : $- 0.4 < g(10^+ \text{ isomer}) < 0$

The lower bound reflecting the lifetime limit $\tau > 300 \text{ ns}$ ⁵⁾

In addition, the rudiments of a negative parity band built on a 5^- state at $E_x = 2174 \text{ keV}$ have been observed.

The feeding times to the G.S.B. members below the 14^+ state are long compared to the ion stopping times of approx. 1 ps. Thus, the transient field precession(TF) is inherited from the predominantly collective statistical states above. The precession contribution from the G.S.B. levels themselves is entirely due to the static hyperfine field. Values for $g(10^+ \text{ backbend})$ and the static and transient fields in Fe, Gd have been extracted by minimizing χ^2 for all internal-field precession data simultaneously, using the measured spectroscopic quantities wherever available and assuming $g = + 0.3$ for all other levels. This procedure yielded TF precessions of 30, 50 mrad/g and static HF fields of -350, -310 KG in Fe, Gd respectively. Moreover, we obtain

$$g(10^+ \text{ backbend}) = - 0.20(20)$$

which deviates significantly from the collective value. Assuming a smooth variation of g -factors over the states around backbending does not appreciably change this result, since the sensitivity to the g -factors of the neighbouring levels is low.

The magnetic moments of both 10^+ states support the hypothesis that decoupled $h_{11/2}$ neutron pairs play a major role in the structure at 3-4 MeV excitation. In contrast, backbending of nuclei at the beginning of the neutron shell ($^{126,128}\text{Ba}$ and $^{128,130}\text{Ce}$) has been attributed to decoupled protons $6,7$). This transition is possibly related to the observed reduction in 10^+ to 8^+ $E2$ rates $1)$ from ^{130}Ce to ^{134}Ce and to the weakening of band structure for the heavier isotopes $1,2)$. Further measurements are in progress.

We would like to thank J.C. Adloff, A. Gelberg and Y. Niv for assistance with some of the measurements, P. Federman and I. Talmi for interesting discussions and A. Meens and L. Sapir for expertise in target making.

1. D. Husar, S.J. Mills, H. Graef, U. Neumann, D. Pelte and G. Seiler-Clark, Nucl. Phys. A292, 267 (1977) and Refs. Therein.
2. M. Mueller-Veggian, Y. Gono, R.M. Lieder, A. Neskakis and C. Mayer-Boericke, Nucl. Phys. A 304, 1 (1978) and annual report, KFA Juelich (1977) p.30.
3. J.C. Merdinger, F.A. Beck, E. Bozek, T. Byrski, C. Gehringer, Y. Schutz and J.P. Vivien, Contribution to this conference.
4. R. Arlt, G. Beyer, V. Fominykh, E. Herrmann, A. Jasinski, H.G. Ortlepp, H. Strusny, H. Tyrroff and Z. Usmanova, Pol. Phys. Acta B4, 301 (1973).
5. G.L. Smith and J.E. Draper, Phys. Rev. C1, 1548 (1970)
6. D. Ward, H. Bertschat, P.A. Butler, P. Colcbani, R.M. Diamond and F.S. Stephens, Phys. Lett. 56B, 139 (1975).
7. C. Flaum, D. Cline, A.W. Sunyar, O.C. Kistner, Y.K. Lee and J.S. Kim, Nucl. Phys. A 264, 291 (1976).

THE g-FACTOR OF THE $I^\pi = 10^+$ ISOMERS IN ^{138}Ce AND ^{140}Nd

J.C. Merdinger, F.A. Beck, T. Byrski, C. Gehringer, Y. Schutz, J.P. Vivien
Centre de Recherches Nucléaires et Université Louis Pasteur,
Strasbourg, France.

E. Bozek
Institute of Nuclear Physics, Cracow, Poland.

There is much interest in the study of the detailed structure of the numerous high spin yrast isomers identified in nuclei near the shell closure at $N = 82$. The features of the yrast level spectra can be understood in a picture where, for oblate nuclei, a number of quasi-particles have their angular momenta aligned along the axis of rotation. Shell-model treatment, using ^{146}Gd as a doubly closed core, led also to a satisfactory description.

Isomeric states were recently found in the $N = 80$ isotones ^{144}Gd , ^{142}Sm , ^{140}Nd and ^{138}Ce . In particular an $I^\pi = 10^+$ isomer was observed in all these nuclei. The recent g-factor measurement ¹ of this isomeric state in ^{144}Gd is in complete disagreement with a $(\nu h_{11/2})^{-2}$ description expected so far for these states. We have measured the g-factors for the 10^+ isomers in ^{138}Ce and ^{140}Nd with the aim of obtaining information about the main configuration of these states.

The levels in ^{138}Ce were populated via the $^{130}\text{Te}(^{12}\text{C}, 4n)$ reaction using a pulsed beam of 60 MeV energy. The 1 mg cm^{-2} thick target was evaporated onto a thick lead backing serving as an implantation medium. Angular distribution and γ -linear polarisation measurements with a five Ge Compton polarimeter assigned definitively $I^\pi = 10^+$ to the previously reported isomeric state at $E_x = 3538.1 \text{ keV}$. For the g-factor measurement an external field $B = 1.175 \pm 0.020 \text{ T}$ was applied perpendicular to the reaction plane and reversed every minute. The time distributions of delayed γ -rays relative to the beam bursts were observed with a 1 cm thick planar detector and a 22 cm^3 coaxial detector set at angles $\theta = \pm 45^\circ$ to the beam direction. The yields $N(t)$ of the 430 keV ($3538 \text{ keV}, 10^+ \rightarrow 3108 \text{ keV}, 8^+$) and 815 keV ($3108 \text{ keV}, 8^+ \rightarrow 2293 \text{ keV}, 6^+$) γ -rays were recorded. The usual ratios $R(t) = (N_+ - N_-) / (N_+ + N_-)$, where $N_\pm = N(\pm H, t)$, were formed. In fig.1 the ratio $R(t)$ for the 430 keV transition is displayed.

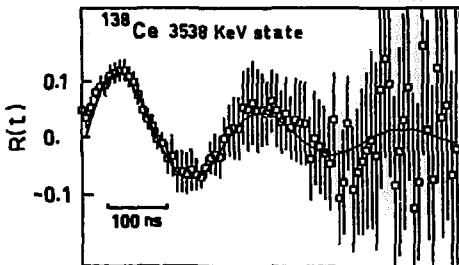


Figure 1
Time-differential pattern $R(t)$ of the 430 keV γ -rays in ^{138}Ce . The smooth curve is a least-squares fit to the data.

The reaction $^{128}\text{Te}(^{16}\text{O}, 4n)^{140}\text{Nd}$ at a bombarding energy of 70 MeV was used to populate high spin levels in ^{140}Nd . A spin of $I = 10$ was unambiguously determined for the isomeric state ² located at $E_x = 3621.4 \text{ keV}$. The small energy of the $10 \rightarrow 9^-$ transition ($E_\gamma = 167 \text{ keV}$) did not allow a reliable linear polarization

measurement for the parity determination of this state. Comparison with ^{144}Gd and ^{138}Ce however favors strongly the $I^\pi = 10^+$ assignment. For the g-factor determination the same experimental technique as for ^{138}Ce was used. Here the yields of the 167 keV (3621 keV, $10^+ \rightarrow 3454$ keV, 9^-) and 215 keV (3454 keV, $9^- \rightarrow 3239$ keV, 8^-) γ -rays were recorded. The ratio $R(t)$ for the 215 keV transition is displayed in Fig.2.

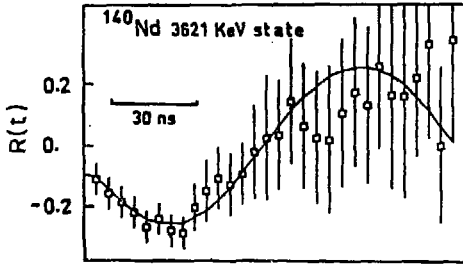


Figure 2
Time-differential pattern $R(t)$ of the 215keV γ -rays in ^{140}Nd .

The measured g-factors for the 10^+ isomers, $g = -0.176(4)$ in ^{138}Ce and $g = -0.185(7)$ in ^{140}Nd , are almost identical suggesting similar configurations for both states. The observed values are very close to the effective g-factor value ($g \sim -0.2$) for a $h_{11/2}$ neutron configuration deduced from experimental data in Sn, Te and Xe isotopes. This gives strong evidence that the 10^+ isomers in ^{138}Ce and ^{140}Nd are rather pure two $h_{11/2}$ neutron-holes states.

1. O. Häusser, P. Taras, W. Trautmann, D. Ward, T.K. Alexander, H.R. Andrews, B. Haas and D. Horn, Phys. Rev. Lett. 42, 1451 (1979).
2. F.A. Beck, T. Byrski, C. Gehringer, A.Z. Hrynkiewicz, J.C. Merdinger, Y. Schutz and J.P. Vivien, Proc. Int. Conf. on Structure of Medium-Heavy Nuclei, Rhodos (1979) p.114.

HIGH SPIN LEVEL STRUCTURE OF ^{147}Sm

M. Piiparinen, Y. Nagai, J. Styczen, P. Kleinheinz
 Institut für Kernphysik, KFA Jülich, D-5170 Jülich, F.R. Germany

We have continued our investigations of N=85 isotones studying the level structure of the ^{147}Sm nucleus which has three neutrons and two proton holes compared to the closed ^{146}Gd core using $(\alpha,3n)$ and $(\alpha,5n)$ reactions with α -particle beams between 35 and 57 MeV from the cyclotron. γ -ray angular distributions and four parameter $\gamma\gamma$ coincidences were measured.

The ^{147}Sm level scheme resulting from these studies is shown in fig. 1. To a large extent this scheme strongly resembles that of $^{149}\text{Gd}^1$. Most of the levels up to 2.6 MeV excitation can be characterized with similar spherical shell model configurations. The $7/2^-$ ground state together with the $5/2^-$, $11/2^-$ and $15/2^-$ levels are formed from the $\nu f_{7/2}^3$ configuration. The 809 keV $9/2^-$ level is clearly analogous to the 796 keV $9/2^-$ level in ^{149}Gd which was characterized as $h_{9/2}$ single neutron state. In ^{147}Sm this interpretation is further supported by transfer reaction data². Above the $\nu h_{9/2}$ state we have the characteristic $(\nu f_{7/2}^2)^0$, 2^+ , 4^+ and 6^+ pattern of the two remaining valence neutrons in $f_{7/2}$ forming $9/2^-$, $13/2^-$, $17/2^-$ and $21/2^-$ levels between 0.8 and 2.6 MeV excitation.

5 - MeV

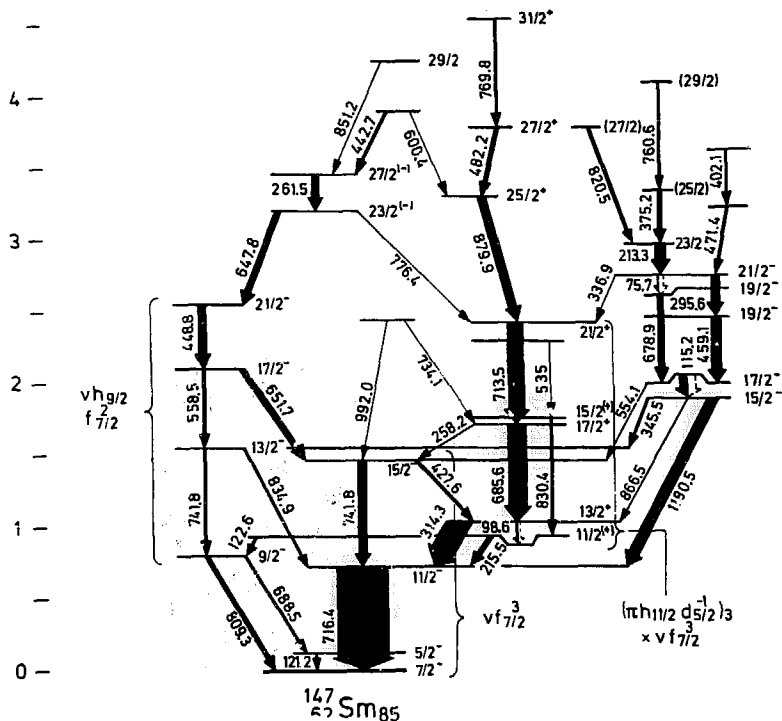


Fig. 1: High spin levels and shell model configurations of ^{147}Sm . Gamma ray intensities as observed with 57 MeV α particles in $(\alpha,5n)$ reactions are shown.

Similar as in ^{149}Gd , we interpret the $13/2^+$ level at 1030 keV in ^{147}Sm as $(\nu f_{7/2}^3 \times 3^-)_{13/2}$ configuration rather than $\nu i_{13/2}$ single particle state. The parity of the $11/2$ state at 932 keV is not unambiguously clear from our data, but positive parity is slightly preferred (in contrast to an earlier³ negative parity assignment). In analogy to ^{149}Gd , we interpret that level as the $(j^3)_{j-1}$ member of the $f_{7/2}^3$ multiplet which in combination with the octupole is lowered below the $(\nu f_{7/2}^3 \times 3^-)_{13/2}^+$ level. The $15/2$ level at 1762 keV probably also belongs to the same multiplet with the $(\nu f_{7/2}^3)_{9/2} \times 3^-$ configuration.

The states shown to the right in the ^{147}Sm level scheme has no analogous levels in ^{149}Gd . Most likely they have contributions from the two proton holes. However, the level scheme of the neighbouring $N=84$ ^{146}Sm nucleus in this energy range is highly complex, which prevents detailed interpretations of the corresponding levels in ^{147}Sm .

1. M. Piiparinen, R. Pengo, Y. Nagai, P. Kleinheinz, N. Roy, L. Carlen, H. Ryde, Th. Lindblad, A. Johnson, S.A. Hjorth, separate contribution on ^{149}Gd to this conference
2. B. Harmatz, W.B. Ewbank, Nucl. Data Sheets 25 (1978) 113
3. J. Kownacki, Z. Sujkowski, E. Hammaren, E. Liukkonen, M. Piiparinen, Th. Lindblad, H. Ryde, V. Paar, Nucl. Phys. A in press

DEFORMATION OF A HIGH-SPIN YRAST ISOMER IN ^{147}Gd

H.-E. Mahnke⁺, O. Häusser, T.K. Alexander, H.R. Andrews,
J.F. Sharpey-Schafer⁺⁺, M. Swanson, P. Taras⁺⁺⁺, D. Ward
Atomic Energy of Canada Limited, Chalk River Nuclear La-
boratories, Chalk River, Ontario, Canada K0J 1J0

The recently discovered discrete high-spin states in the neutron deficient rare-earth nuclei $^{152}\text{Dy}^1$ and $^{154}\text{Er}^2$ are believed to exhibit a new kind of collective motion: many individual particles align their angular momenta along the symmetry axis, thereby producing an oblate deformation. So far experimental evidence for such a deformation stems only from the effective moment of inertia in ^{152}Dy which exceeds the rigid-body value by about 10 %¹. The occurrence of isomeric states along the yrast line allows the determination of the deformation of discrete states at various spin values by measuring the static quadrupole moments.

We have now observed the static quadrupole interaction of three isomers along the yrast line in ^{147}Gd , the 500-ns isomer with a spin of $I \sim 49/2$, the $27/2^-$ -isomer, and the $13/2^+$ -isomer. The isomeric nuclei populated and aligned by the $^{124}\text{Sn} (^{28}\text{Si}, xn)$ -reaction were recoil-implanted into Gd single crystals. The quadrupole interaction with the axially symmetric electric field gradient of the hexagonal Gd metal was measured, using the standard time differential perturbed angular distribution technique³. Figure 1 displays the quadrupole modulation patterns obtained for the 500-ns isomer. The symmetry axis of the electric field gradient (i.e. the crystal \hat{c} axis) was at 45° to the beam direction in the plane of the two Ge(Li)-detectors to maximize the modulation effect (top and center panel); the quadrupole modulation disappears when the symmetry axis coincides with the beam direction (lower panel) demonstrating that the recoils substitute in the Gd lattice and are subject to a well-defined axially symmetric field gradient, eq.

The electric field gradient previously known only in the ferromagnetic phase at 4K^4 was calibrated at a temperature above the Curie point in a separate PAD experiment by using Coulomb excitation of the 2^+ states of the rotational nuclei $^{156,158,160}\text{Gd}$, and additionally the temperature dependence of the field gradient was measured in the paramagnetic region with the 10^+ -isomer of ^{144}Gd as the probe nucleus⁵.

The quadrupole moments $|Q_{\text{exp}}|$ deduced from the quadrupole coupling constants are shown in Table 1. They are compared with shell-model calculations for the most likely quasiparticle structure assuming charges of 1.53 and 1.0 for protons and neutrons, respectively. Obviously unrealistic high effective charges would be needed to reproduce the experimental values. Alternatively the quadrupole moments can be explained with bare nucleon charges if the aligned quasiparticles producing the spin move outside a deformed core. The deformation parameters β inferred from the experimental quadrupole moments are given in the last column of Table 1. The deformation increases with spin, acquiring a substantial value of $|\beta| \sim 0.2$ for the 500-ns yrast isomer in ^{147}Gd . Since the spin is produced by aligning mainly valence particles rather than holes, the oblate solution with the negative sign is strongly favored over the prolate solution given in square brackets.

⁺ summer visitor, from Bahn-Meitner-Institut, Berlin, W. Germany

⁺⁺ summer visitor, from University of Liverpool, Liverpool, U.K.

⁺⁺⁺ permanent address: Université de Montréal, Québec, Canada

TABLE I. Quadrupole moments in ^{147}Gd ($1b = 10^{-28} \text{m}^2$)

$T_{1/2}$ (ns)	I^π	Quasiparticle Structure	$ Q_{\text{exp}} $ (b)	QSM (b)	β
22	$13/2^+$	$\nu i_{13/2}$ $\pi 3^- \nu f_{7/2}$	0.73(7)	-0.36	-0.05 [0.05]
27	$27/2^-$	$\pi 10^+ \nu f_{7/2}$	1.26	-0.78	-0.06 [0.10]
500	$49/2^+$	$\pi 10^+ \nu f_{11/2}^- f_{7/2}^+ i_{13/2}$	3.14(17)	-0.84	-0.18 [0.20]
	$49/2^+$	$\pi 10^+ \nu f_{7/2} i_{13/2} h_{9/2}$		-1.36	
	$59/2^-$	$\pi 15^- \nu f_{7/2} i_{13/2} h_{9/2}$		3.80(20)	-1.40

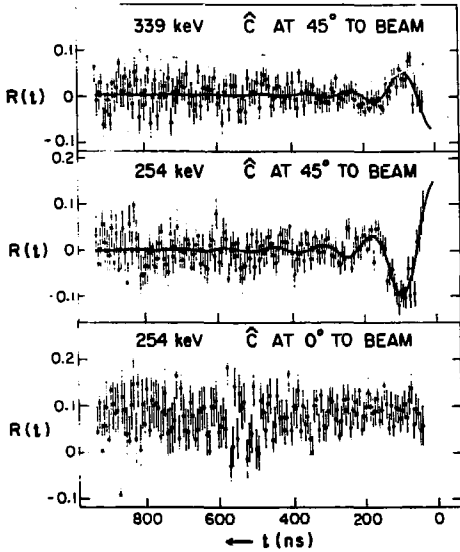


Fig. 1: Quadrupole modulations for the 500-ns yrast trap of ^{147}Gd in Gd at 413 K.

1. T.L. Grob et al., Phys.Rev.Lett. **41**, 1027 (1978).
2. C. Baktash et al., Phys.Rev.Lett. **42**, 637 (1979).
3. H. Frauenfelder and R.M. Steffen, in Alpha-, Beta- and Gamma-Ray Spectroscopy, Vol. II, ed. K. Siegbahn, North Holland Publishing Co. Amsterdam, 1965
4. E.R. Bauminger et al., Phys.Rev.Lett. **34**, 962 (1975).
5. O. Häusser et al., to be published.

ON THE STRUCTURE OF THE HIGH SPIN ISOMERS IN $^{147}\text{Gd}^+$

T. Døssing
NORDITA, Copenhagen, Denmark

K. Neergård
Justus-Liebig-Universität, Giessen, West Germany

H. Sagawa
Niels Bohr Institute, Copenhagen, Denmark

Recently, we reported¹ calculations of yrast states of $^{146,147}\text{Gd}$ in a deformed independent particle model with empirical spherical single particle energies.

The calculated configurations in the lower part of the yrast line agree with the result of a shell model analysis². Additionally, the calculations suggest the configurations

$[\pi\{(d_{\frac{1}{2}}^{5-2})_0(h_{\frac{1}{2}}^{11-2})_0\} \nu\{(d_{\frac{1}{2}}^{3-2})_0(f_{\frac{1}{2}}^{13})\}]_{20}$ and $[\pi\{(d_{\frac{1}{2}}^{5-2})_0(h_{\frac{1}{2}}^{11-2})_0\} \nu\{(d_{\frac{1}{2}}^{3-2})_0(f_{\frac{1}{2}}^{13} h_{\frac{1}{2}}^9)\}]_{49+}$
of the 4.1 ns isomer in ^{146}Gd and the 510 ns isomer in ^{147}Gd , respectively.

Since then, g factors and electric quadrupole moments of several isomeric states in ^{147}Gd have been measured^{3,4}. The table shows, along with the empirical values, the results for these quantities given by the model of ref. 1. The electromagnetic moments were obtained by summation of the single particle contributions. For the effective single particle charge and gyromagnetic ratios we used, respectively, $e_{\text{eff}}=e_{\text{free}}$, $g_{l,\text{eff}}=g_{l,\text{free}}$ and $g_{s,\text{eff}}=0.6g_{s,\text{free}}$. A Strutinsky renormalisation of the independent particle quadrupole moment was performed, but is insignificant within the experimental accuracy.

The table displays an increase of the quadrupole deformation β with the number of particle-hole pairs excited across the Z=64 and the N=82 gaps in the single particle spectrum. This is due to a mechanism discussed in detail in ref. 5 for nuclei close to ^{208}Pb . The resulting equilibrium deformation of a particular configuration is rather insensitive to the details of the single particle spectrum.

The agreement between the empirical and theoretical results supports an interpretation of the observed isomeric states in terms of the configurations given in the table. (The discrepancy for the gyromagnetic ratio of the $^{13/2}^+$ level is explained³ by the admixture of the configuration $f_{\frac{1}{2}}^3 \otimes 3$ in the observed state.) The configuration^{3,4} $[\pi\{(d_{\frac{1}{2}}^{5-2})_0(h_{\frac{1}{2}}^{11-2})_0\} \nu\{(h_{\frac{1}{2}}^{11-1} i_{\frac{1}{2}}^{13})_{11} f_{\frac{1}{2}}^3\}]_{49+}$ lies in this model 1.4 MeV above the yrast line, has $Q = -1.59$ eb, $g = 0.36$, and is not a trap. (Cfr the discussion of similar states in ref. 5.)

⁺Work supported in part by BMFT, GSI Darmstadt, and the Danish Scientific Research Council.

References:

1. K. Neergård et al., Proc. Int. Symp. High-Spin States in Nuclei, Argonne 1979, to be published
2. R. Broda et al., Z. Phys. **A290**, 279 (1979)
3. O. Häusser et al., Phys. Rev. Lett. **42**, 1451 (1979)
4. O. Häusser et al., Phys. Rev. Lett. **44**, 132 (1980)
5. K. Matsuyanagi et al., Nucl. Phys. **A307**, 253 (1978)

Table
Isomeric states in ^{147}Gd

I^π	E (MeV)	Calculation Configuration ^a	β	\bar{Q} ^b (eb)	Q^c (eb)	g	Experiment ^{3,4}			
							E (MeV)	$t_{1/2}$ (ns)	Q (eb)	g
$\frac{3}{2}^-$	0	$\nu f_{7/2}^2$	0.03	-0.52	-0.45	-0.33	0			
$\frac{13}{2}^+$	0.8	$\nu i_{13/2}^2$	0.04	-0.69	-0.61	-0.18	0.997	22.2(5)	0.73(7)	-0.04(1)
$\frac{27}{2}^-$	4.2	$\pi \{(d_{5/2}^{5-2})_0 (h_{7/2}^{11-2})_0\} \nu f_{7/2}^2$	0.06	-1.02	-1.45	0.61	3.582	26.8(7)	1.26(8)	0.84(2)
$\frac{49}{2}^+$	8.1	$\pi \{(d_{5/2}^{5-2})_0 (h_{7/2}^{11-2})_0\} \nu \{(d_{5/2}^{3-2})_{1/2} \{i_{13/2}^{13} h_{7/2}^9\}\}$	0.19	-3.14	-3.35	0.47		510(20)	3.14(17)	0.45(1)
$\frac{57}{2}^-$	11.2	$\pi \{(d_{5/2}^{5-2})_{1/2} (h_{7/2}^{11-2})_{1/2}\} \nu \{(d_{5/2}^{3-2})_{1/2} \{i_{13/2}^{13} h_{7/2}^9\}\}$	0.20	-3.30	-3.57	0.60				

^a The configuration develops continuously into this state for $\beta \rightarrow 0$.

^b Quadrupole moment of a homogeneously charged ellipsoid with the deformation β .

^c Quadrupole moment calculated from our model.

IDENTIFICATION OF HIGH SPIN ISOMERS NEAR $N = 82$

S. André, J. Genevey, A. Gizon, J. Gizon
Institut des Sciences Nucléaires, IN2P3, Grenoble, France

J. Jastrzębski, J. Łukasiak, M. Moszyński, Z. Preibisz
Institute for Nuclear Research, Swierk, Poland

Targets of $10\text{-}20\text{ mg/cm}^2$ ^{141}Pr , ^{144}Sm and ^{147}Sm were bombarded with $70\text{-}130\text{ MeV}$ ^{12}C , ^{14}N and ^{16}O beams from the Grenoble variable energy cyclotron. The Ge(Li) gamma ray spectra were recorded between the beam bursts in coincidence with γ -rays detected by a multiplicity filter consisting of 14 NaI(Tl) detectors.

The unambiguous identification of many high spin isomers near $N = 82$ was achieved through excitation function measurements, cross bombardments and γ - γ coincidence data.

Short half-lives (up to $\sim 20\text{ ns}$) were measured in Ge(Li)-RF coincidence experiments and long ones (from $\sim 20\text{ ns}$ to $\sim 1\mu\text{s}$) deduced from Ge(Li)-NaI coincidences. The very long half-lives in ^{151}Er and ^{149}Dy were obtained from γ decay using a mechanical beam chopper. The average delayed multiplicities are deduced from the ratios of γ -intensities in the x -fold coincidence spectra.

The table given in the following page precises and extends informations partly reported previously ¹. The excitation energy of the compound nucleus (listed in column 4 and calculated at the half-thickness of the target) corresponds to the maximum cross-section for the formation of the isomer. Spins in column 7 are estimated from the expression $I_{is} = 1.7 \bar{M}_d + I_0$ where I_0 is the spin of the ground state or of a lower isomeric state; values in parenthesis are taken from the literature or deduced from systematics.

References to parallel search of high spin isomers in this region by other groups are given in reference 1 or quoted below ²⁻⁶.

1. J. Jastrzębski et al., Proc. Conf. on Large Amplitude Collective Nuclear Motions, Balaton, June 1979, p. 71.
2. T.L. Khoo, Proc. Symp. on High Spin Phenomena in Nuclei, Argonne, March 1979, p. 95.
3. P. Kleinheinz, *ibid.* p. 125.
4. D. Hageman et al., Phys. Lett. **84B**, 301 (1979).
5. L. Carlen et al., Nordic Symposium on Nucl. Phys., Lysekil, Sweden, (1979).
6. J. Borggreen et al., to be published.

Table of identified isomers

Final Nucleus	$T_{1/2}$	Identified transitions (keV)	C.N. and peak ex. en. (MeV)	\bar{M}_d		
				\bar{M}_d	E_{is} (MeV)	I_{is}
^{153}Er	450 ± 50 ns	300, 340, 588 712, 812	^{156}Er (47)	5.6 ± 1.0	≥ 2.75	25/2
	350 ± 50 ns	349, 356, 363, 418, 746, 910	^{156}Er (57)	8.6 ± 1.0	≥ 5	37/2
^{152}Er	3.5 ± 1.0 ns	280, 423, 554, 673, 764, 787, 808	^{156}Er (59)	9 ± 2 (a)	≥ 4.29	14
	35 ± 10 ns	previous and 175, 230, 330, 518, 561, 564, 730, 940, 1052, 1210	^{156}Er (65)	14 ± 2 (b)	≥ 7	24
^{151}Er	6 ± 2 ns	1141	^{156}Er (≥ 75)		1.14	(13/2)
	0.62 ± 0.02 s	289, 1100, 1141		3.0 ± 0.5	> 2.5	(27/2)
^{153}Ho	40 ± 10 ns	533, 557, 576, 632	^{156}Er (50)	≥ 4.8		$> (27/2)$
	240 ± 20 ns		^{157}Ho (≤ 59)			
^{152}Ho	10 ± 3 ns	143	^{156}Er (59)	6.5 ± 1.0	≥ 2.87	20
	55 ± 10 ns	143, 198, 451, 511, 704, 865	^{157}Ho			
	70 ± 10 ns $2 \leq T_{1/2} \leq 200\mu\text{s}$	604, 712, 734, 759	^{156}Er (64) ^{157}Ho			
^{151}Ho	3 ± 1 ns	129, 246, 297 309, 414, 456, 486, 597, 789, 1024, 1397	^{156}Er (≥ 75)	12 ± 1	> 6.14	$\geq 51/2$
	$5 \leq T_{1/2} \leq 200\mu\text{s}$		^{157}Ho	11 ± 1	> 6.14	$\geq 49/2$
^{150}Ho	20 ± 10 ns	1097	^{156}Er (> 75)	7 ± 2	≥ 2.5	(11)
	80 ± 15 ns	226, 264, 280, 313, 629, 1097	^{157}Ho			23
^{149}Dy	0.51 ± 0.01 s	110, 298, 1073, 1178	^{156}Er (75)	2.7 ± 0.5	2.66	(27/2)
	25 ± 5 ns	200, 240, 255, 270, 430, 490, 742, 985, 1336, 1393	^{156}Er (≥ 75)	8 ± 1	> 6.1	53/2
^{148}Tb	20 ± 2 ns	1006	^{153}Tb (72)	11.8 ± 1.0	> 6.6	(11)
	1.3 ± 0.5 μs	140, 214, 240, 284, 340, 351, 427, 454, 522, 621, 634, 743, 780, 803, 828, 930, 1006, 1334				29

(a) The delayed multiplicity \bar{M}_d is measured at $\bar{E}_{lab} = 74$ MeV

(b) \bar{M}_d measured at $\bar{E}_{lab} = 90$ MeV

HOW PARTICLE-OCTUPOLE EXCHANGE COUPLING AFFECTS THE YRAST LINES OF DYSPROSIUM NUCLEI

P.J. Daly[†], P. Kleinheinz, R. Broda, S. Lunardi, H. Backe*, J. Blomqvist**
 Institut für Kernphysik, KFA Jülich, D-5170 Jülich, F.R. Germany

Isomeric states involving two $h_{11/2}$ valence protons have been identified^{1,2} in the N=82 and N=83 nuclei ^{148}Dy and ^{149}Dy . A final analysis of the in-beam data showed that in both cases these yrast isomers are dominantly fed through E1 transitions of about 1 MeV. The next higher yrast transition in ^{148}Dy is of M1 character, whereas only $\lambda = 1$ is known for the corresponding yrast transition in ^{149}Dy (cf. fig. 1).

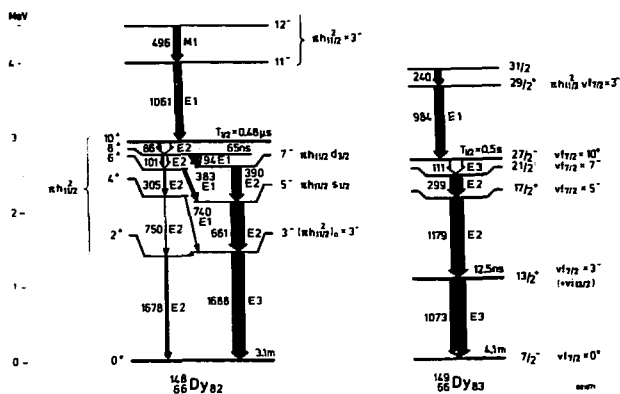


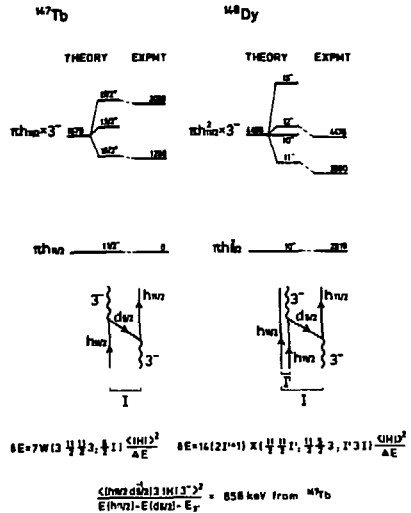
Fig. 1: Yrast states in ^{148}Dy and ^{149}Dy . Intensities from (α, xn) experiments; multiplicities from conversion electron data.

At $I = 10$ the ^{148}Dy valence spin is exhausted, and higher yrast states must involve breaking of the ^{146}Gd core. Since the 3^- octupole state is the lowest core excitation, one would expect the yrast line to continue by excitations of the type $10^+ \times 3^-$, and we interpret the 3980 keV 11^- level as the lowest lying member of an octupole multiplet built on the $(\pi h_{11/2}^-)10^+$ state. Since the $(\pi h_{11/2}^- d_{5/2}^-)3^-$ configuration provides the dominant amplitude of the core 3^- excitation, one expects that the energies of the $\pi h_{11/2}$ particle plus octupole multiplet members will be strongly affected by the Pauli principle.

The figure 2 shows the particle-phonon exchange diagram appropriate to the ^{148}Dy case. The corresponding diagram³ for the Z=65 nucleus ^{147}Tb , which has one $h_{11/2}$ proton in its ground state, is included for comparison. The equations giving the energy shifts δE for the individual particle plus octupole multiplet members are also given, where W denotes a Racah coefficient and X is a 9j symbol. The crucial point here is that the energy factor containing the interaction matrix element is the same as in the ^{147}Tb case, and this makes it possible to use that empirical energy factor from one particle-phonon coupling to describe the exchange interaction of two particles with the phonon. The measured³ 772 keV $15/2^+$ to $17/2^+$ energy splitting in ^{147}Tb gives for that factor a value of $\langle |H| \rangle^2 / \Delta E = 856 \text{ keV}$ which we have used to calculate the expected energy shifts for the four highest spin members of the $\pi h_{11/2}^- \times 3^-$ octupole

multiplet in ^{148}Dy as shown to the right. The $\pi h_{11/2}^2$ couplings $I' = 10$ and $I' = 8$ both contribute to the 11^- and 10^- states and the theoretical energies shown are the lower energy solutions from diagonalizing the interaction in this two dimensional basis. The good agreement gives strong support for the identification of the observed 3.980 MeV 11^- and 4.476 MeV 12^- states in ^{148}Dy with the calculated $\pi h_{11/2}^2 \times 3^-$ multiplet members.

Fig. 2: One particle-phonon and two particle-phonon exchange coupling and observed $\pi h_{11/2}^2 \times 3^-$ and $\pi h_{11/2}^2 \times 3^-$ particle-phonon multiplet members in ^{147}Tb and ^{148}Dy .



The interpretation of the ^{149}Dy $29/2^+$ level at 3.645 MeV is quite analogous, and we note that such $\Delta I = 1$ octupole excitations also occur in the yrast lines of the heavier Dysprosium isotopes. E.g. an E1 transition of 742 keV in ^{150}Dy connects⁴ the 5.813 MeV 19^- yrast state to the $(\pi h_{11/2}^2 \nu f_{7/2} h_{9/2}) 18^+$ level, and in ^{151}Dy the $(\pi h_{11/2}^2 \nu h_{9/2} f_{7/2}) 41/2^-$ state is fed⁵ by an 839 keV E1 γ -ray from the $(41/2^- \times 3^-) 43/2^+$ yrast state at 5.744 MeV. In all cases these $\Delta I = 1$ octupole excitations are built upon yrast states where all valence nucleons are aligned and where the $\pi h_{11/2}$, $\nu f_{7/2}$, and $\nu h_{9/2}$ valence spin is exhausted. The fact that octupole core excitation competes with lifting of a neutron into the $i_{13/2}$ single particle state reemphasizes the rather high⁷ single particle energy of that orbital.

1. P.J. Daly et al., Z. Physik A288 (1978) 103
2. A.M. Stefanini et al., Nucl. Phys. A258 (1976) 34, and Phys. Lett.62B(1976)405
3. R. Broda et al., Z. Physik A293 (1979) 135
4. S. Lunardi et al., Proc. ASHPIN, ANL/PHY-79-4, p. 403
5. M. Piiparinen et al., Z. Physik A290 (1979) 337
6. our recent αK measurement gave E1 for the 839 keV transition, contrary to the earlier adopted M1 multipolarity and in accord with the results of T.L. Khoo, Proc. ASHPIN, ANL/PHY-79-4, p. 95
7. S. Lunardi et al., Proc. ASHPIN, ANL/PHY-79-4, p. 393

+ Visitor from Dept. of Chemistry, Purdue University, Lafayette, Ind., USA
 * TH Darmstadt, F.R. Germany
 ** Research Institute for Physics, Stockholm, Sweden

HIGH SPIN SHELL MODEL EXCITATIONS IN ^{149}Gd

M. Piiparinen, R. Pengo, Y. Nagai, P. Kleinheinz, N. Roy*, L. Carlen*,
H. Ryde*, Th. Lindblad†, A. Johnson†, S.A. Hjorth†, E. Hammarén††,
Institut für Kernphysik, KFA Jülich, D-5170 Jülich, F.R. Germany

We have studied the high spin level structure of the ^{149}Gd nucleus which has three neutrons outside the doubly closed ^{146}Gd core using standard in-beam γ ray spectroscopy methods. With α -particle beams between 38 and 69 MeV from the IKP or AFI cyclotrons the $(\alpha,3n)$, $(\alpha,4n)$, and $(\alpha,5n)$ reactions leading to ^{149}Gd were investigated; the experiments included excitation function-, angular distribution-, linear polarization-, and two parameter (E_γ , $t_{\gamma\text{RF}}$) timing measurements as well as extensive four-parameter $\gamma\gamma$ -coincidence studies.

The ^{149}Gd level scheme resulting from these experiments is shown in fig. 1. The lifetime measurements have located a $T_{1/2} = 6.2 \pm 0.3$ ns isomeric level at 3.39 MeV which has $I^\pi = 27/2^-$. Another, shorter half life of 1.6 ± 0.5 ns could be attributed to the $11/2^+$ level at 0.87 MeV.

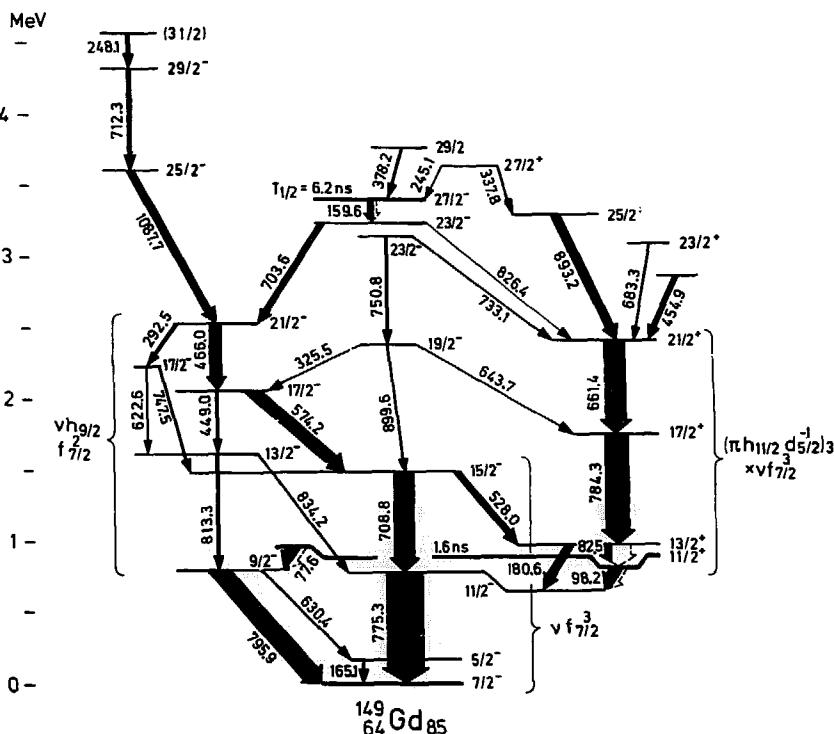


Fig. 1: High spin levels and shell model configurations of ^{149}Gd . Gamma ray intensities as observed with 66 MeV α particles in $(\alpha,5n)$ are shown.

Most of the ^{149}Gd levels up to 2.8 MeV excitation can be characterized within the spherical shell model. The (measured¹ $I=7/2$) ground state together with the strongly fed $11/2^-$ and $15/2^-$ levels are formed by the three $f_{7/2}$ valence neutrons. This characteristic $\nu f_{7/2}^3$ yrast triplet occurs repeatedly in $N=85$ isotones. The low-lying $5/2^-$ level is interpreted as the $(\nu f_{7/2}^3)_{5/2}$ configu-

ration. Its low excitation is due to the large negative quadrupole moment of the $(j^3)_{j-1}$ configuration which gives rise to a lowering of the energy through the quadrupole interaction.

Beta decay data² characterize the 796 keV level as $h_{9/2}$ single neutron state. The two remaining valence neutrons in $f_{7/2}$ form the characteristic $(f_{7/2}^2)0^+, 2^+, 4^+$, and 6^+ levels known from the N=84 isotones. Combined with the 796 keV $vh_{9/2}$ state levels with spins 9/2, 13/2, 17/2 and 21/2 are formed which are all observed. The 17/2 member lies irregularly low in energy, apparently due to interaction with the (so far not interpreted) second $17/2^-$ state at 2.21 MeV.

The lowest $13/2^+$ level of odd N nuclei in this region is usually attributed to the expected $i_{13/2}$ neutron single particle state. However it has recently been shown^{3,4} that the ^{146}Gd core octupole state lies lower than the unperturbed $vi_{13/2}$ single particle state at N=83, which suggests that the ~ 1 MeV $13/2^+$ states in N=83 and 85 are predominantly $(vf_{7/2} \times 3^-)_{13/2^+}$ excitations rather than $vi_{13/2}$ single particle states, although one of course expects the two configurations to be strongly admixed. This interpretation is further supported by the present results for ^{149}Gd , where the characteristic $vf_{7/2}^3$ yrast states are combined with the $13/2^+$ level, forming the $11/2^+$, $13/2^+$, $17/2^+$, and $21/2^+$ states in the energy range from 0.8 to 2.4 MeV. The $(vf_{7/2}^3)_{5/2}$ state, which lies at 165 keV, in combination with the predominant proton particle hole octupole excitation is further lowered through the quadrupole interaction and occurs here 83 keV below the $(vf_{7/2}^2)_{7/2} \times 3^-$ state, an effect which is repeatedly found in the N=85 isotones. The levels above 2.8 MeV could so far not be interpreted in detail. One knows³ however from the neighbouring ^{148}Gd nucleus that proton particle hole excitations play a dominant role in the yrast states at these energies, and one therefore should expect rather complex structure for the ^{149}Gd yrast levels above 2.8 MeV.

The $f_{7/2}^3$ and $h_{9/2}f_{7/2}^2$ yrast configurations observed in ^{149}Gd strongly resemble those in the other N=85 $^{147}\text{Sm}^5$ and $^{151}\text{Dy}^6$ isotones as well as of the odd-odd nucleus $^{150}\text{Tb}^7$. The occurrence of these characteristic three-neutron multiplets proved to be a valuable tool in determining shell model configurations. In particular the observation of an $(f_{7/2}^2)0^+, 2^+, 4^+, 6^+$ sequence indicates the removal of one valence neutron from the $f_{7/2}$ shell, whereas $f_{7/2}^2$ level sequences are associated with e.g. proton excitations in the N=85 isotones.

1. G.E. Holland, Nucl. Data Sheets 19 (1976) 337
2. K.S. Toth, E. Newman, C.R. Bingham, A.E. Rainis, W.-D. Schmidt-Ott, Phys. Rev. C11 (1975) 1370
3. S. Lunardi, M. Ogawa, M.R. Maier, P. Kleinheinz, Contr. to ASHPIN, Argonne, March 1979, p. 393
4. P.J. Daly, P. Kleinheinz, R. Broda, S. Lunardi, H. Backe, and J. Blomqvist, Z. f. Physik, in press
5. M. Piiparinen, Y. Nagai, J. Styczen, P. Kleinheinz, separate contribution on ^{147}Sm to this conference
6. M. Piiparinen, S. Lunardi, P. Kleinheinz, H. Backe, J. Blomqvist, Z. f. Physik A290 (1979) 337
7. R. Broda, M. Ogawa, P. Kleinheinz, R.K. Sheline, L. Richter, Contr. to ASHPIN, Argonne, March 1979, p. 401, and IKP, KFA Jülich Annual Report 1978, p. 29

* University of Lund, Sweden

+ AFI Stockholm, Sweden

++ University of Jyväskylä, Finland

A STUDY OF THE γ -RAY CONTINUUM FEEDING HIGH SPIN STATES IN $^{151,152}\text{Dy}$

J.F.Sharpey-Schafer[†], A.J.Ferguson, H.R.Andrews, O.Häusser,
H-E.Mahnke[‡], D.Ward
Chalk River Nuclear Laboratories, Chalk River, Ontario, Canada

Previous experimental data¹ on γ -ray continuum feeding in $^{151,152}\text{Dy}$ indicated that these nuclei may undergo a shape change from weakly oblate² to strongly prolate deformations at spins greater than $40\hbar$. The purpose of the present experiment was to try to distinguish experimentally between this proposed shape change and the continuum radiation that would be produced by decay to the yrast line down oblate bands based on the yrast states as band heads.

The reactions used were $^{124}\text{Sn}(^{32}\text{S};5,4n)^{151,152}\text{Dy}$ the ^{32}S beam being pulsed in bunches less than 5 ns wide with 400 ns between bunches. Gamma rays were detected in two GeLi detectors at 0° and 55° to the beam direction and in an array of four 12.5 cm by 15 cm NaI detectors at angles 90° , 120° , 135° and 150° . Only γ -rays prompt with the beam were accepted in the large NaI detectors, neutrons being excluded by time-of-flight over the 50 cm distance between target and NaI. A further array of four smaller NaI detectors (7.5 cm by 7.5 cm) were used to detect delayed γ -rays from the higher spin isomers at 5035 keV ($J = 15$) with mean-life ~ 60 ns in ^{152}Dy and at 6033 keV ($J = 49/2$) with mean-life ~ 13 ns in ^{151}Dy . These delayed pulses were used to trigger the large NaI detectors and the GeLi detectors, which were also required to observe γ -rays that were prompt with the beam pulse, so that the GeLi spectra consisted mainly of γ -rays from levels above the high spin isomers³. By requiring different delays on the trigger pulse, GeLi spectra could be obtained containing different amounts of ^{151}Dy and ^{152}Dy γ -rays. Linear combinations of these spectra were then made so that both GeLi and NaI spectra could be obtained which contained either only ^{151}Dy , γ -rays or only ^{152}Dy γ -rays.

γ - γ coincidences between GeLi detectors and the large NaI detectors were recorded at 155 MeV beam energy, and the multiplicity was measured of the γ -rays in coincidence with the discrete yrast γ -rays above the high spin isomers. At 135 MeV γ - γ coincidences were measured where the trigger was now prompt with the beam so that the angular distribution of the continuum radiation directly feeding levels below the high spin isomers could be measured. An excitation function was measured over the range 135(10)165 MeV with only coincidences required between the delayed trigger and either a GeLi or a NaI detector.

The discrete transitions have been subtracted from the NaI spectra which have then been unfolded. These spectra show a maximum intensity at about 1.3 MeV and a sharp drop below about 0.9 MeV. Preliminary indications are that these γ -rays are directly feeding the yrast line and do not arise from a shape change above $40\hbar$.

1. W.Trautmann et al P.R.L. 43 991 (1979).
2. O.Häusser et al P.R.L. 44 132 (1980).
3. T.L.Khoo et al P.R.L. 41 1027 (1978).

[†] Summer visitor from the University of Liverpool, U.K.

[‡] Summer visitor from the Hahn-Meitner-Institut, Berlin, F.R.G.

HIGH SPIN YRAST STATES IN ^{151}Ho

J. Gizon, A. Gizon, S. André, J. Genevey
 Institut des Sciences Nucléaires, IN2P3, Grenoble, France

J. Jastrzębski, J. Łukasiak, M. Moszyński, Z. Preibisz
 Institute for Nuclear Research, Swierk, Poland

Levels in ^{151}Ho have been populated in ^{12}C and ^{16}O induced reactions on ^{144}Sm and ^{141}Pr targets, respectively, with beams delivered by the Grenoble variable energy cyclotron. The nucleus ^{151}Ho has been identified by excitation function measurements and cross bombardments.

The partial level scheme shown in the figure is obtained from studies of in-beam and out-of-beam singles spectra, angular distribution and linear polarization of γ -rays and four dimensions (γ - γ - $t_{\gamma\text{-RF}}$ - $t_{\gamma\gamma}$) coincidence events.

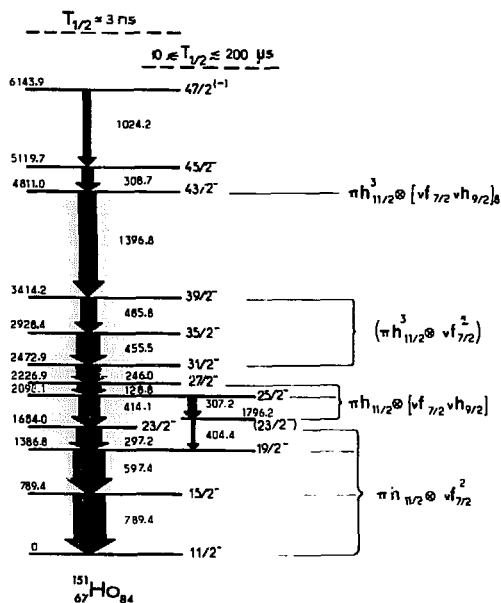
The existence of a short-lived isomer ($T_{1/2} = 3 \pm 1$ ns) has been revealed by means of a multiplicity filter made of fourteen $2'' \times 2''$ NaI(Tl)

detectors. The delayed multiplicity \bar{M}_d associated with the cascade generated from this isomer was determined to be 12 ± 1 .

A long-lived isomer ($10 \mu\text{s} \lesssim T_{1/2} \lesssim 200 \mu\text{s}$) very weakly excited has been observed in a delayed γ - γ (Ge(Li)-NaI) coincidence experiment. Its multiplicity is $\bar{M}_d \approx 11$. The ratio of the cross-sections

$\sigma_{\text{short}}/\sigma_{\text{long}}$ is roughly 80.

The three strongest stretched E2 transitions depopulate the three lowest excited levels with energies similar to those of the 2^+ , 4^+ and 6^+ levels in the core nucleus ^{150}Dy . So,



the $11/2^-$, $15/2^-$, $19/2^-$ and the lower $23/2^-$ levels correspond to the coupling of a fully aligned $h_{11/2}$ proton with two $f_{7/2}$ neutrons. The $27/2^-$ and $25/2^-$ levels, which are de-excited by transitions having strongly negative A_{22} angular distribution coefficients typical of $M1 + E2$ admixtures, and a second $23/2^-$ state are very likely the result of the coupling between 8^+ , 7^+ , 6^+ core states ($\nu f_{7/2} \otimes \nu h_{9/2}$) and an $h_{11/2}$ proton.

A second cascade of three stretched E2 transitions gives rise to $31/2^-$, $35/2^-$ and $39/2^-$ levels which could be members of the multiplet resulting in the coupling of a third $h_{11/2}$ neutron with the $(\pi h_{11/2}^2)_{10} \otimes \nu f_{7/2}^2$ states. A 1.4 MeV gap exists between the $39/2^-$ and $43/2^-$ levels. This $43/2^-$ state whose energy is similar to the one of the 18^+ core level has very likely a $\pi h_{11/2}^3 \otimes (\nu f_{7/2} \nu h_{9/2})_8$ configuration. Such an assignment is also very well supported by the energy difference (2584 keV) between the $43/2^-$ and $27/2^-$ levels which fits perfectly the difference in excitation (2669 keV) between the 18^+ and 8^+ levels in ^{150}Dy . The Yrast sequence is established up to a $I = 47/2^{(-)}$ level at 6.1 MeV excitation energy.

In conclusion, it appears that the low energy part of the ^{151}Ho level structure has similarities with those of neighbouring odd-A nuclei (isotones and ^{151}Tb) and that the observed levels are qualitatively understood in terms of coupling of an $h_{11/2}$ proton to the core nucleus ^{150}Dy .

1. P. Kleinheinz, Proc. Symp. on High-Spin Phenomena in Nuclei, Argonne, 1979, p. 125.

ROTATION-ALIGNED BAND IN THE ODD-ODD ^{152}Eu NUCLEUS.

J.A.Pinston, R.Bengtsson, D.Barneoud^{††}, A.Monnand, F.Schussler
 Centre d'Etudes Nucléaires - DRF/CPN, 85 X, 38041 Grenoble Cedex, France
^{††}Institut des Sciences Nucléaires (IN2P3), 38044 Grenoble Cedex, France

The rotational bands in the odd-odd ^{152}Eu have been studied by means of the $^{150}\text{Nd} (^7\text{Li}, 5n)$ reaction. The experiments were performed at the Grenoble cyclotron and conventional in beam γ -spectroscopic methods were used. The complicated low energy part ($E < 200$ keV) of ^{152}Eu level scheme was earlier investigated by (n, γ) reaction¹ and it was then possible to make the connection between these known levels and the rotational structures fed by ^7Li reaction. Two rotational bands have been evidenced in this work : i) a strongly coupled band based on the isomeric state 8^- ($T_{1/2} = 96$ m) of configuration (ν $11/2^-$ [505], π $5/2^+$ [413]) and populated up to the spin value $I = 16$, ii) a decoupled system starting on a 286 keV level ($T_{1/2} = 3.5$ ns) of spin and parity $I^\pi = 7^-$, populated up to the spin $I = 17$ and belonging to the configuration (π h $11/2$, ν i $13/2$). The more interesting case, namely the system based on the two unique parity states is discussed.

In ref.² a method was described for calculating the aligned angular momentum of excited configurations, using the experimental rotational bands. By introducing a reference configuration with angular momentum $I_x^0(\omega) = \mathcal{J}_0\omega + \mathcal{J}_1\omega^3$ the aligned angular momentum can be calculated as $i_x(\omega) = I_x(\omega) - I_x^0(\omega)$.

For light rare earth nuclei the same method cannot be used, since the potential energy surface is here relatively flat, and the presence of excited quasiparticles has a non-negligible influence on the quasiparticle vacuum, and a unique reference configuration cannot be determined. However, for such configurations where the excited quasiparticles are in the $h_{11/2}$ -proton or $i_{13/2}$ -neutron shell, theoretical calculations predict a practically constant value of $i_x(\omega)$ over a quite large interval in ω . Making the ansatz $I_x(\omega) \approx \mathcal{J}_0\omega + \mathcal{J}_1\omega^3 + i_x$ then allows to fit \mathcal{J}_0 and \mathcal{J}_1 , necessary for describing the reference configuration, as well as an average value of the aligned angular momentum, i_x , of each configuration.

The corresponding moment of inertia $\mathcal{J}^{\text{eff}}(\omega) = I_x(\omega)/\omega = \mathcal{J}_0 + \mathcal{J}_1\omega^2 + i_x/\omega$ goes to infinity when ω goes to zero. This should be a characteristic property of all configurations, having a finite aligned angular momentum, and it is well confirmed by experiment as seen in Fig.1. Fig.2 shows $i_x(\omega) = I_x(\omega) - \mathcal{J}_0\omega - \mathcal{J}_1\omega^3$. Note especially that $i_x(\omega)$ for the odd-odd nucleus ^{152}Eu can be satisfactorily explained as the sum of a neutron contribution (estimated to be approximately the same as in ^{153}Gd) and a proton contribution (taken from ^{153}Eu). The neutron is always placed in the $[i_{13/2}; \alpha = 1/2]$ while the proton may be placed either in the $[h_{11/2}; \alpha = -1/2]$ giving $\alpha = 0$ (even spin) in ^{152}Eu or in the $[h_{11/2}; \alpha = 1/2]$ level giving $\alpha = 1$ (odd spin) in ^{152}Eu .

1. T.Von Egidy et al. Z. Physik A286 (1978) 341.
2. R. Bengtsson, S. Frauendorf, Nucl. Phys. A327 (1979) 139.

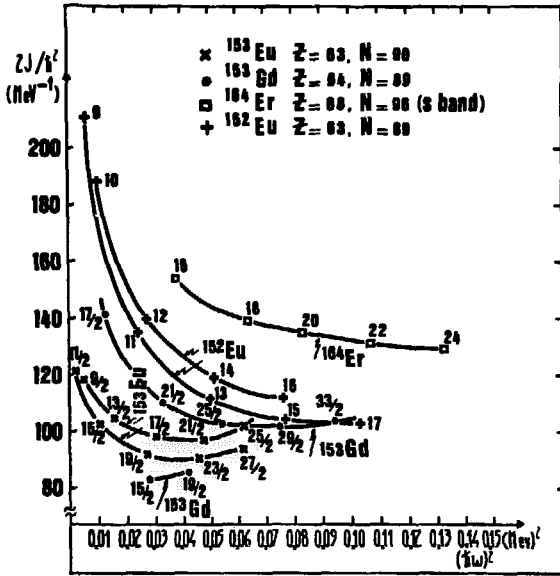


Fig.1 - The effective moment of inertia as a function of ω^2 for e-e, o-e, e-o and o-o nuclei in the mass region $A \sim 152$. The strong increase of \mathcal{J} when ω goes to zero is a characteristic property of all configurations having $i_x = 0$, and follows directly from the relation $\mathcal{J}^{\text{eff}} \approx \mathcal{J}_0 + \mathcal{J}_1 \omega^2 + i_x/\omega$.

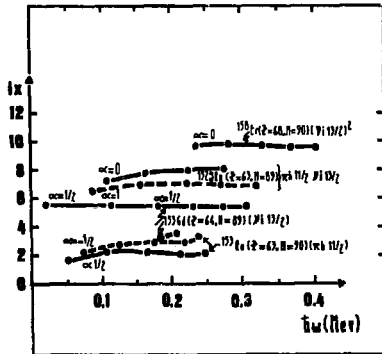


Fig.2 - The experimental aligned angular momentum as a function of ω for e-e, o-e, e-o and o-o nuclei in the mass region $A \sim 152$.

THE X- (OR Δ) TRANSITION IN ^{152}Dy

Y. Nagai, J. Styczen, M. Piiparinen, P. Kleinheinz
Institut für Kernphysik, KFA Jülich, D-5170 Jülich, F.R. Germany

The ^{152}Dy nucleus has attracted great interest since some time ago¹ its yrast levels up to 12.7 MeV excitation have been observed. More recently, $T_{1/2}$ and polarization measurements have established relative spins and parities for the states above 5 MeV. However, the data from different groups^{1,3,4} on the low-lying levels so far are incomplete or contradictory. In particular, disagreement⁴ exists about the occurrence of a low energy isomeric transition (X^3 , or Δ^1) feeding the 5035 keV state. Since furthermore the multipolarity of the lower lying 604 keV transition is not clear^{1,3} the presently available data would allow $I = 15, 16, 17$ or 18 for the 50 ns isomer in ^{152}Dy , with equal uncertainties for all higher lying yrast states. These short comings have greatly impeded comparison with experiment of several⁵ yrast level calculations for ^{152}Dy .

We have reinvestigated ^{152}Dy with the $(\alpha, 4n)$ reaction at 60 MeV using a $200 \mu\text{g}/\text{cm}^2 > 99\%$ enriched ^{152}Gd metal target on a $\sim 50 \mu\text{g}/\text{cm}^2$ C foil backing. In a four parameter $\gamma\gamma$ coincidence experiment one detector (1 cm^3 Ge) was optimized for detection of low energy γ -radiation. In order to eliminate the very intense Gd K and L X-rays arising from target ionization the 1 cm^3 detector was shielded from the target by a .5 mm thick Pd absorber, whereas the γ radiation coming from the recoil catcher .7 cm behind the target was observed unattenuated. With this technique reliable in-beam coincidence data could be obtained for low energy γ -rays down to ~ 5 keV.

The coincidence data reveal a previously unknown 53.3 ± 0.2 keV transition which can be shown to be the 50 ns isomeric transition in ^{152}Dy . The transition is not resolved from the Dy $K_{\beta 2}$ X-ray at 53.5 keV which however can be estimated to contribute little to the 53.3 keV peak from comparison with the observed Dy $K_{\beta 1}$ intensity.

The multipolarity of the 53.3 keV isomeric transition must be extracted from the coincidence data since in the singles spectra the transition cannot be resolved from the 53.4 keV ($T_{1/2} = .5$ s) transition in ^{73}Ge . Our data give three independent intensity ratios which determine that multipolarity. The Dy K_{α} to 53 keV intensity ratio can be extracted from spectrum where due to recoil shadow and t_{YRF} timing conditions only K_{α} X-rays originating from K-conversion of post 50 ns isomeric transitions are recorded. From a coincidence spectrum extending to energies up to 700 keV the 604 + 610 to 53 keV intensity ratio can be determined. Finally, a recoil shadow coincidence spectrum including the Dy L X-rays gives the Dy L X-ray to 53 keV intensity ratio. The results are compiled in the Table and compared with ratios calculated from our measured γ -intensities in the decay of the 50 ns isomer assuming different multiplicities for the 53 keV transition. All three results give E2 for the 53 keV isomeric transition.

From the present work the spins of the ^{152}Dy yrast states above 5 MeV are now determined if one accepts $\lambda = 1$ for the 604 keV transition suggested in Ref.1, which makes comparison with calculated yrast levels more attractive. However, still only relative parities are known for the ^{152}Dy yrast states above 4.5 MeV.

Table 1: Measured intensity ratios compared to values calculated for different multipolarities of the 53 keV transition

	E1	M1	E2	M2	Expmt.
Dy KX/53	14	5.3	.56	.21	.48(16)
1/2 (604+610)/53	1.0	2.7	26	67	21(6)
Dy LX/53	.04	.26	3.2	9.1	1.5(6)

1. T.L. Khoo et al. Phys. Rev. Lett. 41 (1978) 1027
2. B. Haas et al. Phys. Lett. 84B (1979) 178
3. J.F.W. Jansen et al. Nucl. Phys. A321 (1979) 365
4. J.C. Merdinger et al. Phys. Rev. Lett. 42 (1979) 23
5. C.G. Andersson et al. Nucl. Phys. A309 (1978) 141;
 M. Cerkaski et al. Nucl. Phys. A315 (1979) 269;
 A. Faessler et al. Proc. ASHPIN, Argonne, March 1979, p. 551 and to be publ.
 in Z. Phys. A;
 G. Leander et al. Proc. ASHPIN, Argonne, March 1979, p. 197 and references
 given therein

CONTINUUM γ -RAY SPECTRA AND EXCITATION FUNCTIONS
OF YRAST STATES IN ^{152}Dy *

I. Ahmad, J. Borggreen, ** P. Chowdhury, T. L. Khoo, R. K. Smither
Argonne National Laboratory, Argonne, Illinois 60439, U.S.A.

S. R. Faber, C. L. Dors, J. Wilson, P. J. Daly
Purdue University, W. Lafayette, Indiana 47907, U.S.A.

Beams of ^{34}S from the Argonne superconducting linac booster have been utilized to populate states in ^{152}Dy in an attempt to study the nature of the γ -ray transitions connecting the entry region with the yrast line and to understand in detail the population process of the yrast line.¹

Two series of experiments have been done. In one, the population intensities of yrast states in ^{152}Dy were studied as a function of bombarding energy with $144 \leq E_S \leq 184$ MeV. In the other, continuum γ spectra were measured at $E_S = 150$ and 162 MeV with a 25 cm diam. \times 30 cm NaI crystal with a 7.5 cm diam. central collimator. The γ rays in both experiments were observed in coincidence with a sum-spectrometer consisting of two 33 cm \times 15 cm NaI crystals; enhancement of high- ℓ events was obtained by selecting higher sum energies.

For bombarding energies ≥ 160 MeV, corresponding to $\ell_{\text{max}} \approx 57 \hbar$, states with spins of up to $29 \hbar$ receive close to 100% of the $(^{34}\text{S}, 4n)^{152}\text{Dy}$ cross section, indicating little or no side-feeding below this spin. The population of states with higher spin does not increase even at higher bombarding energies (corresponding to higher angular momentum input). In contrast, a monotonic decrease in yrast population with spin is usually observed in studies on prolate deformed nuclei.

The NaI spectra exhibit an enhanced yield between 1.2 and 1.6 MeV, well separated from any known discrete lines. Anisotropy measurements of this energy region suggest that it consists of many unresolved stretched quadrupole transitions.

These results imply that the deexcitation of high- ℓ events ($\ell \gtrsim 35 \hbar$) is not feeding the yrast line directly via statistical transitions, but is diverted by continuum cascades of E2 character, and only reaches the yrast line at $\ell \sim 29$ - $37 \hbar$. The fact that the high energy edge of the "bump" remains fairly constant over a large range of incoming ℓ -values implies a moment of inertia which seems to increase with spin.

* Supported by the U. S. Department of Energy.

** Supported by the Danish National Science Research Council.

K-SHELL IONIZATION YIELDS FOR ($^{40}\text{Ar}, 4n$) REACTIONS LEADING TO THE NUCLEI ^{152}Dy AND ^{162}Yb

K. Cornelis[†], R. Holzmann^{*}, M. Huyse[†], R. Janssens^{*}, G. Lhersonneau[†],
J. Lukasiak^{*}, C. Michel^{*}, Z. Sujkowski^{**}, M.A. Van Hove^{*}, J. Verplancke[†],
J. Vervier[†]

[†] I.K.S., Katholieke Universiteit te Leuven, Leuven (Belgium)

^{*} I.P.C., Université Catholique de Louvain, Louvain-la-Neuve (Belgium)

^{*} K.V.I., Groningen (The Netherlands)

^{**} I.B.J., Swierk-Warsaw (Poland)

There is a long-standing interest in the possible existence of a strong low-energy magnetic-dipole component in the quasi-continuum γ -ray spectrum following (heavy ion, $xn\gamma$) reactions. This has triggered several experimental (e.g. 1-4) and theoretical (e.g. 1,5,6) works. Rather accurate limits on the intensity of such a component can be obtained from the K-shell ionization yield per reaction³). The subject of the present work is to determine this yield for two nuclei of different structure, ^{152}Dy and ^{162}Yb , studied with ($^{40}\text{Ar}, 4n$) reactions. The nucleus ^{152}Dy was chosen because of its well studied yrast line⁷), and of recent linear polarization experiments on the quasi-continuum²). It has a typical vibrational spectrum at low spins and the yrast line at high spins is determined by single-particle rather than collective properties. The nucleus ^{162}Yb seems to rotate collectively up to very high angular momenta⁸).

The experiment consisted in recording coincidences between a large Ge(Li) spectrometer and a high-resolution hyperpure Ge detector. The intensity ratios of the K X-rays to the low-energy γ -rays in the hyperpure detector spectra, gated with discrete γ -transitions in the Ge(Li) spectrometer, are then a measure of the K-shell ionization yields, provided the level scheme and the relative γ -ray intensities are known. Any excess of the measured ionization yields, compared to that expected from the conversion of the observed discrete γ -transitions, can then be attributed, partly or totally, to the internal conversion of the quasi-continuum.

Partial analysis of the data yields a value of this excess for ^{152}Dy consistent with zero for the reactions populating states above $6076 + \Delta$ keV excitation energy: $\bar{x}_{\text{excess}} = (0.07 \pm 0.15)$ K-shell ionization per reaction. Here Δ is the energy of the unobserved transition depopulating the 60-ns isomeric state⁷). There is a sizeable excess found for the state at $5299 + \Delta$ keV depopulated by the 253.6 keV transition⁷). This might indicate that there is a strongly converted side-feeding to this state. Such a conclusion seems however premature, especially in view of the observed self-coincidence 254-254 keV, too strong to be explained on the basis of the known level scheme⁷) and of the experimental conditions.

Preliminary analysis of the ^{162}Yb data indicates slight ionization excess. A more thorough analysis is in progress.

REFERENCES

1. J.O. Newton and S.H. Sie, *Nucl. Phys.* A334, 499 (1980)
2. J.P. Vivien et al, *Phys. Lett.* 85B, 325 (1979); W. Trautmann et al, *Phys. Rev. Lett.* 43, 991 (1979)
3. Z. Sujkowski et al, *Phys. Rev. Lett.* 43, 998 (1979)
4. J. Vervier, *Proc. Int. School Phys. "Enrico Fermi"*, Varenna, 1979 (to be published), and references therein
5. L.K. Peker et al, *Phys. Rev. Lett.* 41, 457 (1978)
6. R.J. Liotta, *Phys. Scripta* 21, 135 (1980)
7. J.F.H. Jansen et al, *Nucl. Phys.* A321, 365 (1979); T.L. Khoo et al, *Phys. Rev. Lett.* 41, 1027 (1978); J.C. Merdinger et al, *Phys. Rev. Lett.* 42, 23 (1979); B. Haas et al, *Phys. Lett.* 84B, 178 (1979)
8. F. Riess et al, private communication

PATHS OF γ -DECAYS FROM HIGHLY EXCITED STATES AND THE EFFECT OF THE K-QUANTUM NUMBER

M. Wakai and M. Sano

Department of Physics, Osaka University, Toyonaka, Osaka 560, Japan

A. Faessler

Institut für Theoretische Physik, Universität Tübingen, W-Germany

One of the main subjects of analyses of γ -rays from a highly excited compound nucleus is the competition between the statistical and the collective γ -transitions. Band structures are expected to be held even in highly excited region and the γ -transitions (especially E2) along a rotational band play an important role in the decay process. Such collective transitions pass through two different types of paths depending on shapes of the nucleus. When the nucleus is deformed prolate, yrast states are produced by rotations around the axis perpendicular to the symmetry axis and the paths are roughly parallel to the yrast line (fig. 1(a)). But in the case of oblately deformed nuclei, rotations around the symmetry axis produce yrast states and paths along a collective band are steeper than the yrast line with a smaller moment of inertia than that of the yrast band (fig. 1(b)).

In the previous works¹ we analyzed the distribution of emitted γ -rays and population intensities to the yrast states of ¹⁵²Dy accompanied by the reaction ¹²⁴Sn(³²S, 4n)¹⁵²Dy, E = 145 MeV^{2,3}. The steeper paths of collective transitions than that of the yrast line result a bump of the collective E2 transitions at larger γ -energy with a somewhat reduced height.

The above results are, however, obtained by neglecting the K-quantum number. Yrast states have large values of K, projection of spin I on the symmetry axis, in the cases of nuclei with oblate deformation, and states with large K are distributed densely near the yrast line. The expression of B(E2) between two states ($\Delta I = 2$) in the same band contains a factor $(1-K^2/I^2)^2$, which reduces the strength of collective E2 transition at large K,

$$c_{E2}^{coll} \approx c_{E2}^{coll}(0)(1-K^2/I^2)^2, \quad I \gg 0. \quad (1)$$

To investigate this effect we did analysis considering the K-quantum number. The level density formula adopted⁴ is

$$\rho(E, I, K) = \frac{1}{24\sqrt{2}} \left(\frac{1}{2\mathcal{J}_I \mathcal{J}_K} \right)^{1/2} a^{1/2} (u'+t)^{-2} \exp(2\sqrt{au'}), \quad (2)$$

$$u' = E - E^{(0)}(I, K).$$

where $E^{(0)}(I, K)$ is the minimum value of energies of states with spin I and K, assumed here to be

$$E^{(0)}(I, K) \equiv \frac{1}{2\mathcal{J}_I} I(I+1) + \left(\frac{1}{2\mathcal{J}_H} - \frac{1}{2\mathcal{J}_I} \right) K^2 + \text{const}. \quad (3)$$

The values of moments of inertia are taken $2\mathcal{J}_I/\hbar^2 = 107 \text{ MeV}^{-1}$, $2\mathcal{J}_H/\hbar^2 = 148 \text{ MeV}^{-1}$ so as to reproduce almost same paths and the yrast line in fig. 1(b).

The results of calculations are plotted in fig. 2(a), compared with the results of the calculations¹ with paths in fig. 1(b) neglecting the K-quantum

number fig. 2(b)). The effect of the K-quantum number is clearly seen as the decrease of the ratio of γ -rays emitted in the intraband transitions (E2). The collective transition is much hindered also in high spin region and the collective γ -rays are emitted in comparably low spin region near the yrast states. This effect causes the shift of the bump of the intraband transition to the lower γ -energy as seen in fig. 2(a).

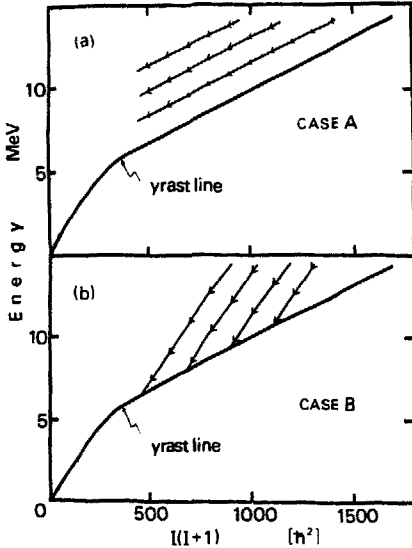


Fig. 1: Schematic representation of the yrast line and paths of collective E2 transitions in ^{152}Dy .
 (a) The paths are parallel to the yrast line ($2\mathcal{J}/h^2 = 142 \text{ MeV}^2$).
 (b) The paths are steeper than the yrast line, with smaller moment of inertia ($2\mathcal{J}/h^2 = 107 \text{ MeV}^2$) than that of the yrast band.

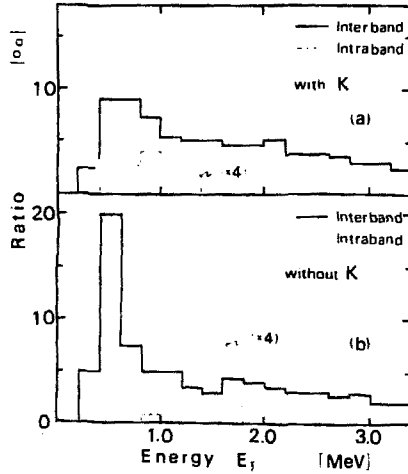


Fig. 2: Theoretical distributions of E_2 from ^{152}Dy excited by $^{129}\text{Sn}(32\text{S}, 4n)^{152}\text{Dy}$, $E_{\text{lab}} = 145 \text{ MeV}$, obtained (a) by considering K-quantum number and (b) by neglecting. In both cases, path of intraband transitions (E2) are same to those in fig. 1(b).

References

1. M. Wakai, M. Sano and A. Faessler, contributed paper to the Int. Conf. on Band Structure and Dynamics, March (1980), New Orleans, and references therein.
2. T. L. Khoo et al., Phys. Rev. Lett. 41, 1027 (1978).
3. J. C. Merdinger et al., Phys. Rev. Lett. 42, 23 (1978).
4. M. Sano and M. Wakai, Prog. Theor. Phys. 48, 160 (1972).

HIGH SPIN ISOMERIC STATES IN THE $N = 84$ NUCLEUS ^{152}Er

R. Holzmann, Y. El Masri, C. Michel, M.A. Van Hove and J. Vervier
Institut de Physique Corpusculaire, B - 1348 Louvain-la-Neuve, Belgium

In the trend of our investigation of high spin isomers in light erbium nuclides ¹) and the study of the detailed properties of their level scheme, we have investigated high-spin states in ^{152}Er using the reaction $^{116}\text{Sn}(^{40}\text{Ar}, 4n)^{152}\text{Er}$. The experiments were performed with 170 MeV ^{40}Ar beams accelerated at the CYCLONE isochronous cyclotron of Louvain-la-Neuve. Self-supporting enriched ^{116}Sn foils of 1 mg/cm² and 10 mg/cm² thicknesses were used as targets. A multiplicity-filter consisting of six 7.5 cm x 7.5 cm NaI(Tl) detectors mounted in a "halo" set-up around the beam axis was used, coupled either to a 66 cc Ge(Li) detector positionned at 0° relative to this axis, or to two 66 cc Ge(Li) detectors in γ - γ coincidences placed at $\pm 30^\circ$ with respect to the beam direction. The data were recorded event by event in a multiparameter procedure, allowing the definition of prompt and delayed events (singles or coincidences) with respect to the beam burst; the timing properties restricted the observation of isomers to those with $5 \text{ ns} \lesssim T_{1/2} \lesssim 65 \text{ ns}$. The experimental set-up also allows to record the γ -ray energies, the time signals and up to seven fold coincidences (0-fold scaled down) between the Ge(Li) and the NaI(Tl) detectors. By gating on delayed or prompt γ -rays observed in the Ge(Li) energy spectra, time spectra could be obtained for each transition.

Figure 1 shows the one-, two- and three-fold γ -spectra delayed with respect to the beam burst ($t \geq 10 \text{ ns}$), the Ge(Li) counter being positionned at 0° relative to the incident beam direction. The assignment of the delayed γ -transitions shown in this figure is in agreement with references 2 and 3, and is confirmed by the concordance of their mean delayed multiplicity shown in table 1. In this table, we show the multiplicity values associated with some delayed γ -transitions observed in our spectra. These values take into account the contributions of the multiple angular correlations ⁴) to the different folds. The time spectra of these delayed γ -rays assigned to ^{152}Er display the existence of an isomeric state, with a half lifetime $20 \text{ ns} \leq T_{1/2} \leq 30 \text{ ns}$, and with a multiplicity of 16 units, in good agreement with the results of reference 2, and in contradiction with previously reported results ^{5,6}). The multiplicity data also show a set of unassigned delayed γ -ray transitions, with distinct mean multiplicity of 21 ± 1 units, suggesting a possible higher spin isomeric state in ^{152}Er . We could not confirm the existence of the 10 ns possible higher spin isomeric state also reported in reference 2. These findings suggest a strong dependence of the cross section to populate these isomers on the reaction mechanism and on the feeding patterns.

The complete analysis of these data, i.e. the prompt singles γ -spectra and the γ - γ coincidence measurements, is in progress.

Delayed gamma transitions	Mean delayed multiplicity	Assignment
230 KeV	16.2 +/- 2	^{152}Er
280 KeV	16.2 +/- 2	^{152}Er
399 KeV	5.5 +/- 0.3	$^{153}\text{Er}^?$
330 KeV	16.1 +/- 2	^{152}Er
422 KeV	16.4 +/- 1	^{152}Er
493 KeV	7.8 +/- 0.5	^{152}Dy
556 KeV	15.0 +/- 1	^{152}Er
614 KeV	7.5 +/- 0.5	^{152}Dy
648 KeV	8.4 +/- 0.5	^{152}Dy
671 KeV	16.0 +/- 1	^{152}Er
686 KeV	9.0 +/- 0.5	^{152}Dy
712 KeV	8.0 +/- 0.5	$^{151,152}\text{Ho}^?$
766 KeV	16.5 +/- 1	^{152}Er
787 KeV	16.1 +/- 1	^{152}Er
808 KeV	17.5 +/- 1	^{152}Er
910 KeV	9.8 +/- 1	?

Table 1

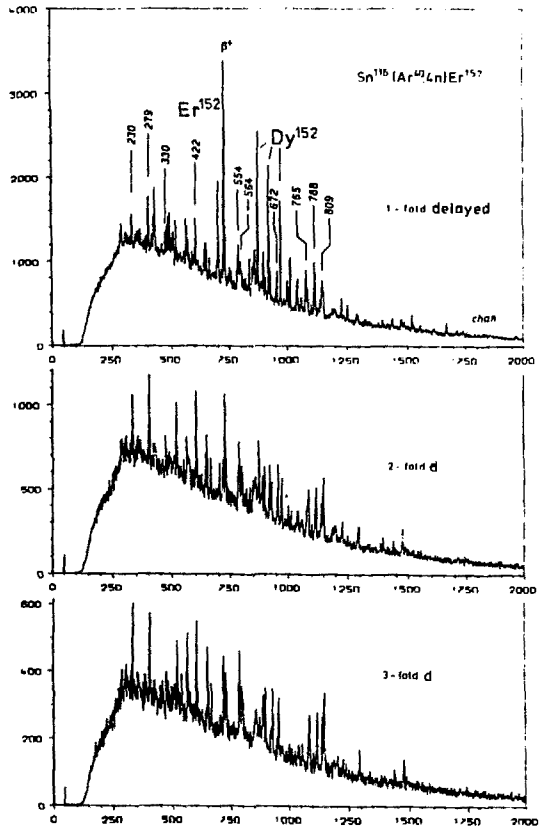


Fig.1

REFERENCES

1. P. Aguer *et al.*, *Phys. Lett.* **82B**, 55 (1979)
2. S. Björholm *et al.*, private communication, *Z. Phys.* (1980) to appear
3. J.F.W. Janssen *et al.*, *Nucl. Phys.* **A321**, 365 (1979)
4. S.Y. Van der Werf, *Nucl. Instr. Meth.* **145**, 295 (1977)
5. D.C.J.M. Hageman *et al.*, *Phys. Lett.* **84B**, 301 (1979)
6. G. Bastin *et al.*, *Nordic Symposium on Nuclear Physics*, p.56 (1979)

HIGH SPIN ISOMERS IN ^{153}Er

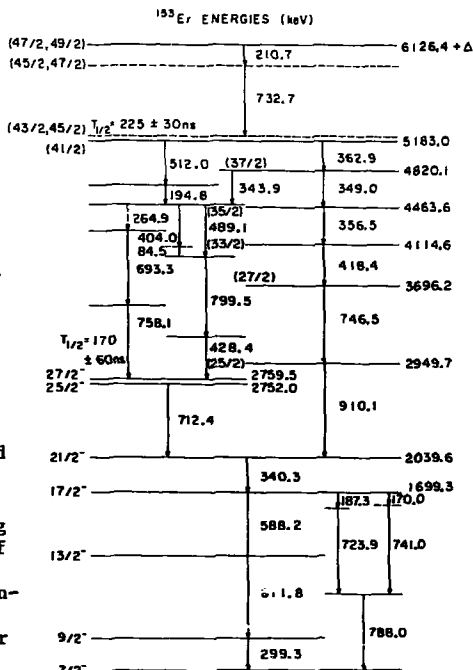
D. Horn, G.R. Young*, C.J. Lister, C. Baktash
 Brookhaven National Laboratory, Upton, New York 11973

The N=85 isotones have provided striking examples of shell structure at high spins. For example, the signature of valence neutron states and their coupling to aligned proton configurations in ^{151}Dy has been discussed by Kleinheinz.¹ Such coupling frequently gives rise to isomeric states. Several survey experiments have reported evidence of high spin isomers in ^{153}Er .^{2,3} Our investigation of ^{153}Er confirmed two long lived high spin isomers, and established their positions and decays.

An array of 4 NaI detectors in delayed coincidence with a Ge(Li) detector served to isolate those transitions associated with lifetimes $\geq 10\text{ns}$. Identification of the delayed transitions was obtained from excitation functions and cross bombardments using $^{12}\text{C}+^{144}\text{Sm}$, $^{11}\text{B}+^{144}\text{Sm}$, and $^{32}\text{S}+^{124}\text{Te}$. Measurements of angular distributions, half-lives (pulsed beam), and γ - γ coincidences were all obtained using the $^{144}\text{Sm}(^{12}\text{C},3n)^{153}\text{Er}$ reaction at 82 MeV.

The level ordering is based on coincidence timing, intensities at 82 MeV (A_0 from angular distribution), and relative intensities from the excitation functions. Due, in part, to the number of different reaction channels open, uncertainties remain and the level scheme shown at right should be considered tentative. The energy of the unobserved transition deexciting the

$T_{1/2}=170 \pm 60\text{ns}$ isomer is deduced to be 7.5 keV from crossovers which feed the isomer from the main cascade. Comparing this isomer with the analogous isomeric state in ^{151}Dy ¹ yields a similar transition rate, indicating M1 character. The near-Yrast states are established up to an excitation energy of 5183.0 keV. Transitions deexciting this state show a half life of $225 \pm 30\text{ns}$. Since tentative assignments do not suggest M2 or E3 character for the 362.9 keV γ -ray, the isomerism may



arise from an unobserved low-energy transition. Bjørnholm et al.³ have reported an isomer at 5.2 ± 0.25 MeV, but with a longer half-life than observed here.

Levels up to 2039.6 keV may be described in analogy with the other $N=85$ isotones as: (i) a $\nu(f_{7/2}^3)$ ground state configuration with two excited states, and (ii) a $\nu(h_{9/2}f_{7/2}^2)$ sequence with $J^\pi=9/2^-$ to $21/2^-$. The $27/2^-$ and $25/2^-$ states may be interpreted as $\pi(h_{11/2}^2) \otimes \nu(f_{7/2}^3)$ with the $5/2$ projection of $(f_{7/2}^3)$ falling below the $7/2$ projection as discussed in ref. 1. The pattern above the isomer certainly resembles that below, but further configuration assignments should await determination of level parities from our planned linear polarization measurements. The existence of a long-lived isomer of spin $\approx 22\hbar$, the complex feeding pattern, and the irregular energy spacings in this nucleus all favor the aligned single-particle picture for ^{153}Er at high spin.

* Summer visitor. Permanent address: Oak Ridge National Laboratory, Oak Ridge, Tennessee 37830

1. P. Kleinheinz, Proc. Symp. on High-Spin Phenomena in Nuclei, Argonne, Ill. (1979) 125.
2. D.J.C.M. Hageman, M.J.A. de Voight, and J.F.W. Jansen, Phys. Lett. **84B** (1979) 301.
3. S. Bjørnholm, J. Borggreen, O. Christensen, A. DelZoppo, B. Herskind, J. Pedersen, and G.Sletten, Proc. Symp. on High-Spin Phenomena in Nuclei, Argonne, Ill. (1979) 421.

NATURE OF HIGH SPIN STATES IN NEUTRON DEFICIENT ERBIUM ISOTOPES

P. Aguer⁺, G. Bastin⁺, A. Péghaire⁺, J.P. Thibaud⁺, N. Perrin⁺⁺,
H. Sergolle⁺⁺, Ph. Hubert^{*}

⁺ C.S.N.S.M. Bât. 104 - 91406 Campus ORSAY- FRANCE

⁺⁺ I.P.N. - Bât. 100 - 91406 Campus ORSAY- FRANCE

^{*} C.E.N.B.G. - Le Haut Vigneau 33170 GRADIGNAN- FRANCE.

In an earlier experiment, neutron deficient erbium isotopes ($N \sim 86$)¹⁾ have been explored at very high spin, using the multiplicity filter technique. The continuum γ ray spectra, observed with a 7.6×7.6 cm NaI showed out two bumps. The upper energy one, centered around 1.4 MeV, and mainly composed of stretched E2 transitions, strongly suggested a collective structure. The multiplicity spectrum also exhibits two peaks at the corresponding bump energies and support the conclusion that such a structure comes out at spin above 40 \hbar for these nuclei lying in the transitional region.

Recently, it has been pointed out that the sum spectrometer method is a powerful tool to select the high angular momentum nuclei produced in a (HI,xn) reaction^{2,3)}. The method has been successfully applied in the study of good rotor nuclei like ^{164}Er ³⁾. We have applied that method to the case of erbium isotopes in the $N \sim 86$ region in order to observe the behaviour of this high spin bump with increasing angular momentum.

The experiments were run at the Alice accelerator at Orsay using a 185 MeV ^{40}Ar beam on a ^{118}Sn target. The total γ ray energy spectra were recorded with a NaI sum spectrometer (31 cm diameter, 31 cm length) of 0.8 efficiency.

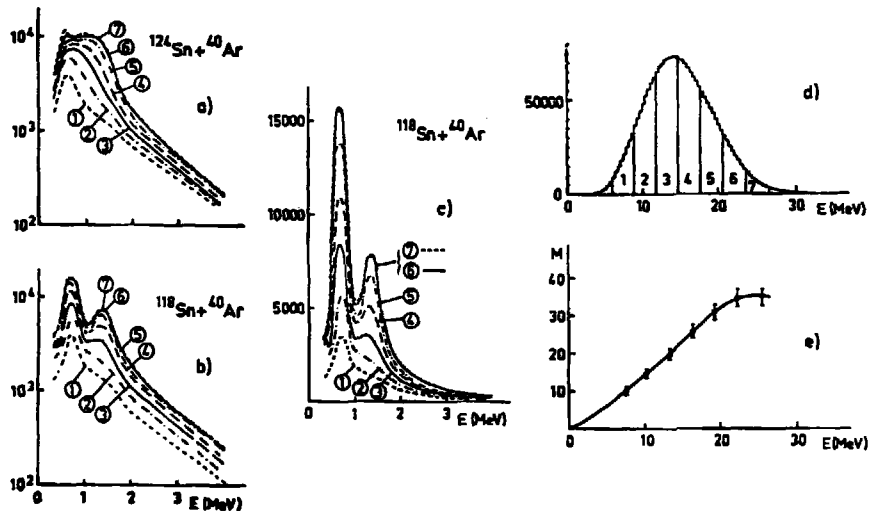
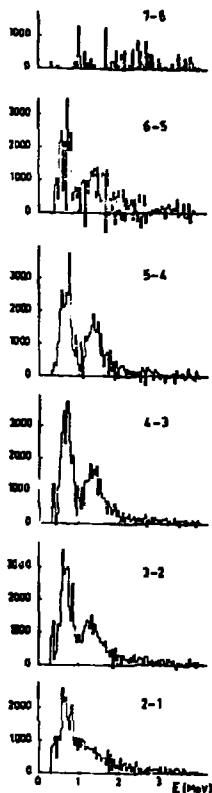


Figure 1

NaI spectra corresponding to seven slices in the total sum spectrum (1d) for the systems $^{124}\text{Sn} + ^{40}\text{Ar}$ (fig. 1a) and $^{118}\text{Sn} + ^{40}\text{Ar}$ (fig. 1b and 1c). Figure 1e displays the multiplicity versus sum energy for the system $^{118}\text{Sn} + ^{40}\text{Ar}$.

Figure 2 - Differences between the adjacent spectra of figure 1c.



This spectrometer is optically divided in four sectors. A Ge(Li) detector placed in a hole in the sum spectrometer at 90° with respect to the beam allows a selection of the outgoing channels. Spectra of individual γ rays were recorded with a 7.6 cm x 7.6 cm NaI located at 0° , 60 cm from the target.

Figures 1^{b,c} show the unfolded 0° NaI spectra for the $^{118}\text{Sn} + 40\text{Ar}$ system, in coincidence with successive adjacent 3 MeV slices in the sum spectrum (fig. 1^d). The spectra of the $^{124}\text{Sn} + 40\text{Ar}$ system are displayed for comparison (fig. 1^a): our results for that system are in agreement with the one previously obtained in ref.3. All the spectra are normalised to the multiplicity for each slice and multiplicities values have been deduced from an analysis of the counting rates of each sector of the sum spectrometer used as an efficient multifold spectrometer (fig. 1^e).

The first salient feature of these results is that the low energy bump (at 650 keV) is connected with the higher slices in the sum spectrum and thus with the higher multiplicities in the nuclei.

Preliminary angular distribution results are consistent with an intense dipole component in this low energy bump. $M_1 \gamma$ rays have already been observed in other systems 4), and some theoretical explanations have already been proposed 5,6).

Moreover, the high energy bump ($E_\gamma \sim 1.4$ MeV) starts developing at about 35 h suggesting at such a spin a change in the nuclear structure. But the average energy of the bump remains constant when increasing the sum energy (i.e. when increasing the spin). This appears clearly in the NaI spectra differences displayed in fig.2 and is in a sharp contrast with the behaviour of the $^{124}\text{Sn} + 40\text{Ar}$ system 3).

The constant energy of the upper bump observed in the $^{118}\text{Sn} + 40\text{Ar}$ system might lead, in the framework of the rotational model, to the conclusion of the existence of an effective moment of inertia uncorrelated with the rotational frequency; this trend recalls a vibrational behaviour. Another explanation could arise from successive particle pairing break up. This last point of view could be in agreement with the strong correlation observed between the two bumps (see Ph. Hubert et al. this conference).

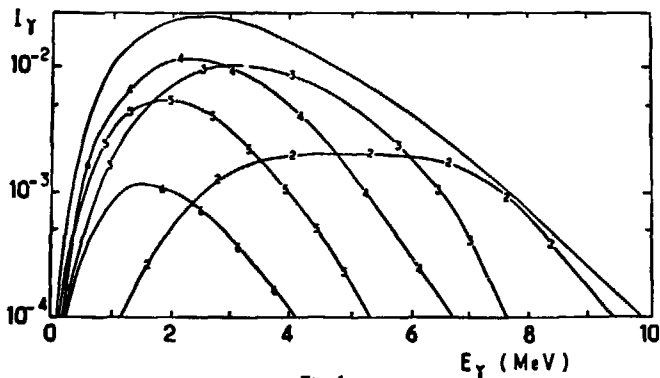
- 1) M.A. Deleplanque, J.P. Hussion, N. Perrin, F.S. Stephens, G. Bastin, C. Schück, J.P. Thibaud, L. Hildingsson, S. Hjorth, A. Johnson, Th. Linblad, Phys. Rev. Lett. 43, 1001 (1979).
- 2) P.O. Tjøm, I. Espe, G.B. Hayemann, B. Herskind, D.L. Hillis, Phys. Lett. 723, 439 (1978).
- 3) H.J. Körner, D.L. Hillis, C.P. Roulet, P. Aguer, C. Ellegaard, D.B. Fossan, D. Habs, M. Neiman, F.S. Stephens, R.M. Diamond, Phys. Rev. Lett. 43 (490) (1979).
- 4) J.O. Newton, S.R. Sie, G.D. Dracoulis, Phys. Rev. Lett. 40 (625) 1978.
- 5) R.J. Liotta, Physica Scripta 21, 135 (1980)
- 6) L.K. Peker, J.H. Hamilton, J.O. Rasmussen, Phys. Rev. Lett. 41, 457 (1978).

CALCULATIONS OF THE CONTINUUM γ -RAY SPECTRA IN (HI,xn) REACTIONS

Ph. Hubert, F. Leccia, R. Liotta, P. Mennrath, M.M. Villard
 Centre d'Etudes Nucléaires de Bordeaux-Gradignan, Gradignan, France

Recent (HI,xn) experiments have shown the rich variety of phenomena occurring at high spin in different nuclei. Thus, in ref.¹ the gamma-ray spectrum of light Er nuclei shows two bumps. The low energy bump corresponds mainly to low spin (below spin 37) transitions. The higher energy bump seems to be the by now classical bump produced by collective (rotational) transitions at high spin. However, the edge of this bump does not move with increasing entry-state energy² (i.e. increasing spin) as would be expected if the corresponding gamma-rays were produced by rotational transitions. On the other hand, in ref.³ it is shown that rotational nuclei decaying at high spin produced also two bumps, but in this case it seems that the low energy bump consists mainly of M1 transitions while the high energy bump consists of E2 transitions. In all cases, the high energy part of the spectra decays exponentially, in disagreement with theoretical predictions⁴.

To study these somehow contradictory features we analysed the high-energy part of these spectra including only statistical E1 transitions. The understanding of these transitions is fundamental not only to elucidate the above mentioned disagreement between theory and experiment but also, from an experimental point of view, to be able to separate the background statistical gamma-ray at low energies from the gamma-ray produced by collective transitions (both M1 and E2). To carry out this analysis we have assumed that the statistical cascade proceeds at random but all $\Delta L(=1,0)$ transitions were allowed to occur. Utilizing a Monte-Carlo method we obtained the spectrum of fig. 1 corresponding to nuclei with $A \sim 150$. In general, we have so far found that this spectrum is sensitive to changes in the density of states.

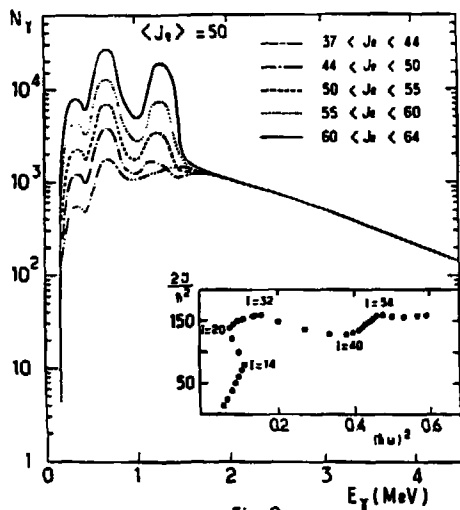


— Fig. 1 —

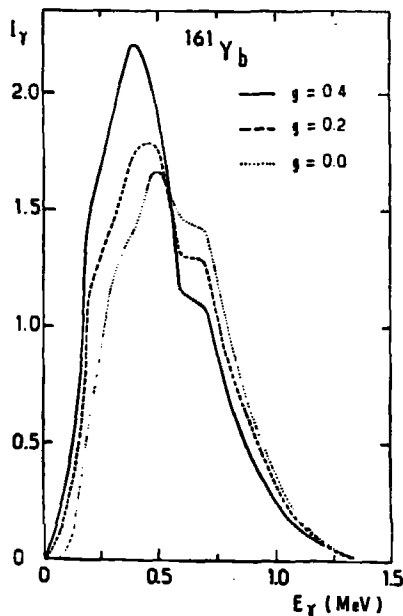
Statistical γ -ray spectrum (full line) calculated for a nucleus with $A \sim 150$ and the partial components (numbers) associated with different γ -ray multiplicities

Regarding the high-energy bump we found that it is very dependent upon the structure of the yrast line. For instance, the fact that the edge of this bump does not move with increasing energy seems to indicate that a series of backbendings occurs beyond spin 40 (fig. 2), although we are not yet sure whether or not there are other possible explanations.

Finally, we analysed the low energy bump of ref.³ using the wobbling model⁴ but including both E2 and M1 collective transitions among different high spins tracks. We then obtained, using reasonable g-values, spectra which have the same feature than the experimental ones as shown in fig. 3.



— Fig. 2 —



— Fig. 3 —

Calculations of the γ -ray spectrum for a quasi spherical nucleus around $A \sim 150$ using a Monte-Carlo method. The backbending plot associated to the yrast line used in the calculation is shown in the insert. No other collective band is included in the calculation.

Total gamma-ray spectrum of the collective transitions (E2+M1) in ^{161}Yb calculated in the wobbling model for different g-factors.

References

1. M.A. Deleplanque et al., Phys. Rev. Lett. **43**, 1001 (1979)
2. P. Aguer et al., Contribution to this Conference
3. J.O. Newton and S.H. Sie, Nucl. Phys. **A334**, 499 (1980)
4. R.J. Liotta and R.A. Sorensen, Nucl. Phys. **A297**, 136 (1978)

∴ Laboratoire de Physique Théorique, Bordeaux, France
 On leave from Research Institute of Physics, Stockholm, Sweden

IRREGULARITIES IN THE YRST LINE OF ^{156}Er

T.Byrski, F.A.Beck, C.Gehringer, J.C.Merdinger, Y.Schutz and J.P.Vivien
Centre de Recherches Nucléaires et Université Louis Pasteur,
67037 STRASBOURG Cedex

In the present work, we have carried on our research of second backbending in the yrast spectra of rare earth nuclei. The second irregularity¹ observed in ^{160}Yb fits well within the framework of a Z oscillatory behaviour of the interaction between two specific bands (no backbending² in ^{156}Dy , upbending³ in ^{158}Er). Our purpose was to study the effect of the variation of the neutron number and for this we have investigated the ^{156}Er nucleus.

The heavy ion reaction $^{141}\text{Pr}(^{19}\text{F},4n)^{156}\text{Er}$ was used to populate high spin states in ^{156}Er . Following the results of an excitation curve run between 85 and 110 MeV, a bombarding energy of 95 MeV was chosen to avoid too strong contaminations from the 3n and 5n channels. The $1\text{mg}/\text{cm}^2$ metallic target was rolled onto a 0.1 mm lead foil. The γ - γ coincidences were measured with a three Ge(Li) array so as to increase the counting rate. Detectors were set at $+90^\circ$, -90° , and 0° , with respect to the beam direction, each detector being in coincidence with each other.

From a large amount of coincidences, the yrast level scheme, found to be in agreement with that reported in Ref.4, has been extended up to $I=26\hbar$ and tentatively up to $I=28\hbar$ (fig.2). Special care has been taken for the assignment of the 766 keV γ -ray line since a transition of 765 keV ($21^- \rightarrow 19^-$) is more strongly populated in the negative parity side band of ^{156}Er and a transition of 765 keV also exists in ^{157}Er . The five coincidence spectra obtained with windows set on the transitions decaying the 14^+ , 18^+ , 20^+ , 22^+ and 24^+ states respectively each exhibit clearly a 766 keV γ -ray line without any significant presence of transitions originating from the negative parity side band of ^{156}Er or from ^{157}Er (fig.1). This 766 keV γ -ray line is also in coincidence with itself. Relative intensities and energies extracted from the coincidence spectra favour the attribution of the second 766 keV transition to the yrast level band. DCO ratios obtained from the relative coincidence intensities at 0° and 90° are all near 1 for the transitions of the yrast level band indicating that all transitions have the same E2 multipole character.

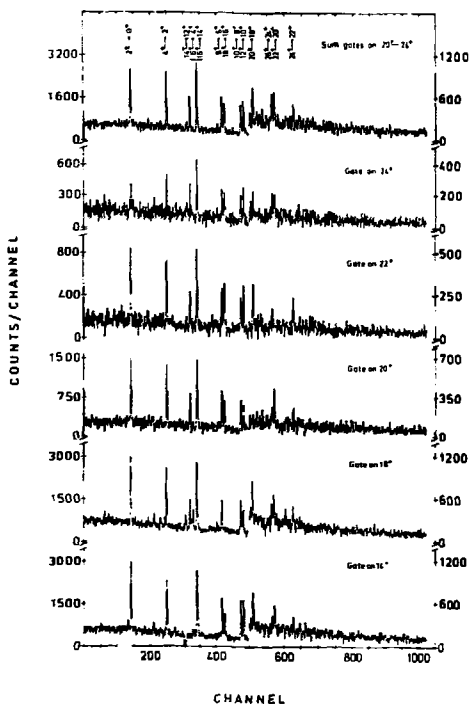


Fig.2 shows a plot of the moment of inertia versus the square of the rotational frequency; the two discontinuities lead to rapid increase of the moment of inertia at $J^\pi \geq 12^+$ and $J^\pi \geq 24^+$. It should be emphasized that the second discontinuity appears at spin value lower than in ^{158}Er or ^{160}Yb and is more pronounced than in these two nuclei: in fact, it is the first time that it appears as a strong back-bending. Preliminary results of calculations, done by the Warsaw group⁵⁾, in the cranked HFB framework, indicate that the second anomaly in ^{156}Er cannot be reproduced by the alignment of a proton pair like in ^{160}Yb , but is rather due to a neutron effect.

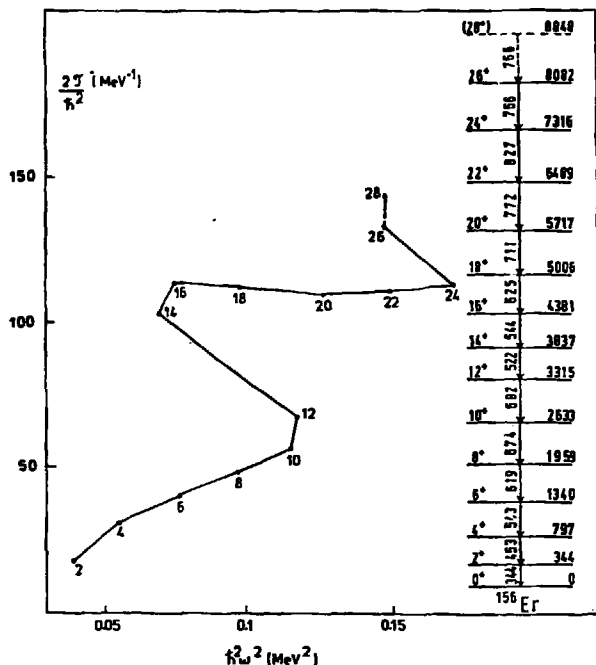


Fig.2

- 1) F.A.Beck, E.Bozek, T.Byrski, C.Gehring, J.C.Merdinger, Y.Schutz, J.Styczen, and J.P.Vivien, Phys.Rev.Lett. 42 (1979) 493.
- 2) D.Ward, O.Häusser, H.R.Andrews, B.Haas, P.Skenved and M.Maynard, Proc. of the Int. Conf. on Nucl. Interact., Canberra 1978.
- 3) I.Y.Lee, M.M.Aleonard, M.A.Delaplanque, Y.El-Masri, J.D.Newton, R.S.Simon, R.M.Diamond, and F.S.Stephens, Phys.Rev.Lett. 38 (1977) 1454.
- 4) A.W.Sunyar, E.de Mateossian, O.C.Kistner, A.Johnson, A.H.Lumpkin, and P.Thieberger, Phys.Lett.62B (1976) 283.
- 5) J.Dudek, private communication.

GAMMA-RAY TRANSITION ENERGY CORRELATIONS IN ^{156}Er and ^{160}Yb

J.P. Vivien, Y. Schutz, F.A. Beck, T. Byrski, C. Gehringer and J.C. Merdinger
Centre de Recherches Nucléaires, Strasbourg, France.

Studies of the rotational nuclei ^{156}Er and ^{160}Yb ^{1,2} show that their yrast and side bands exhibit discontinuities. In particular, in both nuclei a second backband is observed in the yrast band. Gamma transition energy correlation have been measured for these nuclei produced respectively in the heavy ion fusion reactions $^{141}\text{Pr} + ^{19}\text{F}$ at $E_{\text{inc}} = 100$ MeV, and $^{148}\text{Sm} + ^{16}\text{O}$ at $E_{\text{inc}} = 105$ MeV. To record the γ - γ correlation matrix a set of three Ge(Li) detectors with characteristics and gain properly matched has been used.

The two dimensional correlated spectra ΔN_{ij} were obtained via a method which separates correlated events from the uncorrelated background³. In these spectra the rotational behaviour of the nucleus shows up as a valley along the diagonal. The width of the valley $W = 16 \hbar^2 / 2 \mathcal{I} (1)$ depends on the collective moment of inertia which in a rotational band is given by $2 \mathcal{I} / \hbar^2 = 4(I - j_a) / E_{\gamma} (2)$ where E_{γ} is the transition energy and j_a the aligned single particle angular momentum.

Figures 1 and 2 display the bidimensional correlated spectra. The valley can be followed up to 860 keV for ^{160}Yb and to 925 keV for ^{156}Er . These values correspond to the high energy edge of the yrast bump as observed in the direct Ge(Li) spectra. The right-band part of each figure shows the results obtained for different slices perpendicular to the 45° diagonal. For low energy transitions up to ≈ 500 keV, the observed narrowing of the valley for ^{160}Yb with increasing energy reflects the behaviour of the ground band moment of inertia below the first backbending. Beyond the first backbending up to 750 keV, the width of the valley remains almost constant. The ridge which is narrow below the first backbending becomes wider, indicating a spread in the moment of inertia. One can then represent the yrast-like decay by several collective bands with different moments of inertia corresponding to various degrees of alignment of the single particles. A few of these bands are expected to experience crossings at specific frequencies. This phenomenon should be seen as a filling in of the valley. Such a multiband crossing could correspond in the ytterbium data to the disappearance of the valley observed between 750 keV and the second backbending and to the strong necking of the ridge at $\hbar\omega = E_{\gamma}/2 = 0.40$ MeV. The same features are observed in ^{156}Er , but slightly shifted in energy : the necking appears at $\hbar\omega = 0.38$ MeV.

After the second backbending, the end point of the valley is related to the energy of transitions de-exciting the highest spin collective states fed in the reaction. The corresponding moments of inertia deduced from the width are $136 \pm 18 (\text{MeV})^{-1}$ for ^{160}Yb and $111 \pm 22 (\text{MeV})^{-1}$ for ^{156}Er . The maximum angular momentum at the top of the yrast cascade is evaluated to be $I = 44 \hbar$ for both nuclei. Using relation 2, the corresponding single particle aligned angular momentum is found to be $\approx 15 \hbar$ for ytterbium and $\approx 17 \hbar$ for erbium. These values are in good agreement with the alignment obtained for the yrast band after the second crossing².

1. F.A. Beck, E. Bozek, T. Byrski, C. Gehringer, J.C. Merdinger, Y. Schutz, J. Styczen and J.P. Vivien, Phys. Rev. Lett. 42 (1979) 493, and contribution to this conference.
2. L.L. Riedinger, O. Andersen, S. Frauendorf, J.D. Garrett, J.J. Gaardhoje, G.B. Hageman, B. Herskind, Y.V. Makovetzky, J.C. Waddington, M. Guttormsen, P.O. Tjøm, Phys. Rev. Lett. 44 (1980) 568.
3. O. Andersen, J.D. Garrett, G.B. Hagemann, B. Herskind, D.L. Hillis, L.L. Riedinger, Phys. Rev. Lett. 43 (1979) 687.

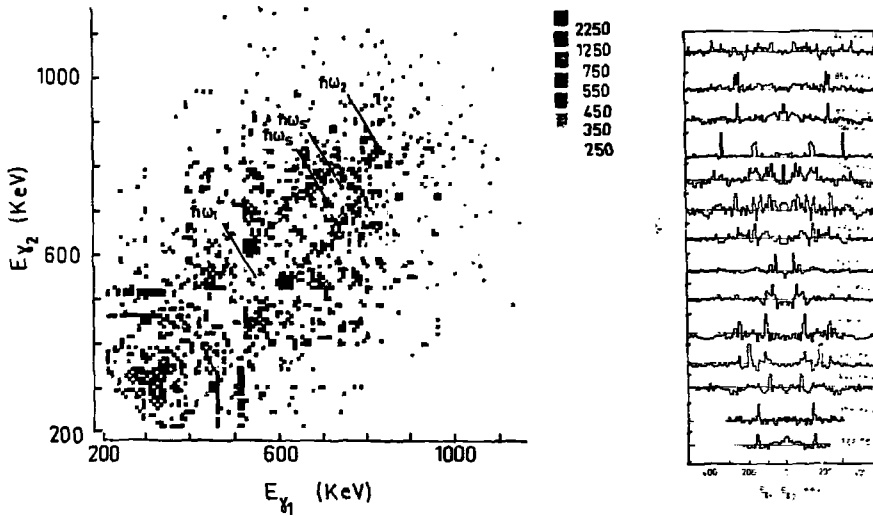


Figure 1
 Positive correlation spectrum N_{ij} for ^{160}Yb and corresponding projections perpendicular to the diagonal. For each slice the mean energy value $(E_{Y1} + E_{Y2})/2$ is indicated. $h\omega_1$ and $h\omega_2$, $h\omega_3$ and $h\omega_4$ are the backbanding frequencies in the grass band respectively side bands.

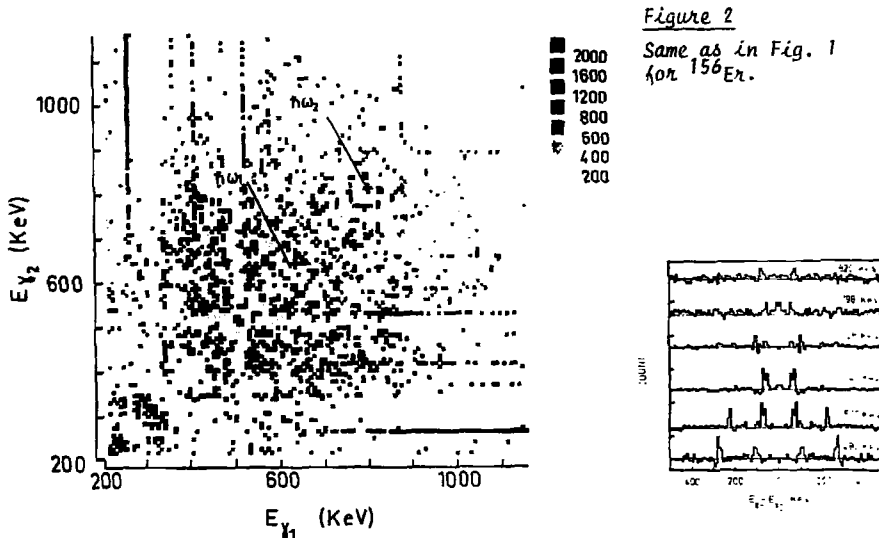


Figure 2
 Same as in Fig. 1
 for ^{156}Er .

B(E2) - VALUES OF HIGH SPIN STATES IN Dy-ISOTOPES

H. Emling, P. Fuchs, E. Grosse, R. Kulesa[†], D. Schwalm, R.S. Simon and H.J. Wollersheim
GSI Darmstadt, Germany

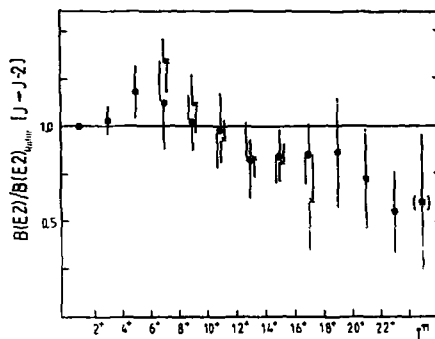
B(E2)-values of high spin states in the three isotopes ^{156}Dy , ^{158}Dy and ^{164}Dy were determined by two independent methods, i.e. multiple Coulomb excitation and lifetime measurements following (HI,xn) reactions.

Special attempts were made (i) to investigate the rotation-vibration coupling at high spins, (ii) to study the interaction between the g-band and the rotational aligned band (s-band) and (iii) to determine the collective properties of the s-band above its crossing with the g-band. The three isotopes were selected with respect to the different behaviour of the yrast band energies spanning from pronounced backbending (^{156}Dy) over upbending (^{158}Dy) to an only smooth variation of the apparent moment of inertia (^{164}Dy).

The Coulomb excitation experiments were performed at the UNILAC using highly enriched targets and ^{208}Pb -beams of 4.7 MeV/A. The use of a special particle- γ -coincidence setup consisting of up to four Ge-Li detectors and two position sensitive parallel plate counters allowed a fast online Doppler shift correction of the γ -spectra. B(E2)-values up to $I^\pi = 20^+$ were obtained by comparing the observed intensities to those calculated in the semiclassical approximation. The wide impact parameter region covered by the large area particle detectors was necessary to determine B(E2)-values at low as well as at high spins.

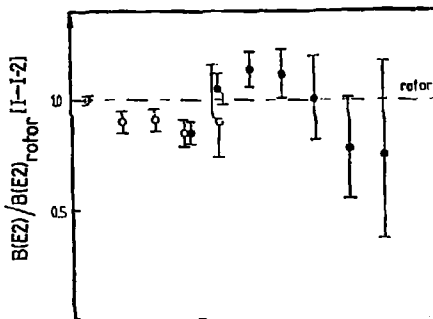
The isotopes ^{156}Dy and ^{158}Dy were additionally investigated using the recoil distance method in the inverse $^{25}\text{Mg} (^{136}\text{Xe},5n)$ and $^{26}\text{Mg} (^{136}\text{Xe},4n)$ reactions. Due to the high recoil velocity of the compound nucleus ($v/c = .08$) lifetimes down to $\sim .3$ ps could be measured with an absolute accuracy of $\sim .1$ ps. Decay curves up to $I^\pi = 26^+$ and $I^\pi = 30^+$ were obtained within the yrastbands of ^{158}Dy and ^{156}Dy respectively. By introducing a thin Au-foil ($\sim 2.5 \mu\text{m}$) instead of a thick stopper we were able to avoid the strong Doppler spread of the stopped components of transitions from shortlived (≤ 1 ps) high spin states. A nearly complete suppression of γ -rays from the Coulomb excited Au-foil was achieved by a NaI multiplicity filter.

Fig. 1 Normalized B(E2)-values of the yrastband in ^{158}Dy obtained from Coulomb excitation (x) and lifetime measurements (•).



The low spin B(E2)-values of ^{156}Dy exceed the rotational model predictions probably due to centrifugal stretching which seems to be saturated at $I^\pi = 8^+$. A similar behaviour was also found for the g-band of ^{156}Dy ¹. In the spin region ($I^\pi > 14^+$) above the upbending however the E2-transition probabilities are significantly reduced compared to the rotational model (fig. 1). This reduction corresponds to the intrinsic quadrupole moment Q_0 in the s-band being 10 % smaller than the one in the g-band. This value agrees to the $Q_0(2^+)$ of ^{156}Dy consistent with the assumption of an aligned neutron configuration in the ^{156}Dy s-band. By analyzing feeding multiplicities and feeding times we also found an average B(E2)-value for the pre-yrast continuum which showed a similar retardation.

Fig. 2 Normalized B(E2)-values of the yrastband in ^{164}Dy obtained from Coulomb excitation. (see ref. 4)



... a detailed study of the coupling between g-band and γ -band was possible since states up to $I^\pi = 22^+$ (g-band) and $I^\pi = 18^+$ (γ -band) were populated by Coulomb excitation. The observed intensities of transitions in the γ -band and between γ -band and g-band require a spin-dependent coupling between both bands deviating at $I^\pi > 6^+$ from a first order perturbation treatment using an effective $\Delta K = 2$ interaction ². A consistent description of the experimental data could be found in the frame of the RV-model ³, however it was necessary to introduce a renormalization of the RV interaction Hamiltonian. With a reduction factor of 2.7 and $Q_{0\gamma} = 1.10 Q_0$ a reasonable fit to the measured yields was obtained.

* on leave from Dept. of Nucl. Phys. Jagiellonian University, Cracow, Poland

1. D. Ward et al., Nucl. Phys. A332, 433 (1979).
2. A. Bohr and B.R. Mottelson, Nuclear Structure, Vol. II, 158 ff (1975).
3. A. Faessler et al., Nucl. Phys. 70, 33 (1965).
4. R.O. Sayer et al., Phys. Rev. 177, 1026 (1978).

DISCRETE γ -RAYS ABOVE 1-MeV IN Er NUCLEI

H. Yamada*, D.C. Hensley[†], A.V. Ramayya*, C.F. Maguire*
J.H. Hamilton*, and A. Ahmed*

*Vanderbilt University, Nashville, Tennessee, USA

[†]Oak Ridge National Laboratory, Oak Ridge, Tennessee, USA

Bumps consisting of multiple γ -rays above 1-MeV for Er nuclei have been observed for the first time. The observation was made with a well collimated 12.7x12.7-cm NaI detector in coincidence with fast forward protons from the $^{154}\text{Sm}(^{14}\text{N}, \text{pxn})^{167}\text{Er}$ reactions. The nitrogen beam at 167-MeV from the Oak Ridge Isochronous Cyclotron was chosen to favor the (p9n) leading to ^{158}Er . In earlier work by Yamada et al.¹ such fast forward protons were attributed to a massive transfer reaction for which a simple particle- γ coincidence experiment turned out to be a very useful probe to investigate high spin states.

In the present work, a technique combining particle- γ coincidence and γ -ray multiplicity was used to select high spin transitions. The proton telescopes were placed at forward angles of 22° on each side of the beam. The NaI was positioned at 145° and 50 cm from target to discriminate against neutrons by time of flight and to reduce coincident summing.

Two of the NaI spectra associated with different numbers of coincident detectors in the γ -multiplicity array and gated on high energy protons are shown in Fig. 1. No unfolding was applied. The solid line under the 5-fold spectrum was obtained by smoothing the structure in the 1-fold spectrum and normalizing the height by the ratio C_5/C_1 , where C_j is the integral of the counts above 1-MeV in the j-fold spectrum. This estimate of the continuum background should give an upper limit since the ratio was calculated including the bumps.

There are bumps at 0.33, 0.61, 0.87, 1.2 and 1.7-MeV in the 5-fold spectrum, while indications of these bumps exist even in the 1-fold spectrum. The 0.33-MeV bump corresponds to the 4-2 transition in ^{158}Er . Bunching of discrete γ -rays at the turning points of the first and second backbendings of the moment of inertia in ^{158}Er give the correct energies to account for the second and third bumps at 0.61 and 0.87-MeV, respectively. The analysis of the Ge(Li) spectra taken simultaneously in coincidence with the fast protons shows that the transitions in ^{158}Er are dominant and are observed up to spin 28 \hbar . The remaining γ -rays were assigned mainly to ^{157}Er and ^{159}Er , each with one half of the γ -yield of ^{158}Er (the intensities drop down quickly with spin and the highest spin observed was 41/2 \hbar). It seems unlikely that the high energy bumps originate from neutrons or from quasi-elastic reactions, because such γ -rays should not have high γ -multiplicity.

In analogy to the lower energy bumps, it is possible that the 1.2 and 1.7-MeV bumps may be associated with third and fourth backbending in Er nuclei. If this interpretation is correct, these additional backbendings would occur around spin 40h and 56h on the assumption that the moment of inertia is 130 MeV^{-1} . Spin 56h is consistent with the average angular momentum transferred into the fused system as estimated from the γ -ray multiplicity of about 30 obtained for the discrete lines of ^{158}Er in the Ge(Li) spectrum. The observation of backbends at high spin suggests that some high-j orbitals might not yet be fully aligned up to spin 56h, from the point of view that the lower backbends of ^{158}Er are produced by the alignment of $\nu(1\ 13/2)^2$ and $\pi(h\ 11/2)^2$ orbits.² If so, a prolate shape may be expected even at such high spin, and an oblate shape may occur above spin 56h. In any case these data suggest that the high j-orbitals may maintain the character and influence at much higher spin than previously thought possible. Further experiments with improved techniques are planned to verify the existence of the bumps.

¹H. Yamada, et al., Phys. Rev. Lett. 43, 605 (1979).

²F. S. Stephens, Reviews of Modern Physics, Vol. 47, No. 1 (1975).

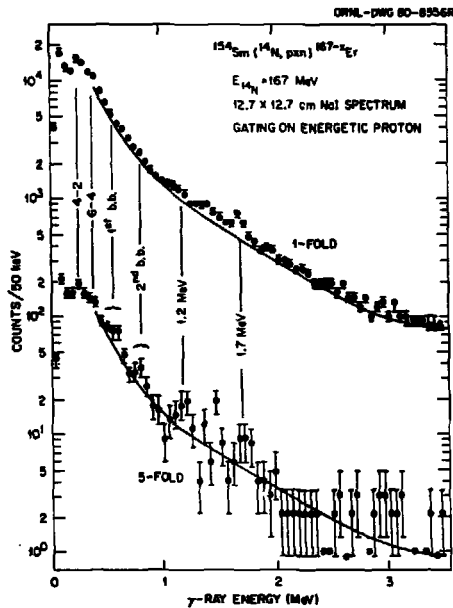


Fig. 1

ALIGNMENT OF PARTICLE ANGULAR MOMENTUM IN DEFORMED NUCLEI

L.K. Peker, NNDC, Brookhaven National Laboratory, Upton, LI, New York

J.H. Hamilton, Physics Department, Vanderbilt University, Nashville, TN

J.O. Rasmussen, Lawrence Berkeley Laboratory, Chemistry Department, University of California, Berkeley, California

The sudden changes in the moment of inertia, backbending in yrast cascades in even-even rare earth nuclei, are understood in terms of the crossing of the ground rotational band (GRB) with a rotational aligned band built on a $(j \geq 9/2)^2$ configuration-Stockholm band (SB). An important characteristic of the SB band is the magnitude of the alignment I_0 — the projection of the intrinsic angular momentum of both unpaired aligned particles on the axis of rotation¹. Recently Bohr and Mottelson² proposed a way to extract the information on I_0 from an analysis of experimental data on the function $I = I(\omega)$, where the angular frequency $\hbar\omega \approx E_Y(I + 1/2 - I - 1)/2$. In the approximation, $E_{rot} = A_1 R(R + 1)$, where $R = I - I_0$, and I is the total angular momentum of the rotational state, the function $I = I(\omega)$ for a given rotational band is $I = 1/4A_1 E_Y + \text{const.}$ and is described by a straight line with a slope proportional to the moment of inertia $\mathcal{J} = \hbar^2/2A_1$. For the GRB and SB, these lines would be displaced by a quantity $i_\alpha(\omega) = I_{SB}(\omega) - I_{GRB}(\omega)$. Bohr and Mottelson² call $i_\alpha(\omega)$ the "aligned angular momentum" and propose to consider it as a measure of the alignment of the SB.

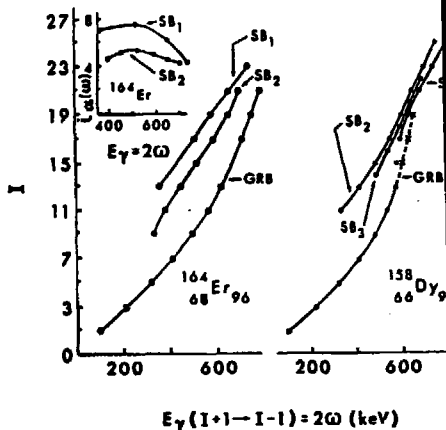
Because of the importance of the effect of Coriolis alignment for the understanding of the nature of high spin collective states, we have analysed their proposed interpretation² of $i_\alpha(\omega)$ in more detail. The function $I_\alpha(\omega)$ depends not only on the properties of the SB (including alignment) reflected in the function $I_{SB}(\omega)$, but as we shall see by definition depends on the properties of the GRB and the strength of coupling of these two bands, $\hbar\omega/\Delta E(I)$. The GRB and the SB have very different dependences on I . To illustrate, consider the next approximation $E_{rot} = A_1 [R(R+1)] - A_2 [R(R+1)]^2$ (eq. 1) where A_2 characterises the nuclear softness. From eq. 1, the two leading terms of $E_Y(I)$ are $E_Y(I) = 4A_1 R - 8A_2 R^3 + \dots$. With $A_2/A_1 \approx 10^{-2} - 10^{-3}$, the influence of the first term is dominant at low R . But with increasing R , the influence of the second term on E_Y increases very fast. For states with the same I , $R_{GRB} \gg R_{SB}$ since $R_{GRB} = I$ and $R_{SB} = I - I_0$. Therefore, the energies of the GRB at a given I are much more strongly affected by the second and higher order terms in equation 1 than are the energies in the SB at the same I . Thus, we can expect that in the GRB as I increases E_Y increases not as fast as in the SB, and the $I = I_{GRB}(\omega)$ curve up bends faster than the $I = I_{SB}(\omega)$ curve. Our conclusions are the same for a more realistic expansion $E_{rot} = \sum i_\alpha \omega^{2i}$. Therefore $i_\alpha(\omega)$ which reflects the difference in the behavior of the SB and the GRB, at large I is expected to decrease with increasing I , independent of the magnitude of the real alignment I_0 of the SB. This effect is illustrated for the GRB and the SB in ^{164}Er and ^{158}Dy (insert in Fig. 1, refs. 3-6).

Now consider the effects of the mixing of the GRB and SB on the magnitude of $i_\alpha(\omega)$. If only the Coriolis effect is responsible for $i_\alpha(\omega)$ in the aligned bands in odd-A and even-even A nuclei, then according to Bohr and Mottelson² $i_\alpha^{e-e}(\omega)_{\text{calc}} = i_{\alpha_f}^{e-o}(\omega) + i_{\alpha_{uf}}^{e-o}(\omega)$ where $i_\alpha^{e-o}(\omega) = I_{AL}^{e-o}(\omega) - I_{GRB}^{e-e}(\omega)$, and i_{α_f} and $i_{\alpha_{uf}}$ are alignments for the favored and unfavored parts of the $113/2$ band. We calculated the values of $i_\alpha^{e-e}(\omega)_{\text{calc}}$ from ^{159}Dy , ^{161}Er and ^{165}Er . We emphasize that calculated in this way values of $i_\alpha^{e-e}(\omega)$ do not include the effect of mixing GRB - SB. The values of $\Delta i_\alpha = i_\alpha^{e-e}(\omega)_{\text{calc}} - i_\alpha^{e-e}(\omega)_{\text{exp}}$ are 4.2, 0.7 and 0.1 for ^{158}Dy , ^{160}Er and ^{164}Er , respectively. It is known that the backbending in ^{158}Dy (refs. 3, 6) is much smaller than in ^{160}Er (refs. 3, 7) and ^{164}Er (Fig. 1). So in ^{158}Dy , \mathcal{J}_{SB} is close to \mathcal{J}_{GRB} , $E(I)_{SB_1}$ is close to $E(I)_{GRB}$, $\Delta E(I)$ is small, and the mixing of the SB_1 and GRB is strong. This

can lead to a strong decrease of $i_{\alpha}(\omega)$ in ^{158}Dy in comparison with the strong back-bender ^{164}Er (where the GRB-SB₁ mixing is weak). So the large difference between $i_{\alpha}^{e-e}(\omega)_{\text{exp}}$ and $i_{\alpha}^{e-e}(\omega)_{\text{calc}}$ can be considered as an effect of the mixing of the GRB and SB₁. Also the configuration $(j \geq 9/2)^2$ can produce many aligned bands with even and odd spins with different degrees of rotational alignment I_0 . The band with maximal alignment I_0^{max} , SB₁, and with strongest Coriolis effect has the largest moment of inertia \mathcal{J}^{max} and is the lowest. The bands with smaller degrees of alignment SB₂, SB₃ have by definition smaller I_0 and larger energies. Because of weaker Coriolis coupling, they also have a smaller moment of inertia. If the SB₁ - GRB mixing is sufficiently strong, the observed $i_{\alpha}^{e-e}(\omega)$ for SB₁ can be smaller than $i_{\alpha}(\omega)$ for SB₂ (with even I) which are higher and therefore have larger $\Delta E(I) = E_{\text{SB}_2}(I) - E_{\text{GRB}}(I)$ and weaker mixing. The same is true for $i_{\alpha}(\omega)$ for SB₃ (with odd I) and for the aligned negative parity bands (NPB). Thus in ^{164}Er , where the GRB - SB₁ mixing is weak, we can expect that $i_{\alpha}(\text{SB}_1) > i_{\alpha}(\text{SB}_2, \text{SB}_3 \text{ or NPB})$, whereas in ^{158}Dy with strong GRB - SB₁ mixing $i_{\alpha}(\text{SB}_1)$ can be smaller than $i_{\alpha}(\text{SB}_2, \text{SB}_3 \text{ or NPB})$. As seen in Fig. 1, the observed properties of the side bands in these nuclei ^{164}Er and ^{158}Dy completely support these predictions and therefore demonstrate the influence of the mixing of the GRB and SB₁ on $I_{\alpha}(\omega)$.

Thus, we have shown that the magnitude of the "aligned angular momentum", $i_{\alpha}^{e-e}(\omega)$, introduced by Bohr and Mottelson² reflects not only the real alignment in SB₁ but also the properties of the GRB and the strength of the mixing of the GRB and SB₁. Thus, i_{α} is not a measure of the real alignment of the SB. The research at Brookhaven and Lawrence Berkeley Laboratories and in part at Vanderbilt University are supported by the Department of Energy.

Figure 1: The functions of $I = I(\omega)$ for GRB and observed aligned bands SB₁, SB₂ and SB₃ in $^{164}\text{Er}_{96}$ and $^{158}\text{Dy}_{92}$. For ^{164}Er we also present data on $i_{\alpha}(\omega)$ for the two even spin aligned bands SB₁ and SB₂. Note that $i_{\alpha}(\omega)_{\text{SB}_1} > i_{\alpha}(\omega)_{\text{SB}_2}$ for ^{164}Er and $i_{\alpha}(\omega)_{\text{SB}_1} < i_{\alpha}(\omega)_{\text{SB}_2}$ for ^{158}Dy . It is possible that the SB₂ and/or SB₃ shown may have negative parity. This change would not alter any of the conclusions we presented.



List of references

1. F.S. Stephens, R. Simon, Nucl. Phys. A183, (1972) 257.
2. A. Bohr, B.R. Mottelson, J. Phys. Soc. Japan 44, (1978) 157.
3. C. Saethre, et al, Nucl. Phys. A207, (1973) 486.
4. N.R. Johnson, et al, Rev. Lett. 40, (1978) 151.
5. O.C. Kistner, et al, Phys. Rev. 17C, (1978) 1417.
6. A.W. Sunyar, Symp. on High Spin Phenomena in Nuclei, Argonne (1979) 77.
7. B. Haas, et al, International Conference on Nuclear Interactions, Canberra, August (1978)

YRST SPECTRUM AND g -FACTOR FOR $^{158}\text{Dy}^*$

M. Diebel, A.N. Mantri[†] and U. Mosel
Institut für Theoretische Physik,
Universität Giessen, 6300 Giessen, West Germany.

Inclusion of pairing correlations in Strutinsky-*cranking* calculations is desirable to get realistic results for energies in the spin region ($I \lesssim 20$) where most of the experimental informations are available. To achieve this we have recently suggested¹ a prescription in which the total energy of a nucleus consists of three terms: 1) the energy of a rotating classical liquid drop, 2) the shell correction energy for the unpaired system as given in the Strutinsky approach, and 3) the pairing energy defined as the difference of HFB and shell energies. We performed a HFB calculation in which a fully selfconsistent treatment of pairing was done and the single particle potential was replaced by a triaxial Nilsson potential. The results for ^{158}Dy are presented in this paper. Fig. (1) gives the calculated yrast energies along with the experimental energies. It is seen clearly that the pairing term contributes significantly and with its inclusion an excellent agreement with experiments is obtained.

Using the cranked HFB wavefunctions we have also calculated the gyromagnetic factors $g(I)$ as a function of spin. Experiments² give a constant g -factor ($g = 0.36 \pm 0.06$) for states up to $I = 8$ and a tendency to decrease for $I = 10$ state. Fig. (2) shows the calculated spin variation of $g(I)$. We also give therein the ratio of proton spin to total spin as a function of spin. The two quantities have the similar trend and decrease with spin. It is clear that the experimental uncertainties are to be reduced to test this variation for $I \leq 8$. However, making use of the enhanced transient field effect³ it should be possible to verify the predicted large decrease in g -factors for spin states $I = 10-14$.

The spin variation of g -factors is found to be very sensitive on the occupation of valence nucleons. Calculations for ^{164}Dy which has a slightly bigger deformation, for example, do not show any appreciable variation. The decrease of $g(I)$ for ^{158}Dy is a rotational alignment effect. Using cranked HFB wavefunctions we determined the spin carried out by the $i 13/2$ neutrons of which there are two pairs in ^{158}Dy (deformation $\epsilon = 0.25$). The decoupling of these neutron pairs is found to be complete at spin $I = 14$ where the g -factor and the spin ratio reaches a minimum. Furthermore, the difference between these two quantities comes mainly

* Work supported by GSI Darmstadt and BMFT.

† Fellow of the A.V. Humboldt Foundation and on leave of absence from Department of Physics, Banaras Hindu University, Varanasi 221005, India.

from the spin contribution of the aligning neutrons. As higher spin states are reached the alignment of $h \ 11/2$ protons starts and causes a rise in the g -factor. However, a significant measurable rise will take place only at much higher spins ($I \sim 30$).

- 1) M.Diebel and U.Mosel, Z. Physik A293, 53 (1979).
- 2) R.Kalish, B.Herskind and G.B.Hagemann, Phys. Rev. 8, 757 (1973).
- 3) D.Ward, O.Häusser, H.R.Andrews, P.Taras, P.Skensved, N.Rud and C.Broude, Nucl. Phys. A330, 225 (1979).

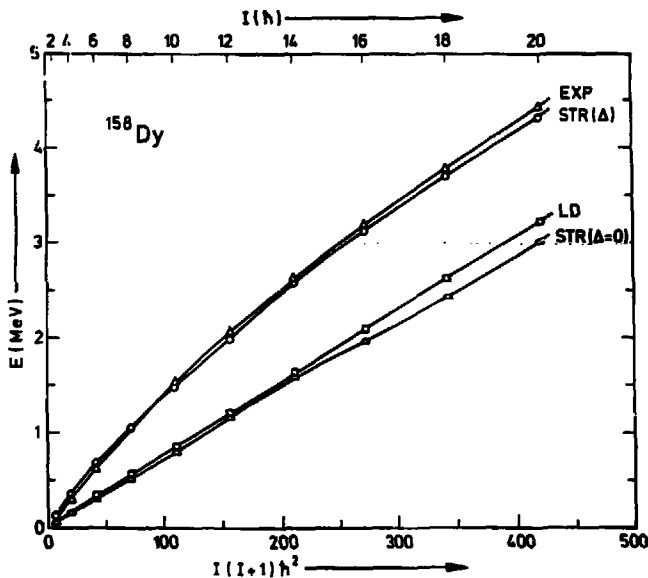


Figure 1

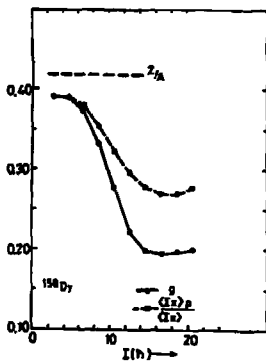


Figure 2

Fig. 1. Yrast spectrum of ^{158}Dy . The results of Strutinsky calculations with inclusion of pairing effects are denoted by STR(A). For comparison we also show the LD energy and the energy of Strutinsky calculations without pairing STR(A=0). The deformation of the nucleus is $\epsilon = 0.25$. The pairing interaction strengths G for neutrons and protons are 0.124 MeV and 0.101 MeV respectively.

Fig. 2. Spin variation of gyromagnetic factor (points on full line) for ^{158}Dy . For comparison, the variation of the ratio of proton spin to total spin is also shown (points on dashed line).

HIGH SPIN STATES IN NEUTRON RICH DEFORMED NUCLEI *

H.Bohn, T.Faestermann, F.v.Feilitzsch, and P.Kienle
Physik-Department, TU - München, D-8046 Garching, F.R. Germany

H.Enling, P.Fuchs, E.Grosse, D.Schwalm, and H.J.Wollersheim
GSI, D-6100 Darmstadt, F.R. Germany

Information on the high spin structure in neutron rich deformed rare earth nuclei is scarce mainly because these nuclei cannot be excited by the usually applied fusion type reactions. On the other hand an extension of the existing knowledge about the behaviour at high spin from the neutron deficient to the more neutron rich nuclei is highly desirable for a more complete microscopic understanding of the underlying structural effects.

In continuing our study of high spin states in the most neutron rich stable nuclei throughout the rare earth region we investigated ^{160}Gd and ^{176}Yb . ^{160}Gd is located in a region where the deformation at low angular momentum still increases with increasing neutron number. This is not true for the Yb isotopes in that for the most neutron rich stable isotope, ^{176}Yb , the deformation already drops.

The nuclei have been excited via inelastic scattering employing a ^{208}Pb beam from the UNILAC. Thin, highly enriched ^{160}Gd and ^{176}Yb targets were bombarded at beam energies between 4.7 and 5.1 MeV/A. Particle - γ coincidences were measured in a set-up similar to the one described previously ¹.

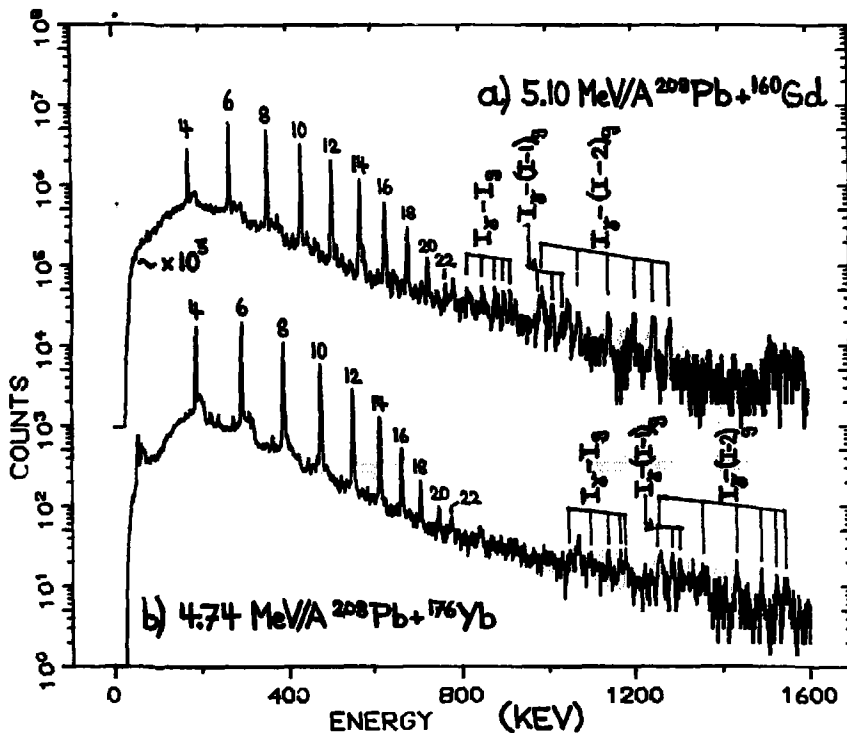
Fig. 1a shows as an example a Dopplershift corrected Ge(Li) spectrum for ^{160}Gd , coincident to recoil nuclei detected in the whole angular range covered by the particle detectors. In ^{160}Gd accurate energy information on the ground state band (g.s.b.) was known before only up to the 4^+ state. We observe excitation of the g.s.b. up to $I^\pi = 22^+$ at $E^* = 5186$ keV. The two highest lying transitions are much more clearly visible in γ - spectra (not shown) coincident to recoils scattered at small impact parameters. In addition, excitation of the γ - band is observed up to the 12^+ level at $E^* = 2584$ keV.

Fig. 1b shows an analogous γ - spectrum for ^{176}Yb . Levels in ^{176}Yb up to $I^\pi = 18^+$ have been investigated before employing ^{86}Kr and ^{136}Xe beams ². We extend the g.s.b. up to $I^\pi = 22^+$ at $E^* = 5502$ keV. For the first time we also observe excitation of the γ - band up to the 10^+ level at $E^* = 2478$ keV.

* Work supported by the Bundesministerium für Forschung und Technologie.

1. H.Bohn, T.Faestermann, F.v.Feilitzsch, P.Kienle, A.W.Sunyar, H.Emling, P.Fuchs, E.Grosse, D.Schwalm, and H.J.Wollersheim, Proceed. Int. Conf. on High-Spin Phenomena in Nuclei, March 15-17, 1979, p. 447, Argonne National Laboratory.

2. D.Ward et al., Nucl. Phys. A266, 194 (1976).



HIGH FREQUENCY BAND CROSSING IN ^{161}Yb

J.J.Gaardhøje, O.Andersen, J.D.Garrett, G.B.Hagemann, B.Herskind and L.L.Riedinger
The Niels Bohr Institute, University of Copenhagen, DK-2100 Copenhagen, Denmark
P.O.Tjøm
Institute of Physics, University of Oslo, Oslo, Norway

The systematics of the crossing between the ground-state rotational band and a band with a large particle angular momentum aligned along the rotational axis¹ ("backbending") are well studied. In ^{158}Er (ref.²) and ^{160}Yb (refs.^{3,4}) two band crossings are known in the yrast sequence. The present contribution reports a band crossing in ^{161}Yb at the same rotational frequency, $\hbar\omega \approx 0.42$ MeV, as the known higher frequency crossings in ^{158}Er and ^{160}Yb .

The level scheme shown in fig.1 was established from γ - γ coincidence and γ -ray angular distribution data obtained using the $^{140}\text{Sm}(^{16}\text{O},3n)$ reaction and experimental techniques similar to those described in ref.⁴. Both signatures of the ground-state configuration ($\alpha^\pi = +\frac{1}{2}^-$, band 2, and $= -\frac{1}{2}^-$, band 3) and the two signatures of the yrast configuration ($\alpha^\pi = +\frac{1}{2}^+$, yrast band, and $= -\frac{1}{2}^+$, band 1) as well as a third $\alpha^\pi = +\frac{1}{2}^-$ band (band 4) extend to large values of $\hbar\omega$ ($\approx E_x/2$). A sharp "backbend" is observed in the ground-state band (see fig.2) at the $\hbar\omega$ of the first band crossing of the yrast band in ^{160}Yb . A "backbend", however, is not observed at this frequency for the two positive parity bands. The alignment of the quasiparticle pair AB (see fig.3) which would be responsible for such a "backbend", is "blocked" by unpaired particles A and B in the yrast band and band 1, respectively. These two bands, however, upbend at a larger $\hbar\omega$, which corresponds to the alignment of quasiparticles BC and AD respectively.

Only the $\alpha^\pi = -\frac{1}{2}^-$, band 3, which is associated with the three-quasiparticle configuration FAB after the first band crossing, is established to the $\hbar\omega$ of the second "backbend" in ^{158}Er and ^{160}Yb . An upbend is observed in this band at $\hbar\omega = 0.42$ MeV. If the identification of this band with the configuration FAB is correct, alignments involving neutron quasiparticles F, A and B are "blocked" for this crossing. Therefore alignments BC, AD, EF and FG are blocked, and the remaining allowed neutron quasiparticles, e.g. CD, EH and GH, would be expected to align at much higher frequency ($\hbar\omega \approx 0.55$ MeV). Calculations indicate that the first proton alignment ($h_{11/2}$ particles) should occur at $\hbar\omega \approx 0.41$ MeV, resulting in a 5-q.p. configuration FAB(2p) which crosses the FAB band. Such a proton alignment also would cause an upbend in all observed bands at the same frequency. The band crossing at this $\hbar\omega$ in the yrast sequence of ^{158}Er and ^{160}Yb previously has been associated with the alignment of proton quasiparticles from theoretical considerations⁵. The present data, the first in which a high frequency "backbend" is observed in an odd neutron system, are the first, however, to experimentally support such an identification.

1. F.S.Stephens and R.S.Simon, Nucl.Phys. **A183**, 257 (1972).
2. I.Y.Lee et al., Phys.Rev.Lett. **38**, 1454 (1977).
3. F.A.Beck et al., Phys.Rev.Lett. **42**, 493 (1979).
4. L.L.Riedinger et al., Phys.Rev.Lett. (in press).
5. See e.g. A.Faessler and M.Ploszajczak, Phys.Lett. **76B**, 1 (1978).

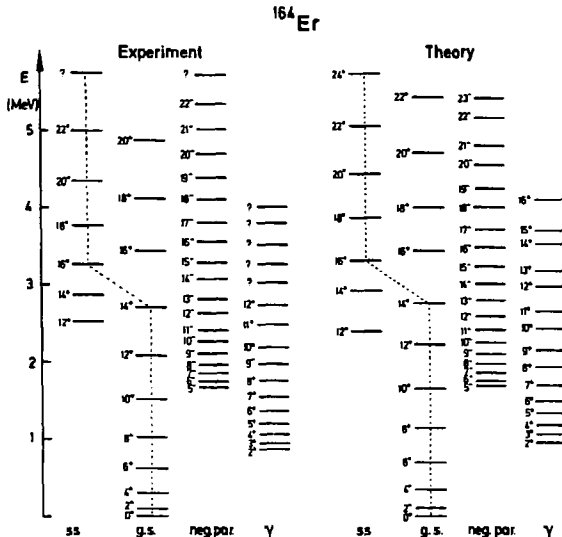
THE MICROSCOPIC STRUCTURE OF THE VIBRATIONAL LEVELS IN ^{164}Er AT LARGE ANGULAR MOMENTA

J.L.Egido, H.J.Mang, P.Ring
 Physik-Department, Techn. Univ. München, D-8046 Garching, W-Germany

Rotational bands in the vicinity of the yrast line of ^{164}Er , which have been recently measured up to rather high angular momenta, were studied in the framework of the mean-field approximation with projection on particle number and angular momentum. Starting from a time-dependent generalized Slater determinant in the intrinsic frame, one ends up in the limit of small amplitudes and approximate axial symmetry with the random-phase approximation in the rotating system. It has several advantages:

- (i) For low angular momenta it goes over into the well-known deformed RPA which has been used with great success for the calculation of vibrational states in deformed nuclei.
- (ii) The self-consistency of the underlying single-particle basis guarantees the spurious solutions arising from the violation of symmetries to decouple completely from the other excitations.
- (iii) The so-called rotation-vibrational coupling is fully taken into account because for each angular momentum a new basis is used for the calculation of the vibrational levels.

For a residual interaction of pairing plus quadrupole type, whose parameters have been adjusted to the ground-state properties, the RPA-equations were solved. For low angular momenta we find the well-known quadrupole oscillations (β, γ), the pairing vibrations for protons and neutrons and several non-collective two-quasiparticle bands. In the high-spin region additional aligned bands develop. They are dramatically lowered in energy by the Coriolis interaction and several band crossings with other collective bands and with the ground-state band ("backbending") occur. The calculated spectrum is in fair agreement with experimental data.



ANALYSIS OF ANGULAR DISTRIBUTIONS IN (PARTICLE, XN) REACTIONS

V.A. Ionescu, J. Kern, Cl. Nordmann, S. Olbrich
Physics Department, University of Fribourg, Switzerland

It is well known that gamma ray emission following (particle, xn) reactions is strongly anisotropic: $W(\theta) = 1 + \sum A_\lambda P_\lambda(\cos\theta)$. A special experimental effort was made in our work on $^{165}\text{Ho}(\alpha, 2n)^{167}\text{Tm}$ reaction in order to obtain precise values for the A_4 coefficients¹. It was then possible, for quadrupole stretched transitions, to experimentally determine the statistical tensors $\rho_\lambda(J_i) = A_\lambda^{\text{exp}} / B_\lambda(J_f J_i L \delta = 0)$ of the initial levels. In this case, the geometrical B_λ coefficients are simply the well known F coefficients. The statistical tensors describe the initial level orientation:

$$(1) \rho_\lambda(J_i) = (2J_i + 1)^{1/2} \sum_m (-1)^{J_i + m} \langle J_i - m J_i m | \lambda 0 \rangle g(m) / \sum_m g(m)$$

where $g(m)$ is the distribution of the magnetic substate population. It has become customary to assume a Gaussian distribution $g(m) = \exp(-m^2/2\sigma^2)$. Before completion of the present work this Gaussian hypothesis has been found not to be correct in experiments with low Z targets^{2,3}. Figure 1 shows that also for our heavy target the Gaussian hypothesis is not satisfactory. The same conclusion can be drawn from fig. 2, curve A, where the best values of $\sigma \pm \Delta\sigma$ is searched by the minimisation of

$$(2) \chi^2 = \sum w_i [A_\lambda^{\text{exp}} - \rho_\lambda(J_i \sigma) B_\lambda(J_f J_i L \delta = 0)]^2$$

The χ^2_{min} is 5 which corresponds to a confidence level of only 5%.

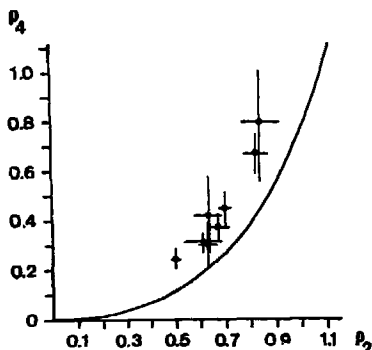


Fig. 1 Experimental ρ_2 ρ_4 statistical tensors and relation corresponding to the Gaussian hypothesis (solid curve)

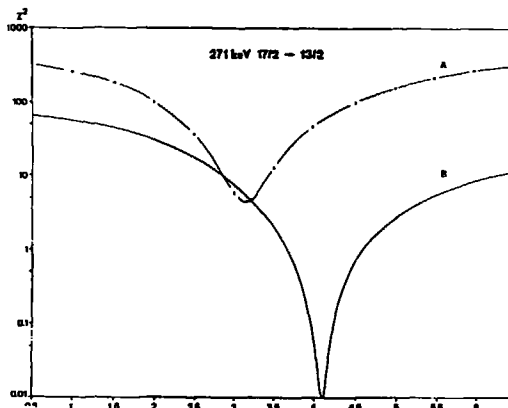


Fig. 2 Fit of $\chi^2(\sigma)$. Curve A: Gaussian hypothesis ; Curve B: present proposition

To resolve this problem we assume that the side feeding contributes effectively a Gaussian distribution $g_s(m)$, but that the discrete transitions bring in the initial level different populations $g_j(m)$. Then $g_t(m) = g_s(m) + \sum g_j(m)$. Using (1), the statistical tensor of the initial level is given by

$$(3) \quad \rho_\lambda(J_i \sigma) = \rho_\lambda^S(\sigma) (I_s/I_T) + \sum \rho_\lambda^{Pj} U(J_i J_j L_j \delta_j) (I_j/I_T)$$

where the ρ_λ^S tensor is computed using the Gaussian hypothesis. I_s is the side feeding intensity, I_j the total (angle averaged and including conversion) intensity of the transition j , $I_t = I_s + \sum I_j$ the total level population, ρ_λ^{Pj} the experimental statistical tensor of the j -th parent state, and $U(J_i J_j L_j \delta_j)$ the corresponding desorientation coefficient. The value of χ^2 obtained by replacing (3) in (2), is much improved (fig 2, curve B) and the A_λ coefficients are now reproduced within their experimental errors. Note that σ_{\min} differs conspicuously from that obtained previously. Similar results are obtained for all the observed quadrupole transitions.

The obtained $\sigma \pm \Delta\sigma$ values are then used to fit the mixing ratios of the dipole transitions originating from the same level.

Our results for ^{167}Tm show that no general trend concerning σ values can be found. For instance, in the $1/2$ (541) band, σ is roughly constant but in the $1/2$ (411) band the ratio σ/J is only approximately constant. Moreover the range of σ values is very large. We therefore find levels with very different degrees of spin orientation. This explains why the population of a given level cannot be described by a single Gaussian distribution, since a relatively small number of discrete transitions contribute populations of quite different widths.

1. S. Olbrich, V.A. Ionescu, J. Kern, Cl. Nordmann, M. Reichart, Nucl. Phys. (in press)
2. L.P. Ekström, A.M. Al-Nasr, P.R.G. Lornie, P.J. Twin, Nucl. Instr. Meth. 158 (1979) 243
3. G.A. Engelbertink, L.P. Ekström, D.E.C. Scherpenzeel, H.H. Eggenhuisen, Nucl. Instr. Meth. 143 (1977) 161

Y_{21} PAIRING AND THE PARTICLE-ROTOR DESCRIPTION OF ^{167}Er

J. Almberger^a, I. Hamamoto^b and G. Leander^c

NORDITA, Copenhagen, Denmark

^aAFI, Stockholm, ^bMIT, Cambridge, USA, ^cLund University, Lund

If the pairing interaction is a short-range two-body force, then its multipole expansion contains more terms than the monopole, with coefficients depending on the range and other characteristics of the force. These terms would give rise to higher multipole components of the pair field. In particular, a Y_{21} pair field would be expected in rotating nuclei with quadrupole deformation, with consequences for the rotational properties of the nucleus depending on the strength of the field. A discussion and results from cranking model calculations can be found in ref. ¹.

Currently we are investigating the effect of the Y_{21} pair field in the particle-rotor model, and here we report on an analysis of the positive-parity rotational bands in ^{167}Er . From the analogy between the frequency ω in the cranking Hamiltonian and the operator $\theta^{-1}\bar{R}$ in the Hamiltonian ²

$$H = \theta^{-1}R^2 + \sum_{\text{valence space}} (\epsilon_i - \lambda) a_i^\dagger a_i + \frac{1}{2} \Delta (a_{i1}^\dagger a_{i-1}^\dagger + a_{i-1} a_i)$$

an additional term corresponding to a Y_{21} pair field in the latter takes the form

$$-\theta^{-1} (\frac{1}{2} \{R_-, F_+\} + \frac{1}{2} \{R_+, F_-\})$$

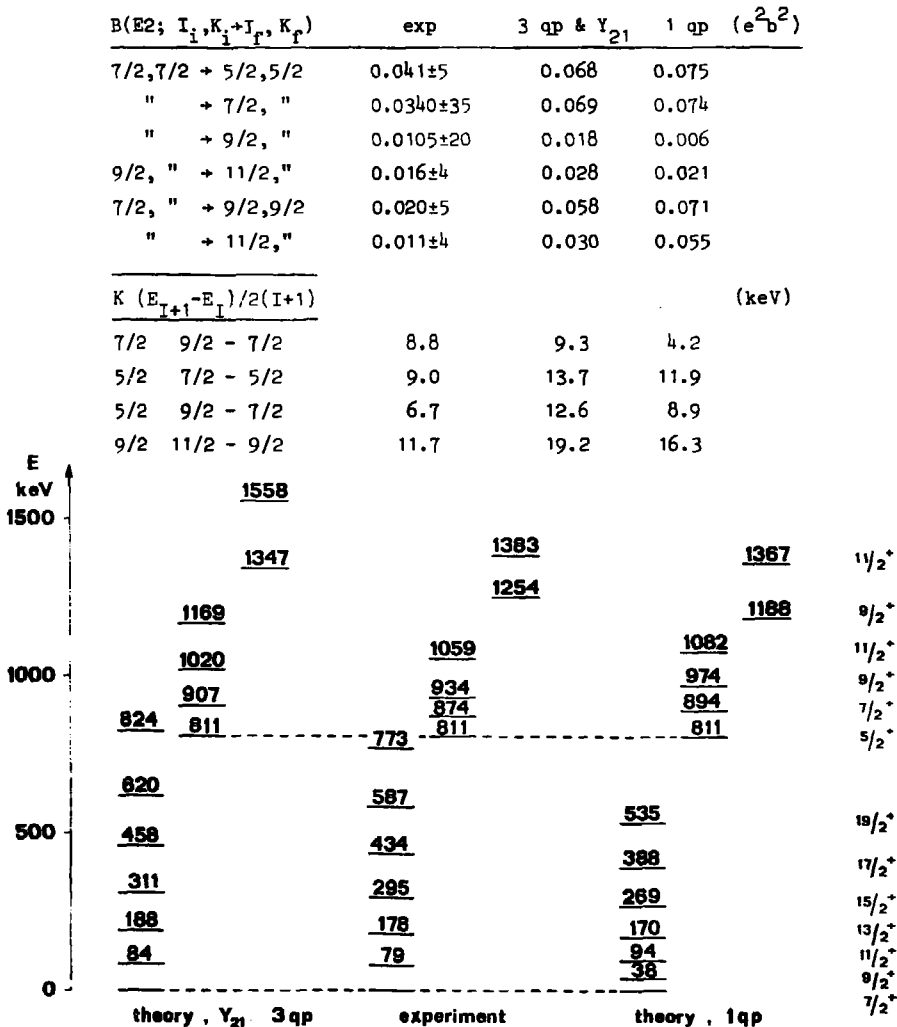
where \bar{R} is well-defined apart from a strength parameter D. The Y_{21} pair field enhances the contribution to the moment of inertia from the valence space, especially for high-j shells. A reasonable contribution from the $i_{13/2}$ neutrons is at most ~50% of the total inertia. In the present calculations, where the single-particle energies ϵ_i correspond to the $i_{13/2}$ shell at deformation $\epsilon=0.26$ and the monopole gap parameter Δ is 0.7 MeV, this sets an upper limit of 0.15 on D. Calculations are made for D=0 and 0.15, with a valence space including all one- and three-BCS-quasiparticle states in the $i_{13/2}$ shell, or alternatively only the 1-qp states. The corresponding even system, intermediate between ^{166}Er and ^{168}Er , is considered to be the rotor plus 0-qp state in the latter case, and the result of diagonalization in the valence space of 0- and 2-qp states in the former. The inertia parameter θ^{-1} and the Fermi level λ is determined for each calculation by requiring a 2^+ excitation energy of 80.2 keV in the even system, and a separation of 811 keV between the $7/2^+$ and $5/2^+$ band heads in the odd system.

The results for D=0 in the 1-qp space, for D=0.15 in the 1+3-qp space and for experiment ³ are compared in the figure and tables below. Actually, the 1-qp and 1+3-qp results for D=0 are very similar. The apparent moment of inertia in the ground band is seen to exceed the experimental value by a factor of two and the value in the even system by a factor of three, due to Coriolis couplings. The Y_{21} pair field attenuates couplings between 1-qp states on opposite sides of the Fermi level ¹, but with the present parameters the effect is modest. However, there is a large effect from taking the Y_{21} couplings to the 3-qp states into account explicitly, and the apparent inertia in the ground band then comes close to the experimental value. Nevertheless, the overall description of ^{167}Er does not improve. The interband E2 transitions are not sufficiently attenuated, and the level spacing increases in the higher bands where it is too large already for D=0. It may be mentioned that all the experimental data are well reproduced by a conventional particle-rotor calculation in the 1-qp space, if the Coriolis matrix

elements across the Fermi surface are attenuated phenomenologically by raising the $uu+vv$ factors to an ad hoc power of $n^{-3.5}$.

In conclusion, the Y_{21} pair field may influence the coupling of an odd nucleon to a rotational core, but when several bands are considered it is seen that this effect alone cannot be used to remove the discrepancy between theory and experiment in ^{167}Er .

1. I. Hamamoto, Nucl. Phys. A232 (1974) 445.
2. J. Almerger, I. Hamamoto and G. Leander, Nucl. Phys. A333 (1980) 184.
3. G.B. Hagemann et al., to be published.



ON THE YRAST-YRARE INTERACTION IN THE CRANKED HFB MODEL

H.-B. Håkansson

Dept. of Mathematical Physics, Lund Institute of Technology, Lund, Sweden

It has been demonstrated by Bengtsson et al. ^{1,2} that the magnitude of the yrast-yrare interaction in the cranked HFB model is an oscillating function of the chemical potential. This character of the model has been much discussed lately, see e.g. the review by Faessler et al. ³. Also in the particle-rotor model ^{4,5,6} this oscillating behaviour exists and furthermore there may be some indications of experimental verification (see e.g. the Yb isotopes ^{1,2}) giving it additional status.

Using Hamamoto's $i_{13/2}$ cranking model ⁷ we have investigated the interaction matrix elements between the 0 q.p. (g)-configuration and the lowest 2 q.p. (s)-configuration. The Hamiltonian reads

$$H = H_{s.p.} - \omega j_x - \Delta(P^+ + P) \text{ where } H_{s.p.} = \kappa \frac{3m^2 - j(j+1)}{j(j+1)} + \epsilon_0$$

and the parameters κ , Δ , ϵ_0 are in units of $M\omega_0$ 0.392, 0.12, 6.655 respectively. In the figure we have plotted the interaction matrix elements of H (solid), $H_{s.p.}$ (dashed) and $\Delta(P^+ + P)$ (dotted) between the non-interacting g and s configurations as a function of λ at the frequency $\omega = \omega_c(\lambda)$ which is defined as the crossing frequency for the non-interacting levels. The procedure for establishing these sharply crossing levels will be presented in a forthcoming publication ⁸.

From the figure we see that it is $H_{s.p.}$ that carries most of the strength, while ωj_x is almost zero for all λ -values and thus not depicted. The total interaction is just the sum of $H_{s.p.}$ and $\Delta(P^+ + P)$ with proper signs chosen. We define the non-interacting levels as those forming strictly straight lines in a quasi-particle energy diagram ^{2,9} and at the same time having constant expectation value of j_x through the crossing ⁸. This is, we believe, the most natural definition of the non-interacting levels in the cranking model. In ref. ¹ it is stated that the interaction matrix element is proportional to j_x , a statement which is not consistent with the definition above.

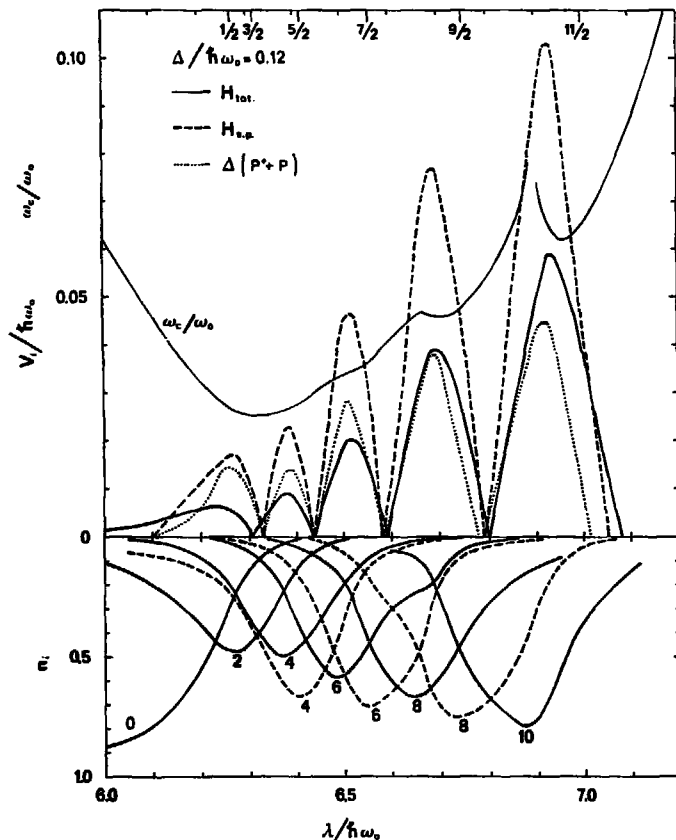
The fact that our non-interacting q.p. levels are almost eigenfunctions to j_x is not surprising if one examines a q.p. energy diagram where the interaction between some of the levels are eliminated ⁹. The levels there form straight lines which approximately can be established by a diagonalization of j_x in the basis of eigenfunctions to H .

In the exact solution of the $i_{13/2}$ model by Andersson and Krumlinde ¹⁰ it is demonstrated how sharp crossing arises if all the single-particle energies are set equal. Consequently, in that model, the yrast-yrare interaction is mainly due to $H_{s.p.}$. On the other hand, in the representation of Grümmer et al. ⁵ the interaction is attributed to the linearized pairing force active between states of particle numbers differing by two units. It is interesting to note, that in the limit $\Delta=0$ in the CHF model the 2 q.p. state goes into a state that differs in particle number by two units to the 0 q.p. vacuum and thus cannot interact by H with the 0 q.p. state. On the other hand, when $\Delta \neq 0$ we see how the interaction is dominated by $H_{s.p.}$ which indicates the connection with the results of ref. ¹⁰. So we see that the mechanism behind the interaction in the different model is highly dependent on the representation chosen and what is defined as interaction-free levels.

In the lower part of the figure we have depicted the distribution over

different particle number (0, 2, 4, ...) for the 0 q.p. vacuum (solid line) and the 2 q.p. configurations (dashed line).

1. R. Bengtsson, I. Hamamoto and B. Mottelson, Phys. Lett. 73B (1978) 259.
2. R. Bengtsson and S. Frauendorf, Nucl. Phys. A327 (1979) 139.
3. A. Faessler, M. Ploszajczak and K.W. Schmid, preprint, Tübingen, 1980.
4. J. Almerger, I. Hamamoto and G. Leander, Phys. Lett. 80B (1979) 153.
5. F. Grümmer, K.W. Schmid and A. Faessler, Nucl. Phys. A326 (1979) 1 and Nucl. Phys. A317 (1979) 287.
6. C.G. Andersson, to be published in Z. Physik.
7. I. Hamamoto, Nucl. Phys. A271 (1976) 15.
8. H.-B. Håkansson, to be published.
9. R. Bengtsson and H.-B. Håkansson, Lund preprint 1980.
10. C.G. Andersson and J. Krumlinde, Nucl. Phys. in press.



STUDY OF BAND CROSSINGS IN ^{182}Os

R.M.Lieder*, G.Sletten, O.Bakander, S.Bjørnholm, J.Borggreen, J.Pedersen
The Niels Bohr Institute, University of Copenhagen, Denmark

Side bands in ^{182}Os have been studied at the Niels Bohr Institute FN tandem accelerator using the ($^{16}\text{O},4n$) reaction, $E(^{16}\text{O}) = 81$ MeV. The studies comprised a γ - γ coincidence experiment and an angular distribution measurement. Three-fold and higher order γ - γ coincidences have been measured with a set-up consisting of 4 Ge(Li) and 3 NaI(Tl) detectors. This coincidence set-up has a large detection efficiency and enhances detection of high multiplicity events. A partial level scheme of ^{182}Os as resulting from this study is shown in fig.1.

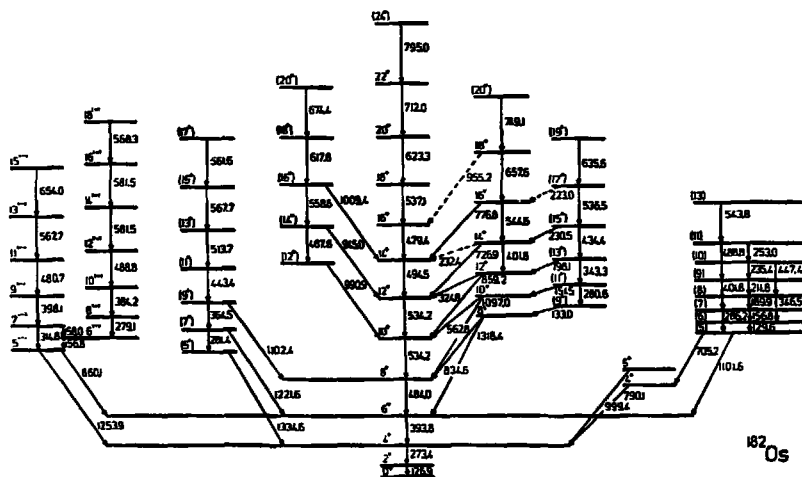


Fig.1. Partial level scheme of ^{182}Os

Spin and parity assignments result from the angular distribution experiments. Complementary conversion electron measurements are planned. The $5(-)$ and $6(-)$ bands are of special interest in connection with the backbending behaviour of the Os nuclei. An analysis of the data in terms of independent particle motion in a rotating deformed potential¹ yields that the $6(-)$ band shows a strong increase of the aligned angular momentum, i , at a rotational frequency of $\hbar\omega = 0.29$ MeV. The $i_{13/2}$ band in ^{181}Os , ref.², of signature $\alpha = 1/2$ aligns at nearly the same frequency, whereas the yrast band in ^{182}Os aligns already at the lower frequency of $\hbar\omega = 0.25$ MeV.

A comparison with cranking model calculations³ in the framework of the above mentioned model indicates that the backbending effect in the yrast band of ^{182}Os is due to the crossing of the ground band with an $i_{13/2}$ two-quasi-neutron band. In the $i_{13/2}$ band in ^{181}Os this crossing is blocked. However, the crossing with an $i_{13/2}$ three-quasi-neutron band occurs already at a frequency $\approx 10\%$ higher. Accordingly, the backbending in the $6(-)$ band results

from the same crossing assuming that the additional neutron has a configuration of opposite parity which does not influence the backbending behaviour of the band. The observation of a backbending effect in the $6^{(-)}$ band of ^{182}Os , therefore, provides a proof that also in the Os nuclei the irregularity in the yrast band is caused by $i_{13/2}$ neutrons.

- * On leave of absence from Institut für Kernphysik, KFA Jülich, D-5170 Jülich, West Germany.
1. R.Bengtsson and S.Frauendorf, Nucl.Phys. A327, 139 (1979).
 2. A.Neskakis, R.M.Lieder, M.Müller-Veggian, H.Beuscher, W.F.Davidson and C.Mayer-Böricke, Nucl.Phys. A261, 189 (1976).
 3. S.Frauendorf, F.R.May and V.V.Pashkevich, preprint, 1979.

ALIGNED QUASIPARTICLES IN EVEN 190-198 Hg ISOTOPES

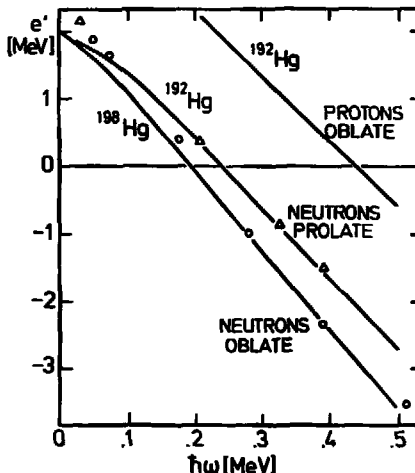
M. Guttormsen[†] and H. Hübel
 Institut für Strahlen- und Kernphysik, Universität Bonn

The level bunching observed around $I^\pi = 10^+$ in the even 190-198Hg isotopes has been interpreted¹⁻⁴ to result from a decoupling of high- j quasiparticles. It was argued that the alignment of angular momentum to $i \approx 10\hbar$ in 190-196Hg can be explained by a $(\pi h_{11/2})^{-2}$ structure whereas the higher alignment to $i \approx 12\hbar$ in 198Hg could be due to a $(\nu i_{13/2})^{-2}$ configuration. However, the proton Fermi surface lies well above the $\pi h_{11/2}$ orbitals in all Hg isotopes. Thus, it is rather surprising that these proton orbitals should play an important role in the aligned structure when going from 198Hg to the lighter isotopes.

In order to pin down the structure of the positive parity high spin states we have performed calculations within a model⁵ of quasiparticles in a rotating Nilsson potential. As an example of our calculations the eigenvalues e' of the Routhian⁵ $h'_{qp} = h_{qp} - \omega j_x$ are compared to experimental data for ¹⁹²Hg and ¹⁹⁸Hg in Fig. 1. The Fermi energies were determined consistent with the number of protons and neutrons in the system. The experimental Routhians in fig. 1 were deduced as prescribed in ref.⁵. The upper curve represents e' for an aligned pair of $h_{11/2}$ protons outside an oblate core. This corresponds to the previous interpretation of the yrast states in 190-196Hg. Although this structure exhibits the correct alignment of $i = \partial e' / \partial \omega \approx 10\hbar$, it is definitely excluded due to the very high excitation energy. We note that this band is situated 2 MeV above the ¹⁹²Hg yrast line and produces backbending first at $\hbar\omega_c \approx 0.43$ MeV.

Fig. 1:

Experimental (triangles and circles) and theoretical (solid curves) Routhians for ¹⁹²Hg and ¹⁹⁸Hg. The experimental values were derived relative to the VMI-core: $\epsilon_0 = 3.6 \text{ MeV}^{-1}\hbar^2$ and $\epsilon_1 = 88 \text{ MeV}^{-3}\hbar^4$. The calculations were performed for oblate ($\epsilon = -0.08$) and prolate ($\epsilon = 0.08$) shapes. The pairing gaps were deduced from the even-odd mass differences. Other parameters: $\hbar\omega_0 = 41A^{-1/3} \text{ MeV}$, $\chi_n = 0.0636$, $\mu_n = 0.390$, $\chi_p = 0.0620$ and $\mu_p = 0.605$.



The calculations for neutrons show much better agreement with the experimental data (see fig. 1). For prolate shape the Fermi surface is located near the high Ω members of the $i_{13/2}$ states. Thus, the alignment is effectively hindered which results in an aligned angular momentum of $i \approx 10\hbar$. For oblate shape we obtain the full alignment of $i \approx 12\hbar$.

The oblate shape for ^{198}Hg has been determined experimentally in Coulomb excitation experiments⁶. Unfortunately there exist no experimental data on the sign of the deformation for the lighter even Hg isotopes. A study⁷ of $B(E2)$ ratios⁸ between in-band and out-of-band transitions in ^{188}Hg indicates that the quadrupole moment of the ground band has the same sign as that for the strongly deformed side band. Since the latter band is expected to be prolate, the ground band is also most probably prolate in ^{188}Hg . On the other hand, theoretical studies⁹ predict oblate deformations for $^{190-196}\text{Hg}$. Thus, the sign of the deformation is not uniquely determined for the light Hg isotopes.

In summary, we predict the s-bands of even Hg isotopes to be built on a decoupled $(\nu i_{13/2})^{-2}$ structure. The attenuated spin alignment i and the critical frequency $\hbar\omega_c$ in $^{190-196}\text{Hg}$ seems to favour prolate shape of the ground bands.

[†]NTNF fellow, permanent address: Institut of Physic, University of Oslo, Norwegen

1. D. Proetel et al., Nucl. Phys. A231, 301 (1974)
2. R.M. Lieder et al., Nucl. Phys. A248, 317 (1975)
3. C. Günther et al., Phys. Rev. C15, 1298 (1977)
4. H.L. Yadav et al., Phys. Rev. Lett. 39, 1128 (1977)
5. R. Bengtsson and S. Frauendorf, Nucl. Phys. A327, 139 (1979)
6. A. Bockisch et al., Z. Physik A291, 245 (1979);
M.T. Esat et al., Phys. Lett. 72B, 49 (1977)
7. M. Guttormsen and H. Hübel, to be published
8. J.H. Hamilton et al., Phys. Rev. Lett. 35, 562 (1975)
9. For references see ref.3,6

HIGH SPIN STATES AND E2 TRANSITION STRENGTHS IN $^{194,196}\text{Pt}^+$

J. Idzko, K. Stelzer, Th.W. Elze, H. Ower
 Institut für Kernphysik, Universität Frankfurt am Main
 H.J. Wollersheim, H. Emling, P. Fuchs, E. Grosse, R. Piercey, D. Schwalm
 Gesellschaft für Schwerionenforschung, Darmstadt

The level structures of the shape transitional nuclei $^{194,196}\text{Pt}$ have been investigated by multiple Coulomb excitation with ^{208}Pb projectiles at the UNILAC of GSI. The measurements included γ -ray singles and γ , γ -coincidences at a bombarding energy of 5.38 MeV/u and particle- γ -coincidences at 4.74 MeV/u, using the coincidence set-up developed at GSI¹. With this apparatus an almost complete Doppler correction was achieved for γ -rays in coincidence with the recoil nuclei, detected at laboratory angles of $15^\circ \leq \theta \leq 60^\circ$, corresponding to center of mass scattering angles of $150^\circ \leq \theta_{C.M.} \leq 60^\circ$. For the γ , γ -coincidence measurements targets of 1 mg/cm² on thick lead backing were used to reduce the Doppler broadening of the γ -lines.

We observe the excitation of the ground state and γ -bands in the two nuclei up to 10^+ and 6^+ respectively. Excitation of levels in the negative parity bands was also identified. Figure 1 shows the positive parity levels observed in our investigations.

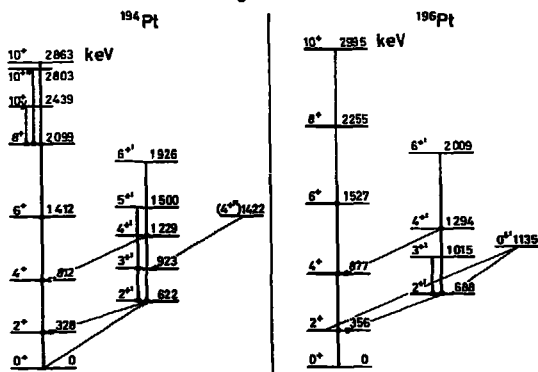


Figure 1.
 Positive parity levels as observed in the Coulomb excitation of $^{194,196}\text{Pt}$ with ^{208}Pb ions.

In ^{194}Pt the ground state band is excited with collective strength to a 10^+ state at 2863 keV, which is 424 keV above the yrast 10^+ state known from (α, xn) -experiments². In the γ , γ -experiments performed at the high bombarding energy we also observe the 10^+-8^+ yrast transition and a transition of 704 keV in coincidence with the lines^y of the ground state band. This transition shows a $0^\circ/90^\circ$ -asymmetry in the coincidence intensities characteristic for a stretched E2-transition. We therefore postulate a third 10^+ level at 2803 keV. From the intensity of the 704 keV line the transition can be estimated to be non-collective with an E2 strength of approximately 1 s.p.u.. The situation is shown in the spin-transition energy-plot of figure 2.

$B(E2)$ values for inter- and intra-band transitions were determined from a comparison of the experimental gamma yields observed in particle- γ -coincidence at the "safe" energy for Coulomb excitation of 4.74 MeV/u with semi-classical Coulomb excitation calculations. Starting with a preliminary set, the E2 matrix elements were systematically varied to achieve a best fit to the experimentally observed yields, and especially their impact parameter dependence.

⁺ This work was supported by the Bundesministerium für Forschung und Technologie

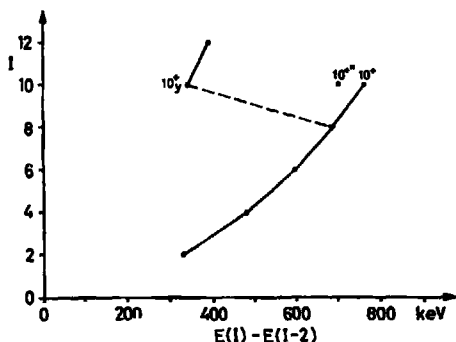


Figure 2:
Spin-transition energy-plot
for the ground state and
yrast transitions in ^{164}Pt .

Figure 3 shows the results for the $B(E2)$ values in the ground state bands. The experimental values are compared with predictions of different models: the rigid symmetric rotor (SRM), the asymmetric rigid rotor with $\gamma_0 = 30^\circ$ (ARM), the Interacting Boson Approximation in the $O(6)$ limit and two calculations^{3,4} on the basis of the Greiner-Gneuss model (GGM) starting from a general potential energy surface.

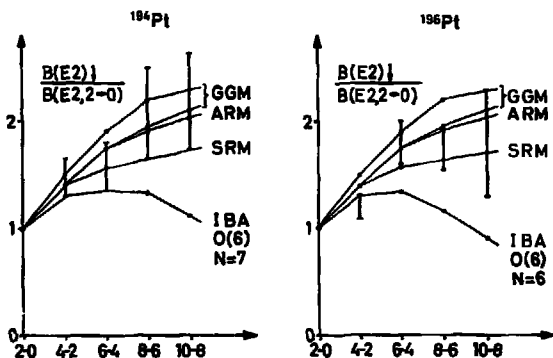


Figure 3:
Experimental and theoretical
 $B(E2)$ values for transitions
in the ground state bands. The
upper of the curves labelled
GGM is for a triaxial ($\gamma_0=30^\circ$)
"γ-stiff" nucleus³, and the
lower corresponds to an oblate
γ-soft nucleus⁴.

The "geometrical" collective models can explain the experimentally observed $B(E2)$ values within their errors. Because of the size of these errors and the small differences in the predictions of especially the more realistic models (GGM and ARM) a distinction between these models is not possible. On the other hand, the reduction of the $B(E2)$ values for the transitions between states of higher spin as predicted by the IBA is not observed.

The analysis of the transitions in the gamma band and between the gamma and ground state band depends more sensitively on the inclusion of additional bands and the sign⁵ of interband $E2$ matrix elements. Calculations for the γ-band are in progress.

1. P. Fuchs et al., GSI Annual Report 1977, p. 195
2. M. Piiparinen et al., Phys. Rev. Lett. 34 (1975), 1110,
S.A.Hjorth et al., Nucl. Phys. A 262 (1976), 328
3. G. Leander, private communication
4. P. Hess, private communication
5. F.T. Baker et al., Phys. Rev. Lett. 37 (1976), 193.

MULTI-STEP SHELL MODEL METHOD

C. Pomar

Dep. de Física, C.N.E.A., Buenos Aires, Argentine

and R. Liotta

Laboratoire de Physique Théorique, Université de Bordeaux I and

Research Institute for Physics, Stockholm, Suède

A method to solve the shell-model equations within a basis that contains correlated pairs of particles was recently presented ¹. This method was found to be very suitable to make drastic truncations of the basis at low spin. In this contribution we extended the method given in ref. ¹ to analyse four- and six-particle systems outside closed-shell cores. The basic idea here is to use the two-particle spectrum components as building blocks to describe the four-particle system. Once the four-particle spectrum is obtained, we use this spectrum and that of the two-particle system as building blocks to describe the six-particle system. The formalism turns out to be very simple. We applied it to analyse the (p,t) reactions ² leading to low-spin states in ²⁰⁴Pb and ²⁰⁶Pb and to calculate the high-spin states in ²⁰⁴Pb. A complete calculation in the low-spin region would be impossible. There would be, for instance, several hundred 2⁺ states in ²⁰⁴Pb and several thousand in ²⁰²Pb. Still, we expect that the lowest states in both nuclei, i.e. states close to the yrast line, are contained in a rather small subspace of the total space spanned by the corresponding correlated basis (which also spans the shell-model space).

We took the two-particle energies and wave-functions from the calculation by J. Blomqvist ³ which, including six single-particle levels, fits well most of the experimental data in ²⁰⁶Pb. To calculate ²⁰⁴Pb we chose for each spin and parity the first 50 states with lowest zeroth order energy. We took this rather large basis because we wanted to have a good description of ²⁰⁴Pb to calculate ²⁰²Pb. To describe ²⁰²Pb we proceeded in the same fashion, but the basis was reduced to 20 elements. The calculated quantities in ²⁰⁴Pb agree well with the experimental data. For ²⁰²Pb the agreement is not as good but still reasonable, as seen in Table 1 where only $\sigma_{rel}(\text{theor}) > 0.03$ are given. The theoretical (experimental) ground state energies, relative to the ²⁰⁸Pb core, are 28.883 (28.925) MeV for ²⁰⁴Pb and 43.983 (44.112) MeV for ²⁰²Pb. In table 2 we give the calculated ²⁰⁴Pb high-spin states.

1. R. Liotta, C. Pomar and B. Silvestre-Brac, Nuov.Cim. 27 (1980) 100.
J.P. Boisson et al., Nucl.Phys. A330 (1979) 307.
2. W.A. Lanford, Phys.Rev. 16C (1977) 988.
3. J. Blomqvist, unpublished.
4. Nucl.Data Sheet 27 (1979) 581.

$^{204}\text{Pb} (p,t) \quad ^{202}\text{Pb} (J^\pi)$					
Exp.			Theory		
J^π	E	σ_{rel}	J^π	E	σ_{rel}
0_1^+	0.	2.31	0_1^+	0.	2.02
2_1^+	0.961	0.56	2_1^+	0.884	0.44
4_1^+	1.383	0.48	4_7^+	1.322	0.65
6_1^+	2.747	0.55	6_{18}^+	2.512	0.15
5_1^-	2.610	1.28	5_5^-	2.093	0.64
—	—	—	5_{12}^-	2.577	0.49
9_1^-	2.172	0.93	9_2^-	1.975	0.66
—	—	—	9_4^-	2.273	0.18

Table 1

State	21^-	20^-	20^+	19^-	$17^{(-)}$	17^-
Exp. ⁴	—	—	—	6.098	6.073	5.664
Theor.	8.781	8.672	7.707	6.095	6.074	5.669
State	16^+	16^+	15^+	14^+	12^+	
Exp. ⁴	5.348	4.887	4.302	4.135	3.516	
Theor.	5.239	4.849	4.306	4.075	3.436	

Table 2

HIGH SPIN STATES IN ^{232}Th , ^{234}U and $^{236}\text{U}^*$

H. Ower, Th. W. Elze, J. Idzko, K. Stelzer,
 Institut für Kernphysik, Universität Frankfurt am Main,
 H. Emling, P. Fuchs, E. Grosse, D. Schwalm, H. J. Wollersheim,
 Gesellschaft für Schwerionenforschung, Darmstadt,
 N. Kaffrell, N. Trautmann,
 Institut für Kernchemie, Universität Mainz

The actinide nuclei ^{232}Th , ^{234}U and ^{236}U have been studied using multiple Coulomb excitation by 5.3 MeV/u ^{208}Pb ions obtained from the UNILAC at GSI. De-excitation gamma rays were observed with Ge(Li) detectors in coincidence with both the scattered projectile and recoil nucleus. These particles were detected by two position sensitive parallel plate counters developed at GSI ¹. By measuring time of flight and scattering angle of both particles it was possible to correct for the large Doppler shifts of the gamma rays and to determine the impact parameter dependence of the gamma yields. A representative corrected spectrum of ^{232}Th is shown in Figure 1. Transition energies were determined to an accuracy of typically 0.5 keV for stronger lines and 1 keV in the higher spin region.

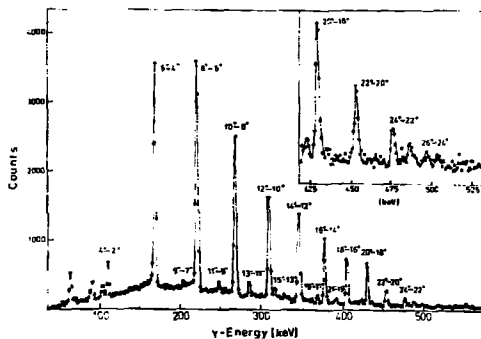


Fig.1: Doppler corrected gamma spectrum of ^{232}Th Coulomb excited by ^{208}Pb ions

The ground state bands are observed up to spin 28^+ in ^{232}Th and ^{234}U and 30^+ in ^{236}U . Levels of the $K = 0^-$ octupole vibrational band were also identified. Partial level schemes of the three nuclei are shown in Figure 2. Levels not deduced from our experiment, in particular the low spin members of the various bands, were taken from Nuclear Data Sheets ². From the apparent up-bending in the ground state bands above spin 14 a rotation aligned angular momentum of 4 to 5 \hbar at $I = 26$ can be deduced.

The experimentally determined gamma yields of the transitions within the ground state band are compared with results of semi-classical Coulomb excitation calculations based on the following nuclear models: rigid rotor, interacting boson model ³, and extended rotation vibration model ⁴. Although this analysis has not been completed, preliminary results can be given. If only ground band levels are included in the calculation, the gamma yields are reproduced by the rigid rotor model. The excitation of side bands, in particular the octupole vibrational band, cannot be neglected, however. Taking these side bands into account, the calculated gamma yields are found to become smaller

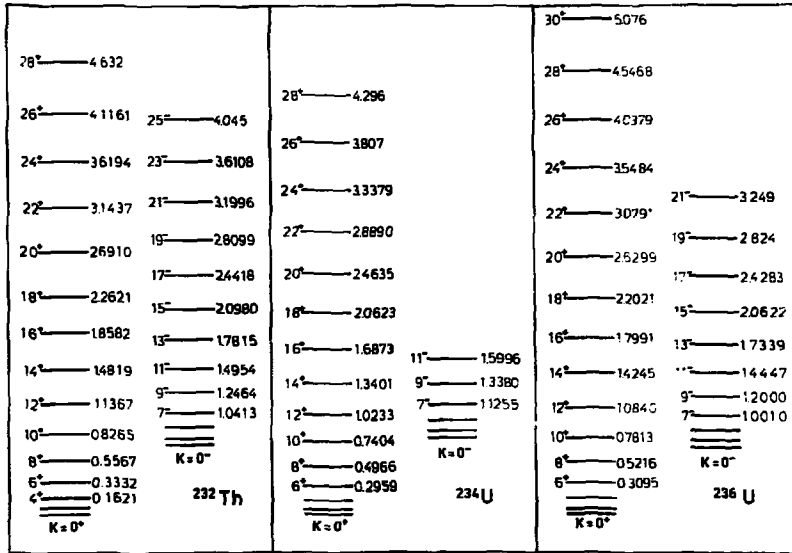


Fig.2: Partial level schemes of ^{232}Th , ^{234}U and ^{236}U showing spins and energies (in MeV) as deduced from the present study

than the measured values. The experimental uncertainties, however, make it difficult to decide to what extent the rigid rotor model has to be modified. The interacting boson model predicts a cut-off in the ground state rotational band at spin 24^+ , 26^+ and 28^+ for ^{232}Th , ^{234}U and ^{236}U , respectively, and a strong reduction of the gamma yields in the high spin region. This is in contrast to our data. Calculations employing the extended rotation vibration model, which predicts larger gamma yields with increasing spin, are still in progress.

* This work was supported by the Bundesministerium für Forschung und Technologie

1. P. Fuchs et al., GSI Annual Report 1977, p. 195
2. Nuclear Data Sheets, Vols. 20 and 21 (1977)
3. A. Arima and F. Iachello, Ann. Phys. (N.Y.) 111 (1978) 201
4. M. Seiwert and P. Hess, private communication

A COMPTON SUPPRESSION SPECTROMETER FOR COINCIDENCE MEASUREMENTS; LARGE SOLID ANGLE AND GOOD SUPPRESSION

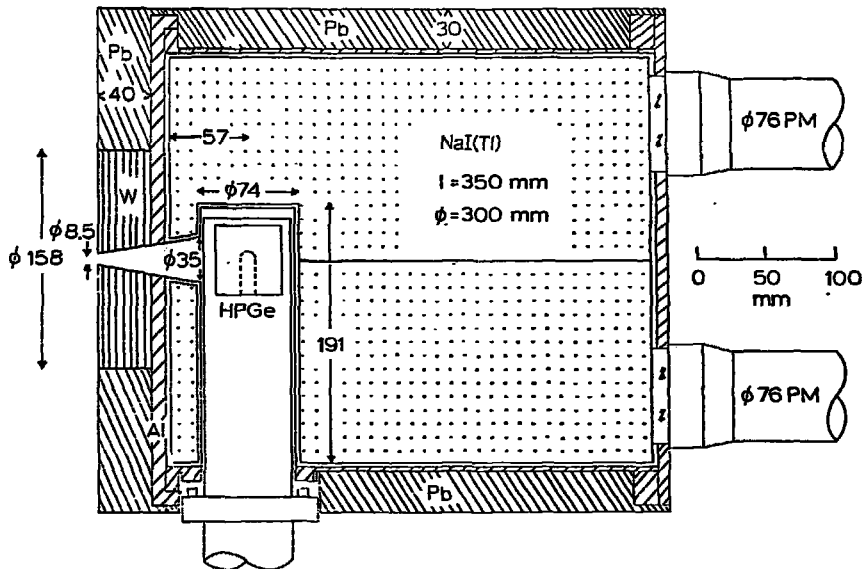
H.J.M. Aarts

Fysisch Laboratorium, Rijksuniversiteit, Utrecht, The Netherlands

For γ - γ coincidence measurements a Compton suppression spectrometer with large solid angle and good suppression has been designed. The dimensions of the NaI anticoincidence shield have been optimized by means of Monte Carlo calculations. The NaI shield^{*)} has a length of 35 cm and a diameter of 30 cm. The solid angle of the central detector is 120 msr. The latter is a 20% efficient HPGe crystal^{*)} with a dead layer of 0.22 mm and a hollow core. The influence of the dead layer of the central Ge detector on the performance of a Compton suppression spectrometer is discussed in ref.¹. For ^{60}Co , the average suppression of the Compton background between 100 and 1100 keV amounts to 11.8 with a photo-peak loss of less than 5%. The area's of the 1173 and 1332 keV peaks taken together amount to 60% of the total number of registered counts for the suppressed spectrum and to 15% for the non-suppressed spectrum. Tests of the spectrometer with the in-beam reaction $^{24}\text{Mg} + (45 \text{ MeV})^{16}\text{O}$ show that its maximum count rate is limited by the maximum count rate of the central HPGe detector.

*) Manufactured by Harshaw Chemie BV, de Meern, The Netherlands.

Ref.¹: H.J.M. Aarts et al., to be published in Nucl. Instr. & Methods.



SPIN POLARIZATION OF LIGHT FRAGMENTS FROM $^{16}\text{O} + ^{58}\text{Ni}$ REACTIONS

W. Trautmann, W. Dahme, W. Dünnweber, W. Hering,
 C. Lauterbach, H. Puchta
 Sektion Physik, Universität München, D-8046 Garching
 W. Kühn, J. P. Wurm
 Max-Planck-Institut für Kernphysik, D-6900 Heidelberg

Using the transmission method ¹ we have measured the circular polarization of γ -rays from the excited projectile-like fragments in the reaction $^{16}\text{O} + ^{58}\text{Ni}$ at 100 MeV. This reaction has been the subject of γ -ray multiplicity ² and circular polarization ³ studies which have determined amount and orientation of the spin transferred to the target like reaction product. From the present investigation we obtain the spin polarization of the light fragment which allows (i) to compare the spin orientation of both fragments individually with the prediction of the friction model and (ii) to study the mechanism of projectile excitation in the quasi-elastic and deep-inelastic regime. The data also yield information on the polarization of the statistical γ -ray continuum deexciting high-spin states in the target-like fragment.

As in former experiments ³ we have used a double-symmetric detector setup consisting of two heavy-ion telescopes at $\pm 35^\circ$ in the reaction plane and two γ -ray polarimeters perpendicular to the reaction plane (Fig. 1). Gamma-rays which had passed through about 7 cm of magnetized iron were accepted at angles $\theta \leq 20^\circ$ relative to the reaction normal and recorded by two 27 cm x 34 cm NaI detectors. In the γ -ray spectra (Fig. 2) we have defined the photopeak regions of discrete lines from excited ejectiles, and the continuum regions, and have determined their respective polarization. Corrections were made for the continuum part underlying the discrete lines.

In Fig. 3 the results are given for the two strongest channels with ejectile atomic number $Z=6$ and $Z=8$. For the discrete lines we find large polarizations, with values of $|P_\gamma|$ up to 100 % in the $^{16}\text{O}, 3^- \rightarrow 0^+$, case. The sign of the polarization is the same as for the heavy fragment for $^{16}\text{O}(3^-)$, and for $Q < -40$ MeV in the $^{12}\text{C}, 2^+ \rightarrow 0^+$, case, as expected assuming a tangential friction force. The heavy-fragment polarization is reflected by the polarization of the continuum (Fig. 3d) which nicely correlates with ³ the results obtained for the energy-integrated γ -ray spectra.

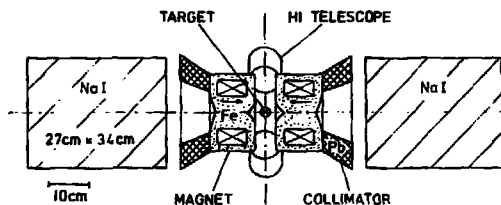
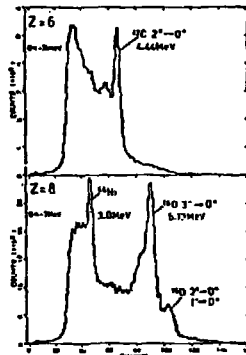


Fig. 1 Detector arrangement. The beam direction points into the drawing plane.

Fig. 2 Recorded γ -ray spectra. An electronic threshold was set at $E_\gamma = 2$ MeV



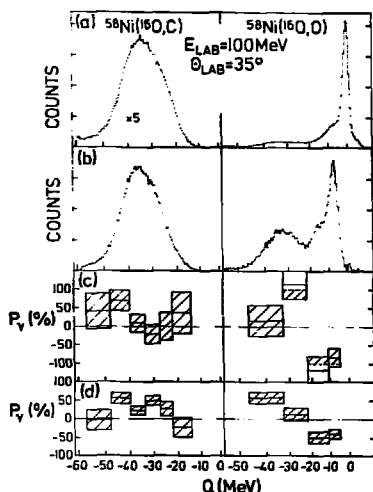


Fig. 3 (a) Free particle spectra, (b) spectra of particles coincident with γ -rays of $E_\gamma > 2$ MeV, (c) circular polarization of the 4.44 MeV ($^{12}\text{C}, 2^+ \rightarrow 0^+$) and 6.13 MeV ($^{16}\text{O}, 3^- \rightarrow 0^+$) transition on the left and right, respectively, and (d) polarization of the continuum with $E_\gamma > 3$ MeV.

The $^{12}\text{C}(2^+)$ polarization decreases from $P_\gamma = 40\%$ at $Q = -15$ MeV to small negative values at $Q = -30$ MeV. ($Q_{\text{opt}} = -24$ MeV in the semiclassical model⁴). A similar Q dependence has been found for the ^{12}B ground state polarization in ($^{14}\text{N}, ^{12}\text{B}$) transfer reactions⁵, and seems to be a general phenomenon associated with quasi-elastic transfer reactions. The increase of P_γ towards positive values with further increasing energy loss is not correlated, however, with the transition from positive to negative scattering angles. In fact, the $^{12}\text{C}(2^+)$ polarization is still small near the maximum of the deep-inelastic component associated with negative scattering angles near $Q = -35$ MeV. For a tentative explanation of this structure one might assume that the correlation of polarization and Q -value established in the quasi-elastic region still holds in the deep-inelastic region. A picture assuming α -transfer after the $^{16}\text{O} + ^{58}\text{Ni}$ system has reached a sticking configuration (and assuming negative scattering angles) would predict $P_\gamma = 0$ at the most probable $Q = -39$ MeV and $P_\gamma > 0$ ($P_\gamma < 0$) at $Q = -45$ MeV ($Q = -33$ MeV).

The P_γ values given for the statistical γ -ray continuum represent a lower limit since the continuum contains about 20% of events which have undergone Compton scattering in the magnetized iron of the polarimeter and for which, consequently, the polarization sensitivity has the opposite sign¹. We estimate that a correction of this effect would lead to $P_\gamma = 70\%$ for the statistical continuum ($E_\gamma > 3$ MeV) in the deep-inelastic region, averaged over Z . This shows that the statistical γ -ray cascades carry away spin on a rate of $0.5 \hbar$ ($1.4 \hbar$) per transition if we assume dipole (quadrupole) radiation. In a purely statistical picture, $P_\gamma = 70\%$ corresponds to a spin dependence of the level density of $\rho(I)/\rho(I+1) = 2.5$ in the populated spin/excitation region.

1. H. Schopper, Nucl. Instr. **3**, 158 (1958)
2. R. Albrecht et al., Phys. Rev. Lett. **34**, 1400 (1975)
3. C. Lauterbach et al., Phys. Rev. Lett. **41**, 1774 (1978)
4. D. M. Brink, Phys. Lett. **40B**, 37 (1972)
5. K. Sugimoto et al., Phys. Rev. Lett. **39**, 323 (1977)

ALPHA EMISSION WITH 10 MeV/A ^{14}N PROJECTILES

R.K.Bhowmik[†], E.C.Pollacco^{††}, J.B.A.England, N.E.Sanderson* and
 G.C. Morrison
 Department of Physics, University of Birmingham, Birmingham B15 2TT, England
[†]K.V.I., Gronigen, The Netherlands. ^{††}New University, Msida, Malta.
 *Daresbury Laboratory, .S.R.C., Warrington, England.

We have performed an extensive set of alpha-heavy ion correlation measurements on ^{12}C , ^{27}Al and ^{58}Ni targets with a 148 MeV ^{14}N beam. The heavy ejectiles ($Z=3-8$) were detected at $\theta_{\text{HI}} = 13^\circ$, the grazing angle for the reaction $^{14}\text{N} + ^{58}\text{Ni}$ and also at $\theta_{\text{HI}} = 26^\circ$. Coincident alpha particles were detected in coplanar geometry in a second telescope moved in the range $\theta_\alpha = \pm 70^\circ$ about the beam axis. Singles energy and angular distributions and some out-of-plane correlations have also been measured. The differential alpha-multiplicities, obtained by dividing the coincidence cross-sections by the singles deep inelastic cross sections, are shown in Fig.1.

The results from the ^{58}Ni target have been reported previously¹. For ejectiles with $Z < 6$ they can be summarised as: (i) the α -HI angular correlations are similar in shape to the singles α angular distributions, being symmetric about the beam axis (FWHM $\sim 40^\circ$); (ii) the α and HI projected energy spectra are similar in shape to the corresponding singles data; (iii) no appreciable dependence of the projected α energy spectra on either the ejectile type or ejectile energy is observed.

These features suggest that the two-dimensional energy-correlation data can be factorised according to:

$$d^4\sigma(E_{\text{HI}}, E_\alpha, \theta_{\text{HI}}, \theta_\alpha) \propto d^2\sigma(E_{\text{HI}}, \theta_{\text{HI}}) \cdot d^2\sigma(E_\alpha, \theta_\alpha) ,$$

where the terms on the R.H. side are simply the independent cross sections for HI and α emission, respectively. A quantitative fit to the measured energy and angular correlation data can be obtained from this parametrisation (see e.g. Fig.1). The angle-integrated α multiplicities corrected for out-of-plane anisotropy are estimated to be in the range 0.4-0.8.

The same analysis has been carried through for the data from the ^{12}C and ^{27}Al targets and many of the same features found. The integral α multiplicities from the ^{12}C target are in the range 1.0-2.0 and for the ^{27}Al target in the range 0.6-1.0. A reasonable description of the energy correlation data can be obtained from the factorisation prescription, but the angular correlation peak shows a systematic shift away from the HI direction with increasing $Z \geq 6$ (Fig.1).

For the ^{12}C target such a shift can be understood from reaction kinematics. A Monte-Carlo simulation of the reaction $^{12}\text{C}(^{14}\text{N}, ^{14}\text{N}\alpha)$ has been performed assuming that a compound nucleus ^{26}Al is first formed from which three α particles are successively evaporated². For a fixed HI direction, the calculated α angular correlation is peaked on the other side of the beam. Similar results could also be obtained by assuming that the ^{14}N fragment is emitted first and that the recoiling ^{12}C fragment subsequently breaks up into

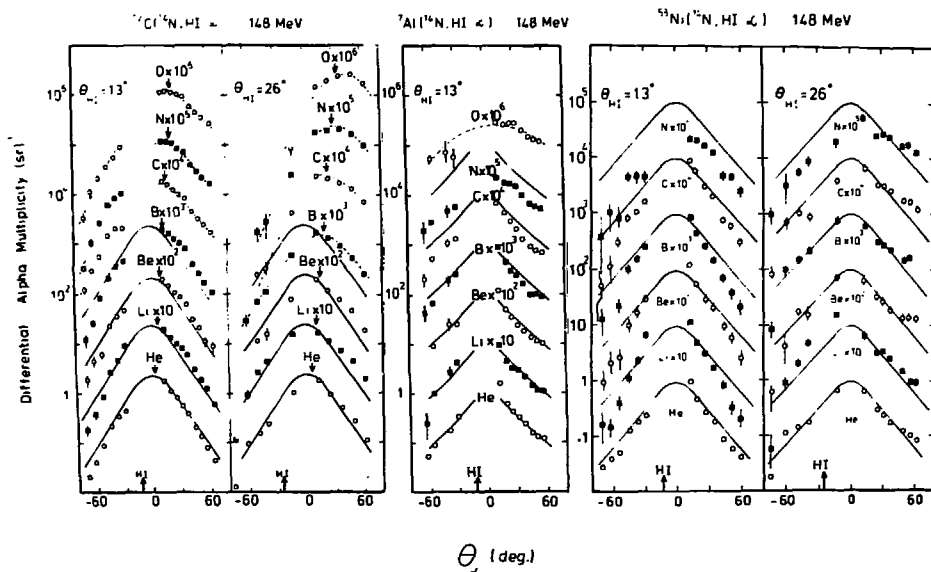


Fig.1. Differential α multiplicities for ^{12}C , ^{27}Al and ^{58}Ni targets for the reaction ($^{14}\text{N}, \text{HI}\alpha$) at 148 MeV. The solid curves are obtained from the singles α angular distributions (interpolated at forward angles).

three α particles. However, the shape of the α angular correlation is not very sensitive to the reaction mechanism and is determined mainly by the momentum constraints imposed by the reaction kinematics. It would be instructive to test to what extent the backward shift is a general feature of the α -HT correlation data for heavy ejectiles.

References:

1. R.K. Bhowmik, E.C. Pollacco, N.E. Sanderson, J.B.A. England and C.C. Morrison, Phys. Rev. Letts 43, 619 (1979).
2. J. Gomez de Campo, R.G. Stokstad, J.A. Biggerstaff, R.A. Dayras, A.H. Snell and P.H. Stelson, Phys. Rev. C. 19, 2170 (1979).

HOW FAST α PARTICLES ARE EMITTED IN "MASSIVE TRANSFER" REACTIONS ?

C. Gerschel, N. Perrin, L. Valentin, H. Tricoire and B. Ader,
IPN, B.P. n° 1, 91406 Orsay, France

D. Paya,
CEN, Saclay, DPhN/MF, BP n° 2, 91190 Gif-sur-Yvette, France

It is known that when a projectile lighter than Ar hits a target, at energies where compound nucleus formation should be the dominant process, a strong emission of p and α particles is observed in the forward direction¹; these are assumed to originate from a direct interaction. More recently^{2,3}, new informations have been obtained about the nature of these reactions in the rare earth region: the direct particles observed are emitted by the projectile without ever being absorbed by the target nucleus. The remainder of the projectile then fuses with the target and leads to compound nucleus. This occurs for the highest impact parameters (just above $l_{critical}$), the residual nuclei reaching then a high angular momentum. We have shown that these conclusions are not general but depend on the angular momentum carried away by the direct particle. Moreover, we think that it is not a special property of light projectiles due to their specific structure but mainly a question of energy involved in the reaction.

We have studied the compound nucleus ^{132}Ce at the same excitation energy by the two reactions: $^{92}Zr+^{40}Ar$ at 193 MeV, $^{116}Sn+^{16}O$ at 125 MeV. In each system we measured the multiplicity of γ rays associated with charged particles detected with a E- ΔE telescope. The channel reactions were identified by known lines in a Ge detector in coincidence with the telescope. With ^{16}O projectile the telescope was set at three angles 15°, 45° and 128° in the laboratory and only at 128° for ^{40}Ar . On fig. 1, we have drawn the α particle spectra detected at 15° in coincidence with specific lines in the Ge detector. Each spectrum exhibits two components: a first one peaked at an energy close to that of the coulomb barrier of the compound nucleus, and another component peaked at an energy close to that of an α particle emitted with a velocity close to that of the incoming projectile. The difference observed with results of ref.^{2,3} is that the multiplicity associated with the high energy α component is rather low: $M_{\gamma} = 8$ for 25 MeV (center of mass) α particles at 15°. This has to be compared with the value $M_{\gamma}=23$ for the same energy evaporation α particles detected at 128°, and to $M_{\gamma}=23$ for 20.5 MeV α particles in the $Ar+Zr$ system. Contrary to ref.^{2,3} we reach much lower spin states with direct particles than with evaporation particles.

We propose a very simple model to account for these experimental facts: the incoming projectile is slowed down by the coulomb field of the target to a velocity v_i . The α particle has then an energy $E_1=2v_i^2$. To allow it to be emitted by the projectile, this energy E_1 must be higher than the coulomb field value B_{ap} between the α particle and the remainder of the projectile. For ^{16}O , $E_1=14MeV$ and $B_{ap}=3.2 MeV$ but for ^{40}Ar $E_1 = 4.4 MeV$ and $B_{ap}=6.5MeV$. With projectiles with masses $A \gg 40$, at the energy usually necessary to produce $^{1}Hl, \alpha xn$ reactions with x of the order of some units, the E_1 value is never high enough to exceed the B_{ap} value and that is why direct components are never observed with heavy projectiles. If the α particle is emitted by the projectile, it is reaccelerated by the composite coulomb field due to the target and the remainder of the projectile. This field is different whether the particle

is emitted by the periphery of the projectile or by the neck between the target and projectile, so that the final energy of the α particle will be different in both cases. For $^{116}\text{Sn} + ^{16}\text{O}$ we calculated a value of 33 MeV if the particle is emitted by the neck and 26 MeV if emitted by the periphery to be compared to the experimental value of 24-28 MeV. Moreover if the α particle is emitted by the periphery it can carry away more angular momentum. That is why in our case we don't reach high spin states in the residual nucleus. In the case of ref.³, the α particle energies measured are all consistent with an emission by the neck of the system, the angular momentum carried away by the α particle is then low and explains the high spins reached in the residual nuclei.

1. H.C. Britt and A.R. Quinton, Phys. Rev. 124, 877 (1961)
2. T. Inamura, M. Ishihara, T. Fukuda, T. Shimoda, Phys. Lett. 68B (1977) 51
3. D.R. Zolnowski, H. Yamada, S.E. Cola, A.C. Kahler, and T.T. Sugihara, Phys. Rev. Lett. 41 (1978) 92

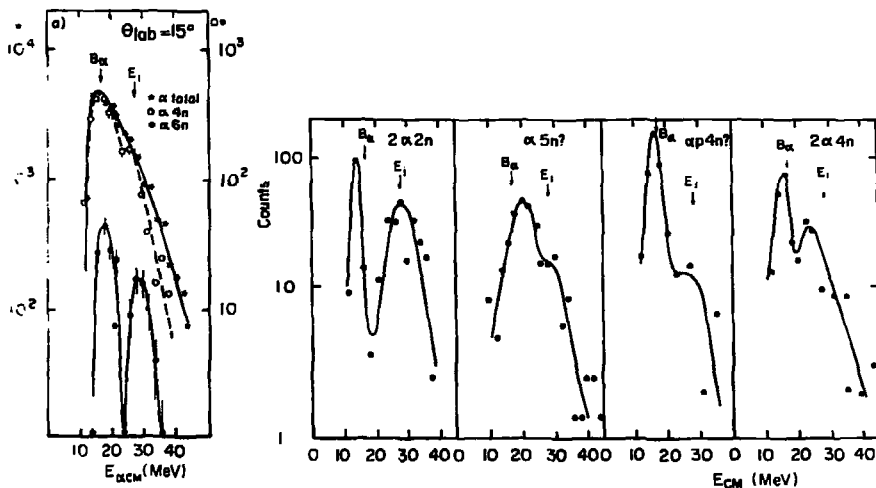


Fig. 1 : α particle spectra in coincidence with discrete γ lines in the Ge detector, for $^{116}\text{Sn} + ^{16}\text{O}$ system. The particle telescope was set at 15° . Reaction channel is indicated for each spectrum. The arrow E_i shows the energy α particles should have if emitted by the periphery of ^{16}O . The arrow B_α indicates the coulomb barrier of the compound nucleus ^{132}Ce .

EMITTED PARTICLES AND GAMMA DEEXCITATION
IN THE REACTION $^{12}\text{C} + ^{55}\text{Mn}$ AT $E(^{12}\text{C}) = 55$ MeV

F. Azgui, J.F. Bruandet, F. Glasser, B. Chambon, A. Dauchy, D. Drain,
A. Giorni, J.P. Longequeue, C. Morand, C. Pastor, Tsan Ung Chan,
J.C. Wells, H. Dumont.

Institut des Sciences Nucléaires, Grenoble, France
+ Institut de Physique Nucléaire, Lyon, France
++ Oak Ridge National Laboratory, Oak Ridge, Tennessee, U.S.A.
& D.P.N.B.E., C.E.N. Saclay, France

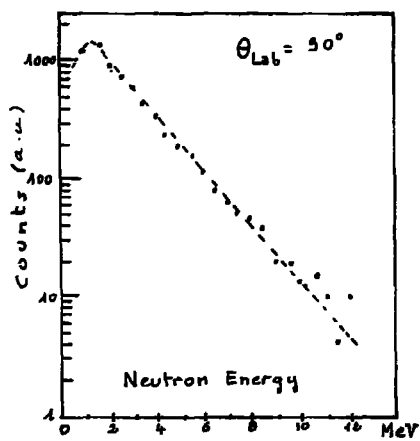


Fig. 1

A set of experiments¹ has been undertaken on the system $^{12}\text{C} + ^{55}\text{Mn}$, at an incident energy of 55 MeV, in order to make an intimate investigation of the fusion-evaporation process by means of gamma and particles detection (singles and coincidences): competition between different channels, complex particle evaporation, access to the upper part of yrast lines, are some of the principal subjects of interest.

A few of preliminary results are presented here :
a/ Fig. 1 : Neutrons energy spectra (Lab Syst) recorded by using time of flight method (cyclotron HF and NE 213 signals)
b/ Fig. 2a - 2b : Mass identification spectra of charged particles (using a three solid-state detector-telescope $\Delta E_1 - \Delta E_2 - E_3$)
c/ Fig. 3a - 3b : Energy spectra (45° Lab Syst) of charged particles detected in coincidence with γ - rays.

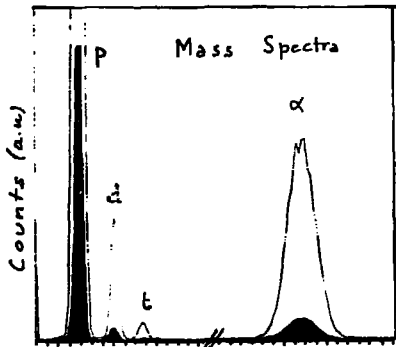


Fig. 2a

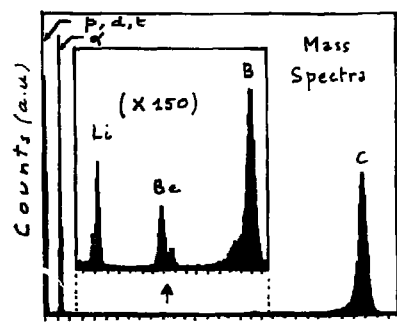


Fig. 2b

Some of the most striking features of the present investigations can be summarized in the following way :

- Maxwellian shapes are observed for energy spectra of light particles (p, d, t, α) and also for ${}^6\text{Li}$, but not for ${}^7\text{Li}$, Be and B, that point out an evolution of the reaction mechanism with the detected particles. A detailed analysis of coincident γ - rays and of angular distribution of particles is needed to give more precise conclusions (this work is in progress).

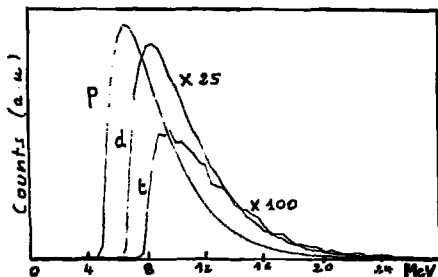


Fig. 3a

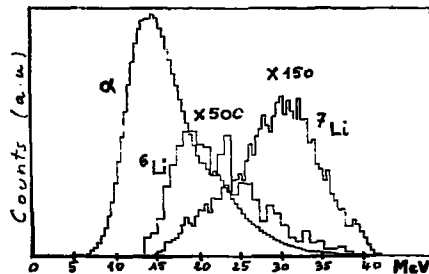


Fig. 3b

- The behaviour of the various evaporation channels appears to be strongly governed by the Q values of the reactions. That is specially obvious for the minor channels which are, in this experiment, the 4-particles-p3n γ and 2p2n γ - and the 2-particles - d γ - channels (the 3 - particles channels p2n γ and 2pn γ being dominant at the CN excitation energy considered). For instance, the γ -rays in coincidence with the d are exclusively the A = 63 residual nuclei γ -rays (competition p3n - d2n and 2p2n - dpn) ; on other way the high energy α select drastically the un channel. So they are some limits for entry states in the (Ex, J) diagramm which, in particular, do not allow to feed substantially the upper part of the yrast lines.

- The energy spread of neutrons emitted from ${}^{67}\text{Ga}(\text{CN}) \rightarrow \text{xnypza}$ is very much narrow than that observed in the evaporation process (α or H1, xn γ) from heavier nuclei. In the deexcitation of a medium-light nucleus such as ${}^{67}\text{Ga}(\text{CN})$ the energy dissipation is essentially due to charged particles, and for an energy balance in the (E, J) diagramm a neutron kinetic energy mean value of $\langle E_n \rangle = 2 \text{ MeV}$ may be use in a first approximation.

It will be mentioned that in the γ - identified charged particles coincidences experiment (three days data recording) a quantitative analysis of the γ rays (Ge-Li) is practicable for γ -p and γ - α coincidences but not for the γ - "complex particles" because of their relative small cross section. Analysis of the angular distributions (single spectra) for charged particles (7 Lab angles) and for neutrons (3 Lab angles only) are in progress. A gamma-rays multiplicity measurement (with a 6NaI - counter) is foreseen in the next experimental programm in order to study angular momentum distribution in the different reaction channels.

MEASUREMENT OF CHARGED PARTICLE MULTIPLICITIES BY PARTICLE- γ COINCIDENCES :
THEIR POSSIBLE ROLE FOR SPECTROSCOPY AND MECHANISM STUDIES

M.G. Saint-Laurent, H. Dumont, H. Yoshikawa* and J. Delaunay
DPH-N/BE, CEN Saclay, BP 2, 91190 Gif-sur-Yvette, France

When a target ($A \sim 50$) is hit by a light-heavy ion (C,N,O), at energy between once and twice the Coulomb barrier, the resulting γ spectrum is usually rather complex, because at each energy more than 10 channels are open simultaneously ($2p_n$, $3n$, $\alpha 2n$, αp_n , etc.). The isotope assignment is therefore a difficult task and the charged particle multiplicity (CPM) of each γ line can help for such assignment. These CPM, M_α , M_p , for each γ line can be deduced by comparison of a γ (singles) spectrum and the γ spectrum gated by the p or the α particles.

We performed such measurements by coincidence between a Ge(Li) detector, 15% efficiency, 2.5 keV resolution at 1.33 MeV, placed at 90° and a Si detector, $\phi = 2$ cm, 250 μ m thick, placed at 150° to the beam. The reaction was $^{48}\text{Ti} + ^{13}\text{C}$ at 46 MeV using the ^{13}C beam of the Saclay tandem accelerator. In this reaction, more than 10 channels are open¹ and we try, as much as the statistics was sufficient, to determine the CPM for ~ 100 γ lines. We use, as normalization between the γ spectra, single and gated by particles, the 308 keV γ line from ^{55}Mn (channel αp_n).

Our present conclusions are the following :

. For spectroscopy studies :

- these CPM confirm the results obtained already by standard γ spectroscopy methods, namely the known lines of the dominant nuclei have the correct CPM : $M_p \sim 1$ and $M_\alpha \sim 0$ for the 321, 332, 433, 707 keV etc. for ^{58}Co (channel $p 2n$) ; $M_p \sim 0$, $M_\alpha \sim 1$ for the lines at 385, 477, 605 keV, etc. of ^{55}Fe (channel $\alpha 2n$) ;

- for a γ line whose energy is common in two residuals, we have the possibility to determine the proportion in each nucleus. For example, the γ line at 1223 keV belongs to ^{57}Co and ^{55}Fe ; we measure $M_\alpha \sim 0.8$ and $M_p \sim 0.5$. This can be very helpful in determining multipolarities of the transitions by γ angular distributions ;

- certain γ lines gave results not yet fully understood : they can be the starting point for more "exotic" channels.

. For mechanism studies :

- the γ lines of ^{57}Fe have $M_p \sim 2$ and $M_\alpha \sim 0$, hence, this nucleus is produced in the channel ($2n 2p$) and not (α) ;

- the γ line at 1381 keV which "signed" the presence of ^{49}Ti ($7/2^- + 3/2^-$ gs) disappears in coincidence with the α gated spectrum. ^{49}Ti is produced in the channel ($^{13}\text{C}, ^{12}\text{C}$) and not (3α) : this was confirmed by the particle angular distribution that we performed with two telescopes².

We intend, in a near future, to do such measurements with a telescope to have a complete p - α separation. With only one thin Si detector, like in the present experiment, this separation is quite good but not complete ($\sim 95\%$). This kind of

* ISN Tokyo, Japan

measurement can be particularly interesting for reactions like ^{28}Si on the Si isotopes that we start to study³, where the CPM is very large.

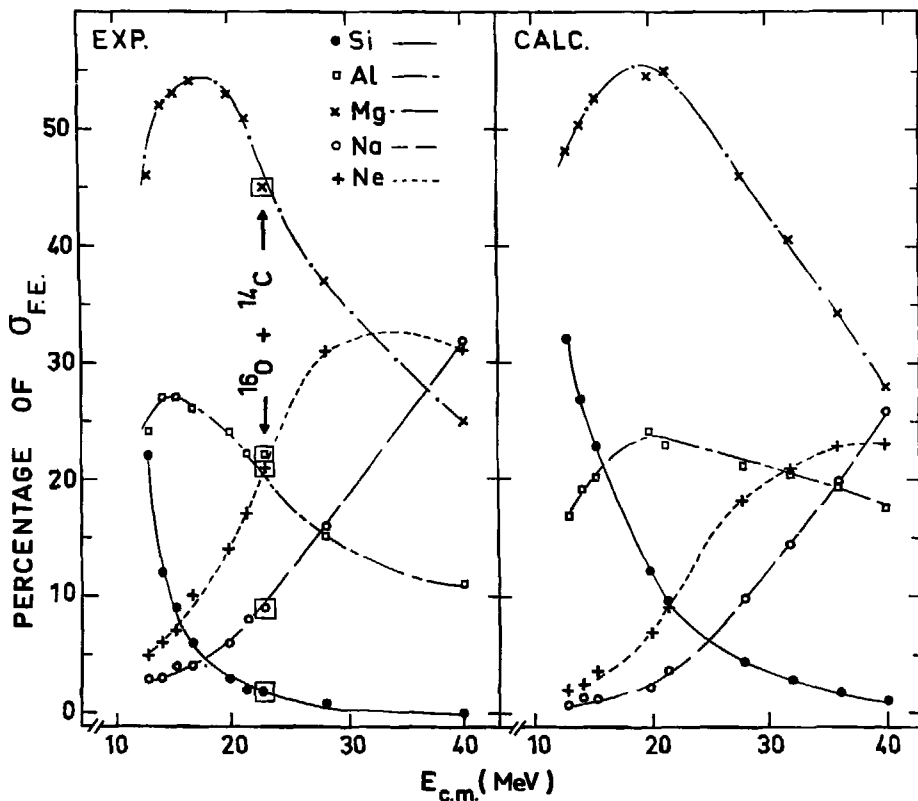
REFERENCE

1. A. D'Onofrio, Thesis Orsay 1979 ; A. D'Onofrio et al., to be published.
2. H. Dumont et al., to be published.
3. M.G. Saint-Laurent et al., to be published.

THE $^{18}\text{O} + ^{12}\text{C}$ FUSION-EVAPORATION REACTION

B. Heusch, C. Beck, J.P. Coffin, R.M. Freeman, A. Gallmann, F. Haas, F. Rami, P. Wagner and D.E. Alburger*.
 Centre de Recherches Nucléaires et Université Louis Pasteur, Strasbourg, France.

The $^{16}\text{O} + ^{12}\text{C}$ reaction is one of the few heavy-ion systems where oscillations have been found in the energy dependence of the total fusion cross-section¹. A similar oscillation appears in the inelastic excitation of the $^{18}\text{O} + ^{12}\text{C}$ reaction² though the total fusion reaction cross-section shows the expected smooth variation with bombarding energy³. In addition the maximum of the fusion cross-section for $^{18}\text{O} + ^{12}\text{C}$ is about 20% greater than for $^{16}\text{O} + ^{12}\text{C}$. To better understand these differences we have made a more detailed study of the $^{18}\text{O} + ^{12}\text{C}$ reaction in which the elemental distributions of the evaporation residues have been measured for $E_{c.m.}$ ranging from 12 to 40 MeV which includes our preceding study at $E_{c.m.} = 40$ MeV⁴.



A time of flight technique has been used with Z identification. The experimental set-up has been described previously ⁴. Cross-sections have been obtained by integration of the angular distributions measured at least at $\theta_{lab} = 5^\circ, 10^\circ, 15^\circ$ and 20° . We used ^{18}O and ^{16}O beams from the Strasbourg MP tandem accelerator. The $^{18}O + ^{12}C$ reaction has been studied for $32 \leq E_{lab}(^{18}O) \leq 100$ MeV and one point at $E_{lab}(^{16}O) = 50$ MeV has also been included for the $^{16}O + ^{14}C$ reaction which leads to the same compound nucleus ^{30}Si . Self supporting ^{12}C targets of $80 \mu g/cm^2$ have been used. The ^{14}C target contained about 20% ^{12}C ; it was self-supporting ($80 \mu g/cm^2$). The ^{12}C contamination could be correctly estimated using the elastic scattering data of the ^{16}O beam on ^{12}C and ^{14}C which were separated for $\theta_{lab} \geq 15^\circ$. The $^{16}O + ^{12}C$ fusion evaporation cross-sections have been independently measured at $E_{lab}(^{16}O) = 50$ MeV, using a ^{12}C self-supporting target, and, by appropriate normalization, have been subtracted from the $^{16}O + ^{14}C$ data.

On the left hand side of fig. 1 are presented the cross sections summed for each element over the corresponding isotopes. This representation has been chosen for simplicity and also because it is directly comparable to the results obtained for other light-heavy systems ¹. The point for the $^{16}O + ^{14}C$ reaction has been included, corrected to the same excitation energy of the compound nucleus. The agreement with the $^{18}O + ^{12}C$ data demonstrates that the results are not measurably dependent on the way in which the compound nucleus is formed.

On the right hand side of fig. 1 are presented the corresponding predictions of the evaporation calculation code LILITA ⁶: it calculates the statistical Hauser Feshbach cross-sections by a Monte-Carlo technique. The critical angular momenta introduced in these calculations are extracted from the total fusion cross-section data from Sperr et al. ³ using the sharp-cut-off approximation. An overall satisfactory agreement with the data is found especially if one considers that with the same set of parameters we could reproduce, with the same quality, the results for about 10 systems ranging from $^{12}C + ^{12}C$ up to $^{16}O + ^{16}O$ for energies $10 \leq E_{c.m.} \leq 40$ MeV.

In this experiment, it has been shown that for the $^{12}C + ^{18}O$ reaction the production of Mg isotopes ($\alpha\alpha n$), which follows closely the energy dependence of the total fusion cross section ², dominates the fusion-evaporation process up to $E_{c.m.} = 30$ MeV. This is not the case for the $^{12}C + ^{16}O$ reaction where the $^{20}Ne(2\alpha)$ channel, the most able channel to carry away angular momenta, is the dominant channel for the same energy range ⁵. In this range, the number of open channels able to evacuate the grazing angular momenta are lower by a factor of 100 for $^{12}C + ^{16}O$ compared to $^{12}C + ^{18}O$. This explains the absence of resonant structure in the $^{12}C + ^{18}O$ fusion channels.

1. D.G. Kovar et al., Phys. Rev. C20, 1305 (1979)
2. R.M. Freeman and F. Haas, Phys. Rev. Lett. 40, 927 (1978)
3. P. Sperr et al., Phys. Rev. Lett. 37, 321 (1976)
4. J.P. Coffin et al., Phys. Rev. C17, 1607 (1978)
5. J.J. Kolata et al., Phys. Rev. C19, 408 (1979)
6. Code LILITA, J. Gomez del Campo and R.G. Stokstad, unpublished

* Brookhaven National Laboratory, Upton, New York

STUDY OF THE DOMINANT CHANNELS IN THE REACTIONS INDUCED BY LIGHT-HEAVY IONS ON INTERMEDIATE-MASS ($A \sim 50$) TARGETS

A. D'Onofrio*, H. Dumont, M.G. Saint-Laurent, F. Terrasi*, B. Delaunay, J. Delaunay and D. Rizzo**
DPh-N/BE, CEN Saclay, BP 2, 91190 Gif-sur-Yvette, France

In order to study the spectroscopy of high-spin states for neutron deficient nuclei like ^{56}Ni , ^{57}Ni , ^{52}Fe , ^{53}Fe , it is necessary to produce them with a reasonable yield. How reliable are the evaporation codes based on the statistical model to predict these yields? It is generally assumed that, in our experimental conditions (C,N,O projectiles, $A \sim 50$ targets, incident energy between ~ 1 and ~ 2 coulomb barriers) the fusion cross section σ_f is very close to the reaction cross section σ_r and the formation of compound nucleus and successive emission of particles are believed to be well described by the statistical model of nuclear reactions.

To perform this study we have first to obtain experimental results to compare with the calculated ones and if the agreement is good this gives confidence to predict cross sections for other systems. So our study had two parts :

a) measurement of absolute cross sections for the dominant channels for a group of reactions, namely $^{13}\text{C} + \text{Ti}$ (46,47,48,49,50) at 36, 46, 56 MeV, and a complete excitation function was performed in the case of $^{48}\text{Ti} + ^{13}\text{C}$ between 18 and 60 MeV by 2.5 MeV steps. We used γ spectroscopic methods^{1,2} and the Saclay Van de Graaff accelerator facilities.

b) We compared the sets of results with different evaporation codes¹, all based on the statistical model of Hauser-Feshbach. The parameters were taken from systematics¹ and we try - as much as it was possible - to use the same parameters in all these calculations. No effort was made to improve the fit.

Our present conclusions are following (Fig. 1) : in general, the code CASCADE³ gives an acceptable agreement (but it is very costly !). For the other codes¹ strong and unexpected discrepancies appear ; attempts with the authors of these codes to amend these discrepancies are underway, in particular for the Monte-Carlo codes, much faster and hence much cheaper than CASCADE and very well suited for studying complex reactions.

* On leave of absence from Istituto di Fisica Sperimentale dell'Universita, Via A. Tari 3, Napoli, Italy.

** On leave of absence from Universidade Catolica, Sao Paulo, Brazil.

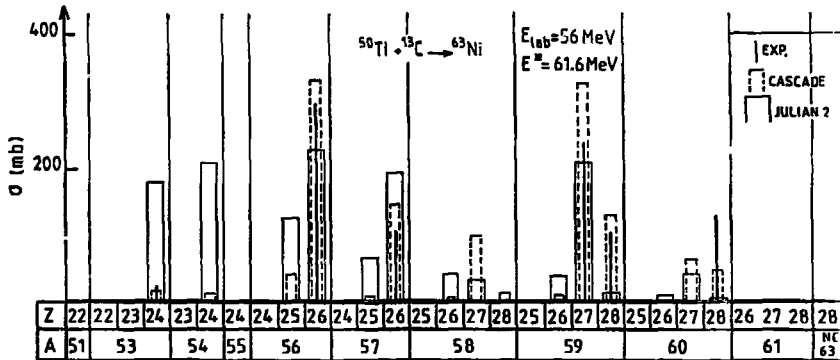


Figure 1 - Experimental and calculated cross sections for different residual nuclei in the $^{50}\text{Ti} + ^{13}\text{C}$ reaction at 56 MeV. (a) ref.¹.

REFERENCES

1. A. D'Onofrio, Thesis Orsay 1979 and references therein.
A. D'Onofrio et al., to be published.
2. F. Terrasi et al., to be published.
3. CASCADE : F. Pulhofer, Nucl. Phys. A280, 267 (1977).

EVAPORATION RESIDUE AND FISSION CROSS-SECTIONS FOR THE SYSTEM $^{40}\text{Ar}+^{110}\text{Pd}$.

C.Cabot, H.Gauvin, Y.Le Beyec
 Institut de Physique Nucléaire, BP n°1, 91406 Orsay, France

H.Delagrance, J.P.Dufour, A.Fleury, Y.Llabador
 CENBG, Allée du Haut Vigneau, 33170 Bordeaux-Mérignac, France

J.M.Alexander
 State University of New York at Stony Brook, Stony Brook, New York 11794 USA

It is of great interest to obtain, for a given compound nucleus formed by heavy ions, maximal informations on the production and deexcitation processes. Measurements of each exit channel cross-section (x_n, p_x, α_x) as well as total evaporation residue and fission cross-sections in the energy range between the Coulomb barrier (B_C) and about 2 times B_C are a first approach in the investigation of these processes. We present here results of such measurements performed for the system $^{40}\text{Ar}+^{110}\text{Pd}+^{150}\text{Gd}$. Partial results have also been obtained for the systems $^{150}+^{134}\text{Ba}$ 1 and $^{68}\text{Zn}+^{82}\text{Se}$ 2 giving the same CN. Gamma multiplicity measurements, which would complete the present investigation, are planned for the near future.

In fig.1, the sum of the cross-sections ($x_n+p_x+\alpha_x$) measured through the stack foil method ¹ is in agreement, in the overlapping energy region, with the direct E.R. cross sections obtained by the well known $\Delta E-E$ telescope counter technique. In this latest experiment, angular distributions were measured between 3° and 12° and absolute cross-sections have been deduced from Rutherford scattering cross-sections and from absolute beam monitoring with a calibrated Faraday cup. The beam energies and the 0° beam axis were carefully determined. During the course of the E.R. experiment, a second telescope was positioned at 90° CM to detect fission fragments which, in the $\Delta E-E$ plane, were separated from deep inelastic events. Therefore, fission cross-sections have been obtained assuming a

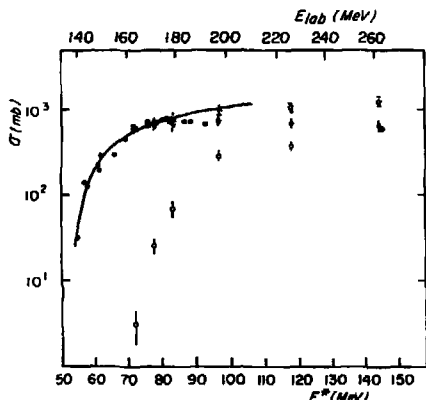


Figure 1 :
 Results for $^{40}\text{Ar}+^{110}\text{Pd}+^{150}\text{Gd}^*$.
 Black star (★) = σ evaporation residues.
 Open circle (○) = σ fission
 Open star (☆) = σ complete fusion
 Black point (●) = σ evaporation residues from ¹.

$1/\sin^2\theta$ angular distribution. The results are given in Table I. In the right part of this table we also indicate additional results on σ fission for the system $\text{Ar}+^{130}\text{Te}$. Based on the assumption that all fission events come from compound nuclei,

Experimental results							Calculated values
E_{lab} (MeV)	E_{cm} (MeV)	Z^2 (NoV)	σ_{tot} (mb)	$\sigma_{fission}$ (mb)	σ_{CF} (mb)	σ_{CRR} (mb)	χ^2_{min} (S) or crit. Ng6 ($\chi^2_{crit}=1.05mb$)
Ar+Pd 110							
166	122	72.5	840±75	1.2±1.6	842-75	59±3.5	56
171	125.5	78	880±100	2±1.5	710±105	62±4.5	63
179	131	83.5	900±145	20±15	720±160	67±7	70
187	140.5	97	760±85	200±60	1050±125	87±4.5	79
225.5	192.5	118	710±75	380±60	1090±115	90±4.5	82
262	192	144.5	645±70	610±80	1275±130	104.5±5.5	108

Experimental results							Calculated values
E_{lab} (MeV)	E_{cm} (MeV)	Z^2 (NoV)	σ_{tot} (mb)	$\sigma_{fission}$ (mb)	σ_{CF} (mb)	σ_{CRR} (mb)	χ^2_{min} (S) or crit. Ng6 ($\chi^2_{crit}=1.05mb$)
Ar+Se 130							
164.5	126	64	-	-	-	-	50
171.5	131	69.5	-	11.5±7	-	-	59
179.5	137	75.5	-	90±25	-	-	68
187	150.5	88	-	240±50	-	-	78
226	173	111.5	670±95	690±60	1160±115	96.5±6.5	94

Table I

one can write $\sigma_{CF} = \sigma_{ER} + \sigma_{fission} \sim \pi R^2 \chi^2$. Values of χ^2 , given in Table I, are in agreement with calculated values from the semi empirical model of Ng6³, even for the highest energies where the concept of critical radius is used in the model. A good agreement with χ values calculated with the Vaz and Alexander approach⁴ was also found for $E_{lab} < 210$ MeV, and the corresponding fusion excitation function is given by the solid line in fig.1. In addition, it is noted that above 225 MeV, $\chi_{CF exp.}$ exceeds $\chi_{BF=0} = 91\%$ calculated from the rotating liquid drop model⁶.

These experimental results on individual residual nuclei, E.R. and fission are now used to obtain restrictive conditions on the choice of the parameters which are involved in statistical evaporation calculations, in the case of competition between particle evaporation, fission and gamma deexcitation. For that purpose, the Groggi F code is used⁵. As a first step, in order to reproduce the rising part of the fission excitation function, we determined values of $a_f/a_n \sim 1.2$ and $B_f \sim 0.80 B_{fLD}$ (B_{fLD} being the rotating liquid drop fission barrier⁶). We recall that Beckermann and Blann⁷ using the MB-II code, determined $a_f/a_n = 1.05$ and a low value of B_f ($0.60 \times B_{fLD}$) to reproduce σ_f and σ_{ER} reported for the ⁴⁰Ar+¹⁰⁹Ag system by Britt et al.⁸. Complete calculations for the Ar+Pd system are being performed.

1. S.Della Negra, H.Gauvin, H.Jungclas, Y.Le Beyec and M.Lefort, Z. für Phys. **A282**, 65-73 and 75-84 (1977).
2. C.Cabot, S.Della Negra, H.Gauvin, to be published.
3. C.Ngô, B.Tamain, J.Galin, M.Beiner and R.J.Lombard, Nucl. Phys. **A240**, 353 (1975).
4. L.C.Vaz and J.M.Alexander, Phys. Rev. **C18**, 2152 (1978).
5. J.R.Grover and J.Gilat, Phys. Rev. **157**, 802 (1967)
H.Delagrance, Report CENBG 7707 (1978).
6. S.Cohen, F.Plasil and W.J.Swiatecki, Ann. Phys. (N.Y.) **82**, 557 (1974).
7. M.Beckermann and M.Blann, Phys. Rev. **C17**, 5, 1615 (1978).
8. H.C.Britt, B.H.Erkkila, R.H.Stokes, H.H.Gutbrod, F.Plasil, R.L.Ferguson and M.Blann, Phys. Rev. **C13**, 4, 1483 (1976).

CROSS SECTION DISTRIBUTION IN NUCLEAR REACTIONS
INDUCED BY ^{12}C , ^{14}N AND ^{16}O IONS ON TARGETS NEAR $N = 82$

J. Jastrzębski, R. Kossakowski, J. Żukasiak, M. Moszyński,
Z. Preibisz, P. Rymuza
Institute for Nuclear Research, Swierk, Poland

S. André, J. Genevey, A. Gizon, J. Gizon
Institut des Sciences Nucléaires, IN2P3, Grenoble, France

The cross sections for the production of final nuclei in ^{12}C , ^{14}N and ^{16}O induced reactions on ^{141}Pr , ^{144}Sm and ^{147}Sm targets were investigated. The experimental method is based on the determination of the gamma ray intensities observed during the cyclotron beam bursts, between bursts and immediately after the beam shut-off. The observed gamma rays are normalized to the target K X-rays. Details of the experimental techniques were reported previously ¹.

	150	151	152	153	154	155	156
Er 68	≈ 13	35	120	20			C.N.
	149	150	151	152	153	154	88
Ho 67		≈ 13	137	202	47		
	148	149	150	151	152		87
Dy 66	33	99	73	36	18		
	146	147	148	149	150		86
Tb 65	20	≈ 49	≈ 91	55	9		
	145	146	147	148			85
Gd 64		≈ 20	33	9			
	81	82	83	84			

Figure 1

$^{12}\text{C} + ^{144}\text{Sm}$
 $\bar{E}^{\text{M}} = 65 \text{ MeV}$
 $\Delta E^{\text{M}} = 14 \text{ MeV}$

Figure 1 shows the cross section distribution on final products of the $^{12}\text{C} + ^{144}\text{Sm}$ reaction at 90 MeV (in mb, assuming that the cross section for the excitation of the target K X-rays is reproduced by the calculation using the Plane Wave Born Approximation ²). As shown in figure 2, the reaction channels in which one or more charged particles are emitted dominate the decay of the ^{156}Er compound nucleus in the whole energy range studied. This is not the case for e.g. $^{12}\text{C} + ^{141}\text{Pr} \rightarrow ^{153}\text{Tb}^*$ reaction (figure 3). Up to about 70 MeV excitation energy the xn channel represents more than 50% of the observed cross section and the pxn channel becomes comparable to the xn and axn channels only at about 85 MeV excitation energy. From the studies of other target-projectile combinations it is concluded that in this region, far from the stability line, the

charged particle emission depends strongly not only on the effective binding energies ³ but also on other factors as e.g. level density of final products (p emission to even-even and odd-even vs. odd-even and odd-odd nuclei). The cross section data obtained during the present investigation were crucial for the identification of high spin isomers reported in another communication ⁴.

1. J. Jastrzębski et al., Proc. Conf. on Large Amplitude Collective Nuclear Motions, Balaton, June 1979, p. 71.
2. G.S. Khandenwal et al., Atomic Data 1, 103 (1969).
3. F.S. Stephens et al., Nucl. Phys. A170, 321 (1971).
4. S. André et al., Contribution to this Conference.

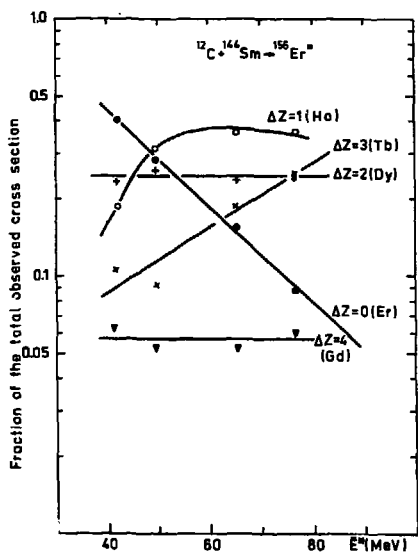


Figure 2

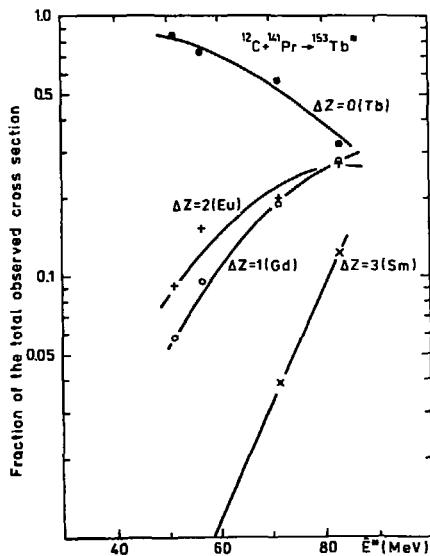


Figure 3

NEW RESULTS ON ANGULAR MOMENTUM TRANSFER FROM SEQUENTIAL FISSION
IN 255 MeV Ar+Bi AND 435 MeV Ni+Pb DEEP INELASTIC COLLISIONS

C. Le Brun, J.F. Lecomte, F. Lefebvres, M. L'Haridon, J.P. Patry
J.C. Steckmeyer and R. Chechik⁺

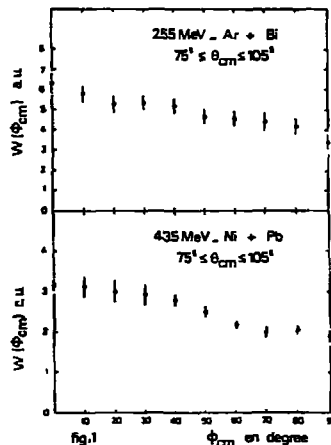
Laboratoire de Physique Corpusculaire, ISMRA
Université de Caen, France

The first experiments⁽¹⁾⁽²⁾ on angular momentum transfer in deep inelastic collisions from sequential fission agree with the fact that the target like fragment spin is aligned along the normal to the reaction plane and its value reaches a limit compatible with the sticking hypothesis for deformed nuclei. Nevertheless they disagree on the depolarisation mechanism since an anisotropy in the in plane angular distribution of the fission fragments is observed only in the experiment of Dyer et al⁽²⁾.

We present new data obtained at ALICE (Orsay) on angular momentum transfer in deep inelastic collisions from sequential fission. The light fragment was identified in a solid state $\Delta E.E$ telescope, the coincidence fragments were detected in a position sensitive parallel plate detector which measured its θ_E and time of flight. With these informations, we can separate without ambiguity the deep inelastic events followed by a sequential fission of the target like reaction products from the other mechanisms. The fission fragment velocity distributions in the center of mass of the target like Pb, Bi are in good agreement with the published results⁽¹⁾; they show clearly the existence of an intermediate system which behaves like a resonance decaying by fission.

From the out of plane angular distributions peaked in the reaction plane, we confirm that the target like Bi, Pb intrinsic angular momenta are aligned along the normal to the reaction plane and reach a limit compatible with the sticking condition for the deformed nuclei coming from the composite system created in the initial reaction.

The in plane angular distributions $W(\phi_{CM})$ shown in figure 1, are clearly anisotropic. These results are fully compatible with the Dyer et al published experiment⁽²⁾ and are in disagreement with the 7.5 MeV/A Pb+Ni experiment⁽¹⁾ (same energy in the CMS as our experiment) that has found an isotropic in plane angular distribution. Nevertheless we can remark that this last experiment presents its in plane angular distribution integrated over a large angular domain of the Ni like reaction product, whereas in our experiment and Dyer's et al one the projectile like reaction fragment was detected in a narrow angular domain.



⁺ Present address : Weizmann Institute of Science, Rehovot, Israël
1 - D.V. Barrach et al, Phys. Rev. Lett. 42 (1979) 1728
2 - P. Dyer et al, Nucl. Phys. A322 (1979) 205

COMPETITION BETWEEN FISSION AND NEUTRON EMISSION OF ^{210}Po AT HIGH SPINS AND EXCITATION ENERGIES

M. Płoszajczak

Institute of Nuclear Physics, 31-342 Krakow, Poland

M. Faber

Institut für Kernphysik, 5170 Jülich, W. Germany

In the fusion reaction between heavy ions it is possible to bring the large angular momentum to the compound system. Cooling of the high spin nucleus is then provided mainly by the emission of neutrons. The competition between the processes of particle emission and fission depends on the appropriate level densities and gives important informations about the nuclear shape changes far above the yrast line. Here we study Γ_f/Γ_n in the framework of the statistical theory for the near spherical nucleus ^{210}Po . The deformation of the saddle and of the equilibrium configuration were obtained minimizing the free energy surface F with respect to the deformation $\beta(\gamma=0^\circ)$ and the neck parameter for all angular momenta and excitation energies above the yrast line. The surfaces F were constructed in the framework of the Strutinsky approach generalized for finite spins and temperatures. The shell corrections were calculated using the energy and spin eigenvalues of the WS potential. The intrinsic level density was approximated by the formula of the back-shifted Fermi gas model. The shift parameter was set equal to the shell correction δF . The neutron separation energy and the fission barrier were calculated from F for each considered state. Absence of the γ -deformation in F explains the excess of the theoretical barrier ($V_f \sim 25\text{MeV}$) above the experimental one for $I=0$ ($V_f \sim 21\text{MeV}$). To improve the agreement with the data the calculated microscopically barriers were decreased by 4 MeV for all spins and excitation energies. Finally the total level densities in Γ_f, Γ_n for a given spin were obtained by summing over the intrinsic densities with $^n|K| \leq I$. The theoretical values of Γ_f/Γ_n are compared with the experimental values¹⁾ (dashed line) for $I=0$. At the excitation energy of ~ 50 MeV ($I=0$) the slopes of both experimental and theoretical curves change. This effect can be interpreted²⁾ as the shape transition from the ground state minimum to the fission isomeric minimum. For angular momenta $I < 30 \hbar$ this critical excitation energy is almost unchanged. For higher spins transition energy from the spherical to the strongly deformed configurations is significantly lowered ($E^* \sim 30\text{MeV}$). At $I > 40 \hbar$ and $E > 25$ MeV the fission process dominates the neutron emission and the probability to form the nucleus ^{210}Po at still higher spins and excitation energies is strongly reduced.

1. A. Khodai - Joopari, UCRL - 16489 (1966), unpublished

2. P.A. Gottschalk, T. Ledergerber, Nucl. Phys. A278, 16 (1977)

FAST FISSION PHENOMENA IN HEAVY ION REACTIONS

C. Grégoire, R. Lucas, C. Ngô, H. Ngô* and B. Schürmann**
 DPh-N/MF, CEN Saclay, BP 2, 91190 Gif-sur-Yvette, France

Until recently the classification, at low bombarding energy, of heavy ion nuclear reactions into 3 categories : quasi elastic, deep inelastic (DI) and compound nucleus (CN) reactions was quite satisfactory. However some experimental data which are associated to the de-excitation of the CN cannot be fully understood within this framework. A CN has completely forgotten about its formation and will de-excite by emitting light particles and γ rays (leading to evaporation residues) or by fissioning into two fragments (symmetric fragmentation component). The effective barrier against fission decreases with increasing angular momentum and for some value l_{Bf} vanishes¹. Consequently, according to this picture a real CN cannot be formed. What is usually called fusion cross section is the sum of the evaporation residues and of the symmetric fragmentation cross sections. This latter is usually associated to the fission of the CN. From the fusion cross section one can deduce, within the sharp cut off approximation, a critical angular momentum l_{crit} . If the fusion cross section is the same as the CN cross section formation l_{crit} should be bound by l_{Bf} . This seems not to be the case for medium systems². The symmetric fragmentation cross section is too large to be entirely associated to the fission of a CN. This is likely to indicate that a new mechanism intermediate between DI and CN formation exists. We can call it fast fission phenomenon (FFP) because the fragments have properties which are similar to those of the CN fission fragments. It turns out that one property seems to be different : the FWHM of the mass distribution seems to be larger for FFP than for ordinary fission^{3,4}. This is illustrated in Fig. 1 where the FWHM of the symmetric fragmentation component of a system ^{208}At increases quite a lot for $l_{crit} > l_{Bf}$ due to the appearance of FFP. We have developed a simple static model to try to understand such an evolution⁵. The collision is assumed to be pictured as follows :

1. The entrance channel is assumed to be dominated by a sudden interaction potential. For a given l value, the trajectory can either be scattered after a loss of kinetic energy (DI) or it can be trapped in the pocket of the potential. In this latter case we will have either CN formation or FFP. Due to the Coulomb field it should be noted that the pocket only exists if $Z_1 Z_2 < 2500-3000$.

2. When the system is trapped in the pocket it will drift along the mass asymmetry coordinate. This drift will lead to a symmetric quasimolecular system if it is not too asymmetric. Indeed it is only if the system is initially not too asymmetric that FFP will be observed.

3. In the last step it is assumed that a reorganization of the densities takes place (transition from a sudden to an adiabatic potential). If $l < l_{Bf}$ a real CN is formed which will forget about its formation : the FWHM of the fission mass distribution will be given by the statistical fluctuations in the adiabatic potential. On the contrary for $l > l_{Bf}$ no real compound nucleus is formed and the memory of the sudden potential will be kept as far as mass asymmetry is concerned. The FWHM will arise from the statistical fluctuations in the sudden potential. In Fig. 1 the full curve shows the result of a simple calculation based on the pre-

* IPN, Laboratoire de Physique Théorique, BP 1, 91406 Orsay.

** Present address : TU München, D-8046 Garching.

ceding assumptions. For $l_{crit} < l_{Bf}$ a FWHM of 29 was taken as an input and for $l_{crit} > l_{Bf}$ the calculation was performed using a sudden potential. This calculation predicts that l_{crit} saturates around 130 which seems to be experimentally observed.

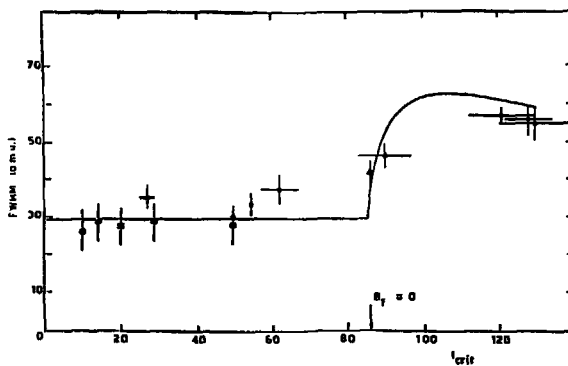


Figure 1 - The FWHM of the mass distribution of the symmetric products is shown as a function of critical angular momentum for the Ar + Ho (\bullet), Ne + Re (\blacktriangle), p + Bi, α + Pb, C + Pt (\blacksquare) systems. The full curve corresponds to the fast fission model.

REFERENCES

1. S. Cohen, F. Plasil and W.J. Swiatecki, *Ann. of Phys.* **82**, 557 (1974).
2. For a compilation of results see M. Lefort, *Symposium on deep inelastic and fusion reactions with heavy ions*, Berlin (1979).
3. C. Lebrun, F. Hanappe, J.F. Lecolley, F. Lefebvres, C. Ngô, J. Peter and B. Tamain, *Nucl. Phys.* **A321**, 207 (1979).
4. C. Grégoire, M. Berlangier, B. Borderie, F. Hanappe, D. Gardès, J. Girard, J. Matuszek, C. Ngô and B. Tamain, preprint 1980.
5. C. Grégoire, R. Lucas, C. Ngô, B. Schürmann and H. Ngô, preprint DPh-N/MF 79/33 (1979).

PRE-EQUILIBRIUM EMISSION IN PROTON-INDUCED REACTIONS ON COBALT AND NICKEL IN
THE ENERGY RANGE 18-84 MeV

S.J. Mills and F.J. Haasbroek
National Accelerator Centre, CSIR, Pretoria, South Africa

Absolute cross-sections for the production of ^{55}Fe , $^{55-58}\text{Co}$ and $^{56,57}\text{Ni}$ in proton bombardment of cobalt and for the production of $^{55-58}\text{Co}$ and $^{56,57}\text{Ni}$ in proton bombardment of nickel have been derived from radioactivity yield data¹ obtained in the energy range 18-84 MeV by means of the stacked-foil technique. The results are shown in fig. 1. The cross-sections for ^{55}Fe and $^{56,57}\text{Co}$ have been corrected for precursor decay and, as in the case of ^{58}Co , refer to the independent formation of the nuclide; those for ^{55}Co and $^{56,57}\text{Ni}$ could not be corrected for contributions of their (short-lived) precursors, but according to our theoretical calculations (see below) the production of all the precursors in question should be negligible. Except for a few points at low energies, the excitation functions obtained are in good general agreement with relevant earlier results²⁻⁴ reported in the literature.

The experimental results were compared with calculations performed by means of the computer program OVERLAID ALICE⁵ for all reactions possibly contributing to the observed radionuclides. As could be expected, pure equilibrium calculations according to Weisskopf-Ewing theory completely failed to yield agreement with the experiment, demonstrating the need for considering pre-equilibrium reactions in calculating the excitation functions. The calculations have consequently been performed within the framework of the geometry-dependent hybrid model for the pre-equilibrium emission of the first neutron or proton (initial configuration: 1p-1n-1h), in combination with the Weisskopf-Ewing formalism for the subsequent equilibrium emission of neutrons, protons, deuterons and alpha-particles. Binding energies were taken from the compilation of Wapstra and Bos⁶ and the intranuclear transition rates used were based on nucleon mean free paths calculated from free nucleon-nucleon scattering cross-sections.

Theoretical results obtained with standard Fermi-gas level densities (with a level-density parameter of $A/8 \text{ MeV}^{-1}$) were found to be in very poor agreement with the experimental data, especially for those radionuclides situated around the closure of the $1f_{7/2}$ neutron and/or proton shells (fig. 1, dashed curves). Satisfactory overall agreement could, however, be obtained by introducing a pairing-energy shift⁷ as well as a shell-correction shift^{8,9} of the ground state in the calculation of the level densities (fig. 1, solid curves).

1. F.J. Haasbroek et al., CSIR research report FIS89 (1976).
2. R. Michel, H. Weigel and W. Herr, Z. Phys. A286, 393 (1978), and references therein.
3. R. Michel, G. Brinkmann, H. Weigel and W. Herr, Nucl. Phys. A322, 40 (1979), and references therein.
4. N.C. Schoen, G. Orlov and R.J. McDonald, Phys. Rev. C20, 88 (1979).
5. M. Blann, Report COO-3494-29 (1976); Report UR-NSRL-181 (1978).
6. A.H. Wapstra and K. Bos, Atomic Data and Nucl. Data Tables 19, 215 (1977).
7. J.W. Truran, A.G.W. Cameron and E. Hilf, Proc. Int. Conf. on properties of nuclei far from the region of beta-stability. Report CERN 70-30 (1970), vol. 1, p.275.
8. N. Rosenzweig, Phys. Rev. 105, 950 (1957); Phys. Rev. 108, 817 (1957).
9. M. Blann, Nucl. Phys. 80, 223 (1966).

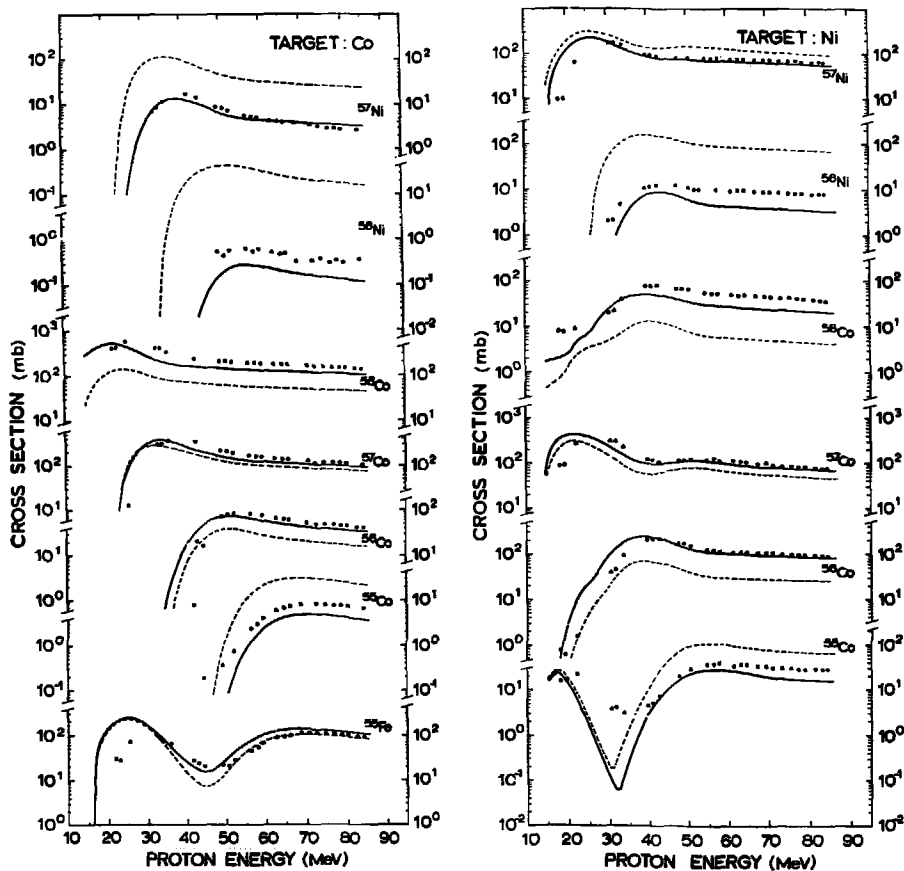


Fig. 1. Comparison between experimental cross-sections and the results of theoretical calculations within the framework of the geometry-dependent hybrid model, in combination with Weisskopf-Ewing theory. The dashed curves and solid curves respectively represent the results obtained with standard Fermi-gas level densities and with level densities calculated with respect to a shifted ground state to account for pairing and shell corrections. The overall uncertainties in the experimental points were, with a few exceptions, estimated¹ to be between 6% and 9%.

FORMATION AND DEEXCITATION OF THE ^{79}Rb COMPOUND NUCLEUS

J. Barreto, M. Langevin and C. Détraz
 Institut de Physique Nucléaire, 91406, Orsay, France

The measurement of the excitation functions of many evaporation channels for the ^{79}Rb formed by the $^{16}\text{O} + ^{63}\text{Cu}$ ¹ and $^{34}\text{S} + ^{45}\text{Sc}$ ² compound nucleus reactions has given evidence for an angular momentum population independent of the entrance channel. Indeed, direct comparison of a large number of individual evaporation channels from both systems shows that the corresponding particles come from the same region of the $(E^* - J)$ plane for the two systems.

The fusion barrier have been determined from the threshold of the first observed evaporation channels. The values thus obtained (table I) are compared to some theoretical predictions; it resorts that although the $^{16}\text{O} + ^{63}\text{Cu}$ fusion barrier is correctly predict, the $^{34}\text{S} + ^{45}\text{Sc}$ one is largely overestimated by the models predictions by about ten MeV.

The variation of the complete fusion cross section (Fig. 1-2) are compared to the predictions of model without and with frictions ^{3,4}. The critical distance model ³ cannot reproduce the experimental results. The classical calculations ⁴ with friction reproduce correctly the $^{16}\text{O} + ^{63}\text{Cu}$ results but not the $^{34}\text{S} + ^{45}\text{Sc}$ ones. This is probably due to a bad determination of the interaction barrier for the latter system. Indeed, an increasing of $\Delta R = 1,4$ Fermi enables good agreement with experimental results. This is certainly due to a large deformation for these nuclei at the contact point.

Statistical model analysis have been performed with codes Alice and Julian for both systems. From the global comparison the code Julian correctly predicts the shapes and magnitudes for almost all the experimental excitation functions. The comparison with the predictions of the Code Alice shows that a critical angular momentum parameter must be introduced in the calculations for the $^{16}\text{O} + ^{63}\text{Cu}$ system ¹ and an additionnal preequilibrium assumption is necessary for the $^{34}\text{S} + ^{45}\text{Sc}$ reaction ⁵ in order to obtain agreement between predictions and calculations.

Table I

Système	B_{fc} (MeV)	$B_{coul.}^a$ (MeV)	B_{Bass}^a (MeV)	$B_{VAZ et al.}^a$ (MeV)	$B_{NGO et al.}^a$ (MeV)	$B_{NGO-NGO}^a$ (MeV)
$^{16}\text{O} + ^{63}\text{Cu}$	27,5 \pm 2,0	35,5	30,0	32,3	32,9	32,6
$^{34}\text{S} + ^{45}\text{Sc}$	36 \pm 4,0	47,5	43,8	46,1	46,8	46,5

a - see Ref. 3

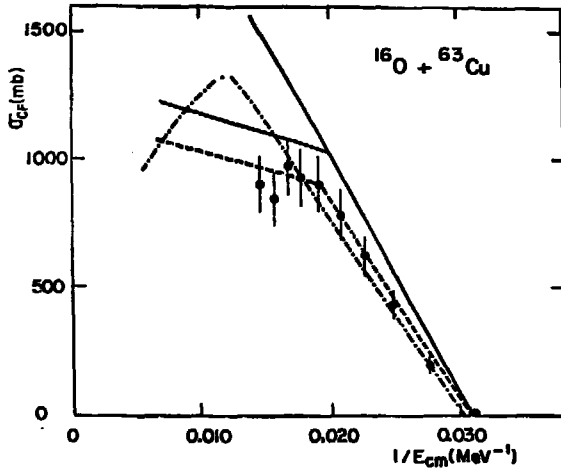


Fig. 1 : Experimental variation of the complete fusion cross section (full points) for the $^{16}\text{O} + ^{63}\text{Cu}$ system as a function of the inverse center of Mass energy. The solid and dashed line curves are the predictions of Ref. 3 ; the dashed dotted line curve are the predictions of ref. 4. The dotted line curve representing the best fit Glas and Mosel parametrization of the experimental results.

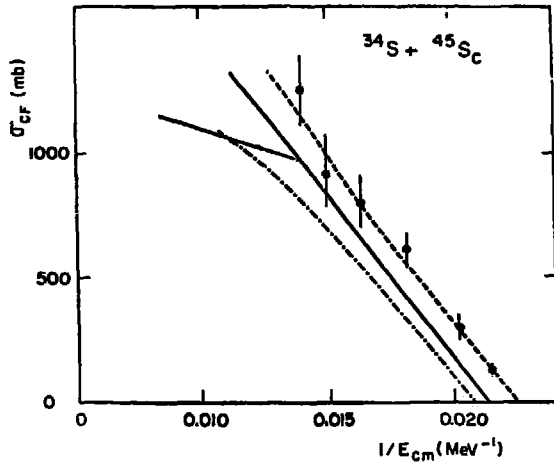


Fig. 2 : Experimental variation of the complete fusion cross section (full points) for the $^{34}\text{S} + ^{45}\text{Sc}$ system (see fig. 1 caption).

1. M. Langevin, J. Barreto and C. Détraz, Phys. Rev. C14(1976) 152.
2. J. Barreto, M. Langevin and C. Détraz, To be published.
3. C. Ngô et al. Nucl. Phys. A240(1975) 353.
4. J.R. Birkelund, Phys. Rev. Vol. 56(1979), n°3, 108.
5. J. Barreto, M. Langevin, To be published.

POST DEAD - LINE

CONTRIBUTED PAPERS

ANGULAR MOMENTUM PROJECTION OF TWO QUASIPARTICLE STATES[†]

F. Grümmer, K.W. Schmid, A. Faessler

Institut für Theoretische Physik, Universität Tübingen, Germany

The aim of the present work is to investigate the method of angular momentum projection^{1),2)} of two quasiparticle states³⁾ built on a Hartree-Fock-Bogoliubov vacuum state. In order to learn something about the important features of this method and the numerical problems connected with it we first did some model calculations in the $i^{13/2}$ -shell, where we can compare our results to the exact solutions. We start from a deformed BCS-state

$$|\phi_0\rangle = \prod_{K>0} (u_K + v_K c_K^+ c_{\bar{K}}^+) |0\rangle \quad (1)$$

with the desired expectation value of the particle number $\langle \phi_0 | \hat{N} | \phi_0 \rangle = N_0$. In terms of the quasiparticle creation operators (1) can be written as

$$|\phi_0\rangle = \left(\prod_{K>0} \beta_K \right) |0\rangle \quad (2)$$

In addition we construct all two quasiparticle states with the K-quantumnumber K=0

$$|K\rangle = \beta_K^+ \beta_{\bar{K}}^+ |\phi_0\rangle \quad (3)$$

so that we have a basis space of 8(=1+7) HFB-wavefunctions for the case of the $i^{13/2}$ -shell. All these wavefunctions are neither eigenfunctions of the angular momentum operator nor of the particle number operator, so that we have to apply the corresponding projection operators. We have to calculate now the projected matrixelements

$$\begin{pmatrix} H_{KK'}^I \\ N_{KK'}^I \end{pmatrix} = \langle K | \begin{pmatrix} \hat{H} \\ \hat{I} \end{pmatrix} \hat{P}_I \hat{P}_{N_0} | K' \rangle \quad (4)$$

where we have to include $|K=0\rangle \equiv |\phi_0\rangle$, and to solve the matrixequation

$$\sum_{K'} \left\{ H_{KK'}^I - E_{\nu}^I N_{KK'}^I \right\} f_{K',\nu}^I = 0 \quad (5)$$

which yields the final solution for the energies E^I and the wavefunctions

$$|\phi_{\nu}^I\rangle = \sum_K f_{K\nu}^I \hat{P}_I \hat{P}_{N_0} |K\rangle \quad (6)$$

The matrixelements (4) are calculated in the framework introduced already in ref. 2 using the surface delta hamiltonian for H and adopting the angular momentum projection method by Kelemen and Dreizler⁴⁾ in order to perform this projection exactly. The resulting energies and wavefunctions can be compared to the exact solutions for N_0 particles in the $i^{13/2}$ -shell. It can be easily shown that for $N_0=2$ the angular momentum projection of $|\phi_0\rangle$ alone gives already the exact spectrum provided the particle number projection is done exactly.

For $N_v=4$ it turns out that the diagonalisation of (5) yields also the exact spectrum of the $(i^{13/2})^4$ -configuration, which is already quite complex. For $N_v=6$ the results are no longer exact as can be seen in table 1, where some exact energy levels are compared to the ones obtained with our model. Nevertheless our model seems to exhaust the space of the $(i^{13/2})^4$ -configurations so well, that the results of a coupling calculation, where the exact and the approximate valence solutions are coupled to a rigid rotor are in extreme agreement. Thus in the case of a single j -shell our model is very well comparable to an exact shellmodel-diagonalisation, a fact, which encourages us to apply it also in more realistic configuration spaces.

- 1) F. Grümmer, K.W. Schmid, A. Faessler, Nucl. Phys. A239 (1975) 289
- 2) R. Beck, H.J. Mang, P. Ring, Z. Phys. 231 (1970) 26
- 3) K.W. Schmid, H. Mütter, K. Goeke, A. Faessler, F. Grümmer, Phys. Lett. 63B (1976) 399
- 4) A. Kelenen, R.M. Dreizler, Z. Phys. 278 (1976) 269

⁺Supported by the BMFT

I	$E_{Q.P.}^I$	E_{exact}^I
0	-21.00	-21.00
2	-15.72	-15.72
4	-14.51	-14.93
6	-13.78	-14.61
8	-14.12	-14.42
10	-14.12	-14.28
12	-14.09	-14.16
14	-10.00	-10.03
16	- 9.10	- 9.12
18	- 8.65	- 8.65
20	- 8.33	- 8.33
22	- 5.29	- 5.29
24	- 4.33	- 4.33

Table 1: For 6 particles in the $i^{13/2}$ -shell the approximate energies $E_{Q.P.}^I$ and the exact ones E_{exact}^I in units of the SDI-strength A are compared.

ON THE STRUCTURE OF THE LOWEST BANDS IN ^{188}Hg *

S.B. Khadkikar, University of Tübingen, 7400 Tübingen

Detailed band mixing calculations for ^{188}Hg based on particle-hole excitations on Hartree-Fock state have been already reported¹⁾. The purpose of the present note is to reinterpret these results so that a new scheme to obtain these bands in other nuclei could be made feasible, and possible improvements can be made.

The microscopic description of the ground and first excited band-structure is given best in terms of the occupancy level of the last pair of neutrons:¹⁾ (1) $(7/2^+)^2$, (2) $(5/2^-)^2$, (3) $(3/2^-)^2$ and (4) $(1/2^-)^2$ for the four intrinsic single determinants. The band mixing coefficients for 0^+ and 14^+ states of the two bands are given in the table (1). From these numbers it is quite clear that the ground band has coherent Cooper-pair of neutrons while the excited band this coherence is broken for $(7/2^+)$ pair only. This exactly corresponds to number and angular momentum projected HF-BCS state as the intrinsic state for ground state while the excited 0^+ state is obtainable from two quasi particle states in $(7/2^+)$ ortho-normalised to ground intrinsic state. At the angular momentum 14 however the occupancy in the ground band of $(7/2^+)$ becomes large and the coherence is reduced which vanishes by complete occupancy of $(7/2^+)^2$ state at $I^\pi=16^+$. For the excited band however reverse thing happens i.e. the occupancy of $(7/2^+)$ -belonging to $i_{13/2^-}$ becomes as small as the angular momentum increases. That is to say the Cooper-pair transforms in to $(i_{13/2^-})^2$ configuration at high angular momentum for ground band. An alternate description in terms of aligned pair may then accrue!

Thus it is seen that the band mixing calculation involving several bands would be equivalent to a model in which zero and two quasiparticle states are mixed with number projection and angular momentum projection restricting the quasiparticle states to the "intruder"- $i_{13/2}$ in this case-state.

Table 1:

Coefficients of band mixing

J^π	1	2	3	4
0^+	.45	-.52	-.52	-.52
0^{++}	.89	.25	.24	.29
14^+	0.98	-.13	-.10	-.10
14^{++}	.19	0.71	.46	.45

1) C.R. Praharaj and S.B. Khadkikar, J. Phys. G: Nucl. Phys. 6 (1980) 241.

* Supported by the BMFT

**Imprimé
au Centre de
Recherches Nucléaires
Strasbourg
1980**